THE PHYSICAL REVIEW

VOLUME 47 | Second Series | NUMBER 10

MAY 15, 1935

Published for the

AMERICAN PHYSICAL SOCIETY

by the

AMERICAN INSTITUTE OF PHYSICS

LANCASTER, PA., AND NEW YORK, N. Y.

...OCIETY

OFFICERS OF THE SOCIETY

...*President*
...Johns Hopkins University
...Baltimore, Maryland

...*Secretary*
...Columbia University
...New York, New York

...*Editor*
...University of Minnesota
...Minneapolis, Minnesota

J. K. ROBERTSON, *Vice President*
Cornell University
Ithaca, New York

G. B. PEGRAM, *Treasurer*
Columbia University
New York, New York

L. B. LOEB, *Local Secretary for the Pacific Coast*
University of California
Berkeley, California

THE PHYSICAL REVIEW

BOARD OF EDITORS

...T. TAUSS, *Editor* J. W. BUCHTA, *Assistant Editor*

Associate Editors

...BARROW A. ELLETT W. V. HOUSTON
...BLEEKER L. A. TURNER R. S. MULLIKEN
...CLARK G. E. UHLENBECK I. I. RABI

...PHYSICAL REVIEW, which was established ..., is a journal of experimental and ... physics. It is published for the American Physical Society by the American Institute of Physics Incorporated. There are two volumes annually with twelve issues in each volume.

... for publication should be submitted to ..., University of Minnesota, Minneapolis, ...

... correspondence concerning papers in the ..., should be addressed to the Editorial ..., American Institute of Physics, 11 East 38th ..., New York.

... within United States and Possessions and ... Foreign, $40.00. Subscriptions and orders ... should be addressed to Lancaster, Pennsylvania, or to the American Institute of Physics, 11 East 38th Street, New York.

... is not accepted for the *Physical Review* but ... to the *Review of Scientific Instruments* ... Physics, a semi-monthly publication of ... through which the field of physics can be reached most effectively. Rates and other information will be furnished on request to the Editorial Secretary.

Changes of address and complaints of failure to receive the *Physical Review*, in the case of members of the American Physical Society, should be addressed to the Treasurer; in the case of other subscribers, to the Editorial Secretary. Back copies can be sent free in response to complaints of non-delivery only if notice of non-delivery is received within three months of date of issue.

The Physical Review is published semi-monthly at Prince and Lemon Streets, Lancaster, Pennsylvania.

Entered at the Post Office at Lancaster, Pennsylvania, as second class matter.

Acceptance for mailing at special rate of postage provided for in section 1103, Act of October 3, 1917, authorized December 6, 1926.

THE
PHYSICAL REVIEW
A Journal of Experimental and Theoretical Physics
VOL. 47, NO. 10 MAY 15, 1935 SECOND SERIES

Some Bands in the Extreme Ultraviolet Spectrum of Helium

J. L. NICKERSON, *Mount Allison University, Sackville, New Brunswick, Canada*
(Received March 18, 1935)

The band at λ600 in the extreme ultraviolet spectrum of helium, first observed by Lyman and first attributed to the helium molecule He_2 by Sommer, has been investigated under various discharge conditions. Low voltage arc, Schüler hollow cathode and uncondensed capillary discharges have been used as sources with a one-meter vacuum spectrograph. The helium used was circulated from the spectrograph back to the discharge tube through the purifying system of a misch metal arc and a chabazite trap in liquid air. The band at λ600 appeared under those conditions of purity which favored the appearance of the visible bands of helium and under such conditions that there can be little doubt that it is due to helium. The intensity of this λ600 band varied directly with the first power of the current in the discharge, whereas the visible bands are known to vary as the square of the current. This suggests a difference of mechanism in the two cases, and in the light of this, various explanations of the origin of the λ600 band are considered but none found satisfactory. A possible explanation of the diffuse structures appearing at λ647 and λ662 is advanced.

THE ultraviolet spectrum of helium as obtained by Lyman[1] contained a prominent line at λ600.3±0.6 which was of a diffuse character and occasionally showed a suggestion of a prolongation toward the regions of long wavelengths. Its persistence of occurrence and intensity relative to the $1^1S_0-m^1P_1^0$ series, as the impurity of the gas decreased, made it doubtful whether it was carbon λ600.2 or other impurity, while its diffuse width λ599.9−λ601.3 not falling over the region of the forbidden line of helium, $1^1S_0-2^1S_0$, at λ601.4 was not consistent with its being a helium line. Further doubts about its being the forbidden line were raised by the fact that it occurs in discharges with steady currents while the forbidden transitions are made more probable by disruptive discharges where the fields are stronger. Lyman also observed diffuse structures at λ647 and at λ662. These shaded toward the regions of short wavelengths and were said to be due to impurities although the actual impurity was not stated.

The line λ600 was next discussed by Dorgelo and Abbink[2] who suggested that it was not any of the possibilities advanced by Lyman but was the $1p-4s_2$ $(2p^1S_0-5s^1P_1^0)$ of neon excited by collisions of the second kind with metastable helium atoms. This conclusion is based on the appearance on their plates of a line at λ600.03, which is within the limit of experimental error of the calculated position of the neon line, and the observation that in neon (with a trace of helium) the higher energy levels are less strongly developed than in helium (with a trace of neon). This is taken to indicate that the higher states of neon are excited by impacts of the second kind with helium metastable atoms.

It was suggested by Sommer[3] that λ600.03 is a

[1] T. Lyman, Astrophys. J. **60**, 1 (1924).

[2] H. B. Dorgelo and J. H. Abbink, Zeits. f. Physik **37**, 667 (1926).

[3] L. A. Sommer, Proc. Nat. Acad. Sci. **13**, 213 (1927).

helium band because of its bandlike appearance and its association with helium of reasonable purity.

In the work of Compton and Boyce[4] the structure at λ600.03 had none of the bandlike appearance described by Sommer and was enhanced by the addition of a further trace of neon to the helium in the discharge. Consequently they incline to the view of Dorgelo and Abbink but suggest there are possibly two or three causes which independently give radiation near λ600 and that the experimental conditions determine which cause predominates.

Paschen[5] mentions the structure at λ600.019 which appears on plates taken by P. G. Kruger[6] and states definitely that it originates in helium and is not the forbidden transition, which is found at λ601.418. The structure at λ600.019 is distinctly bandlike being sharp on the short wavelength edge and shading away toward the red.

The present work was carried on at Princeton University in an attempt to determine the origin of the band at λ600. Spectrograms in the extreme ultraviolet were made of the low voltage arc, Schüler hollow cathode, and uncondensed capillary discharges. The vacuum spectrograph, used formerly by Compton and Boyce,[4] had a one-meter grating ruled fifteen thousand lines to the inch, and covered the region from the zero order to λ1250 with a dispersion of about 12A/mm. This investigation was made at pressures above 2 mm of mercury in order to favor the appearance of the visible bands of helium and it was found that λ600 appeared strongly when the gas purity was sufficient to give the visible bands. Purification of the gas was difficult. The system had several wax seals and since a volume equivalent to several hundred cubic centimeters of gas at atmospheric pressure was in circulation, the purifying system had to be efficient. The best method was circulation of the gas through a misch metal arc using heavy currents and through a chabazite trap immersed in liquid air. These processes removed the inert gases neon and argon and the more active gases, including even hydrogen after long running. However, as hydrogen provided good standards for some regions of the plates it was not always completely removed. This was satisfactory providing Hα (λ6563) was kept less in intensity than the neighboring red line of helium (λ6678), otherwise mild excitation particularly with the uncondensed capillary discharge gave the hydrogen band spectrum very strongly. Occasionally it was necessary to use liquid air traps filled with glass beads to remove mercury vapor. Circulation of the gas at pressure from 2 mm to 12 mm was maintained by one Langmuir pump which kept a pressure ratio of 5 : 1 between the discharge tube and the body of the spectrograph. Purification of the gas for several days in a misch metal arc was always a necessary preliminary to circulation. The increase of strength of the λ600 band with continued purification is strong support for the identification of its origin.

A 94½-hour exposure of a 40-volt arc in helium was obtained. The plate current was 0.3 ampere and the gas pressure 8.8 mm. The filament of the arc consisted of a 15-mil tungsten wire wound in a helix of eight turns on a 30-mil wire as mandrel. The plate was a one-inch diameter circular disk of nickel with its plane 3 mm from the filament. Here, as in all other cases, the metal parts were baked out by the induction furnace while the pumps were running to remove gas contamination. The filament was parallel to the slit and just out of the direct line from it to the grating. This exposure showed the helium band at λ600 but not with extreme intensity. For quick and easy production of the band this method was not suitable, the long exposure time making it very difficult to keep the gas pure. There is a slight continuum observed which extends from λ600 to approximately λ900. This was observed by Hopfield.[7] In plates by the other methods the development of this continuum is not so well marked although the λ600 band appears more readily.

A series of Schüler hollow cathodes were next investigated. These cathodes were made of sheet tungsten bent into hollow cylinders varying from 25 to 50 mm in length and from 6 to 10 mm in internal diameter. The anode was a one-inch

[4] K. T. Compton and J. C. Boyce, J. Frank. Inst. **205**, 497 (1928).
[5] F. Paschen, *Sitzungberichte der Preussischen Akademie der Wissenschaften*, Berlin, p. 662, 1929.
[6] P. G. Kruger, Phys. Rev. **36**, 855 (1930).
[7] J. J. Hopfield, Phys. Rev. **35**, 1133 (1930).

diameter nickel disk. The cathode axis was directly in line with the slit of the spectrograph. With this source a typical exposure was produced in 48 hours from a Schüler cathode discharge in helium at 2.5 to 3-mm pressure. The plate current was 0.2 ampere and the voltage applied 700 d.c. The helium band at λ600 was but poorly developed. The conclusion from several plates was that this method of excitation was not favorable to the strong excitation of the band at λ600.

In order to make intensity comparisons of the band under different current densities, it was desirable to have short exposure under constant conditions of pressure and purity. The most satisfactory type of discharge was the one finally used, the uncondensed capillary type which enables one to have good exposures within an hour. The capillary was a Pyrex tube 8.8 cm long and 3.2 mm internal diameter lined up with, and its near end 4 mm from the slit. The discharge was produced by a 15,000-volt, 8-kilowatt transformer controlled by a resistance in the primary making it possible to vary the discharge current from 10 ma to 350 ma. Considerable care was taken to prevent overheating, air blasts being turned on the discharge tube continuously, and with the higher currents the discharge was intermittent, one second on and one second off, the intervals being timed by a motor-driven interrupter. During any one set of observations for intensity comparisons the same rate of intermittency was maintained. Approximate photometry was attained by a series of carefully timed and regulated exposures with the gas pressure and purity constant. The latter was judged by visual observations and by photographs taken in the visible region simultaneously with those in the vacuum region. In a typical run, for example, a forty-minute exposure with a discharge current of 150 ma was followed by two exposures, one of ten minutes and the other of twenty minutes, both of these with the doubled discharge current of 300 ma. Lines whose excitation depended on the square of the discharge current would then be expected to show equal blackening in the first and second of these exposures while those for which the excitation depends on the first power of the current would be equally blackened in the first and third exposure. The assumption of approximate reciprocity between current and time in producing plate darkening was checked by the variation of the helium resonance series members from one exposure to another, an excitation process known to depend directly on the first power of the current.

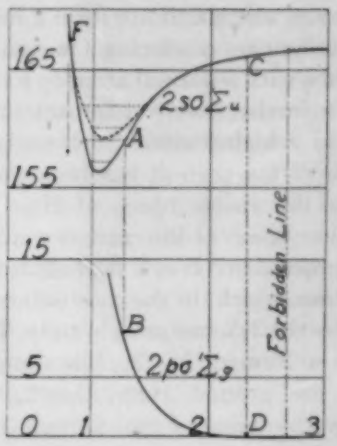

FIG. 1. Energy curves for the helium molecule. Energy in thousands of wave numbers plotted against the internuclear distance in Angstrom units.

From a number of sets of exposures and current ratios of 2/1 and 3/1 it is found that the band at λ600 varies more nearly with the first power of the current[5] than with the square of the current. It was also observed that the diffuse structures at λ647 and λ662 occur in all cases where the gas is quite pure and the current density relatively large.

In seeking an explanation of the band at λ600 one observes that the conditions of gas purity and type of discharge favor the presence of metastable helium atoms (atoms in the $1s2s\,^1S_0$ state). Kruger[6] has found that this band is frequently accompanied by the forbidden line ($1\,^1S_0 - 2\,^1S_0$), and that the line never appears without the band although the band sometimes appears alone. This suggests an association of the band with the forbidden line. That the band edge at 166,660 cm^{-1} represents 385 cm^{-1} greater energy than the forbidden line at 166,275 cm^{-1} raises a difficulty, which will be considered in the remainder of this paper.

Variation of the intensity of a band with the square of the current indicates a process involving two electron impacts, producing either two

[5] J. L. Nickerson, Phys. Rev. **38**, 1907 (1931).

excited atoms which unite to form a molecule, or one electron impact producing a metastable atom which unites with a normal atom to form a molecule and a further electron impact raising that molecule to a higher state. Such variation with the square of the current has been observed by Weizel for the visible bands of He_2.[9] Variation with the first power of the current would indicate that the process involves a normal atom and an excited atom, which, in the case we are considering, may be the 2^1S_0 metastable state. The molecular state so formed, $2S\sigma^1\Sigma_u$, has allowed transitions to the ground state, $2p\sigma^1\Sigma_g$, which is formed by the union of two normal atoms.[10]

The potential energy curve of the ground state is known with considerable accuracy in the region concerned in this problem. This is found in the work of Lennard-Jones, Slater, Slater and Kirkwood, and Margenau.[11] Slater's curve in Fig. 1 shows the energy relations to be expected. The depth of the minimum is less than 20 cm^{-1} with its lowest point at an internuclear distance of 2.9A.

For the upper state the potential energy curve was obtained in the form of Morse's function:[12]

$$U(r)=166{,}275+10{,}000\,e^{-6.9(r-r_0)}.$$
$$-20{,}000\,e^{-3.45(r-r_0)}$$

where $r_0=1.05$A.[13]

The determination of the constants of this equation depended on the estimation of the heat of dissociation for the state. The value assumed, namely $D\sim10{,}000$ cm^{-1} is reasonable from three viewpoints:

(1) Using the data of Imanishi[14] and of Dieke, Takamine and Suga[15] in the rotational energy relation of Kratzer:

$$\omega_0=2(B_0^3/\beta_0)^{\frac{1}{2}} \quad \text{gives} \quad D=8600.$$

(2) Considering the extent of the development of the rotational levels for $2s\sigma^1\Sigma_u$ in the work of Imanishi it can be found that D must be greater than 6500 to prevent dissociation before the higher rotational states are reached.

(3) For the level $3p\pi^3\Pi_g$ $D\sim20{,}000$ has been estimated[16] and this would allow a value of the same order for $2s\sigma^1\Sigma_u$. Transitions from the upper to the lower state will produce diffuse bands because of the steep slope of the ground state potential energy curve in the regions to which transitions occur, see *C–D* in Fig. 1, and this together with transitions discussed in the next section will account for some of Hopfield's continuum[7] which extends from λ600 to about λ900. It is impossible to obtain from this type of radiation sufficient energy to account for the high frequency edge of the λ600 band. A glance at the curves in Fig. 1 will show that they are nowhere else as far apart in ordinates as at complete dissociation. It is hence impossible to obtain, from any transitions between these two states, bands of higher frequency than that associated with the forbidden line λ601.418.

Besides radiation from this definite molecular state there may be radiation from the temporary states formed momentarily during impact. Born and Franck[17] have shown that for two atoms on collision to form a stable molecule there is necessarily present a third body, wall or atom, in order to have conservation of energy and momentum. Very frequently a third body will not be at hand, and in the present problem, when a stable molecule is not formed, there is with decreasing radius of collision an increasing probability of electron transition from the metastable state accompanied by the radiation of energy. Two-body collisions have been used by Kuhn and Oldenberg[18] and by Finkelnburg[19] to describe the origin of bands appearing in the spectra of mixtures of argon and mercury. In Fig. 1 transitions from point F to the ground state are illustrative of this process as applied to the present problem. However, it is again obviously impossible to have frequencies greater than the forbidden line because of the position of the ground state potential energy curve. Sufficient energy could be obtained if the electronic transitions were probable at internuclear distances of the order of 2.5A or

[9] W. Weizel, Zeits. f. Physik **59**, 320 (1930).
[10] F. Hund, Zeits. f. Physik **63**, 719 (1930).
[11] J. E. Lennard-Jones, Proc. Roy. Soc. **A107**, 157 (1925); J. C. Slater, Phys. Rev. **32**, 349 (1928); J. C. Slater, Kirkwood, Phys. Rev. **37**, 682 (1931); H. Margenau, Phys. Rev. **38**, 747 (1931).
[12] P. M. Morse, Phys. Rev. **34**, 57 (1929).
[13] W. Weizel, *Bandenspektren*, p. 268.
[14] S. Imanishi, Inst. Phys. and Chem. Res. Tokyo **10**, 250 (1929).
[15] G. H. Dieke, T. Takamine and T. Suga, Zeits. f. Physik **49**, 637 (1928).
[16] W. Weizel, *Bandenspektren*, p. 255.
[17] M. Born and J. Franck, Zeits. f. Physik **31**, 411 (1925).
[18] H. Kuhn and O. Oldenberg, Phys. Rev. **41**, 72 (1932).
[19] W. Finkelnberg, Zeits. f. Physik **81**, 781 (1933).

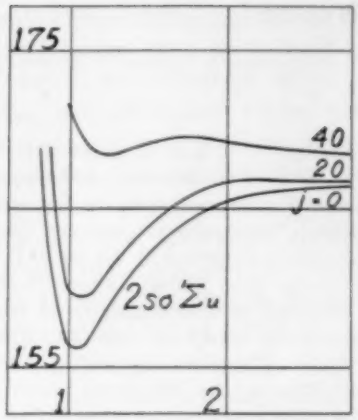

FIG. 2. Energy curves E_u+E_j for the j values indicated.

greater. This would be so if on the approach or recession of the two atoms there were a slowing of their motion in that region. This would occur if the upper state potential energy curve was shaped as in Fig. 2. Such a form of curve actually appears[20] when the combined energy of vibration and rotation is plotted against the internuclear distance. Such curves may be calculated, but the large energies involved in these processes make it very unlikely that in an ordinary gas discharge, where the mean kinetic energy is of the order of 600 to 800 cm^{-1}, the number of high energy atoms would be sufficient to provide the excess 385 wave numbers of energy with the intensity observed. Further since the levels involved are Σ levels there would be only R and P branches and they would be of about equal intensity. One would expect therefore a symmetric distribution of radiation about the forbidden line but one observes that with short exposures the band shades away from λ600.019 but does not always cross λ601.418.

There remains another possibility to be considered:—

That the potential energy curve in the upper state has, for $j=0$, a rise of a few hundred wave numbers above the horizontal asymptote thus producing a potential barrier at large internuclear distances and enabling larger energy contributions to the radiation to be associated with smaller values of j. This rise in the curve would indicate repulsion at large internuclear distances but changing to attraction as the internuclear distance decreases. This would require a nearby perturbing level in the atomic state. The nearest level that combines with 2^1S_0 is $2^1P_1^0$ which lies 4829 cm^{-1} above it, and there are no lower lying levels which combine with 2^1S_0. Now the effect of these perturbing levels is to act repulsively on each other, the higher one being raised and the lower one lowered. Thus clearly there is nothing to make one anticipate a rise in the molecular potential energy curve.

There seems to be then no simple explanation of λ600 considering it as a helium band originating in the molecular $2s\sigma^1\Sigma_u$ level, the only reasonable electronic assignment. One point of interest remains. The appearance of the diffuse structures at λ647 and λ662 (sharper edges at λ648.73 and λ663.23, corresponding to 154,450 cm^{-1} and 150,800 cm^{-1}, approximately) both shading toward the short wavelength side occur only when the gas is pure and when the current density is relatively large. These structures could be transitions from the two known vibrational levels of $2s\sigma^1\Sigma_u$ to the ground state, since the accuracy in the position of these curves is small. One of these is A–B in Fig. 1. The dotted curve in the figure shows the order of change in the upper state necessary to give good agreement in frequency. The observed shading toward short wavelengths would also be expected from the shape of the curves. It is significant that associated plates of the visible region show the helium bands in the region of λ4723 strongly developed only when these two structures appear in the ultraviolet. The bands that appeared were identified with the $4s\sigma^1\cdot{}^3\Sigma_u$ to $2p\pi^1\cdot{}^3\Pi_g$. The lower of the singlet levels can radiate further only by going into the $2s\sigma^1\Sigma_u$ level which is the upper state suggested for the diffuse structures at λ647 and λ662.

In conclusion grateful acknowledgment is made to Dr. K. T. Compton for suggesting this problem, and to Dr. J. C. Boyce and Professor E. U. Condon for encouragement and criticism, and to the Carnegie Institution of Washington for financial assistance.

[20] O. Oldenberg, Zeits. f. Physik **56**, 563 (1929).

The Third Spectrum of Krypton

C. J. HUMPHREYS, *George Eastman Research Laboratory of Physics, Massachusetts Institute of Technology*

(Received March 25, 1935)

The spectrum characteristic of the Kr^{++} ion has been selected from the various krypton spectra excited in a Geissler tube discharge. The distinction between lines of Kr III or higher spark spectra and those of Kr II is based on the partial or complete suppression of the former by inductance in the discharge circuit. Wavelength measurements, based mainly upon observations with the Rowland grating at the Bureau of Standards, extend from λ2100 to λ7400. A total of 369 lines has been classified arising from 88 levels of Kr III. The low states of Kr^{++} are ^3P, ^1D and ^1S, due to the $4s^24p^4$ configuration. The higher excited states are built upon the ^4S, ^2D and ^2P states of Kr^{+++} by the addition of *ns*, *np* or *nd* to the normal $4s^24p^3$ configuration. All but 8 of the 76 levels comprising the first excited states have been found. The connection between these and the low states has been established by the use of J. C. Boyce's extreme ultraviolet data. Numerous inter-limit combinations have permitted precise evaluation of relative term values. Calculations based on the $4p^3(^4S)ns^3S^0$, and $4p^3(^4S)nd^3D^0$ and $^5D^0$, series have led to an estimated value of 298,020 cm^{-1} for the lowest $4p^4(^4S)^3P_2$ level, corresponding to an ionization potential of 36.8 volts.

THE wavelength data reported in this paper were obtained in the spectroscopy laboratory of the Bureau of Standards during a series of investigations of the spectra of krypton and the other rare atmospheric gases in various stages of ionization.[1, 2, 3] The spectra were obtained from Geissler tubes operated by a.c. transformers in a circuit containing a spark gap and condensers. Various amounts of self-inductance were inserted in the circuit for some exposures in order to distinguish between lines arising from different stages of ionization. Full details are given in the paper on Kr II[3], in which a selected list of spark lines arising from the Kr^+ ion was published. After this selection was made about 600 lines remained, which, judging by their behavior in the discharge, originate in Kr^{++} or higher stages. In the present investigation 369 of these including practically all the intense sharp lines are classified as Kr III. In view of the uncertain origin of the remaining lines the published list is confined to the classified lines.

In determining the stage of ionization in which a line originates, by aid of discharge behavior, the essential criterion is the weakening of intensity or complete suppression of higher spark lines when inductance is placed in the circuit. The method is not entirely critical because, for a given ion, lines from higher energy states are affected in much the same way as those from the next ion. L. Bloch, E. Bloch and G. Déjardin[4] made a selection of the rare gas lines on the basis of their length when the spectrograph slit was illuminated by an electrodeless discharge exposed end-on. This method is subject to the same limitations. In the paper quoted the lines are designated 1, 2 or 3, accordingly as they are regarded as belonging to the first, second or third spark spectrum. The identification of the lines marked 1 is practically perfect, but it was found in the course of this analysis that, not only the lines marked 2, but also a considerable number of those marked 3, belong to Kr III. Here again the basis of the distinction seems to be the elevation of energy states within the ion. On the whole the two methods of sorting show satisfactory agreement. It is now known also that the discharge conditions in an electrodeless discharge can be made to favor a certain ion by a proper selection of pressure and electrical excitation.

The wavelengths used in the analysis are based mainly on observations with the 21-ft. Rowland grating over the range from λ2400 to λ10,000. No Kr III lines are classified beyond λ7400. The probable error of the grating observations seldom exceeds 0.01A except in the case of very broad hazy lines which in general have not been accounted for by this analysis. The corresponding

[1] Wm. F. Meggers, T. L. de Bruin and C. J. Humphreys, Bur. Standards J. Research **3**, 129 (1929); **7**, 643 (1931).
[2] Wm. F. Meggers and C. J. Humphreys, Bur. Standards J. Research **10**, 427 (1933).
[3] T. L. de Bruin, C. J. Humphreys and Wm. F. Meggers, Bur. Standards J. Research **11**, 409 (1933).
[4] L. Bloch, E. Bloch and G. Déjardin, Ann. de physique **10**, 461 (1924).

wave number precision ranges from 0.17 cm^{-1} at λ2400 to better than 0.02 cm^{-1} at λ7400. Quartz prism observations go down to λ2100 and overlap the ultraviolet region covered by the grating spectrographs. The fainter ultraviolet lines were observed only with the quartz instrument. The wavelengths in air, wave numbers in vacuum, estimated relative intensities, and identifications of the classified lines, are given in Table I. The relative intensities from the beginning of the list to λ2407 are estimated from quartz prism observations. The rest are based mainly on the grating observations. In any case the intensity estimates are comparable only over short ranges. Lines marked *h* or *H* are hazy or very broad and diffuse, respectively.

In addition to the experimental material just discussed, the author had at his disposal the wavelength measurements in the extreme ultraviolet, made by Professor J. C. Boyce, which the latter very kindly permitted him to use. These data were obtained by use of the electrodeless discharge and the two-meter vacuum spectrograph of the Carnegie Institution of Washington, at the Massachusetts Institute of Technology. The identified lines of the extreme ultraviolet are given in Table III of the following paper.[5] This material proved to be of inestimable value, not only for establishing the connection between terms which had already been found and the lowest states, but also for indicating the relative positions of the groups of terms converging to different limits based on the Kr^{+++} ion.

Two previous attempts at the analysis of Kr III have been reported. Acharya[6] supplemented published wavelengths with quartz prism observations and gave a list of terms part of which were identified as the quintets of the (^4S) system. A different partial analysis of the term system converging to the (^4S) limit has been published by Deb and Dutt.[7] We are in complete disagreement with both of these analyses. The wavelengths already published, consisting of the measurements of Baly,[8] and of Bloch, Bloch and Déjardin,[4] are hardly of sufficient precision for use in a term analysis.

The electron configurations of the Kr^{++} ion are obtained by adding the valence electron to the configuration, $4s^24p^3$, of the Kr^{+++} ion. The lowest states of the Kr^{+++} ion, ^4S, ^2D and ^2P, become accordingly the convergence limits of three sets of terms. The normal configuration of Kr^{++} is $4s^24p^4$, giving (^4S)^3P, (^2D)^1D and (^2P)^1S states. The configuration $4s4p^5$ yields $^3P^0$ and $^1P^0$. These latter terms combine both with those of the low and first excited states but all the lines lie in the Schumann region or extreme ultraviolet. The term scheme, predicted by the Hund theory, because of the addition of an electron to the $4s^24p^3$ configuration, is shown in Table II. When the principal quantum number of the valence electron is increased by one, the corresponding array is repeated. Bold-face type indicates that all or part of the levels of a term have been identified. The predicted arrays for *nf* electrons are omitted inasmuch as no such terms have been found.

Altogether 97 levels have been found including 68 of the 76 belonging to first excited states. Identifications are given for all but two of the observed terms. Inter-system and inter-limit combinations appear with considerable intensity. The relative values of the terms converging to the different ion limits are fixed by the inter-limit combinations in the range covered by this investigation and supported by such combinations in the extreme ultraviolet. Transitions between terms converging to different ion limits are associated theoretically with perturbations between terms separated by a small interval.[9] The rare gas spectra approach the *jj* type of coupling so that perturbations may be expected to occur between terms of like *j* values irrespective of *l* or *s*. Consequently in many cases there may be a sharing of configurations between different terms, leading to peculiar interval ratios, partial term inversions, or unusual combining intensities. The unusually high relative intensities of the inter-limit combinations among the higher terms among the first excited states converging to (^2D) and (^2P) have added to the difficulty of assigning these terms to their proper system. Table III contains the observed terms and their identifications, including those fixed only by extreme ultraviolet transitions.

[5] J. C. Boyce, Phys. Rev. **47**, 718 (1935).
[6] D. P. Acharya, Ind. J. Phys. **5**, 385 (1930).
[7] S. C. Deb and A. K. Dutt, Zeits. f. Physik **67**, 138 (1931).
[8] E. C. C. Baly, Phil. Trans. **202**, 183 (1904).
[9] E. U. Condon, Phys. Rev. **36**, 1121 (1930).

TABLE I. *Lines of krypton III.*

INT.	λ (air)	ν (vac.)	TRANSITION
1	2116.00	47243.96	$(^4S)5s^5S^0_2 - (^2D)5p^3P_1$
1	2129.75	46938.98	$(^4S)4d^3D^0_3 - (^2D)5p^3F_4$
1	2138.70	46742.58	$(^4S)4d^3D^0_2 - (^2D)5p^1F_3$
1	2142.49	46659.91	$(^2D)4d^1D^0_2 - (^2P)5p^1D_2$
2	2148.58	46527.67	$(^4S)5s^5S^0_2 - (^2D)5p^3P_2$
1	2158.43	46315.36	$(^4S)4d^3D^0_2 - (^2D)5p^1P_1$
3	2162.50	46228.20	$(^4S)4d^3D^0_3 - (^2D)5p^3F_4$
2	2170.83	46050.84	$(^4S)4d^3D^0_2 - (^2D)5p^3F_2$
1	2172.25	46020.73	$(^4S)4d^3D^0_2 - (^2D)5p^3D_3$
2	2215.60	45120.40	$(^4S)4d^3D^0_2 - (^2D)5p^3F_2$
1–	2219.14	45048.45	$(^4S)4d^3D^0_1 - (^2D)5p^1P_1$
1	2230.69	44815.21	$(^2D)5s^3D^0_2 - (^2P)5p^3D_3$
1	2232.35	44781.89	$(^2D)5p^3D_2 - 2^0_2$
6	2259.76	44238.76	$(^4S)5p^5P_3 - (^4S)5d^3D^0_3$
3	2273.76	43966.40	$(^4S)4d^3D^0_2 - (^2D)5p^3D_2$
4	2279.79	43850.12	$(^2P)5p^3S_1 - (^2P)6s^1P^0_1$ $(^2D)5p^1P_1 - 1^0_1$
1	2290.52	43644.72	$(^2D)5p^3F_3 - 2^0_2$
3	2291.28	43630.25	$(^4S)4d^3D^0_1 - (^2D)5p^3D_2$
3	2299.15	43480.91	$(^2D)5p^3D_3 - (^2D)6s^1D^0_2$
2	2303.00	43408.23	$(^2D)4d^3F^0_2 - (^2D)5p^3P_2$
1	2317.87	43129.78	$(^2D)5p^1F_3 - 2^0_2$
1	2322.32	43047.14	$(^2D)4d^1D^0_2 - (^2P)5p^3D_2$
3	2329.22	42919.64	$(^4S)4d^3D^0_2 - (^2D)5p^3D_1$
6	2345.45	42622.67	$(^2D)5p^3D_1 - (^2D)5d^1D^0_2$
3	2358.48	42387.21	$(^2D)5p^3D_1 - (^2D)6s^3D^0_2$
3	2360.14	42357.40	$(^2D)5p^3D_2 - (^2D)6s^1D^0_2$
4	2361.82	42327.27	$(^2D)5p^3F_2 - (^2D)6s^1D^0_2$
3	2363.26	42301.48	$(^2P)5p^3S_1 - (^2P)6s^3P^0_2$
1	2364.70	42275.73	$(^4S)5s^5S^0_2 - (^2D)5p^3F_2$
4	2368.19	42213.43	$(^4S)5p^5P_1 - (^4S)6s^5S^0_2$
1	2376.69	42062.47	$(^2D)5p^1P_1 - (^2D)6s^1D^0_2$
1	2387.90	41865.03	$(^2D)5p^3D_2 - (^2D)6s^3D^0_3$
40	2393.94	41759.41	$(^4S)5p^5P_2 - (^4S)6s^5S^0_2$
4	2400.10	41652.24	$(^4S)4d^3D^0_1 - (^2D)5p^3D_1$
1	2401.58	41626.57	$(^2P)5p^1P_1 - (^2P)6s^3P^0_2$
2	2402.40	41612.36	$(^4S)4d^5D^0_1 - (^4S)5p^3P_2$
3	2402.96	41602.67	$(^4S)4d^5D^0_2 - (^4S)5p^3P_2$
1	2403.29	41596.96	$(^4S)5p^5P_2 - (^4S)5d^3D^0_2$
3	2403.65	41590.73	$(^4S)4d^5D^0_0 - (^4S)5p^3P_2$
10	2407.10	41531.12	$(^2D)5p^3D_2 - (^2D)5d^1G^0_4$
1	2414.78	41399.05	$(^2D)4d^3F^0_2 - (^2D)5p^3F_2$
1	2427.48	41182.47	$(^4S)4d^5D^0_0 - (^4S)5p^3P_1$
1	2428.92	41158.06	$(^4S)4d^5D^0_1 - (^4S)5p^3P_1$
1	2431.04	41122.17	$(^4S)5s^5S^0_2 - (^2D)5p^3D_2$
2	2434.64	41061.37	$(^2D)5d^1P^0_1 - (^3P)5p^3P_2$
6	2439.21	40984.45	$(^4S)5p^5P_1 - (^4S)5d^5D^0_2$
1	2439.78	40974.87	$(^2D)4d^3F^0_2 - (^2D)5p^3F_4$
6	2440.05	40970.34	$(^4S)5p^5P_1 - (^4S)5d^5D^0_1$
5	2440.89	40956.24	$(^4S)5p^5P_1 - (^4S)5d^5D^0_0$
4	2451.52	40778.67	$(^2D)4d^3F^0_2 - (^2D)5p^1F_3$
1c	2452.29	40765.86	$(^4S)5p^5P_2 - (^4S)5d^5D^0_2$
8	2453.28	40749.41	$(^4S)5p^5P_2 - (^4S)5d^5D^0_2$
1	2453.74	40741.48	$(^2D)5p^3D_2 - (^2D)6s^3D^0_2$
3	2454.12	40735.47	$(^4S)5p^5P_3 - (^4S)5d^5D^0_3$
10h	2457.72	40675.80	$(^4S)5p^5P_2 - (^4S)5d^5D^0_2$
5h	2459.63	40644.22	$(^2D)5p^3D_2 - (^2D)5d^1D^0_2$
3	2462.76	40592.57	$(^2D)4d^3D^0_2 - (^2P)5p^3P_2$
6h	2468.43	40499.39	$(^2D)5p^3P_2 - 2^0_2$
4	2473.96	40408.81	$(^2D)5p^3D_2 - (^2D)6s^3D^0_2$
3h	2474.90	40393.47	$(^2D)5p^3F_3 - (^2D)5d^1G^0_4$
2	2478.37	40336.92	$(^2P)5p^1D_2 - (^2P)6s^1P^0_1$
1	2481.04	40293.51	$(^2D)4d^3F^0_2 - (^2D)5p^3F_2$
2	2482.99	40261.87	$(^2D)4d^3F^0_3 - (^2D)5p^3D_3$
1	2487.03	40196.47	$(^2P)5p^3P_1 - (^2P)6s^1P^0_1$
2	2491.35	40126.78	$(^2D)4d^1P^0_1 - (^2P)5p^1D_2$
40	2494.01	40083.98	$(^4S)5p^5P_2 - (^4S)5d^5D^0_4$
15	2497.71	40024.50	$(^4S)5p^5P_3 - (^4S)5d^5D^0_2$
3	2498.77	40007.63	$(^4S)5p^5P_3 - (^4S)5d^5D^0_2$
8	2500.64	39977.71	$(^4S)5p^5P_1 - (^4S)6s^5S^0_2$
5h	2506.86	39878.53	$(^2D)5p^1F_3 - (^2D)5d^1G^0_4$
1	2507.84	39862.95	$(^2D)5p^3P_2 - 1^0_1$
1	2511.92	39798.20	$(^2D)4d^3D^0_2 - (^2P)5p^3P_1$
6h	2512.92	39782.37	$(^2D)5p^3P_1 - 2^0_2$
10	2512.42	39742.83	$(^4S)5p^5P_2 - (^4S)6s^5S^0_2$
6h	2519.29	39681.78	$(^2D)5p^3F_4 - (^2D)5d^1G^0_4$
2	2520.32	39665.57	$(^4S)5p^5P_1 - (^4S)5d^5D^0_1$
2h	2524.27	39603.51	$(^2D)5p^3F_3 - (^2D)6s^3D^0_2$
10	2524.97	39592.53	$(^2D)4d^3F^0_4 - (^2D)5p^3F_4$
2	2525.51	39584.06	$(^2D)4d^3D^0_1 - (^2P)5p^3P^0$
1	2529.52	39521.32	$(^2D)5p^3D_3 - (^2D)5d^1D^0_2$
1–	2531.46	39491.02	$(^2D)5p^3F_2 - (^2D)5d^1D^0_2$
1	2537.16	39402.31	$(^2P)5p^3P_2 - (^2P)6s^1P^0_1$
6	2537.57	39395.95	$(^2D)4d^3F^0_4 - (^2D)5p^1F_3$
3h	2544.72	39285.26	$(^2D)5p^3D_3 - (^2D)6s^3D^0_2$
1	2546.36	39259.97	$(^2D)5s^3D^0_2 - (^2D)5p^1D_2$
1	2546.67	39255.18	$(^2D)5p^3F_2 - (^2D)6s^3D^0_2$
4h	2548.60	39225.46	$(^2D)5p^1P_1 - (^2D)5d^1D^0_2$
2	2549.51	39211.46	$(^4S)5p^5P_3 - (^4S)5d^5D^0_1$
2	2551.49	39181.03	$(^2D)5p^3P_0 - 1^0_1$
8	2553.16	39155.41	$(^2D)4d^3F^0_3 - (^2D)5p^3F_2$
1	2553.81	39145.44	$(^2D)5p^3P_1 - 1^0_1$
8	2554.25	39138.70	$(^2D)4d^3F^0_2 - (^2D)5p^3D_2$
10	2555.13	39125.22	$(^2D)4d^3F^0_3 - (^2D)5p^3D_2$
1	2557.55	39088.20	$(^2D)5p^1F_3 - (^2D)6s^3D^0_2$
5h	2558.00	39081.33	$(^2D)4d^3D^0_1 - (^2P)5p^1P_1$
30	2563.25	39001.29	$(^4S)5p^5P_3 - (^4S)6s^5S^0_2$
10h	2570.48	38891.60	$(^2D)5p^3F_4 - (^2D)6s^3D^0_3$
6	2571.19	38880.86	$(^2D)4d^3F^0_4 - (^2D)5p^3F_3$
3h	2586.78	38646.55	$(^2D)5p^3P_1 - (^2P)6s^3P^0_2$
3	2589.47	38606.40	$(^2D)4d^3D^0_2 - (^2P)5p^3P_2$
8	2604.35	38385.84	$(^2D)5s^1D^0_2 - (^2P)5p^1P_1$
1	2609.66	38307.74	$(^2D)4d^3D^0_1 - (^2P)5p^3D_2$
3	2615.19	38226.74	$(^2P)4d^3F^0_3 - (^2P)5p^3P_2$
1	2623.11	38111.33	$(^2D)4d^3G^0_3 - (^2D)5p^3F_2$
2h	2625.64	38074.61	$(^2D)5p^3P_2 - (^2D)6s^1D^0_2$
6	2628.08	38039.26	$(^4S)4d^5D^0_2 - (^4S)5p^5P_3$
25	2628.90	38027.40	$(^4S)4d^5D^0_3 - (^4S)5p^5P_3$
15	2630.66	38001.95	$(^2D)4d^3F^0_3 - (^2D)5p^3D_2$
60	2639.76	37870.91	$(^4S)4d^5D^0_4 - (^4S)5p^5P_2$
4h	2641.00	37853.18	$(^2P)5p^3P_2 - (^2P)6s^3P^0_2$
2	2641.74	37842.63	$(^2D)5s^3D^0_2 - (^2D)5p^1D_2$
4	2648.43	37746.99	$(^4S)5p^5P_1 - (^4S)5d^3D^0_2$
10	2648.69	37743.29	$(^2D)4d^3F^0_4 - (^2D)5p^3D_3$
1h	2650.96	37710.97	$(^2D)5s^1D^0_2 - (^2P)5p^3S_1$
4	2653.66	37672.60	$(^2D)4d^3D^0_3 - (^2P)5p^1D_2$
2	2658.00	37611.10	$(^2D)5s^1D^0_2 - (^2P)5p^3D_2$
20	2670.67	37432.68	$(^2D)4d^1D^0_2 - (^2D)5p^1D_2$
3	2672.79	37402.99	$(^2D)4d^3D^0_2 - (^2P)5p^3D_2$
8h	2676.00	37358.12	$(^2D)5p^3P_1 - (^2D)6s^1D^0_2$
15	2679.62	37307.66	$(^4S)4d^3D^0_1 - (^4S)5p^5P_2$
30	2680.32	37297.91	$(^4S)4d^3D^0_2 - (^4S)5p^5P_2$
7	2680.72	37292.35	$(^4S)5p^5P_2 - (^4S)5d^3D^0_2$
40	2681.19	37285.95	$(^4S)4d^5D^0_3 - (^4S)5p^5P_2$
15	2690.23	37160.53	$(^2D)4d^3F^0_2 - (^2D)5p^3D_1$
20	2694.81	37097.37	$(^4S)4d^5D^0_0 - (^4S)5p^5P_1$
25	2696.59	37072.89	$(^4S)4d^5D^0_1 - (^4S)5p^5P_1$
25	2697.30	37063.13	$(^4S)4d^5D^0_2 - (^4S)5p^5P_1$
3	2698.07	37052.55	$(^2P)4d^3F^0_2 - (^2P)5p^3P_1$
2h	2698.71	37043.77	$(^2P)5p^1D_2 - (^2P)6s^3P^0_1$
1	2708.34	36912.06	$(^2P)4d^3F^0_2 - (^2P)5p^1D_2$
1	2709.02	36902.79	$(^2P)5p^3P_1 - (^2P)6s^3P^0_1$
2	2710.27	36885.78	$(^4S)5p^5P_1 - (^4S)5d^5D^0_1$
7	2715.19	36818.94	$(^2D)4d^3D^0_2 - (^2P)5p^1P_1$
5	2730.41	36613.72	$(^2D)4d^1P^0_1 - (^2P)5p^3S_1$
2h	2741.84	36461.09	$(^4S)5p^5P_2 - (^4S)5d^5D^0_2$
5h	2742.05	36458.30	$(^2D)5p^3P_2 - (^2D)6s^3D^0_2$
3	2743.03	36445.14	$(^4S)5p^5P_2 - (^4S)5d^5D^0_2$
2	2744.05	36431.73	$(^4S)5p^5P_2 - (^4S)5d^5D^0_1$
10	2750.36	36348.15	$(^2D)5s^1D^0_2 - (^2P)5p^3D_1$
8	2756.53	36266.80	$(^2P)4d^3D^0_2 - (^2P)5p^3P_2$
2	2765.90	36143.94	$(^2D)4d^3D^0_2 - (^2P)5p^3S_1$
4h	2768.54	36109.48	$(^2P)5p^3P_2 - (^2P)6s^3P^0_1$
2	2785.26	35892.72	$(^4S)5p^3P_1 - (^4S)6s^5S^0_2$
20	2806.07	35626.56	$(^2D)4d^3S^0_1 - (^2P)5p^3S_1$
25	2811.67	35555.60	$(^2D)5s^3D^0_1 - (^2D)5p^3P_1$
15	2813.97	35526.54	$(^2D)4d^3S^0_1 - (^2P)5p^3D_2$
15	2814.48	35520.10	$(^2D)5s^3D^0_1 - (^2D)5p^3P_0$
2	2817.53	35481.66	$(^2D)4d^3G^0_3 - (^2D)5p^1F_3$
4h	2820.95	35438.64	$(^4S)5p^3P_2 - (^4S)6s^5S^0_2$
6	2822.63	35417.55	$(^2D)4d^3D^0_3 - (^2P)5p^3D_2$
6	2829.41	35332.69	$(^2P)4d^3D^0_2 - (^2P)5p^1D_2$
6	2835.94	35251.33	$(^2D)4d^1P^0_1 - (^2P)5p^3D_1$
30	2841.00	35188.55	$(^2D)5s^3D^0_2 - (^2D)5p^3P_1$
30	2851.16	35063.16	$(^2D)4d^3G^0_4 - (^2D)5p^1F_3$
2	2853.22	35037.85	$(^2P)4d^3F^0_3 - (^2P)5p^3D_3$
5h	2856.09	35002.64	$(^2D)5p^3P_2 - (^2D)6s^3D^0_2$
4	2859.05	34966.40	$(^2D)4d^3G^0_3 - (^2D)5p^3F_2$
50	2870.61	34825.60	$(^2P)4d^3F^0_4 - (^2P)5p^3D_3$
5	2872.85	34798.45	$(^2P)5s^3P^0_1 - (^2P)5p^3P_2$
2	2874.24	34781.62	$(^2D)4d^3D^0_2 - (^2P)5p^3D_1$
2	2884.55	34657.31	$(^2P)4d^3F^0_2 - (^2P)5p^3D_2$
100	2892.18	34565.89	$(^2D)4d^3G^0_5 - (^2D)5p^3F_4$
40	2893.68	34547.97	$(^2D)4d^3G^0_4 - (^2D)5p^3F_3$
1h	2895.92	34521.25	$(^2D)5p^3P_1 - (^2D)5d^1D^0_2$
20	2900.04	34472.21	$(^2D)5s^1D^0_2 - (^2D)5p^1P_1$
30	2909.17	34364.02	$(^4S)5s^5S^0_2 - (^4S)5p^3P_2$
6h	2915.78	34286.13	$(^2D)5p^3P_1 - (^2D)6s^3D^0_2$
10	2917.67	34263.92	$(^2D)4d^3S^0_1 - (^2P)5p^3D_1$
10	2934.00	34073.22	$(^2P)4d^3F^0_2 - (^2P)5p^1P_1$
20	2935.23	34058.95	$(^2D)4d^3D^0_2 - (^2P)5p^3D_2$
4	2938.56	34020.35	$(^2P)5s^3P^0_0 - (^2P)5p^3P_1$
15	2939.91	34004.73	$(^2P)5s^3P^0_1 - (^2P)5p^3P_1$
10	2948.13	33909.92	$(^4S)5s^5S^0_2 - (^4S)5p^3P_1$
4	2952.09	33864.44	$(^2P)5s^3P^0_1 - (^2P)5p^1D_2$
50	2952.56	33859.05	$(^2D)4d^3G^0_3 - (^2D)5p^3F_2$
3	2955.20	33828.80	$(^2D)4d^3G^0_5 - (^2D)5p^3D_3$
20	2968.31	33679.40	$(^2P)4d^3F^0_3 - (^2P)5p^3D_3$
60	2992.22	33410.29	$(^2D)4d^3G^0_4 - (^2D)5p^3D_3$
2	2993.27	33398.57	$(^2P)4d^3F^0_2 - (^2P)5p^3S_1$
20	2996.60	33361.45	$(^2D)4d^1D^0_2 - (^2D)5p^3P_1$
6	3002.24	33298.78	$(^2P)4d^3F^0_2 - (^2P)5p^3D_2$

TABLE I.—*Continued*

INT.	λ (air)	ν (vac.)	TRANSITION
50	3022.30	33077.78	$(^3P)4d^3D_2 - (^3P)5p^3D_2$
80	3024.45	33054.27	$(^3D)5s^3D_3 - (^3D)5p^3P_2$
6	3044.80	32833.36	$(^3D)4d^1G^0_4 - (^3D)5p^3F_4$
50	3046.93	32810.40	$(^3P)5s^3P^0_2 - (^3P)5p^3P_2$
30	3056.72	32705.33	$(^3D)4d^3G^0_5 - (^3D)5p^3D_3$
3	3062.43	32644.35	$(^3D)4d^1D^0_2 - (^3D)5p^3P_2$
60	3063.13	32636.89	$(^3D)4d^1G^0_4 - (^3D)5p^1F_3$
40	3097.16	32278.30	$(^4S)4d^3D^0_3 - (^4S)5p^3P_2$
60	3112.25	32121.81	$(^3D)4d^1G^0_4 - (^3D)5p^3F_3$
30	3120.61	32035.76	$(^2P)4d^3F^0_2 - (^2P)5p^3D_1$
20	3122.46	32016.78	$(^2P)5s^3P^0_2 - (^2P)5p^3P_1$
100	3124.39	31997.00	$(^3D)5s^1D^0_2 - (^3D)5p^1D_2$
10	3136.20	31876.51	$(^2P)5s^3P^0_2 - (^2P)5p^1D_2$
15	3139.58	31842.20	$(^3D)5s^3D^0_3 - (^3D)5p^1F_3$
60	3141.35	31824.26	$(^4S)4d^3D^0_2 - (^4S)5p^3P_1$
20	3141.88	31818.89	$(^2P)4d^3D^0_2 - (^2P)5p^3S_1$
9	3144.32	31794.20	$(^2P)5s^1P^0_1 - (^2P)5p^3P_2$
10	3151.75	31719.25	$(^2P)4d^3D^0_2 - (^2P)5p^3D_2$
10h	3156.63	31670.21	$(^3D)5p^1D_2 - (^2D)6s^3D^0_2$
20	3170.93	31527.40	$(^2P)5s^1P^0_1 - (^2P)5p^3P_0$
100	3189.11	31347.68	$(^4S)4d^3D^0_3 - (^4S)5p^3P_2$
80	3191.21	31327.05	$(^3D)5s^3D^0_2 - (^3D)5p^1F_3$
20	3220.62	31040.99	$(^2P)5s^3P^0_0 - (^2P)5p^1P_1$
10	3222.24	31025.38	$(^2P)5s^3P^0_1 - (^2P)5p^1P_1$
3	3223.74	31010.94	$(^4S)4d^3D^0_1 - (^4S)5p^3P_2$
20	3224.85	31000.27	$(^2P)5s^1P^0_1 - (^2P)5p^3P_1$
2h	3235.21	30901.01	$(^2D)4d^1P^0_1 - (^2D)5p^1D_2$?
40	3239.52	30859.89	$(^3P)5s^1P^0_1 - (^2P)5p^1D_2$
40	3240.44	30851.14	$(^3D)5s^3D^0_1 - (^3D)5p^1P_1$
300	3245.69	30801.23	$(^4S)5s^5S^0_2 - (^4S)5p^5P_2$
5	3246.62	30792.41	$(^2P)4d^3D^0_1 - (^2P)5p^3P_2$
150	3264.81	30620.86	$(^2D)5s^3D^0_2 - (^2D)5p^3F_4$
100	3268.48	30586.48	$(^2D)5s^3D^0_1 - (^2D)5p^3F_2$
30	3271.65	30556.84	$(^4S)4d^3D^0_1 - (^4S)5p^3P_1$
2	3279.42	30484.44	$(^3D)5s^3D^0_2 - (^3D)5p^1P_1$
3	3285.25	30430.35	$(^2D)4d^3D^0_2 - (^2D)5p^1D_2$
30	3285.89	30424.42	$(^3D)5s^3D^0_3 - (^2D)5p^1F_3$
1	3292.21	30366.02	$(^2P)5s^1P^0_0 - (^2P)5p^3S_1$
4	3293.88	30350.62	$(^2P)5s^1P^0_1 - (^2P)5p^3S_1$
30	3304.75	30250.80	$(^2P)5s^3P^0_4 - (^3P)5p^3D_3$
20	3308.16	30219.61	$(^3D)5s^3D^0_3 - (^2D)5p^3F_2$
1h	3308.73	30214.41	$(^2D)5p^1D_2 - (^2D)6s^3D^0_2$
50	3311.47	30189.41	$(^3D)5s^3D^0_3 - (^2D)5p^3D_3$
200	3325.75	30059.79	$(^4S)5s^5S^0_2 - (^4S)5p^5P_2$
60	3330.76	30014.58	$(^3D)4d^1D^0_2 - (^3D)5p^1F_3$
10	3332.50	29998.90	$(^2P)4d^3D^0_1 - (^2P)5p^3P_1$
50	3342.48	29909.33	$(^2D)5s^3D^0_3 - (^2D)5p^3F_3$
10	3348.17	29858.51	$(^2P)4d^3D^0_1 - (^2P)5p^1D_2$
100	3351.93	29825.02	$(^4S)5s^5S^0_2 - (^4S)5p^5P_1$
40	3374.96	29621.50	$(^3P)5s^3P^0_2 - (^3P)5p^3D_3$
20	3388.93	29499.40	$(^2D)4d^1D^0_2 - (^2D)5p^3F_3$
15	3396.58	29432.96	$(^2D)5s^3D^0_1 - (^2D)5p^3D_2$
10	3428.83	29156.14	$(^3P)4d^1F^0_3 - (^3P)5p^1D_2$
100	3439.46	29066.03	$(^2D)5s^3D^0_2 - (^2D)5p^3D_2$
6	3442.86	29037.33	$(^3P)5s^3P^0_2 - (^3P)5p^1P_1$
8	3446.85	29003.72	$(^2P)5s^3P^0_0 - (^2P)5p^3D_1$
10	3448.71	28988.07	$(^2P)5s^3P^0_1 - (^2P)5p^3D_1$
3	3471.02	28801.76	$(^3D)5s^3D^0_3 - (^2D)5p^3F_2$
70	3474.65	28771.67	$(^2D)5s^3D^0_2 - (^2D)5p^3D_2$
1—	3485.08	28685.56	$(^2P)5p^1P_1 - 1^0_1$
100	3488.59	28656.70	$(^3D)4d^1D^0_2 - (^3D)5p^1P_1$
8	3492.80	28622.16	$(^3D)4d^3D^0_1 - (^2D)5p^3P_1$
10	3497.13	28586.73	$(^2D)4d^3D^0_1 - (^2D)5p^3P_0$
200	3507.42	28502.86	$(^4S)5s^5S^0_2 - (^4S)5p^5P_2$
15	3514.55	28445.04	$(^3D)4d^3D^0_3 - (^2D)5p^1D_2$
4	3521.11	28392.05	$(^3D)4d^1D^0_2 - (^2D)5p^3F_2$
5	3524.78	28362.49	$(^2P)5s^3P^0_2 - (^2P)5p^3S_1$
2	3537.20	28262.90	$(^2P)5s^1P^0_2 - (^2P)5p^3D_2$
20	3549.42	28165.60	$(^2P)4d^3D^0_3 - (^2P)5p^3P_2$
2	3562.09	28065.50	$(^2P)4d^3F^0_3 - (^2D)5p^1D_2$
100	3564.23	28048.57	$(^4S)5s^5S^0_1 - (^4S)5p^3P_1$
15	3567.72	28021.13	$(^2P)5s^1P^0_1 - (^2P)5p^1P_1$
2	3579.95	27925.41	$(^2D)5s^1D^0_2 - (^2D)5p^1P_1$
5h	3582.48	27905.69	$(^2D)4d^3D^0_1 - (^2D)5p^3P_2$
1	3598.04	27785.01	$(^4S)4d^3D^0_2 - (^4S)5p^3P_2$
2	3603.96	27739.45	$(^4S)4d^3D^0_2 - (^4S)5p^3P_1$
5	3611.06	27684.83	$(^2P)4d^3F^0_2 - (^2D)5p^1D_2$
20	3615.82	27648.39	$(^2D)5s^3D^0_3 - (^2D)5p^3D_2$
1	3632.5	27521.43	$(^2P)4d^3D^0_1 - (^2P)5p^3P_0$
30	3641.34	27454.62	$(^2D)5s^3D^0_1 - (^2D)5p^3D_1$
1	3655.77	27346.26	$(^2P)5s^1P^0_1 - (^2P)4d^3S_1$
4	3670.23	27238.52	$(^2D)4d^1D^0_2 - (^2D)5p^3D_2$
1	3671.14	27231.77	$(^2P)4d^3D^0_3 - (^2P)5p^1D_2$
4	3674.23	27208.87	$(^2D)5s^1D^0_2 - (^2D)5p^3P_2$
30	3690.65	27087.81	$(^2D)5s^3D^0_2 - (^2D)5p^3D_1$
5	3696.69	27043.56	$(^4S)4d^3D^0_2 - (^4S)5p^3P_2$
2	3699.98	27019.44	$(^3P)4d^3D^0_1 - (^2P)5p^1P_1$
5	3726.32	26828.53	$(^2D)4d^1P^0_1 - (^2D)5p^3P_1$
2	3769.69	26519.87	$(^2D)4d^3F^0_2 - (^4S)5p^3P_2$
15	3792.70	26358.98	$(^2D)4d^3D^0_2 - (^2D)5p^3P_1$
7	3809.16	26245.08	$(^2P)4d^3D^0_1 - (^2P)5p^3D_2$
1	3829.57	26105.21	$(^2P)4d^3D^0_2 - (^2D)5p^1D_2$
2	3835.37	26065.73	$(^2D)4d^3F^0_2 - (^4S)5p^3P_1$
3	3847.49	25983.63	$(^3P)5s^1P^0_1 - (^2P)5p^3D_1$
40H	3868.70	25841.18	$(^2D)4d^3S^0_1 - (^2D)5p^3P_1$
3	3874.04	25805.56	$(^2D)4d^3S^0_1 - (^2D)5p^3P_0$
10	3898.70	25642.34	$(^2D)4d^3D^0_2 - (^2D)5p^3P_2$
3	3913.90	25542.75	$(^3P)4d^1F^0_3 - (^3P)5p^3D_3$
4	3938.53	25383.02	$(^2D)4d^3F^0_3 - (^4S)5p^3P_2$
25	3957.67	25260.27	$(^2D)4d^1D^0_2 - (^2D)5p^3D_1$
3	3979.05	25124.54	$(^2D)4d^3S^0_1 - (^2D)5p^3P_2$
15	4002.61	24976.66	$(^3P)4d^3D^0_3 - (^3P)5p^3D_2$
1	4027.17	24824.34	$(^3P)4d^1P^0_1 - (^3P)5p^3P_2$
50	4067.37	24578.99	$(^2D)5s^1D^0_2 - (^2D)5p^1F_3$
40	4131.33	24198.48	$(^4S)5s^3S^0_1 - (^4S)5p^3P_2$
40	4154.46	24063.76	$(^2D)5s^1D^0_2 - (^2D)5p^3F_2$
4h	4160.21	24030.50	$(^3P)4d^1P^0_1 - (^3P)5p^3P_1$
15	4171.79	23963.79	$(^4S)5s^3S^0_1 - (^4S)5p^3P_1$
2h	4184.59	23890.49	$(^3P)4d^1P^0_1 - (^3P)5p^1D_2$
1h	4195.91	23826.04	$(^3P)5p^1P_1 - (^3D)6s^3D^0_2$
20	4225.92	23656.83	$(^2D)4d^3D^0_3 - (^2D)5p^3P_2$
25	4226.58	23653.15	$(^2D)4d^3D^0_1 - (^2D)5p^3F_2$
2	4232.82	23618.28	$(^3P)4d^3D^0_2 - (^3P)5p^3D_2$
1h	4233.72	23613.26	$(^3P)4d^3F^0_3 - (^3D)5p^3P_2$
5h	4244.33	23554.24	$(^3P)4d^1D^0_2 - (^3P)5p^1D_2$
10	4294.83	23277.28	$(^2P)4d^3F^0_3 - (^3D)5p^3P_2$
9	4305.20	23221.22	$(^3D)5s^1D^0_2 - (^3D)5p^1P_1$
8h	4344.24	23012.54	$(^3D)4d^3D^0_2 - (^2D)5p^1F_3$
1	4360.63	22926.04	$(^2D)5s^1D^0_2 - (^2D)5p^3D_2$
8	4378.68	22831.54	$(^3P)4d^3P^0_1 - (^3P)5p^3P_2$
15	4443.28	22499.60	$(^3D)4d^3D^0_1 - (^2D)5p^3D_2$
3	4443.72	22497.37	$(^2D)4d^3D^0_2 - (^3D)5p^3F_2$
2	4518.64	22124.37	$(^3D)4d^3P^0_1 - (^3D)5p^1P_1$
10	4536.46	22037.46	$(^3P)4d^3P^0_1 - (^3P)5p^3P_1$
6	4537.25	22033.62	$(^3P)4d^3D^0_2 - (^3D)5p^3P_1$
1h	4565.51	21897.24	$(^3P)4d^3P^0_1 - (^3P)5p^1D_2$
1h	4621.40	21632.42	$(^3P)5s^1P^0_1 - (^3D)5p^1D_2$
3	4673.80	21389.90	$(^2D)4d^3D^0_2 - (^3D)5p^3F_2$
3h	4693.65	21299.44	$(^3P)4d^1D^0_2 - (^3P)5p^3D_2$
10	4710.48	21223.34	$(^2D)4d^3D^0_3 - (^2D)5p^3F_4$
4	4729.72	21137.01	$(^2D)4d^3S^0_1 - (^2D)5p^1P_1$
2h	4749.00	21051.20	$(^3P)4d^1P^0_1 - (^3P)5p^1P_1$
6	4754.48	21026.93	$(^2D)4d^3D^0_2 - (^3D)5p^1F_2$
7	4789.74	20872.14	$(^2D)4d^3S^0_1 - (^2D)5p^3F_2$
2h	4826.08	20714.98	$(^2P)4d^1D^0_2 - (^2P)5p^1P_1$
1	4841.9	20647.30	$(^2P)4d^3F^0_3 - (^2D)5p^1F_3$
2	4845.62	20631.45	$(^3P)4d^3F^0_4 - (^3D)5p^3F_4$
1h	4873.87	20511.86	$(^2D)4d^3D^0_3 - (^2D)5p^3F_3$
5h	4892.21	20434.97	$(^3P)4d^3F^0_4 - (^3D)5p^1F_3$
6h	4906.28	20376.36	$(^2P)4d^1P^0_1 - (^3P)5p^3S_1$
2	4940.21	20236.42	$(^2D)4d^3D^0_2 - (^3D)5p^3D_2$
2	4965.78	20132.22	$(^2P)4d^3F^0_3 - (^3D)5p^3F_4$
2h	4977.08	20086.51	$(^2D)4d^3G^0_5 - (^4S)5p^3P_2$
10	4988.52	20040.45	$(^3P)4d^1D^0_2 - (^3P)5p^3S_1$
20h	5016.45	19928.87	$(^3P)4d^1F^0_3 - (^3D)5p^1D_2$
2h	5018.72	19919.86	$(^3P)4d^3F^0_4 - (^3D)5p^3F_3$
2h	5042.86	19824.51	$(^2D)5s^1D^0_2 - (^3D)5p^3D_1$
2	5061.46	19751.65	$(^2P)4d^3F^0_2 - (^3D)5p^3F_2$
4	5069.96	19718.54	$(^2D)4d^3S^0_1 - (^2D)5p^3D_2$
1h	5110.98	19560.29	$(^2P)4d^3P^0_1 - (^3P)5p^3P_0$
2	5151.68	19405.75	$(^3P)4d^3P^0_2 - (^3P)5p^3P_2$
3h	5152.01	19404.51	$(^2D)4d^3D^0_2 - (^3D)5p^3F_2$
1	5160.09	19374.12	$(^2D)4d^3D^0_3 - (^3D)5p^3D_2$
2	5257.83	19013.98	$(^3P)4d^1P^0_1 - (^3P)5p^3D_1$
1	5263.18	18994.65	$(^3P)4d^3F^0_3 - (^3D)5p^3D_2$
2h	5338.20	18727.71	$(^3D)4d^1P^0_1 - (^3D)5p^3D_1$
2	5349.77	18687.21	$(^3P)4d^3D^0_2 - (^3D)5p^1F_3$
1	5362.11	18644.20	$(^3P)4d^3F^0_2 - (^3D)5p^3F_2$
4	5371.40	18611.96	$(^3P)4d^3P^0_2 - (^3P)5p^3P_1$
2h	5381.39	18577.41	$(^3P)5s^3P^0_2 - (^3D)5p^3P_1$
5	5412.19	18471.69	$(^3P)4d^3P^0_2 - (^3P)5p^1D_2$
2h	5438.20	18383.34	$(^2P)4d^3P^0_1 - (^3P)5p^3S_1$
1h	5475.49	18258.15	$(^2D)4d^3D^0_2 - (^2D)5p^3D_1$
2	5477.66	18250.91	$(^2D)4d^3D^0_2 - (^2D)5p^3D_2$
10	5501.43	18172.06	$(^3P)4d^3D^0_1 - (^3D)5p^3F_2$
5	5597.32	17860.75	$(^3P)5s^3P^0_2 - (^3D)5p^3P_2$
1h	5715.80	17490.52	$(^3P)4d^3F^0_2 - (^3D)5p^3D_2$
1h	5873.50	17020.92	$(^2P)4d^3P^0_1 - (^2P)5p^3D_1$
8h	5935.03	16844.46	$(^3P)5s^1P^0_1 - (^3D)5p^3P_1$
10h	6037.17	16559.47	$(^2P)4d^3D^0_1 - (^3D)5p^3P_1$
3h	6050.11	16524.06	$(^2P)4d^3D^0_1 - (^2D)5p^3P_0$
10h	6078.38	16447.21	$(^3D)5s^3D^0_2 - (^4S)5p^3P_2$
5h	6110.81	16359.92	$(^3D)5s^3D^0_1 - (^4S)5p^3P_1$
1h	6164.76	16216.75	$(^3P)4d^3P^0_2 - (^3P)5p^3D_3$
5	6250.98	15993.08	$(^3D)5s^3D^0_3 - (^4S)5p^3P_1$
10h	6310.22	15842.94	$(^2P)4d^3D^0_1 - (^3D)5p^3P_2$
2	6395.09	15632.68	$(^2P)4d^3P^0_2 - (^3P)5p^1P_1$
1h	6444.70	15512.35	$(^2P)4d^3F^0_2 - (^3D)5p^3D_1$
10h	6602.90	15140.69	$(^2P)4d^3F^0_3 - (^3D)5p^3P_2$
10h	6651.75	15029.49	$(^2D)5s^3D^0_3 - (^4S)5p^3P_2$
1h	6683.55	14957.98	$(^2P)4d^3P^0_2 - (^3P)5p^3S_1$
1h	6728.41	14858.26	$(^2P)4d^3P^0_2 - (^3P)5p^3D_2$
3h	6793.53	14715.83	$(^2P)5s^3P^0_2 - (^3D)5p^3F_2$
1H	6818.13	14662.74	$(^2P)4d^1P^0_1 - (^3D)5p^1D_2$
3h	6977.95	14326.91	$(^2P)4d^1D^0_2 - (^3D)5p^1D_2$
2h	7057.45	14165.52	$(^2D)4d^1D^0_2 - (^4S)5p^3P_1$
1H	7353.42	13595.37	$(^2P)4d^3P^0_2 - (^2P)5p^3D_1$

TABLE II. *Electron configurations and spectral terms for Kr III.*

ELECTRON CONFIGURATION	TERM LIMIT $4s^24p^3\ ^4S$		TERM LIMIT $4s^24p^3\ ^2D$				TERM LIMIT $4s^24p^3\ ^2P$		
$4s^24p^4$	^3P		^1D				^1S		
$4s^24p^3\ 5s$	$^5S^0$	$^3S^0$	$^1D^0$		$^3D^0$		$^1P^0$		$^3P^0$
$4s^24p^3\ 5p$	^5P	^3P		^1P	^1D	^1F	^1S	^1P	^1D
				^3P	^3D	^3F	^3S	^3P	^3D
$4s^24p^3\ 4d$	$^3D^0$	$^1D^0$	$^1S^0$	$^1P^0$	$^1D^0$	$^1F^0$ $^1G^0$	$^1P^0$	$^1D^0$	$^1F^0$
			$^3S^0$	$^3P^0$	$^3D^0$	$^3F^0$ $^3G^0$	$^3P^0$	$^3D^0$	$^3F^0$
$4s^24p^3\ 6s$	$^5S^0$	$^3S^0$	$^1D^0$		$^3D^0$		$^1P^0$		$^3P^0$
$4s^24p^3\ 5d$	$^3D^0$	$^1D^0$	$^1S^0$	$^1P^0$	$^1D^0$	$^1F^0$ $^1G^0$	$^1P^0$	$^1D^0$	$^1F^0$
			$^3S^0$	$^3P^0$	$^3D^0$	$^3F^0$ $^3G^0$	$^3P^0$	$^3D^0$	$^3F^0$
$4s4p^5$	$^1P^0$	$^3P^0$							

The principal evidence for the identifications is in the combining intensities. In the region studied we expect the strongest combinations to be $(^4S)5s\,^5S^0_2-(^4S)5p\,^5P_3$ and $(^4S)5s\,^3S^0_1-(^4S)5p\,^3P_2$. The strongest lines observed, ν, 30,801.14, and ν, 28,502.86, are assigned to these respective transitions. Trial arrays with constant differences involving these and other strong lines in the same region lead to the ^5P and ^3P intervals, which in turn appear in the $(^4S)nd\,^5D^0-(^4S)5p\,^5P$ and $(^4S)nd\,^3D^0-(^4S)5p\,^3P$ multiplets. Failure to find $(^4S)5p\,^3P_0$ seems explainable only on the assumption that two of these ^3P levels have coalesced or else that the interval separating it from the other ^3P levels is abnormally large inasmuch as all lines of appreciable intensity in the expected range have been classified. We expect the odd terms to give far ultraviolet combinations with the $4s^24p^4$ terms. The clew to the identification of these low terms was found by Dr. Boyce in the multiplets, $(^4S)s^2p^4\ ^3P-sp^5\ ^3P^0$, and $(^2D)s^2p^4\ ^1D-sp^5\ ^3P^0$. The $s^2p^4\ ^2P$ intervals, together with the separations between these and ^1D, were found to occur repeatedly among the extreme ultraviolet data. In almost all cases these constant differences were found to be associated with real odd levels which combined with higher even levels to give lines in the visible and near ultraviolet.

Of the (^2D) odd terms those arising from $5s$ are expected to yield the most intense combinations. The interpretation of the second most intense group of lines among the data as combinations of $(^2D)5s\,^3D^0$ and $^1D^0$ with $(^2D)5p\,^3F$, ^3D, ^3P, and ^1F, ^1D, ^1P, is thus supported. These multiplets are an outstanding feature of the observed spectrum. The remaining (^2D) odd levels fall into fairly well isolated groups and are identified on the basis of j values and combining intensities. The $^3G^0_5$ level is identified necessarily on the basis of a single combination, but is supported by a strong line in the expected position. The $^3P^0$, $^1F^0$, and $^1S^0$ terms of this group have not been found. Considerable assistance in placing the even (^2D) levels has been obtained from the isoelectronic spectrum, Se I, recently analyzed

TABLE III. *Kr III terms.*

ELECTRON CONFIGURATION		LIMIT $^4S_{3/2}$: 0		LIMIT $^2D_{3/2}$ $^2D_{5/2}$		LIMIT $^2P_{1/2}$ $^2P_{3/2}$	
$4s^2$		$^3P_2$	298020				
$3d^{10}$	$4p$	$^3P_1$	293472	$^1D_2$	283376	$^1S_0$	264941
$4p^3$		$^3P_0$	292707				
				$^2D^0_1$	134749.99	$^1P^0_1$	119775.54
	$5s$	$^5S^0_2$	152300.00	$^2D^0_2$	134383.17	$^3P^0_1$	119759.88
		$^3S^0_1$	146438.74	$^2D^0_3$	132965.45	$^3P^0_2$	117771.90
				$^1D^0_2$	127119.98	$^1P^0_1$	116755.47
		$^5P_1$	122474.95	$^3D_1$	107295.36	$^3D_1$	90771.82
		$^5P_2$	122240.26	$^3D_2$	105317.07	$^3D_2$	89508.96
		$^5P_3$	121498.82	$^3D_3$	104193.76	$^3S_1$	89409.26
	$5p$			$^3F_2$	104163.51	$^1P_1$	88734.57
		$^3P_0$	———	$^1P_1$	103898.80	$^3P_0$	88232.55
		$^3P_1$	118390.17	$^3F_3$	103056.13	$^3D_3$	88150.43
		$^3P_2$	117935.88	$^1F_3$	102541.01	$^1D_2$	85895.48
				$^3F_4$	102344.56	$^3P_1$	85755.19
				$^3P_2$	99911.12	$^3P_2$	84961.44
				$^3P_0$	99229.89	$^1S_0$	———
				$^3P_1$	99194.51		
				$^1D_2$	95122.92		
		$^5D^0_0$	159572.32	$^3F^0_2$	144455.82	$^3F^0_2$	123188.34
		$^5D^0_1$	159547.88	$^3F^0_3$	143318.95	$^3F^0_4$	122976.02
		$^5D^0_2$	159538.08	$^3F^0_4$	141937.04	$^3F^0_3$	122807.72
		$^5D^0_3$	159526.22	$^3G^0_3$	138022.48	$^3D^0_3$	121228.17
		$^5D^0_4$	159369.73	$^3G^0_4$	137604.12	$^3D^0_1$	115754.00
				$^3G^0_5$	136910.45	$^1F^0_3$	115051.73
		$^3D^0_3$	150214.30	$^1G^0_4$	135177.93	$^3D^0_2$	113127.15
	$4d$	$^3D^0_2$	149283.56	$^1D^0_2$	132555.55	$^1P^0_1$	109785.72

ELECTRON CONFIGURATION		LIMIT $^4S_{3/2}$: 0		LIMIT $^2D_{3/2}$ $^2D_{5/2}$		LIMIT $^2P_{1/2}$ $^2P_{3/2}$	
		$^3D^0_1$	148947.01	$^3D^0_1$	127816.62	$^1D^0_2$	109449.70
				$^1F^0_3$	?126023.09	$^3P^0_0$	———
				$^3D^0_2$	125553.49	$^3P^0_1$	107792.76
				$^3D^0_1$	?125035.67	$^3P^0_2$	104367.20
				$^3D^0_3$	123567.95		
				$^1F^0_3$	———		
				$^3P^0_0$	———		
				$^3P^0_1$	———		
				$^3P^0_2$	———		
				$^1S^0_0$	———		
		$^5S^0_2$	82497.43	$^1D^0_2$	———	$^3P^0_0$	———
	$6s$			$^1D^0_2$?	64908.37	$^3P^0_1$	48852.02
		$^3S^0_1$	76176.60	$^3D^0_3$	63452.80	$^3P^0_2$	47108.17
				$^1D^0_2$?	61836.33	$^1P^0_1$	45558.88
		$^5D^0_0$	81518.71	$^1D^0_2$?	64672.62		
		$^5D^0_1$	81504.70	$^1G^0_4$	62662.64		
		$^5D^0_2$	81490.68	1^0_1	60048.87		
	$5d$	$^5D^0_3$	81474.36	2^0_2	59411.68		
		$^5D^0_4$	81414.84				
		$^3D^0_2$	80643.34				
		$^3D^0_1$	78724.56				
		$^3D^0_3$	77260.07				
		$^3P^0_2$	182078				
$4s4p^5$		$^3P^0_1$	178639				
		$^3P^0_0$	176476				
		$^1P^0_1$	156144				

by Ruedy and Gibbs,[10] in which this set of terms is fully developed. Almost the same order of even (^2D) levels occurs in both spectra.

The even terms of the first excited state based on (^2P) are complete except for $5p\,^1S_0$. The relative positions make practically certain the interpretation of those of j value 2. $^3D_2$ has a unique j value among the group. Those with J value 1 are given the most plausible assignment on the basis of the combinations. This group has not been found in Se I.

Of the odd (^2P) levels those yielding the most intense combinations are assigned to $(^2P)5s\,^3P^0$ and $^1P^0$. The $(^2P)5d\,^3F^0$ levels seem to be quite certain because of the intensity distribution in the $(^2P)5d\,^3F^0-(^2P)5p\,^3D$ multiplet. The $^3F^0_4$ level is checked by interlimit combinations. Two levels assigned to the (^2D) system, $(^2D)4d\,^3S^0_1$, and $(^2D)4d\,^1P^0_1$, combine very strongly with the (^2P) even terms. The assignments are made therefore with reservations. The $(^2P)4d\,^3D^0$ levels show unexpected intervals but no other reasonable assignment seems possible. The remaining (^2P) odd terms $^3P^0$ and $^1D^0$ are supported by faint but numerous and numerically consistent combinations with no plausible alternatives.

It is not possible to estimate precisely the intervals between the various ion limits on the basis of the data here reported. Either the low terms of Kr IV or sufficiently long series for precise evaluation of the limits would be required. A fair estimate of the relative positions of the limits is obtained by extrapolation from the homologous spectra, Ne IV, and A IV. The centers of gravity of the term groups should also be separated by roughly the separation of the limits. Calculations based on series of which two members have been found indicate an interval of from 16,000 to 19,000 cm^{-1} between ^4S and ^2D and from 34,000 to 38,000 cm^{-1} between ^4S and ^2P. These intervals are to be regarded as approximations, however, because it is improbable that the series are well represented by a Rydberg formula and free from perturbations. Furthermore the identifications of the second series members are too uncertain to establish beyond doubt which of the levels of the doublet ion limit is approached in each case. These estimated intervals compare reasonably well with the separations between the groups of levels belonging to first excited states which are associated with the second series members and also with the intervals between the low terms, $^3P_2-^1D_2$, 14,644 cm^{-1}, and $^3P_2-^1S_0$, 33,079 cm^{-1}.

The absolute value of the terms is based on calculations of the limits of the $(^4S)nd\,^5D^0_3$, $(^4S)nd\,^3D^0_3$, and $(^4S)ns\,^3S^0_1$ series. The calculated limits expressed in terms of the position of $^5D^0_3$ are as follows:

$^5D^0_3$,	159,049
$^3D^0_3+(^5D^0_3-^3D^0_3)$,	159,751
$^3S^0_1+(^5D^0_3-^3S^0_1)$,	159,778.

An earlier estimate was based on $(^4S)ns\,^5S^0_2$ which is expected to give the most regular series. Such a calculation, however, places $5s\,^5S^0_2$ at 146,000 and $4d\,^5D^0_3$ at 153,226 differing by 6300 from the average of the above values. It was assumed therefore that the $^5S^0_2$ series was perturbed more than the others which were chosen as the basis of the absolute values. The actual procedure was to add 6300 to 146,000 to bring it up to 152,300 to give the absolute value of $^5S^0_2$ and to fix all other levels by their relative positions. The calculation places the lowest level of Kr III, $(^4S)4s^24p^4\,^3P_2$ at 298,020, corresponding to an ionization potential of 36.8 volts. The experimental value given by Tate and Smith[11] is 38.7$\pm$0.5 volts.

In conclusion the author is very happy to acknowledge his indebtedness to all who have contributed to the progress of the analysis, in particular to Dr. Wm. F. Meggers of the Bureau of Standards, who collaborated in the experimental work and in the measurement of the spectrograms, to Dr. T. L. de Bruin,[12] of the University of Amsterdam, for making the first suggestions as to the identity of some of the (^4S) terms, and to Professor J. C. Boyce, of the Massachusetts Institute of Technology, for the use of his extreme ultraviolet data.

[10] J. E. Ruedy and R. C. Gibbs, Phys. Rev. **46**, 880 (1934).

[11] J. T. Tate and P. T. Smith, Phys. Rev. **46**, 773 (1934).

[12] A letter, dated Amsterdam, 8 Jan. 1933, from Dr. de Bruin to Dr. Meggers contained the first Kr III regularities. These consisted of the combinations of $(^4S)5p\,^5P$, ^3P with $(^4S)5s\,^5S^0$, $^3S^0$, $6s\,^5S^0$, $^3S^0$, and $(^4S)4d\,^5D^0$, $^3D^0$, based on wavelength and intensity data obtained at the Bureau of Standards and confirmed by Zeeman effects of λλ3507.42 and 3564.23 observed at Physica. Some revisions of these identifications have been made.

The Spectra of Krypton in the Extreme Ultraviolet

J. C. BOYCE, *George Eastman Research Laboratory of Physics, Massachusetts Institute of Technology*

(Received March 25, 1935)

Increased dispersion and resolving power have made possible a revision and extension of the work of previous investigators on the spectra of krypton in the extreme ultraviolet. Lists of classified lines are given for Kr I, Kr II and Kr III, and for one multiplet of Kr IV, in the range from λ2000 to λ500. No new lines were found for Kr I, but the accuracy of the measurements is considerably improved. 82 lines of Kr II are given including 31 lines newly identified. 138 lines of Kr III have been identified in collaboration with C. J. Humphreys. The consolidated term table for Kr III is included in the previous paper.

THE extreme ultraviolet spectra of krypton have been investigated by using the two-meter normal incidence vacuum spectrograph[1] of the Carnegie Institution of Washington, which is located in the Spectroscopy Laboratory of the Massachusetts Institute of Technology. The method of reduction of the plates has been discussed with the results on neon[2] and the standards used have been published.[3] For lines whose wavelength is given to three decimal places the probable error ranges from 0.005A to 0.01A, and this estimate is confirmed by the accuracy of the term combinations. When the character of the line did not permit precise measurement, the wavelengths are given to two decimal places and here the error may be as great as 0.02A. The lines newly identified in the present investigation are denoted by an asterisk. The presence of Roman numerals in the intensity column denotes that the line is a blend with a line of the other spectrum. Previous measurements on krypton in this spectral range were made by Taylor[4] and by Abbink and Dorgelo.[5] The gas used in the present investigation was purchased from the Air Reduction Company and was found to be quite free from xenon. Exposures were made of electrodeless discharges at different pressures, both of the pure gas and of mixtures of it with helium, neon and argon. Lines due to different stages of ionization were distinguished by this means.

Kr I. Classified lines are given in Table I. As this type of discharge does not favor the strong excitation of first spectra, these lines are few and faint. The notation used for the upper levels from which these lines arise corresponds to that in the revised term table given by Meggers and Humphreys.[6] The ground state is located at 112,915.7 cm^{-1} when referred to the other terms of that table. This alters by a trivial amount the older result of Meggers, de Bruin and Humphreys[7] which was based on the extreme ultraviolet measurements of Abbink and Dorgelo.[5] The ionization potential, 13.94 volts, already published[7] is unchanged.

TABLE I. *Kr I classified lines.*

λ	INT.	ν	CLASSIFICATION
1235.819	13	80,917.9	$^1S_0-1s^0_4$
1164.868	4	85,846.6	$^1S_0-1s^0_2$
*1030.020	2	97,085.5	$^1S_0-3d^0_3$
1003.542	2	99,647.1	$^1S_0-3d^0_2$
1001.048	2	99,895.3	$^1S_0-2s^0_4$
963.34	1	103,805	$^1S_0-4d^0_3$
953.42	1	104,886	$^1S_0-2s^0_2$
*951.06	0	105,144	$^1S_0-3s'^0_1$
946.52	1*d*	105,650	$^1S_0-4d^0_2$
945.45	1*d*	105,770	$^1S_0-3s^0_4$

Kr II. The classified lines given in Table II make no extension or revision in the term table of de Bruin, Humphreys and Meggers.[8] 31 additional lines have now been identified in the extreme ultraviolet, but these involve terms already known from other combinations in the more accessible portion of the spectrum. The ionization potential is 24.47 volts.[8]

Kr III. The principal group of lines was located by analogy with the $s^2p^4\,{}^3P-sp^5\,{}^3P^0$ groups of Ne III and A III. Other multiplets

[1] K. T. Compton and J. C. Boyce, R.S.I. **5**, 218 (1934).
[2] J. C. Boyce, Phys. Rev. **46**, 378 (1934).
[3] J. C. Boyce and C. A. Rieke, Phys. Rev. **47**, 653 (1935).
[4] L. B. Taylor, Proc. Nat. Acad. Sci. **12**, 658 (1926).
[5] J. H. Abbink and H. B. Dorgelo, Zeits. f. Physik **47**, 221 (1928).
[6] W. F. Meggers and C. J. Humphreys, Bur. Standards J. Research **10**, 427 (1933).
[7] W. F. Meggers, T. L. de Bruin and C. J. Humphreys, Bur. Standards J. Research **3**, 129 (1929).
[8] T. L. de Bruin, C. J. Humphreys and W. F. Meggers, Bur. Standards J. Research **11**, 409 (1933).

TABLE II. *Kr II classified lines.*

λ	Int.	ν	Classification
964.962	30	103,631	$s^2p^4\ ^2P^0_{\frac{3}{2}} - s p^4\ ^2S_{\frac{1}{2}}$
917.434	20	109,000	$s^2p^4\ ^2P^0_{\frac{1}{2}} - s p^4\ ^2S_{\frac{1}{2}}$
911.384	25	109,723	$s^2p^4\ ^2P^0_{\frac{1}{2}} - (^2P)5s^4P_{\frac{1}{2}}$
890.982	20	112,236	$s^2p^4\ ^2P^0_{\frac{3}{2}} - (^2P)5s^4P_{\frac{3}{2}}$
886.302	30	112,828	$s^2p^4\ ^2P^0_{\frac{1}{2}} - (^2P)5s^4P_{\frac{5}{2}}$
884.144	30	113,104	$s^2p^4\ ^2P^0_{\frac{3}{2}} - (^2P)5s^2P_{\frac{1}{2}}$
868.869	25	115,092	$s^2p^4\ ^2P^0_{\frac{1}{2}} - (^2P)5s^4P_{\frac{1}{2}}$
864.812	20	115,632	$s^2p^4\ ^2P^0_{\frac{3}{2}} - \begin{cases}(^2P)4d^4D_{\frac{1}{2}}\\(^2P)5s^2P_{\frac{1}{2}}\end{cases}$
859.040	20	116,409	$s^2p^4\ ^2P^0_{\frac{3}{2}} - (^2P)4d^4D_{\frac{3}{2}}$
850.318	6	117,603	$s^2p^4\ ^2P^0_{\frac{1}{2}} - (^2P)5s^4P_{\frac{1}{2}}$
844.058	25	118,475	$s^2p^4\ ^2P^0_{\frac{1}{2}} - (^2P)5s^2P_{\frac{1}{2}}$
830.377	18	120,427	$s^2p^4\ ^2P^0_{\frac{1}{2}} - (^2P)4d^4D_{\frac{3}{2}}$
826.432	22	121,002	$s^2p^4\ ^2P^0_{\frac{1}{2}} - \begin{cases}(^2P)4d^4D_{\frac{1}{2}}\\(^2P)5s^2P_{\frac{1}{2}}\end{cases}$
821.161	20	121,779	$s^2p^4\ ^2P^0_{\frac{1}{2}} - (^2P)4d^4D_{\frac{1}{2}}$
818.147	25	122,227	$s^2p^4\ ^2P^0_{\frac{3}{2}} - (^2D)5s^2D_{\frac{3}{2}}$
799.083	9	125,143	$s^2p^4\ ^2P^0_{\frac{3}{2}} - (^2P)4d^4F_{\frac{3}{2}}$
*796.678	6	125,521	$s^2p^4\ ^2P^0_{\frac{3}{2}} - (^2P)4d^4P_{\frac{1}{2}}$
783.715	20	127,597	$\begin{cases}s^2p^4\ ^2P^0_{\frac{1}{2}} - (^2D)5s^2D_{\frac{3}{2}}\\s^2p^4\ ^2P^0_{\frac{3}{2}} - (^2P)4d^2D_{\frac{3}{2}}\end{cases}$
782.084	25	127,864	$s^2p^4\ ^2P^0_{\frac{1}{2}} - (^2D)5s^2D_{\frac{5}{2}}$
773.684	18	129,252	$s^2p^4\ ^2P^0_{\frac{3}{2}} - (^2P)4d^2P_{\frac{1}{2}}$
771.024	18	129,698	$s^2p^4\ ^2P^0_{\frac{3}{2}} - (^2P)4d^4F_{\frac{5}{2}}$
766.202	9	130,514	$s^2p^4\ ^2P^0_{\frac{3}{2}} - (^2P)4d^4P_{\frac{3}{2}}$
763.976	11	130,894	$s^2p^4\ ^2P^0_{\frac{1}{2}} - (^2P)4d^4P_{\frac{1}{2}}$
761.050	18	131,376	$s^2p^4\ ^2P^0_{\frac{1}{2}} - (^2P)4d^4P_{\frac{5}{2}}$
752.051	30	132,970	$s^2p^4\ ^2P^0_{\frac{1}{2}} - (^2P)4d^2D_{\frac{3}{2}}$
743.122	9	134,567	$s^2p^4\ ^2P^0_{\frac{3}{2}} - (^2P)4d^2D_{\frac{5}{2}}$
*742.821	9	134,622	$s^2p^4\ ^2P^0_{\frac{1}{2}} - (^2P)4d^2P_{\frac{1}{2}}$
729.402	20	137,099	$s^2p^4\ ^2P^0_{\frac{3}{2}} - (^2P)4d^2F_{\frac{5}{2}}$
722.036	50*III*	138,497	$s^2p^4\ ^2P^0_{\frac{1}{2}} - 59,687$
712.036	8	140,442	$s^2p^4\ ^2P^0_{\frac{3}{2}} - (^1S)5s^2S_{\frac{1}{2}}$
690.557	11	144,811	$s^2p^4\ ^2P^0_{\frac{3}{2}} - (^1D)4d^2D_{\frac{3}{2}}$
685.812	11	145,813	$s^2p^4\ ^2P^0_{\frac{1}{2}} - (^1S)5s^2S_{\frac{1}{2}}$
682.791	16	146,458	$s^2p^4\ ^2P^0_{\frac{3}{2}} - (^1D)4d^2F_{\frac{7}{2}}$
681.119	16	146,817	$s^2p^4\ ^2P^0_{\frac{3}{2}} - (^1D)4d^2P_{\frac{1}{2}}$
668.827	20	149,516	$s^2p^4\ ^2P^0_{\frac{1}{2}} - (^1D)4d^2D_{\frac{3}{2}}$
665.870	9	150,180	$s^2p^4\ ^2P^0_{\frac{1}{2}} - (^1D)4d^2D_{\frac{5}{2}}$
663.039	20*III*	150,821	$s^2p^4\ ^2P^0_{\frac{3}{2}} - (^1D)4d^2F_{\frac{5}{2}}$
*658.637	5	151,829	$s^2p^4\ ^2P^0_{\frac{1}{2}} - (^1D)4d^2P_{\frac{1}{2}}$
657.088	13	152,187	$s^2p^4\ ^2P^0_{\frac{3}{2}} - (^1D)4d^2P_{\frac{3}{2}}$
*655.677	5	152,514	$s^2p^4\ ^2P^0_{\frac{3}{2}} - (^2P)6s^4P_{\frac{1}{2}}$
643.404	9	155,423	$s^2p^4\ ^2P^0_{\frac{3}{2}} - (^2P)5d^4P_{\frac{1}{2}}$
640.870	5	156,038	$s^2p^4\ ^2P^0_{\frac{3}{2}} - (^2P)5d^4P_{\frac{3}{2}}$
639.263	5	156,430	$s^2p^4\ ^2P^0_{\frac{3}{2}} - (^2P)5d^4D_{\frac{1}{2}}$
638.952	5	156,506	$s^2p^4\ ^2P^0_{\frac{3}{2}} - (^2P)6s^4P_{\frac{1}{2}}$
*638.214	4	156,687	$s^2p^4\ ^2P^0_{\frac{3}{2}} - (^2P)6s^2P_{\frac{1}{2}}$
*636.154	3	157,195	$s^2p^4\ ^2P^0_{\frac{3}{2}} - (^2P)6s^2P_{\frac{3}{2}}$
634.265	4	157,663	$s^2p^4\ ^2P^0_{\frac{3}{2}} - (^2P)5d^4D_{\frac{3}{2}}$
633.373	5	157,884	$s^2p^4\ ^2P^0_{\frac{1}{2}} - (^2P)6s^4P_{\frac{1}{2}}$
621.910	5	160,795	$s^2p^4\ ^2P^0_{\frac{1}{2}} - (^2P)5d^4P_{\frac{1}{2}}$
621.071	5	161,012	$s^2p^4\ ^2P^0_{\frac{1}{2}} - (^2P)5d^4P_{\frac{3}{2}}$
*619.548	2	161,408	$s^2p^4\ ^2P^0_{\frac{1}{2}} - (^2P)5d^4P_{\frac{5}{2}}$
*619.379	2	161,452	$s^2p^4\ ^2P^0_{\frac{1}{2}} - (^2P)5d^4D_{\frac{5}{2}}$
*618.879	3	161,582	$s^2p^4\ ^2P^0_{\frac{3}{2}} - (^2P)5d^2F_{\frac{5}{2}}$
*618.515	2	161,678	$s^2p^4\ ^2P^0_{\frac{3}{2}} - (^2P)5d^4F_{\frac{7}{2}}$
*618.042	4	161,801	$s^2p^4\ ^2P^0_{\frac{1}{2}} - (^2P)5d^4D_{\frac{1}{2}}$
*617.750	4	161,878	$s^2p^4\ ^2P^0_{\frac{3}{2}} - (^2P)6s^4P_{\frac{3}{2}}$
*617.068	6	162,059	$s^2p^4\ ^2P^0_{\frac{1}{2}} - (^2P)6s^2P_{\frac{1}{2}}$
*615.225	4	162,542	$s^2p^4\ ^2P^0_{\frac{3}{2}} - (^2P)5d^2D_{\frac{3}{2}}$
*615.134	4*III*	162,566	$s^2p^4\ ^2P^0_{\frac{1}{2}} - (^2P)6s^2P_{\frac{3}{2}}$
*613.366	4	163,035	$s^2p^4\ ^2P^0_{\frac{1}{2}} - (^2P)5d^4D_{\frac{3}{2}}$
608.124	5	164,440	$s^2p^4\ ^2P^0_{\frac{1}{2}} - (^1S)6s^2S_{\frac{1}{2}}$
605.776	5	165,078	$s^2p^4\ ^2P^0_{\frac{1}{2}} - (^2P)5d^4F_{\frac{9}{2}}$
*605.536	5	165,143	$s^2p^4\ ^2P^0_{\frac{1}{2}} - (^2P)5d^2P_{\frac{1}{2}}$
*605.316	5	165,203	$s^2p^4\ ^2P^0_{\frac{3}{2}} - (^1D)6s^2D_{\frac{3}{2}}$
599.944	4	166,682	$s^2p^4\ ^2P^0_{\frac{3}{2}} - (^1S)4d^2D_{\frac{3}{2}}$
*598.968	3	166,954	$s^2p^4\ ^2P^0_{\frac{1}{2}} - (^2P)5d^2P_{\frac{1}{2}}$
*598.791	3	167,003	$s^2p^4\ ^2P^0_{\frac{1}{2}} - 31,181$
*598.66	0	167,051	$s^2p^4\ ^2P^0_{\frac{1}{2}} - (^2P)5d^4F_{\frac{1}{2}}$
*596.944	4	167,520	$s^2p^4\ ^2P^0_{\frac{1}{2}} - (^2P)5d^2F_{\frac{5}{2}}$
595.530	7*III*	167,918	$s^2p^4\ ^2P^0_{\frac{1}{2}} - (^2P)5d^2D_{\frac{1}{2}}$
589.262	5	169,704	$s^2p^4\ ^2P^0_{\frac{1}{2}} - (^2P)5d^2D_{\frac{3}{2}}$
*586.269	1	170,570	$s^2p^4\ ^2P^0_{\frac{1}{2}} - (^1D)6s^2D_{\frac{3}{2}}, \frac{1}{2}$
*585.684	2	170,740	$s^2p^4\ ^2P^0_{\frac{3}{2}} - (^1D)5d^2D_{\frac{1}{2}}$
581.496	3	171,970	$s^2p^4\ ^2P^0_{\frac{1}{2}} - (^1S)4d^2D_{\frac{3}{2}}$
*581.22	1	172,053	$s^2p^4\ ^2P^0_{\frac{3}{2}} - (^1S)4d^2D_{\frac{5}{2}}$
*580.342	3	172,312	$s^2p^4\ ^2P^0_{\frac{3}{2}} - (^1D)5d^2P_{\frac{1}{2}}$
*579.11	0	172,680	$s^2p^4\ ^2P^0_{\frac{3}{2}} - (^2P)7s^4P_{\frac{1}{2}}$
*577.01	0	173,308	$s^2p^4\ ^2P^0_{\frac{1}{2}} - (^2P)7s^2P_{\frac{1}{2}}$
*576.647	4	173,416	$s^2p^4\ ^2P^0_{\frac{3}{2}} - (^1D)5d^2P_{\frac{3}{2}}$
575.902	2	173,641	$s^2p^4\ ^2P^0_{\frac{1}{2}} - (^2P)7s^2P_{\frac{1}{2}}$
*560.788	3	178,320	$s^2p^4\ ^2P^0_{\frac{1}{2}} - (^1D)5d^2D_{\frac{5}{2}}$
*559.320	4	178,788	$s^2p^4\ ^2P^0_{\frac{1}{2}} - (^1D)5d^2P_{\frac{1}{2}}$

TABLE III. *Kr III classified lines.*

λ	Int.	ν	Classification
*1923.88	0	51,978.2	$s p^4\ ^1P^0_1 - (^1D)5p^4F_2$
*1914.086	3	52,244.2	$s p^4\ ^1P^0_1 - (^1D)5p^1P_1$
*1721.637	1	58,084.3	$s p^4\ ^3P^0_0 - (^4S)5p^3P_1$
*1659.809	2	60,247.9	$s p^4\ ^3P^0_1 - (^4S)5p^3P_1$
*1647.359	2*d*	60,703.2	$s p^4\ ^3P^0_1 - (^4S)5p^3P_2$
*1638.816	3	61,019.7	$s p^4\ ^1P^0_1 - (^2D)5p^1D_2$
*1569.886	2	63,698.9	$s p^4\ ^3P^0_2 - (^4S)5p^3P_1$
*1558.802	2	64,151.8	$s p^4\ ^3P^0_2 - (^4S)5p^3P_2$
*1483.429	2	67,411.8	$s p^4\ ^1P^0_1 - (^2P)5p^1P_1$
*1423.553	1	70,246.8	$s p^4\ ^1P^0_1 - (^2P)5p^1D_2$
*1400.90	1	71,382.5	$s p^4\ ^3P^0_1 - (^2D)5p^3D_1$
*1377.833	2	72,577.8	$s p^4\ ^3P^0_0 - (^2D)5p^1P_1$
*1363.853	2	73,321.7	$s p^4\ ^3P^0_1 - (^2D)5p^3D_2$
*1342.678	1	74,478.0	$s p^4\ ^3P^0_1 - (^2D)5p^3F_2$
*1302.586	2	76,770.4	$s p^4\ ^3P^0_2 - (^2D)5p^3D_2$
*1293.988	3	77,280.4	$s p^4\ ^3P^0_1 - (^2D)5p^3P_1$
*1283.798	3	77,893.9	$s p^4\ ^3P^0_2 - (^2D)5p^3D_3$
*1283.313	3	77,923.3	$s p^4\ ^3P^0_2 - (^2D)5p^3F_2$
*1278.943	1	78,189.6	$s p^4\ ^3P^0_2 - (^2D)5p^1P_1$
*1270.204	5	78,727.5	$s p^4\ ^3P^0_1 - (^2D)5p^3P_2$
*1265.315	4	79,031.7	$s p^4\ ^3P^0_2 - (^2D)5p^3F_3$
*1259.309	3	79,408.9	$s p^4\ ^3P^0_1 - (^2D)5p^3P_0$
*1258.745	3	79,442.2	$s p^4\ ^3P^0_1 - (^2D)5p^3P_1$
*1216.896	5	82,176.6	$s p^4\ ^3P^0_2 - (^2D)5p^3P_2$
*1206.346	5	82,894.9	$s p^4\ ^3P^0_2 - (^2D)5p^3P_1$
*1158.724	6	86,301.8	$s^2p^4\ ^1S_0 - s p^4\ ^3P^0_1$
*987.281	18	101,288	$s^2p^4\ ^1D_2 - s p^4\ ^3P^0_2$
*954.774	4	104,737	$s^2p^4\ ^1D_2 - s p^4\ ^3P^0_1$
*919.143	2	108,797	$s^2p^4\ ^1S_0 - s p^4\ ^1P^0_1$
*897.801	40	111,383	$s^2p^4\ ^3P_1 - s p^4\ ^3P^0_2$
*876.674	22	114,068	$s^2p^4\ ^3P_0 - s p^4\ ^3P^0_1$
*870.825	20	114,834	$s^2p^4\ ^3P_1 - s p^4\ ^3P^0_1$
*862.578	35	115,932	$s^2p^4\ ^3P_2 - s p^4\ ^3P^0_2$
*854.733	25	116,996	$s^2p^4\ ^3P_1 - s p^4\ ^3P^0_0$
*837.666	22	119,379	$s^2p^4\ ^3P_2 - s p^4\ ^3P^0_1$
*785.968	25	127,232	$s^2p^4\ ^1D_2 - s p^4\ ^1P^0_1$
*768.104	1	130,191	$s^2p^4\ ^1S_0 - (^2D)5s^3D^0_1$
*750.986	4	133,158	$s^2p^4\ ^3P_0 - (^4S)4d^5D^0_1$
*646.417	20	154,699	$s^2p^4\ ^3P_2 - (^2D)4d^3F^0_3$
*644.521	1	155,154	$s^2p^4\ ^1S_0 - (^2P)4d^1P^0_1$
*642.84	1	155,559	$s^2p^4\ ^1D_2 - (^2D)4d^3D^0_1$
*639.981	15	156,255	$s^2p^4\ ^1D_2 - (^2D)5s^1D^0_2$
*636.348	1	157,147	$s^2p^4\ ^1S_0 - (^2P)4d^3P^0_1$
*633.631	5	157,820	$s^2p^4\ ^1D_2 - (^2D)4d^3D^0_2$
*633.082	7	157,957	$s^2p^4\ ^3P_0 - (^2D)5s^3D^0_1$
*631.550	7	158,341	$s^2p^4\ ^1D_2 - (^2D)4d^3S^0_1$
*630.037	15	158,721	$s^2p^4\ ^3P_1 - (^2D)5s^3D^0_1$
*628.581	15	159,088	$s^2p^4\ ^3P_1 - (^2D)5s^3D^0_2$
*625.758	13	159,806	$s^2p^4\ ^1D_2 - (^2D)4d^3D^0_2$
*625.011	9	159,997	$s^2p^4\ ^3P_2 - (^2D)4d^3G^0_4$
*624.268	3	160,188	$s^2p^4\ ^1D_2 - (^2P)4d^3F^0_3$
*622.795	11	160,566	$s^2p^4\ ^1D_2 - (^2P)4d^3F^0_2$
*621.448	8	160,914	$s^2p^4\ ^3P_1 - (^2D)4d^3D^0_2$
*616.728	5	162,146	$s^2p^4\ ^1D_2 - (^2P)4d^3D^0_1$
*612.485	6	163,269	$s^2p^4\ ^3P_0 - (^2D)5s^3D^0_1$
*611.187	8	163,616	$s^2p^4\ ^1D_2 - (^2P)5s^3P^0_1$
*611.100	9	163,639	$s^2p^4\ ^3P_2 - (^2D)5s^3D^0_2$
*606.460	9	164,891	$s^2p^4\ ^3P_0 - (^2D)4d^3D^0_1$
*605.862	9	165,054	$s^2p^4\ ^3P_1 - (^2D)5s^3D^0_2$
*604.355	4	165,466	$s^2p^4\ ^3P_2 - (^2D)4d^3D^0_2$
*603.849	6	165,604	$s^2p^4\ ^1D_2 - (^1P)5s^3P^0_1$
*603.666	7	165,655	$s^2p^4\ ^3P_1 - (^2D)4d^3D^0_1$
*601.134	7	166,352	$s^2p^4\ ^3P_1 - (^2D)5s^1D^0_2$
*600.167	5	166,620	$s^2p^4\ ^1D_2 - (^1P)5s^1P^0_1$
*599.944	4*II*	166,682	$s^2p^4\ ^3P_0 - (^2D)4d^3P^0_1$
*597.194	6	167,450	$s^2p^4\ ^3P_1 - (^2D)4d^3P^0_1$
*596.576	6	167,623	$s^2p^4\ ^1D_2 - (^2P)4d^3D^0_1$
*596.401	6	167,672	$s^2p^4\ ^3P_0 - (^2D)4d^3S^0_1$
*595.530	7	167,918	$s^2p^4\ ^3P_1 - (^2D)4d^3D^0_2$
*594.090	9	168,325	$s^2p^4\ ^1D_2 - (^2P)4d^1F^0_3$
*593.699	7	168,436	$s^2p^4\ ^3P_1 - (^2D)4d^3S^0_1$
*587.543	4	170,200	$s^2p^4\ ^3P_2 - (^2D)4d^3D^0_3$
*587.374	4	170,249	$s^2p^4\ ^1D_2 - (^2P)4d^3D^0_2$
*585.950	8	170,663	$s^2p^4\ ^3P_1 - (^2P)4d^3F^0_2$
*585.140	8	170,899	$s^2p^4\ ^3P_2 - (^2D)5s^1D^0_2$
*580.577	6	172,242	$s^2p^4\ ^3P_1 - (^2P)4d^3D^0_2$

TABLE III. (*Continued*)

λ	INT.	ν	CLASSIFICATION
*746.834	5	133,899	$s^2p^4\,{}^3P_1 - ({}^4S)4d\,{}^5D^o_0$
*746.695	7	133,924	$s^2p^4\,{}^3P_1 - ({}^4S)4d\,{}^5D^o_{2,\,1}$
*745.763	3	134,091	$s^2p^4\,{}^1D_2 - ({}^4S)4d\,{}^3D^o_2$
*743.870	3	134,432	$s^2p^4\,{}^1D_2 - ({}^4S)4d\,{}^3D^o_1$
*732.259	4	136,564	$s^2p^4\,{}^3P_0 - \quad s\,p^5\,{}^1P^o_1$
*730.264	3	136,937	$s^2p^4\,{}^1D_2 - ({}^4S)5s\,{}^3S^o_1$
*722.036	50II	138,497	$s^2p^4\,{}^3P_2 - ({}^4S)4d\,{}^5D^o_{2,\,3,\,1}$
*719.85	1	138,918	$s^2p^4\,{}^1D_2 - ({}^2D)4d\,{}^3F^o_3$
*714.772	2	139,905	$s^2p^4\,{}^1S_0 - ({}^2D)4d\,{}^3S^o_1$
*713.999	7	140,056	$s^2p^4\,{}^1D_2 - ({}^2D)4d\,{}^3F^o_2$
*708.356	8	141,172	$s^2p^4\,{}^3P_1 - ({}^4S)5s\,{}^5S^o_2$
*704.838	4	141,877	$s^2p^4\,{}^3P_2 - \quad s\,p^5\,{}^1P^o_1$
*698.037	20	143,259	$s^2p^4\,{}^3P_1 - ({}^4S)4d\,{}^3D^o_2$
*695.604	15	143,760	$s^2p^4\,{}^3P_0 - ({}^4S)4d\,{}^3D^o_1$
*691.919	18	144,526	$s^2p^4\,{}^3P_1 - ({}^4S)4d\,{}^3D^o_1$
*687.979	11	145,353	$s^2p^4\,{}^1D_2 - ({}^2D)4d\,{}^3G^o_3$
*686.254	20	145,719	$s^2p^4\,{}^3P_2 - ({}^4S)5s\,{}^5S^o_2$
*683.666	18	146,270	$s^2p^4\,{}^3P_0 - ({}^4S)5s\,{}^5S^o_1$
*680.119	22	147,033	$s^2p^4\,{}^3P_1 - ({}^4S)5s\,{}^3S^o_1$
*676.564	25	147,806	$s^2p^4\,{}^3P_2 - ({}^4S)4d\,{}^3D^o_2$
*674.828	8	148,186	$s^2p^4\,{}^1S_0 - ({}^2P)5s\,{}^1P^o_1$
*672.826	7	148,627	$s^2p^4\,{}^1D_2 - ({}^2D)5s\,{}^3D^o_1$
*672.330	25	148,736	$s^2p^4\,{}^3P_2 - ({}^4S)4d\,{}^3D^o_2$
*671.175	7	148,992	$s^2p^4\,{}^1D_2 - ({}^2D)5s\,{}^3D^o_2$
*671.058	7	149,018	$s^2p^4\,{}^3P_1 - ({}^2D)4d\,{}^3F^o_2$
*670.813	3	149,073	$s^2p^4\,{}^3P_2 - ({}^4S)4d\,{}^3D^o_1$
*670.300	4	149,187	$s^2p^4\,{}^1S_0 - ({}^2P)4d\,{}^3D^o_1$
*664.844	11	150,411	$s^2p^4\,{}^1D_2 - ({}^2D)5s\,{}^3D^o_2$
*663.039	20	150,821	$s^2p^4\,{}^1D_2 - ({}^2D)4d\,{}^3D^o_2$
*659.716	22	151,580	$s^2p^4\,{}^3P_2 - ({}^4S)5s\,{}^5S^o_1$
*651.198	8	153,563	$s^2p^4\,{}^3P_2 - ({}^2D)4d\,{}^3F^o_2$
*579.823	6	172,466	$s^2p^4\,{}^3P_2 - ({}^2D)4d\,{}^3D^o_2$
*578.220	5	172,945	$s^2p^4\,{}^3P_0 - ({}^2P)5s\,{}^3P^o_1$
*578.09	0	172,983	$s^2p^4\,{}^3P_2 - ({}^2D)4d\,{}^3S^o_1$
*576.076	4	173,588	$s^2p^4\,{}^1D_2 - ({}^2P)4d\,{}^1P^o_1$
*575.716	5	173,697	$s^2p^4\,{}^3P_1 - ({}^2P)5s\,{}^3P^o_{1,\,0}$
*574.956	5	173,926	$s^2p^4\,{}^1D_2 - ({}^2P)4d\,{}^1D^o_2$
*573.228	13	174,451	$s^2p^4\,{}^3P_2 - ({}^2D)4d\,{}^3D^o_2$
*571.983	15	174,830	$s^2p^4\,{}^3P_2 - ({}^2P)4d\,{}^3F^o_3$
*570.738	4	175,212	$s^2p^4\,{}^3P_2 - ({}^2P)4d\,{}^3F^o_2$
*569.156	7	175,699	$s^2p^4\,{}^3P_1 - ({}^2P)5s\,{}^3P^o_2$
*565.879	4	176,716	$s^2p^4\,{}^3P_1 - ({}^2P)5s\,{}^1P^o_1$
*565.640	5	176,791	$s^2p^4\,{}^3P_2 - ({}^2P)4d\,{}^3D^o_2$
*565.124	4	176,952	$s^2p^4\,{}^3P_0 - ({}^2P)4d\,{}^3D^o_1$
*562.690	5	177,718	$s^2p^4\,{}^3P_1 - ({}^2P)4d\,{}^3D^o_1$
*560.986	5	178,258	$s^2p^4\,{}^3P_2 - ({}^2P)5s\,{}^3P^o_1$
*558.634	15	179,008	$s^2p^4\,{}^1D_2 - ({}^2P)4d\,{}^3P^o_2$
*554.794	7	180,247	$s^2p^4\,{}^3P_0 - ({}^2P)5s\,{}^3P^o_1$
*551.689	4	181,262	$s^2p^4\,{}^3P_2 - ({}^2P)5s\,{}^1P^o_1$
*548.652	5	182,265	$s^2p^4\,{}^3P_2 - ({}^2P)4d\,{}^3P^o_1$
*546.686	5	182,920	$s^2p^4\,{}^3P_0 - ({}^2P)4d\,{}^1P^o_1$
*546.547	6	182,967	$s^2p^4\,{}^3P_2 - ({}^2P)4d\,{}^1F^o_3$
*544.413	5	183,684	$s^2p^4\,{}^3P_1 - ({}^2P)4d\,{}^1P^o_1$
*543.420	8	184,020	$s^2p^4\,{}^3P_1 - ({}^2P)4d\,{}^1D^o_2$
*540.860	4	184,891	$s^2p^4\,{}^3P_2 - ({}^2P)4d\,{}^3D^o_2$
*540.788	5	184,915	$s^2p^4\,{}^3P_0 - ({}^2P)4d\,{}^3P^o_1$
*538.544	8	185,686	$s^2p^4\,{}^3P_1 - ({}^2P)4d\,{}^3P^o_1$
*531.255	4	188,234	$s^2p^4\,{}^3P_2 - ({}^2P)4d\,{}^1P^o_1$
*530.306	6	188,570	$s^2p^4\,{}^3P_2 - ({}^2P)4d\,{}^1D^o_2$
*528.811	4	189,103	$s^2p^4\,{}^3P_1 - ({}^2P)4d\,{}^3P^o_2$
*525.687	4	190,227	$s^2p^4\,{}^3P_1 - ({}^2P)4d\,{}^3P^o_1$
*516.384	4	193,654	$s^2p^4\,{}^3P_2 - ({}^2P)4d\,{}^3P^o_2$

having differences characteristic of the ground state were then found to give connections with the analysis of visible and near ultraviolet data already undertaken by C. J. Humphreys. The complete identification of the 138 lines classified in Table III was made possible by the very generous cooperation of Dr. Humphreys. All of the low states of Kr III have been located and many intersystem combinations have been found. The consolidated term table for Kr III is given by Humphreys in the previous paper.[9] The ionization potential is 36.8 volts.

Kr IV. A provisional identification has been made in Table IV of the principal multiplet in Kr IV. The investigation of this spectrum is being continued.

[9] C. J. Humphreys, Phys. Rev. **47**, 712 (1935).

TABLE IV. *Kr IV classified lines.*

λ	INT.	ν	CLASSIFICATION
*842.035	22	118,760	$s^2p^3\,{}^4S^o_{1\frac{1}{2}} - s\,p^4\,{}^4P_{2\frac{1}{2}}$
*816.822	18	122,426	$s^2p^3\,{}^4S^o_{1\frac{1}{2}} - s\,p^4\,{}^4P_{1\frac{1}{2}}$
*805.763	7	124,108	$s^2p^3\,{}^4S^o_{1\frac{1}{2}} - s\,p^4\,{}^4P_{\frac{1}{2}}$

The experimental part of this work was made possible by a grant to Dr. K. T. Compton from the Carnegie Institution of Washington. Some of the technical assistance necessary in plate measurement and reduction has been provided by a grant to the writer from the Permanent Science Fund of the American Academy of Arts and Sciences. The careful work of Dr. Carol A. Rieke and Mr. D. H. Clewell in measurement and computation is gratefully acknowledged.

The Emission Spectrum of Diatomic Arsenic

G. M. ALMY AND G. D. KINZER, *Physics Department, University of Illinois*

(Received March 14, 1935)

The emission spectrum of As_2 consists principally of an extensive group of bands in the ultraviolet, which have been analyzed into two overlapping band systems. These two systems have the same lower state. Their upper states lie at about the same electronic energy, have similar vibrational intervals and perturb one another strongly. In one system, called $A \rightarrow X$, predissociation sets in at two points in the upper state, namely, at $v'=9$ and $v'=14$. In the regions where predissociation is occurring absorption bands appear (for low v'') on the emission plates. The heat of dissociation obtained depends upon what assumption is made as to the pair of atomic states standing at the predissociation energy. If this pair is $^4S+^2D$, $D(X)$ is about 4.0 volts in agreement with the value obtained by extrapolation of the vibrational levels, but if this pair is $^2D+^2D$, as appears to be required by the Kronig rules for perturbations and predissociations, $D(X)$ is 2.6 volts.

INTRODUCTION

THE diatomic molecules of nitrogen, phosphorus, arsenic, antimony and bismuth, form an homologous group, each consisting of two atoms whose lowest state is . . . $p^3\,{}^4S$. A comparative study of the spectra of these molecules should provide information as to the variation with mass and type of atomic coupling of the process of molecule formation. The spectrum of each of these molecules has been observed. In the case of N_2,[1, 2] and P_2,[3] the vibrational and rotational structure has been analyzed. A fairly complete vibrational analysis of the absorption spectrum of Bi_2 has been made,[4] and Naudé[5] has published a preliminary report of Sb_2 absorption spectrum. The absorption spectrum of As_2 is the subject of a recent paper by Gibson and MacFarlane.[6] The present paper is an account of the emission spectrum of the same molecule. The emission spectrum contains the system observed in absorption though much more extensively developed and other systems in addition. It yields, therefore, more information about the molecular states than the absorption spectrum.

Gibson and MacFarlane give a good summary of the previous work on the arsenic molecular spectrum as observed in absorption, emission and fluorescence. The only attempt to study the emission spectrum is that of Winand,[7] who used an electrodeless discharge in a tube containing metallic arsenic. The spectrum he obtains is entirely unlike that which we are describing in this paper. In fact, examination of his data makes it practically certain that the bands he reports are largely, if not entirely, due to CO. We have produced Winand's bands by simply heating slightly metallic arsenic in a bulb connected to a discharge tube by several inches of cold glass tubing. A considerable but limited amount of gas is driven from the arsenic and a discharge in this gas discloses the CO bands, attributed by Winand to arsenic. As discussed below we found it necessary to free the arsenic used in obtaining the As_2 bands from impurities by a preliminary heating.

In the present paper only the vibrational analysis of the As_2 bands and conclusions that can be drawn therefrom will be discussed. On the low dispersion plates so far obtained, the rotational structure is in some places partly resolved; we are hoping to secure plates with larger dispersion in order to perform the rotational analysis, which may establish or disprove some of the conclusions tentatively drawn in the following sections

EXPERIMENTAL METHOD

The spectrum was obtained by photographing an electrical discharge in a mixture of arsenic

[1] See Jevons' *Report on Band-Spectra of Diatomic Molecules*, or Weizel, *Bandenspektren*, for work up to 1931.
[2] G. Herzberg and H. Sponer, Zeits. f. physik. Chemie **B26**, 1 (1934).
[3] G. Herzberg, Ann. d. Physik **15**, 677 (1932).
[4] G. M. Almy and F. M. Sparks, Phys. Rev. **44**, 365 (1933).
[5] S. M. Naudé, Phys. Rev. **45**, 280 (1934).
[6] G. E. Gibson and A. MacFarlane, Phys. Rev. **46**, 1059 (1934).
[7] Winand, Bulletin de la classe des sciences, Academie Royale de Belgique (5), **18**, 422 (1932). Results of this work also described in reference 6.

TABLE I. *Observed bands in order of wave number.* Assignment to system *A*, *B*, or *C* and to vibrational quantum numbers. Comparison with calculated wave numbers. Intensities; *s* = sharp, *d* = diffuse, *dd* = very diffuse, *at* = head obscured by atomic line. Bands marked *Abs.* in column 2 were obtained as absorption bands on emission spectrum plates.

System and v', v''	Int.	Wave Number (obs.)	(obs.−calc.)
A 17,0	*Abs.*	44597.2	0.0
A 16,0	*Abs.*	44352.0	0.0
A 15,0	*Abs.At*	44102.9	−1.8
A 14,0	2*s*	43854.4	−2.5
A 13,0	*Abs.*	43603.9	−0.1
A 14,1	2*s*	43428.4	−0.6
A 12,0	*Abs.*	43350.2	−0.1
A 13,1	*Abs.*	43176.5	−0.3
A 11,0	*Abs.*	43095.3	+0.4
A 14,2	1*s*	43003.6	−0.2
A 12,1	*Abs.*	42926.0	+2.7
A 10,0	*Abs.*	42836.9	−0.3
A 11,1	*Abs.*	42670.0	+2.3
A 9,0		42581.5	{+2.8
14,3	2*s*		+0.4
A 10,1	*Abs.*	42412.6	+2.6
B 6,0	0*s*	42392.5	−1.3
A 8,0	1*s*	42321.8	−1.0
	1*d*	42223.0	
A 9,1	2*s*	42151.0	−0.5
A 7,0	1*s*	42080.6	−1.0
B 6,1	1*s*	41965.0	−1.6
B 4,0	0*d*	41918.0	+0.1
A 8,1	3*s*	41895.0	−0.6
A 6,0	1*d*	41833.0	−2.8
A 14,5	2*s*	41743.6	+1.3
B 5,1	1*d*	41734.6	−0.2
A 9,2	3*s*	41726.1	−2.2
	0*s*	41671.3	
A 7,1	3*s*	41653.8	−0.6
B 6,2	2*d*	41543.0	+1.6
B 4,1	0*s*	41487.8	−2.9
A 8,2	4*s*	41470.6	+0.2
A 6,1	3*s*	41407.1	−1.5
B 5,2	4*s*	41308.1	−1.5
A 7,2	5*s*	41227.1	−2.1
A 5,1	1*dd*	41147.5	+0.2
B 6,3	1*dd*	41118.8	+0.1
B 4,2	1*s*	41063.6	−0.9
A 8,3	3*s*	41046.3	−1.4
A 6,2	5*s*	40981.6	−1.8
A 9,4	3*d*	40884.3	{+1.2
B 5,3			−2.6
A 7,3	6*s*	40804.9	−1.6
A 5,2	4*d*	40721.1	−1.0
A 6,3	5*s*	40559.9	−0.8
A 9,5	2*d*	40465.3	{+0.5
B 5,4			−0.9
A 4,2	0*dd*	40445.5	+3.0
A 7,4	2*dd*	40384.5	−1.5
B 3,3	2*dd*	40371.9	−1.1
A 5,3	5*s*	40298.6	−0.8
B 6,5	3*s*	40280.9	+1.0
B 4,4	0*d*	40223.1	+0.8
A 8,5	1*d*	40207.6	−1.3
	1*d*	40177.8	
A 6,4	4*d*	40139.4	−0.8
A 9,6	1*dd*	40048.0	{−0.8
B 5,5			−0.1
A 4,3	2*d*	40017.5	−2.0
B 3,4	1*dd*	39950.0	−2.5
A 5,4	6*s*	39877.8	−1.1
B 6,6	2*s*	39863.6	−0.3
A 8,6	3*d*	39791.7	−1.2
	1*d*	39758.4	
	2*s*	39684.7	
B 2,4	2*s*	39667.9	−0.7
A 9,7	2*d*	39633.8	{−1.2
B 5,6			+1.7
A 4,4	3*s*	39598.6	−0.4
A 7,6	3*s*	39551.6	−0.1
A 5,5	4*s*	39459.7	−0.9
A 8,7	2*d*	39378.9	{−0.2
B 1,4			−1.8
	1*s*	39342.3	
A 6,6	1*dd*	39305.7	−0.2
B 2,5	1*d*	39252.4	+2.1
A 9,8	1*dd*	39224.6	+1.2
A 4,5	5*s*	39179.2	−1.5
A 7,7	5*s*	39137.4	{−0.5
B 0,4			−0.0
B 6,8	3*s*	39037.7	−0.8
B 4,7	2*s*	38973.9	−0.3
B 1,5	3*s*	38961.5	−0.9
A 6,7	5*d*	38891.8	−0.3
A 3,5	5*s*	38876.3	−1.3
A 4,6	4*s*	38764.4	−0.3
B 0,5	3*d*	38718.5	−0.6
A 5,7	4*s*	38628.7	{−2.1
B 6,9			−0.5
	4*d*	38618.6	
A 8,9	4*s*	38557.6	−0.6
B 1,6	3*s*	38545.5	−0.9
	0*s*	38513.6	
A 3,6	2*s*	38460.4	−1.3
B 5,9	1*d*	38398.9	+1.5
A 7,9	0*d*	38318.9	+1.9
B 0,6	2*d*	38303.0	−0.1
B 3,8	2*dd*	38294.1	+1.3
A 2,6	0*s*	38243.1	−3.0
B 6,10	4*s*	38219.7	−2.4
B 4,9	0*s*	38152.0	{−1.3
A 8,10			+0.9
B 1,7	0*d*	38133.5	+0.9
A 6,9	1*d*	38071.1	−0.1
A 3,7	2*s*	38047.2	−0.7
B 2,8	0*d*	38008.3	−0.6
A 9,11	2*d*	38001.5	−0.7
A 1,6	3*s*	37990.1	{+3.3
B 5,10			−0.2
A 7,10	4*s*	37909.9	−0.0
B 0,7	5*s*	37888.4	−0.9
A 2,7	0*s*	37834.3	+2.0
A 5,9	4*s*	37810.0	+0.1
A 0,6	3*s*	37728.8	−2.2
A 6,10	2*s*	37663.7	−0.4
A 3,8	2*s*	37635.8	−0.8
B 2,9	4*s*	37598.3	{−1.3
A 9,12			−1.3
B 5,11	4*d*	37584.7	−0.8
A 4,9	2*s*	37529.9	−0.1
A 7,11	2*s*	37504.5	−0.6
B 0,8	3*s*	37477.7	{−0.0
B 3,10			+1.3
B 6,12	1*dd*	37413.4	−1.3
A 5,10	0*d*	37402.2	−0.6
B 4,11	3*s*	37343.6	+2.2
A 0,7	2*s*	37316.1	−1.1
	2*s*	37288.3	
A 6,11	4*s*	37259.2	−0.1
B 2,10	2*s*	37192.1	−0.4
A 1,8	3*s*	37169.2	+1.2
A 4,10	3*s*	37124.5	+1.6
B 0,9	2*s*	37067.8	−0.6
A 2,9	1*d*	37011.5	{+0.1
B 6,13			−2.8
B 4,12	2*s*	36942.6	+3.8
A 0,8	4*s*	36905.2	{−0.4
B 1,10			+0.6
A 6,12	4*s*	36857.6	+0.9
B 2,11	0*d*	36785.6	{−2.1
B 5,13			+3.1
A 1,9	2*s*	36760.2	+1.5
A 4,11	0*s*	36719.2	+1.1
A 7,13	3*s*	36701.6	−0.5
B 3,12	0*dd*	36669.1	+0.1
B 0,10	1*d*	36662.1	+0.8
B 6,14	1*d*	36617.6	+1.4
A 5,12	3*s*	36595.1	−0.3
A 0,9	5*s*	36500.1	{+3.8
B 1,11			−0.3
B 2,12	1*s*	36386.0	{+0.9
B 5,14			+1.6
A 1,10	3*s*	36354.0	+2.4
A 7,14	4*s*	36304.3	+0.3
B 3,13	2*s*	36268.6	0.0
A 2,11	1*d*	36198.3	−1.2
A 5,13	3*d*	36193.7	−1.3
A 8,15	1*d*	36151.3	+1.9
	1*s*	36122.5	
B 1,12	3*s*	36096.6	−0.6
A 6,14	0*dd*	36061.9	+3.7
A 3,12	0*d*	36012.0	−0.5
B 5,15	0*d*	35988.2	−0.4
A 7,15	1*d*	35909.4	+1.2
B 3,14	1*s*	35870.9	+0.4
B 6,16	1*s*	35825.9	−0.9
	1*s*	35804.7	
A 2,12	2*d*	35795.9	{−1.0
A 5,14			−1.0
A 8,16	3*d*	35755.4	−0.4
	1*s*	35719.2	
B 1,13	3*s*	35696.5	−0.3
A 6,15	4*s*	35662.1	−0.3
B 2,14	2*s*	35586.9	+0.3
A 1,12	1*s*	35545.7	+1.5
A 7,16	2*d*	35517.5	+2.9
A 4,14			+0.5
	1*d*	35453.4	
A 5,15	1*s*	35402.1	+1.0
A 2,13	3*d*	35397.4	+0.9
A 8,17	2*s*	35365.0	+0.5
B 4,16	2*s*	35353.6	+2.7
B 1,14	1*s*	35299.8	+1.1
A 6,16	2*s*	35269.0	+0.2
A 9,18	2*s*	35230.7	−0.6
B 2,15	3*s*	35190.4	−0.4
	1*d*	35170.5	
A 1,13	1*d*	35146.4	+2.6
A 4,15	5*s*	35122.0	{+0.8
A 7,17			−1.3
B 6,18	0*d*	35048.8	+2.4
A 5,16	0*d*	35004.4	−3.1
A 2,14	5*d*	34998.8	+0.4
A 8,18	2*d*	34975.4	0.0
A 6,17	0*d*	34880.3	{+2.8
B 7,19			0.0
A 9,19	2*d*	34842.7	−1.9
A 3,15	1*d*	34815.5	{−2.7
B 5,18			+0.9
B 2,16	2*s*	34797.8	+0.6
A 4,16	2*d*	34728.5	+0.9
B 3,17	1*s*	34689.9	+0.1
B 6,19	2*d*	34659.4	−0.3
A 5,17	3*s*	34616.8	+0.6
A 2,15	5*s*	34602.9	+0.3
A 8,19	3*d*	34587.3	−1.4
	0*d*	34556.1	
B 1,16	1*s*	34508.1	−1.2
A 7,19	1*s*	34346.6	−0.9
B 3,18	2*s*	34300.6	−0.1
B 6,20	2*dd*	34274.8	−0.4
	2*d*	34253.1	
A 5,18	3*d*	34225.9	−1.2
A 2,16	5*s*	34208.8	−0.2
A 8,20	5*s*	34203.0	−1.2
B 1,17	3*s*	34117.0	−1.0
A 6,19	4*d*	34101.7	0.0
A 9,21	1*dd*	34077.1	−0.8
	1*d*	34006.9	
A 4,18	0*d*	33947.1	−0.1
B 3,19	1*s*	33912.4	−1.6
	1*s*	33849.9	
A 5,19	1*s*	33839.7	−0.3
A 2,17	4*s*	33818.7	+1.0
B 1,18	4*s*	33729.1	+0.2
A 6,20	4*s*	33717.3	+0.1
A 9,22	3*d*	33698.0	+0.2
	1*s*	33621.4	
A 7,21	2*s*	33581.1	+0.3
A 4,19	2*s*	33359.2	−1.3
B 3,20	0*d*	33530.0	+0.5
C 0,21	1*d*	33502.1	−0.7
A 2,18	2 *At*	33429.7	+1.1
B 1,19	5*s*	33342.3	+0.1
A 9,23	2*dd*	33319.5	−1.2
B 5,22	1*dd*	33283.3	+1.8
B 2,20	2*s*	33244.5	−1.1
A 7,22	4*s*	33201.2	+0.1
A 4,20	3*s*	33176.8	+0.8
B 3,21	1*d*	33147.2	−0.1
C 0,22	1*dd*	33124.6	+0.9
A 5,21	0*d*	33075.0	+1.3
A 8,23	1*d*	33065.8	+1.0
A 2,19	1*s*	33043.4	+1.5
B 4,22	1*d*	33032.9	−4.5
B 1,20	4 *At*	32958.9	+1.2
B 5,23	0*dd*	32904.8	+0.8
B 2,21	3*s*	32863.0	−0.4
A 7,23	2*s*	32823.5	−0.1
A 4,21	2*s*	32794.6	−0.8
A 14,28	4*s*	32746.7	{+0.9
C 0,23			+0.5
A 5,22	4*d*	32692.3	{−1.3
A 8,24			+2.7
	1*d*	32658.5	
A 6,23			{−2.7
A 9,25	3*s*	32575.1	{+2.5
B 1,21			−0.4
B 2,22	4*s*	32483.2	−0.5
A 4,22	0*d*	32413.8	−0.3
B 3,23	1*d*	32391.1	+1.0
A 5,23	5*s*	32316.3	−0.2
A 9,26	5*d*	32201.6	{−0.5
A 6,24			−1.0
B 1,22	5*d*	32195.6	−0.2
B 2,23	5*s*	32106.2	0.0
B 3,24	2*s*	32016.0	+1.1
A 5,24	2*s*	31942.2	+0.9
A 9,27	4*d*	31832.6	{−1.5
A 6,25			+2.9
B 1,23	5*d*	31819.3	+1.0
B 2,24	5*s*	31731.0	0.0
A 7,26	3*s*	31705.6	+0.6
A 4,24	3*s*	31664.3	+2.9
B 3,25	4*s*	31643.1	+1.1
C 0,26	1*d*	31626.8	−0.8
A 5,25	1*s*	31568.2	−0.2
B 4,26	1*s*	31542.2	+0.9
A 6,26	3*d*	31460.4	+1.2
B 1,24	3*d*	31444.0	+0.9
B 2,25	4*d*	31359.9	+1.8
A 7,27	4*s*	31338.1	+1.1
	3*s*	31308.9	
B 3,26	3*s*	31272.0	+0.5
C 0,27	3*s*	31258.7	−0.9
A 8,28	2*s*	31213.2	+0.8
A 5,26	1*s*	31198.4	+0.5
B 4,27	2*s*	31172.9	−0.4
A 6,27	2*s*	31091.4	+0.2
B 5,28	1*dd*	31052.2	+0.6
B 2,26	2*d*	30987.7	+0.1
A 7,28	3*s*	30971.8	+0.6
B 3,27	3*s*	30905.5	+1.8
C 0,28	3*d*	30893.6	−0.2
A 8,29	4*s*	30850.1	+0.9
	1*d*	30834.2	
B 4,28	2*s*	30807.4	−0.1
B 7,30	1*d*	30781.3	+1.2
A 9,30	1*d*	30744.4	0.0
A 6,28	1*s*	30726.4	+1.0
B 5,29	1*d*	30688.9	+0.5
B 8,31	0*d*	30629.9	−1.3
A 7,29	1*s*	30609.0	+0.9
B 6,30	0*s*	30559.4	−0.1
B 3,28	2*d*	30538.7	+1.0
A 8,30	4*s*	30489.3	+0.8
	1*d*	30473.2	
A 5,28	1*d*	30464.4	+0.3
B 4,29	2*s*	30443.1	+1.2
B 7,31	1*d*	30421.9	+0.2
A 9,31	3*s*	30386.3	+0.3
A 6,29	1*s*	30363.3	+1.1
	1*s*	30349.0	
B 5,30	3*s*	30328.4	+0.7
B 2,28	4*s*	30255.7	+1.9
A 7,30	3*d*	30247.2	−0.1
B 6,31	0*s*	30201.5	+0.4
C 0,30	1*dd*	30169.9	0.0
A 8,31	4*s*	30131.1	+1.0
	1*d*	30117.0	
A 5,29	1*dd*	30103.7	+2.8
B 4,30	1*d*	30085.4	+1.8
B 7,32	0*dd*	30061.6	−4.4
A 9,32	4*s*	30030.3	0.0
A 6,30	0*d*	30003.0	+1.5
B 5,31	2*s*	29968.8	−0.5
B 8,33	2*s*	29922.2	+0.2
	3*s*	29909.4	
A 7,31	2*s*	29888.7	{−0.2
B 2,29			−1.9
B 6,32	1*d*	29845.1	−0.3
A 8,32	3*s*	29774.7	+0.4
	1*d*	29759.8	
A 5,30	1*dd*	29743.8	+3.6
A 9,33	4*s*	29676.1	−0.7
A 6,31	1*s*	29643.1	0.0
B 5,32	2*s*	29612.4	−1.2
B 8,34	0*d*	29571.9	+0.9
	0*d*	29551.3	
A 7,32	1*s*	29533.1	−0.1
	2*d*	29498.6	
C 0,32	0*d*	29456.9	+1.1
A 8,33	2*s*	29420.6	−0.3
A 9,34	3*s*	29324.5	−1.3
A 6,32	0*d*	29288.7	+1.3
A 7,33	1*s*	29181.3	+1.6
A 8,34	3*d*	29069.6	−0.3
	2*d*	28995.5	
A 9,35	3*d*	28976.7	−0.5
A 6,33	0*d*	28933.9	+0.1
	0*d*	28910.8	
A 14,39	3*s*	28885.9	+0.1
A 7,34	1*d*	28831.1	+2.4
A 8,35	1*s*	28720.9	−0.4
A 9,36	1*d*	28631.1	−0.1
A 6,34	0*d*	28583.2	+0.3
A 14,40	4*s*	28550.0	0.0
	0*s*	28497.5	
	0*s*	28376.2	
A 9,37	1*d*	28289.8	+0.3
A 14,41	4*s*	28217.1	+0.3
A 14,42	3*s*	27886.3	0.0
A 14,43	2*s*	27558.4	+0.1
A 14,44	1*s*	27223.0	−0.1

vapor and hydrogen. The discharge tube was constructed so that a continuous flow of hydrogen through it could be maintained when necessary. Its electrodes were hollow nickel cylinders lying along the axis of the discharge column. The spectrum was photographed through a quartz window which was waxed to one end of the discharge tube. In the center of the discharge a side tube containing metallic arsenic was so placed that, by heating it, arsenic vapor could be driven into the hydrogen discharge.

In the procedure used, the tube was exhausted of gas and then a steady flow of hydrogen pumped through it. A discharge in the hydrogen was then maintained and the tube and arsenic heated for a time sufficient to eliminate impurities from the walls and electrodes of the tube as well as the surface impurities such as AsO and carbon compounds from the arsenic. This washing and baking process was essential for eliminating OH, CO, NO and N_2 bands from the spectrum. Finally, the flow of hydrogen was stopped, the pressure in the tube adjusted to between 15 and 40 mm Hg and the arsenic vapor driven into the discharge. It was necessary to heat constantly the discharge column as well as the side tube in order to prevent the arsenic from condensing. The discharge in the arsenic vapor was nearly colorless in contrast to the blue of the discharge in hydrogen.

The bands were most intense at the highest pressure of hydrogen that could be used. The exposure time on a Hilger E1 spectrograph with Eastman I-0 plate was from 10 min. to 1½ hours, the longest time being used in photographing the shortest wavelength portion of the spectrum, because of the loss in the sensitivity of the photographic plates in that region.

The metallic arsenic used in this investigation was tested spectroscopically for impurities and was found to contain traces of Fe, Sb and Bi. The hydrogen used was very carefully dried by passing it through P_2O_5 and then through a liquid air trap. Another liquid air trap was placed between the exhausting oil pump and the discharge tube for collecting any arsine which might have been formed.

A method quite similar to this was used by Pearse[8] in photographing PH bands, but in this investigation no trace of bands was found which could be attributed to AsH.

[8] R. W. B. Pearse, Proc. Roy. Soc. **A129**, 328 (1930).

Description of Band Systems and Vibrational Analysis

The bands observed consisted of an extensive complex group of bands degraded to the red between 2100A and 3700A and a few weak bands similarly degraded in the visible violet region. The latter group is not as yet certainly identified or analyzed and the discussion of them will be deferred until they have been more completely studied experimentally. The wave numbers of the band heads of the ultraviolet group are given in Table I, together with an eye estimate of intensity and sharpness of edge, and vibrational quantum assignment. This group has been arranged into two systems, designated *A* and *B* in Table I, which overlap one another almost completely. There is some indication of a weak,

Table IIa. *Values of* $\Delta G_{v'}$.

v'	$\Delta G_{v'}$ (obs.) Ave. from $A\rightarrow X$, $B\rightarrow X$	$\Delta G_{v'}$ (calc. from Eq. (1))	Obs.–Calc.	v'	$\Delta G_{v'}$ (obs.) Ave. from $A\rightarrow X$, $B\rightarrow X$	$\Delta G_{v'}$ (calc. from Eq. (1))	Obs.–Calc.
1	428.1	427.2	+0.9	23	377.3	377.5	−0.2
2	425.4	425.0	+0.4	24	374.5	375.2	−0.7
3	423.3	422.7	+0.6	25	373.2	372.9	+0.3
4	419.8	420.5	−0.7	26	370.9	370.5	+0.4
5	418.4	418.3	+0.1	27	368.3	368.0	+0.3
6	416.0	416.0	0.0	28	365.9	365.8	+0.1
7	413.3	413.8	−0.5	29	361.9	363.2	−1.3
8	410.9	411.6	−0.7	30	360.9	360.7	+0.2
9	409.4	409.3	+0.1	31	358.8	358.4	+0.4
10	407.2	407.1	+0.1	32	355.9	355.7	+0.2
11	405.4	404.8	+0.6	33	353.4	353.5	−0.1
12	402.1	402.6	−0.5	34	350.9	351.0	−0.1
13	400.1	400.4	−0.3	35	348.6	348.6	0.0
14	398.1	398.1	0.0	36	346.1	346.0	+0.1
15	396.0	395.8	+0.2	37	343.5*	343.5	0.0
16	394.1	393.6	+0.5	38	341.0*	341.0	0.0
17	389.1	391.3	−2.2	39	338.4*	338.4	0.0
18	389.6	389.1	+0.5	40	335.9	335.8	+0.1
19	387.6	386.7	+0.9	41	333.5	333.2	+0.3
20	385.1	384.5	+0.6	42	331.0	330.5	+0.5
21	382.5	382.2	+0.3	43	327.7	328.0	−0.3
22	380.7	379.7	+1.0	44	325.4	325.2	+0.2

* Smoothed in, not observed.

Table IIb. *Term values of states A and B.*

v'	T_A+G_A ($=\nu_A(v',0)$)	ΔG_A	T_B+G_B ($=\nu_B(v',0)$)	ΔG_B	v'	T_A+G_A ($=\nu_A(v',0)$)	ΔG_A
0	40260.9		40833.0		9	42578.7	255.9
1	40523.3	262.4	41076.3	243.3	10	42837.2	258.5
2	40776.0	252.7	41364.2	287.9	11	43094.9	257.7
3	40991.6	215.6	41648.1	283.9	12	43350.5	255.6
4	41294.9	303.3	41917.9	269.8	13	43604.0	253.5
5	41574.5	279.6	42162.0	244.1	14	43856.2	252.2
6	41835.8	361.3	42393.8	231.8	15	44104.7	249.3
7	42081.6	245.8	42614.4	220.6	16	44352.0	247.3
8	42322.8	241.2	42823.9	209.5	17	44597.2	245.2

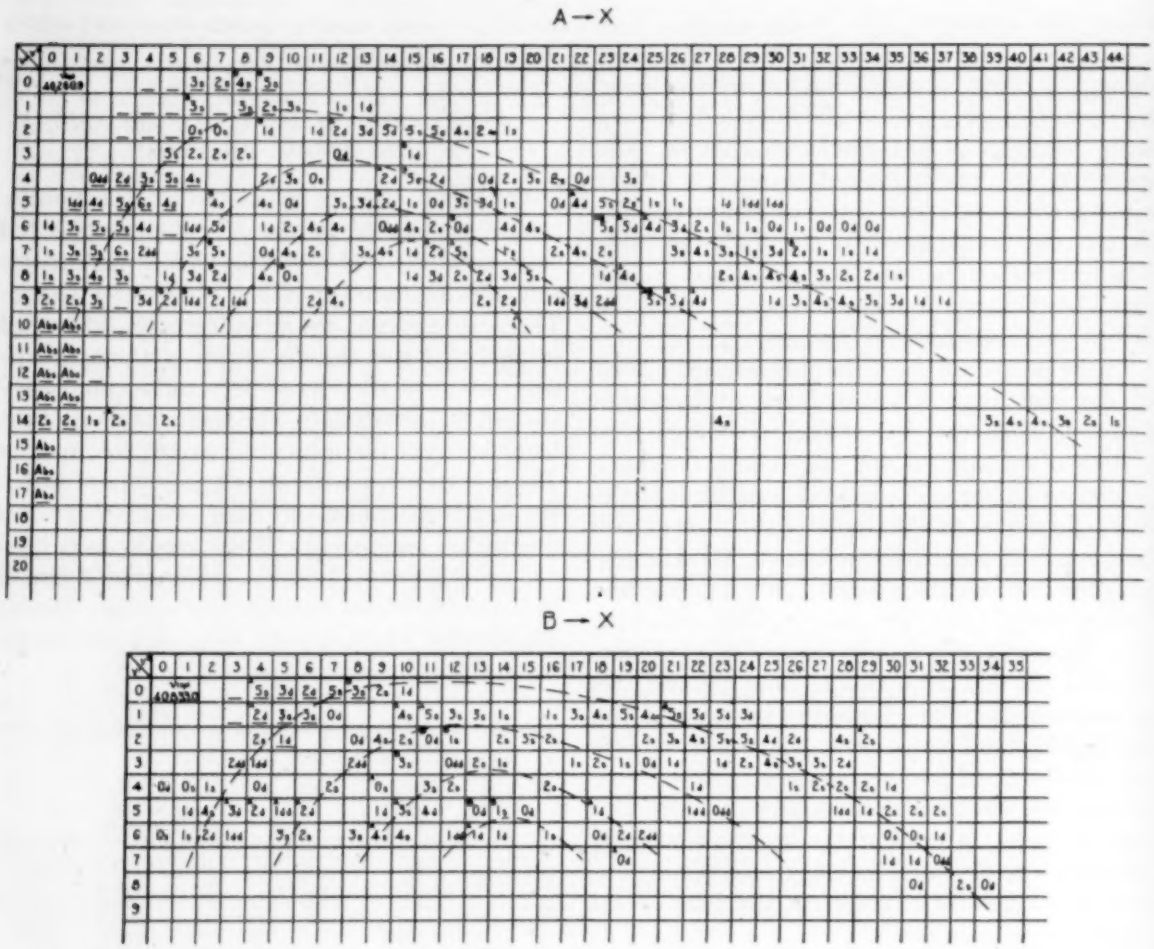

FIG. 1. Observed bands of $A \rightarrow X$ and $B \rightarrow X$ systems, indicated by intensity symbols. A, B, indicates superposed band in A or B system. Underlined bands observed by Gibson and MacFarlane in absorption. "Abs" indicates observed as absorption bands on emission plates.

third, C system overlapping the long wave end of the A and B systems. The (v', v'') arrays of the A and B systems are shown in Fig. 1 where the presence of a band is indicated by its intensity symbol. The values of $\Delta G''$ obtained from this assignment show that the two strong systems (as well as the C system) have a common lower state, which is undoubtedly the normal state of As_2, since the A system is identical with the absorption spectrum observed by Gibson and MacFarlane. Hereafter, therefore, the common lower state will be designated X and the three systems, $A \rightarrow X$, $B \rightarrow X$, $C \rightarrow X$, respectively. In Table IIa values ΔG_X (averages from $A \rightarrow X$ and $B \rightarrow X$) are listed, together with a comparison with ΔG_X calculated by Eq. (1) (below). In Fig. 2 ΔG_X is plotted against G_X. Through the range of observation the lower state follows a normal course. Values of ΔG_X were fitted to a power series by least squares (Birge-Shea method), from which was obtained for ΔG_X,

$$\Delta G_X = 428.32 - 2.238(v+\tfrac{1}{2}) + 0.001374(v+\tfrac{1}{2})^2 - 0.0001025(v+\tfrac{1}{2})^3. \quad (1)$$

From Eq. (1) G_X was obtained,

$$G_X = 429.44(v+\tfrac{1}{2}) - 1.120(v+\tfrac{1}{2})^2 + 0.0005091(v+\tfrac{1}{2})^3 - 0.00002563(v+\tfrac{1}{2})^4. \quad (2)$$

In every v'' progression the observed values of

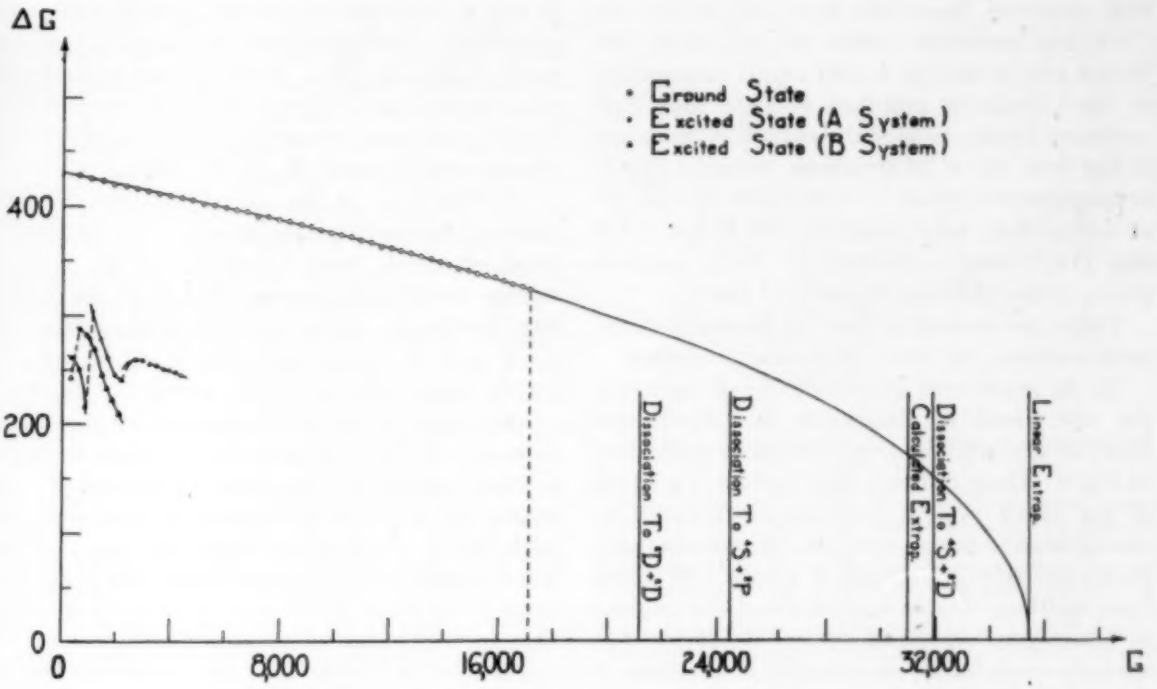

FIG. 2. Plot of ΔG *vs.* G for states X, A, B. Vertical lines indicate values of $D(X)$ as calculated by different methods. For example, the value labeled "Dissociation to $^3D+^1D$" assumes state B dissociates into $^3D+^3D$. It is probably the correct $D(X)$.

ΔG_X fit Eq. (1) sufficiently well that the relative v'' numbering is entirely definite; the progressions cannot be shifted with respect to one another even by one. This was important in making the vibrational anslysis, because of the irregular behavior of the intervals in the upper states. In fact, the analysis was made by arranging practically all of the bands into v'' progressions, then fitting these as smoothly as possible into two systems. The absolute numbering of v'' was secured by the absence of any bands of v'' lower than that of the long first v' progression in system $A \rightarrow X$.

States A and B lie at about the same electronic energy, the $A \rightarrow X$ (0,0) head being at 40,260.9 cm^{-1}, the $B \rightarrow X$ (0,0) head at 40,833.0. The two states have also approximately the same vibrational intervals with the result that one set of levels strongly perturbs the other giving erratic series of values of ΔG (Fig. 2). On account of these irregularities no attempt was made to represent states A and B by equations such as Eq. (1). To test the validity of the quantum assignments the following procedure was adopted for comparing observed and calculated wave numbers of the bands. To each observed $\nu(v', v'')$, $G_X(v'')$, as calculated by summing the ΔG_X's calculated from Eq. (1), was added, giving a value of $\nu(v', 0)$. These values were averaged for each v'' progression and are listed in Table IIb, together with the first differences. Finally, the position of each band was calculated according to

$$\nu(v', v'') = \nu(v', 0)_{\text{ave}} - G_X(v''). \qquad (3)$$

The difference between observed and calculated values is listed in column 4 of Table I. Although the difference is larger in some cases than the probable experimental error (0.5 to 2 cm^{-1} depending on diffuseness and superposition), the calculation, on the whole, strongly supports the assignment.

Certain band heads of the $A \rightarrow X$ system appeared in absorption on the emission plates. These are marked "Abs" in the intensity column of Table I and in Fig. 1. The wave numbers of these absorption bands were not calculated in the same way as the wave numbers of the emission bands, since only two v' progressions

were observed. Since ΔG_A decreases linearly for $v'>9$, the smoothed values of ΔG_A were read from a plot of ΔG_A *vs.* v, and added successively to the calculated positions of (9,0) and (9,1) (emission bands) to give the calculated positions of the first two v' progressions. Since in the v'' progression for which $v'=14$ bands of high v'', as well as low, were observed, the bands (14,0) and (14,1) were calculated by both methods giving values differing by only 0.8 cm^{-1}.

There are several features of intensity distribution among the bands that deserve remark.

(1) As mentioned above, the $A\rightarrow X$ system is the one found in absorption by Gibson and MacFarlane, who reported the bands underlined in Fig. 1. These authors also found a few bands of the $B\rightarrow X$ system (also called B bands by them), noted a fairly constant difference between them and suitably chosen A bands and speculated on the probable association of the two sets of heads into one band system. With the two systems completely developed in emission it seems clear that they are independent.[9] The $B\rightarrow X$ bands observed in absorption are also underlined in Fig. 1.

(2) In each band system there is a fairly definite principal Franck-Condon parabola and several subsidiary parabolas. These are sketched in Fig. 1. This behavior is compatible with the progressive overlapping or "interference" of the wave functions of a given upper vibrational state with those of a progression of lower states. Similar intensity variations were found in the emission spectrum of P_2 by Herzberg.[3]

(3) There is, in the $A\rightarrow X$ system, a pronounced intensity perturbation in the neighborhood of $v'=3$, near which the most violent energy perturbation occurs. At low v'' the intensity minimum along the parabola comes at $v'=2$ with $v'=3$ also quite weak. At higher v'', on the right branch of the parabola, the progression for $v'=2$ is very strong and the minimum is at $v'=3$. The intensity distribution in both systems would be somewhat improved if the strong, A, $v'=2$, progression were interchanged with the B, $v'=0$, progression (see Fig. 1). The wave number displacements are then less pronounced in state B but more so in A. It may be that in this region of greatest perturbation one cannot say definitely that one particular set of rotational levels (associated with a vibrational state) belongs to the A state and the other set of levels to the B state. This difficulty calls for rotational analysis.

(4) Every $A\rightarrow X$ band for which $v'=8$, which is not superposed on another band, shows a very characteristic peculiarity in the partially resolved rotational structure. The head is sharp, and at 15 to 25 cm^{-1} from the head the intensity drops suddenly, beyond which, after a narrow gap, almost resolved but irregularly spaced rotational lines appear. These lines look something like a new head, much weaker than the main head. In Table I several of these subsidiary heads are listed following $A(8,v'')$ heads, but are unassigned.

(5) The $A\rightarrow X$ bands at $v'=9$ which are not obscured by other bands show a sharp drop in intensity at approximately 25 cm^{-1} from the head indicating a break off in the unresolved rotational structure.

(6) $A\rightarrow X$ bands for which $v'=10$, 11, 12, 13 do not appear in emission. But on the emission photographs absorption bands do occur in the first two v' progressions at the proper positions for the emission bands. These progressions were observed by Gibson and MacFarlane. At $v'=14$ a strong emission progression occurs not only for

---

[9] According to our classification of the $B\rightarrow X$ bands the lowest vibrational state is the one labeled $v'=2$ by Gibson and MacFarlane. Accurate measurements on four sharp heads making up what is apparently their B, $v'=1$, $v''=4$ to 7 progression cannot fit in that position but must range from $v''=5$ to $v''=8$. Thus restricted it fits best in the $A\rightarrow X$ system with $v'=3$, where it implies, however, a large perturbation in state A (cf. ΔG_A in Table IIb and Fig. 2). Their B (0,3) and B (0,4) at 39,034 and 38,611, may be our B (6,8) and B (6,9) (or possibly A (5,6) and A (5,7)) although we also list an unassigned band at 38,618.6 cm^{-1}. Their assignment of these two bands would isolate them in our square array, while our assignment separates them from their other observed bands. Although our disposal of these last two bands is not as satisfactory as we should like, we assume, because of lack of data pushing it farther down, that the B, $v'=0$, state lies about two vibrational intervals above the A, $v'=0$, state.

The additional evidence against associating each B band with an A band to form a single system may be summarized as follows: (1) There is no regular intensity relation between corresponding A and B bands. Both may be strong, both weak, or one strong and the other weak. (2) Visual inspection of the plates indicates that the association is erroneous. For example, a strong B head, lying to the violet of the associated A head fades out completely before it gets half-way to the A head. (3) To understand the strong perturbations in either system, it is necessary to assume a nearly coincident state with similar vibrational and rotational constants. The other system provides just such a state.

low v'' but for $v''=39$ to 44, in exactly the positions demanded by the intervals, ΔG_X (extrapolated), and by the intensity distribution. The $(14,v'')$ bands have sharp heads but break off suddenly at about 15 cm^{-1} from the head. Finally the first v' progression ($v''=0$) appears again in absorption and can be followed visually to $v'=26$ on a low dispersion plate although the measurements have not been extended beyond $v'=17$ on the Hilger E1 plates.

(7) In the $B\rightarrow X$ system the general intensity distribution is similar to that of the $A\rightarrow X$ system except that the parabolas are shifted somewhat toward larger v''. The system was not pushed beyond $v'=6$ at low v'' or $v'=8$ at high v''. At low v'' where the structure is fairly well resolved the rotational lines of the $B\rightarrow X(6,v'')$ bands appear diffuse. The structure does not appear to break off suddenly.

Perturbations, Predissociation, Heat of Dissociation

In this section we shall first draw what conclusions we can without making any assumptions as to the kinds of electronic molecular states involved in the band systems. Then we shall discuss, largely by means of the analogy with P_2, the probable electronic molecular states and their parent atomic states.

The vibrational analysis shows that in state A there are large perturbations in the positions and intensities of the band heads. These perturbations seem to center near $v'=3$ and $v'=7$. In the B state there are large perturbations at about the same total energies, or at $v'=0$ or 1 and $v'=4$ or 5. It is therefore probable that the interaction of states A and B is responsible for the perturbations and that their potential energy curves cross in the regions of greatest displacement. Such a relation of the two curves is shown in Fig. 3. The vibrational levels are shown, as well as the directions of their apparent displacements in the lower regions of great perturbation. It is not clear just what the displacements are at the higher perturbation.

To explain such large perturbations as occur, with whole bands apparently displaced, it seems necessary that the sets of rotational levels of close-lying A and B vibrational levels should

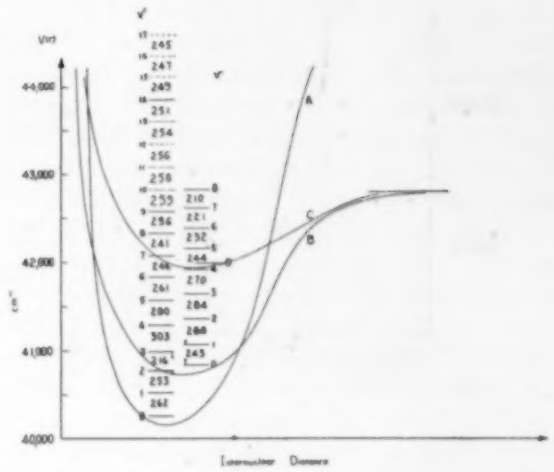

FIG. 3. An assumed set of potential energy curves for states A, B, C, which is consistent with the observed perturbations and predissociations; also vibrational energy levels of these states. Large perturbations are at $v'=3$ and $v'=7$ in state A and at the same total energy in state B; curves are assumed to cross in these regions. Departure of levels from smooth behavior at lower perturbation is indicated by arrows. B dissociates by rotation; A predissociates into B from $v'=9$ to 13, and into C from $v'=14$ on. Dotted levels are upper states of absorption bands on emission plates.

very nearly parallel one another, since one of the selection rules is that $\Delta J=0$. Such approximate coincidence of rotational levels is quite likely in As_2 since (1), each A vibrational level lies just below the nearest B level and (2), the rotational constant $B(=h/8\pi c\mu r^2)$ of an A state is probably slightly greater than the rotational B of a B state. This last is true if the relative positions of the minima of the curves assumed in Fig. 3 are correct; it is also consistent with the intensity distribution in the square array (Fig. 1) where, as mentioned above, the Franck-Condon parabolas are shifted to higher v'', for a given v', in B than in A. Therefore the rotational levels of a vibrational state of A should gradually overtake and pass the rotational levels of corresponding J in the nearby vibrational state of B. A rotational analysis is necessary in order to discuss the perturbations with more certainty and completeness.

Bands of the A system for which $v'=8$ and 9 show, as described above, a sudden drop in intensity if not a complete break-off in rotational structure. This behavior is undoubtedly due to predissociation at a total energy of about 42,600 cm^{-1} ($\nu_A(9,0)=42{,}579$ cm^{-1}). At about the same or slightly greater energy the B system

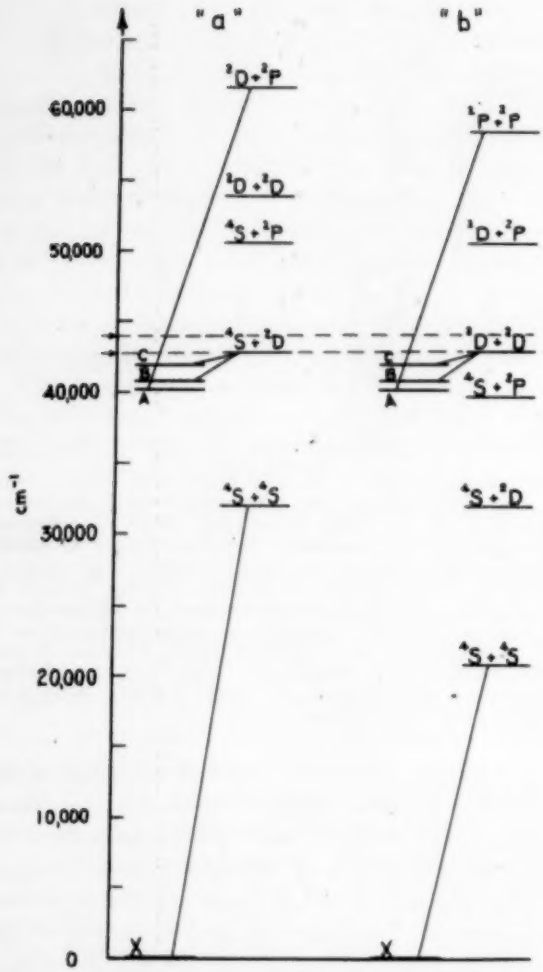

FIG. 4. Term schemes based on assumptions that predissociation occurs at, and B and C dissociate into, atomic states (a) $^4S+^3D$, (b) $^3D+^3D$. The latter is probably correct. Dashed lines indicate predissociation energies.

disappears entirely ($\nu_B(8,0)=42{,}824$ cm^{-1} is the last level observed). This disappearance together with the rapid convergence of the B levels as compared with the A levels and the scarcity of atomic states (Fig. 4) makes it likely that state B dissociates into a pair of atomic states having an energy of about 42,800 cm^{-1}. (It is possible, of course, for stable rotational states to exist having energies somewhat greater than the dissociation energy, as one can see by constructing the effective potential energy curve in which the potential energy is corrected by the rotational kinetic energy.) Finally, the only observed level of the questionable C system has only a little less energy than the predissociation energy of A and the dissociation energy of B. Thus, for example,

$$\nu_c(0,0)=\nu_c(0,22)+G_X(22)$$
$$=33{,}123+8880=42{,}003\ \text{cm}^{-1}.$$

It seems fairly certain, then, that a pair of atomic states stands at about 42,700 cm^{-1} (measured from $v''=0$ of the ground state) and that from these atomic states arise molecular states B and C, as shown in Fig. 3. B dissociates by rotation when its total energy exceeds sufficiently its dissociation energy. From $v'=9$ to $v'=13$ state A predissociates into the continuum of state B. At $v'=14$ A is reappearing in emission, but in the same vibrational level, at not very high J, it predissociates again, this time into C, and continues to go over into C as far as the bands are observed, that is, to $v'=26$. The bands from $v'=10$ to 13 and $v'=15$ to 26 are absorption bands on emission plates, the continuous background being supplied presumably[10] by continuous radiation from transitions $C\rightarrow X$ and $B\rightarrow X$. Finally, it may be remarked that even if the $C\rightarrow X$ bands do not actually represent a third system, there must be at least a repulsive state in the neighborhood to account for the second onset of predissociation in A (at $v'=14$).

We may determine the heat of dissociation of the ground state in two ways, (1) by extrapolating the vibrational levels, and (2) by assuming a particular pair of atomic states at total energy 42,700 cm^{-1}. The extrapolation of the ground state has been done in two ways. First, ΔG_X was plotted against v and the curve extrapolated linearly to $\Delta G_X=0$. The area under the curve gave $D(X)$, equal to 35,500 cm^{-1}. Second, in Eq. (1) the lowest v which made $\Delta G_X=0$ was found by trial and substituted in Eq. (2) to give $G_{X(\text{conv})}=D(X)=31{,}050$ cm^{-1}.[11]

The atomic states of As arising from the $4p^3$ configuration are the normal ^4S, ^2D at 10,785 cm^{-1} (center of gravity), and ^2P at 18,493 cm^{-1}. Since G_X was followed to 17,260 cm^{-1} and since the predissociation occurs at 42,700, the excitation energy of the pair of atoms at 42,700 cannot

[10] Some of the continuum may come from the hydrogen in the tube, but probably not much of it, for there is little continuum on the better plates in the region 2500A to 3500A where the H_2 continuum is ordinarily strongest.

[11] In our preliminary report of this work (Phys. Rev. **47**, 199 (1935)), we gave $D(X)=27{,}500$ cm^{-1}, obtained by extrapolation. We have since discovered an error in the calculation of the frequencies of the $v'=14$ progression, which has increased this earlier value considerably.

be greater than $42{,}700-17{,}260=25{,}440$ cm^{-1}. Thus this pair of atoms must be $^4S+^4S$, $^4S+^2D$, $^4S+^2P$, or $^2D+^2D$. The first pair is ruled out by the fact that it would require that $D(X)$ be 42,700 cm^{-1}, or more than a volt *higher* than the extrapolated value. The other three possibilities give, respectively, for $D(X)$, $42{,}700-10{,}785=31{,}915$ cm^{-1}, $42{,}700-18{,}493=24{,}207$ cm^{-1}, and $42{,}700-21{,}580=21{,}120$ cm^{-1}. The first of these is in good agreement with the extrapolated value obtained above (from Eq. (1)), supporting the conclusion that the rounded figure for $D(X)$ is 4.0 volts. The relative positions of atomic and molecular levels according to this scheme is shown in Fig. 4a.

So far we have made no assumptions as to the kind of molecular states involved. It is worth while to discuss the possible states, for such consideration raises some serious objections to the scheme just proposed (Fig. 4a). We may reasonably assume that, as in N_2 and P_2, the ground state of As_2 is $^1\Sigma_g^+$ arising from two normal ^4S As atoms. It is also probable that, as in P_2, the principal system, $A\rightarrow X$, is $^1\Sigma_u^+\rightarrow{}^1\Sigma_g^+$. Now if state B perturbs A, and if radiationless transitions occur from A to B and A to C, the relations of B and C to A should satisfy the Kronig selection rules for such perturbations or transitions, namely, $\Delta J=0$; $\Delta\Lambda=0, \pm1$; $\Delta S=0$; $g\rightarrow g$ or $u\rightarrow u$, $+\rightarrow+$ or $-\rightarrow-$. Of all possible states arising from the three combinations of atoms permitted by energy considerations, namely, $^4S+^2D$, $^4S+^2P$, $^2D+^2D$, there are only two that could interact with a $^1\Sigma_u^+$ state (A) without violating the selection rules. These are the two $^1\Pi_u$ states arising from two ^2D atoms; these must be states B and C if the selection rules are to be satisfied.[12] But if B and C dissociate into $^2D+^2D$ at 42,700 cm^{-1} the heat of dissociation of the ground state must be $42{,}700-21{,}580=21{,}120$ cm^{-1}, which is much below the value given and disconcertingly close to the maximum observed G_X (17,260 cm^{-1}), when one considers the nearly linear course of ΔG_X as far as observed. The relative positions of the atomic and molecular states according to this scheme are shown in Fig. 4b.

If $^4S+^2D$ stands at 42,700, $D(X)$ is equal to 31,915 cm^{-1}, in good agreement with the value obtained by extrapolating G_X. This assumption, however, implies the violation of the Kronig rules since this pair, $^4S+^2D$, supplies no singlet states to perturb our assumed $^1\Sigma_u^+$ A state. It does provide $^3\Sigma_u^+$ and $^3\Pi_u$ states, which break only the rule $\Delta S=0$; such an intersystem perturbation is of course possible. The third possibility for the pair of states at 42,700 cm^{-1} is $^4S+^2P$, giving $D(X)=24{,}207$ cm^{-1}. $^4S+^2P$ yields no singlet states but does yield two triplet states, $^3\Sigma_u^-$ and $^3\Pi_u$, which might perturb $^1\Sigma_u^+$ though violating the restriction, $\Delta S=0$. In Fig. 2 we have indicated the values of $D(X)$ which would result from the various assumptions as to the products of dissociation of the molecular states.

The situation is very like that found in the case of P_2, by Herzberg.[3] He preferred the choice corresponding to Fig. 4a in which the perturbing state dissociates into $^4S+^2D$, because of the satisfactory agreement then obtained between the values of the heat of dissociation as determined by extrapolation and by predissociation. In P_2 perturbations and predissociation occurred in the system observed but no transitions from the perturbing state were observed and there was no evidence for the presence of a third state such as C. As noted above, the Kronig selection rules are broken if this scheme of states is correct.

For As_2 we are inclined to prefer, in spite of the low value of $D(X)$ which it yields, the situation of states represented in Fig. 4b, in which states B and C dissociate into $^2D+^2D$, for two reasons: (1) It seems very unlikely that such large perturbations should occur between states not satisfying the selection rules, and (2) the recent work on the heat of dissociation of the similar molecule N_2 shows the danger of placing much weight on the extrapolation of ΔG_X. In N_2 the ground state has been followed to more than 5 volts, and extrapolated to 11.5 volts, but recent evidence independent of extrapolation pretty definitely places D very near to 7.3 volts.[2, 12, 14] In As_2 a successful rotational analysis, showing what kind of electronic states A, B and

[12] Although we have in this discussion assumed, for definiteness, state A to be $^1\Sigma_u^+$, the argument requires only that states A, B, C be identified in any order with $^1\Sigma_u^+$, $^1\Pi_u$, $^1\Pi_u$.

[13] R. S. Mulliken, Phys. Rev. **46**, 744 (1934).
[14] W. Lozier, Phys. Rev. **45**, 840 (1934).

C are, should aid the fixing of the scheme of levels and thereby the determination of $D(X)$.

State A appears to be following a normal course in the latter part of its observed range. Extrapolation gives about 19,000 cm^{-1} as its heat of dissociation, which places its total energy of dissociation at $40{,}260+19{,}000=59{,}260$ cm^{-1}. In both schemes in Fig. 4 it is assumed that this extrapolated value of $D(A)$ is approximately correct in determining which pair of atoms give A. In either case, however, if state A were assumed to dissociate into the next lower atomic pair, the values of $D(A)$ would not be impossibly low.

MAY 15, 1935 PHYSICAL REVIEW VOLUME 47

A Note on the Diffraction of Cathode Rays by Single Crystals

KEN'ICHI SHINOHARA, *The Institute of Physical and Chemical Research, Tokyo, Japan*

(Received December 3, 1934)

The black and white line parabolas and circles observed in the diffraction patterns of electrons are shown to be a kind of envelope of the family of Kikuchi lines due to a set of co-zonal planes. That the parabolas appear isolated from the generating Kikuchi lines is due to an effect similar to that which in the case of x-rays accounts for the reduction in density observed at the intersection of two lines in the diffraction pattern. The circle is in fact the envelope of a family of parabolas, its appearance isolated from the generating lines being accounted for in the manner mentioned above. It is shown that the circle is the boundary of a region within which occur no Kikuchi lines of a certain set.

1. INTRODUCTION

When a beam of high voltage cathode rays is sent against a surface of a single crystal at a grazing angle and the scattered beam received on a photographic plate, a diffraction pattern, consisting of Kikuchi lines and spots,[1] is obtained. As the envelopes of certain families of these Kikuchi lines there are observed several parabolas and sometimes also circles. In a previous paper,[2] an account of an investigation on the parabolas in the diffraction patterns for rocksalt and calcite was given. The present paper is concerned with a more general investigation of these curves. The energy of the rays used was of the order of 70 kv.

[1] S. Kikuchi, Jap. J. Phys. **5**, 83 (1928–29). S. Nishikawa and S. Kikuchi, Proc. Imp. Acad. Japan **4**, 475 (1928).

[2] K. Shinohara, Sci. Papers, Inst. Phys. and Chem. Res. **20**, 39 (1932).

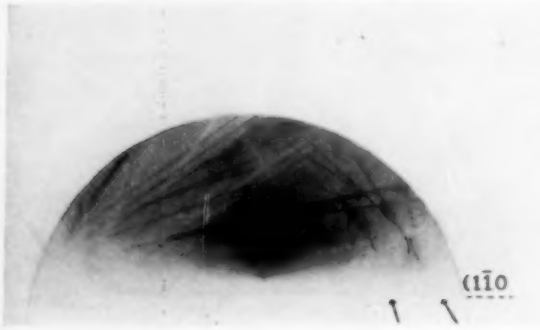

FIG. 1. Zincblende $\lambda=0.043$A (75 kv).

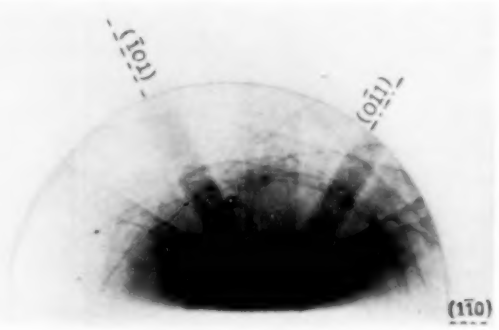

FIG. 2. Zincblende $\lambda=0.044$A (71 kv).

Parabolas

2.

In Figs. 1 and 2, which are photographs taken with the cleavage face of zincblende, there may be seen many black curves looking like parabolas. Their axes are the intersection lines of net-planes of large spacing, *viz.*, the $(1\bar{1}0)$-, $(0\bar{1}1)$- and $(\bar{1}01)$-planes, with the photographic plate. Some of the curves look quite continuous, but most of them show more or less sudden breaks at several points. Some, such as are indicated by the arrows in Fig. 1, are actually formed of short segments of straight lines. It can be seen that these segments are parts of Kikuchi lines and further that the lines belonging to each curve are due to net-planes containing a common zone axis.

White curves also were frequently observed. For example, in Fig. 1 two of them appear in the right corner but may be difficult to see in the reproduction. They appear in case a common zone axis makes a rather large angle with the primary beam, as in this photograph. The geometrical interpretation of their formation is similar to that of the black curves. No white curves had been observed when the previous paper was written, as no photographs having the zone axis suitably directed had been obtained at that time.

Emslie[3] recently observed similar curves in his photographs for stibnite and galena. He considered them to be due to the diffraction of electrons confined to a single net-plane. It was because of the apparent continuity of the curves in his photographs that he preferred this explanation to that of the envelope, and, just on this account, it does not account for the fact that some of the curves have sudden changes of curvature at several points. Moreover, it also seems difficult to explain the existence of white curves. As a matter of fact, the curves seem continuous and without sharp breaks at the intersection points of the generating Kikuchi lines. However this may be expected from the dynamical theory which takes into account the interaction of the electrons with the crystal, as has been shown in the previous paper on the parabolas in the pattern for rocksalt.

[3] A. G. Emslie, Phys. Rev. **45**, 43 (1934).

Reduction in Density of Kikuchi Lines

3.

At the intersection of two Kikuchi lines there is always the disturbing effect of a third plane. Let (l_1, l_2, l_3) and (m_1, m_2, m_3) be the indices of two net-planes and $\mathfrak{l}$ and $\mathfrak{m}$ two radius vectors in the reciprocal lattice, so that

$$\mathfrak{l}=l_1\mathfrak{b}_1+l_2\mathfrak{b}_2+l_3\mathfrak{b}_3,$$

and

$$\mathfrak{m}=m_1\mathfrak{b}_1+m_2\mathfrak{b}_2+m_3\mathfrak{b}_3,$$

where $\mathfrak{b}_1$, $\mathfrak{b}_2$ and $\mathfrak{b}_3$ are the reciprocal axes. Then,

$$\mathfrak{k}_l=\mathfrak{k}_0+2\pi\mathfrak{l}, \tag{1}$$

and

$$\mathfrak{k}_m=\mathfrak{k}_0+2\pi\mathfrak{m}, \tag{2}$$

where $\mathfrak{k}_0$, $\mathfrak{k}_l$ and $\mathfrak{k}_m$ are, respectively, the propagation vectors of the diffracted beam moving in the direction of an intersection of two Kikuchi lines and of the two incident beams which give rise to this common diffracted beam. Therefore,

$$\begin{aligned}\mathfrak{k}_l&=\mathfrak{k}_m+2\pi(\mathfrak{l}-\mathfrak{m})\\&=\mathfrak{k}_m+2\pi\mathfrak{h},\end{aligned} \tag{3}$$

if we write $\mathfrak{h}$ for $\mathfrak{l}-\mathfrak{m}$. From Eqs. (2) and (3) we see that the beam moving initially in the direction of $\mathfrak{k}_m$ is simultaneously reflected by the $(-m_1, -m_2, -m_3)$- and (h_1, h_2, h_3)-planes; in other words, the reflection of the beam from the $(-m_1, -m_2, -m_3)$-plane into the direction of the intersection (i.e. k_0) will be disturbed by the (h_1, h_2, h_3)-plane. The same is true also for the beam moving in the direction of $\mathfrak{k}_l$. As will be shown in §5, this disturbing plane is common for every intersection of two consecutive Kikuchi lines which generate a parabola. Now, the effect of the disturbance increases in general with the reflecting power of the (h_1, h_2, h_3)-plane and is expected to be especially large if the plane is one of cleavage; that is, when the axis of the parabola becomes the intersection line of the cleavage face with the photographic plate. The behavior of black or white lines at such an intersection is shown diagrammatically in Fig. 3. On the other hand, it is also observed that two Kikuchi lines sometimes cross each other without a marked disturbance. In such a case, the angle

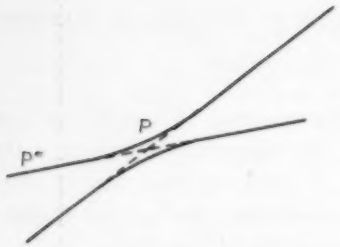

FIG. 3. The broken lines show the behavior when the manner of reflection is not disturbed.

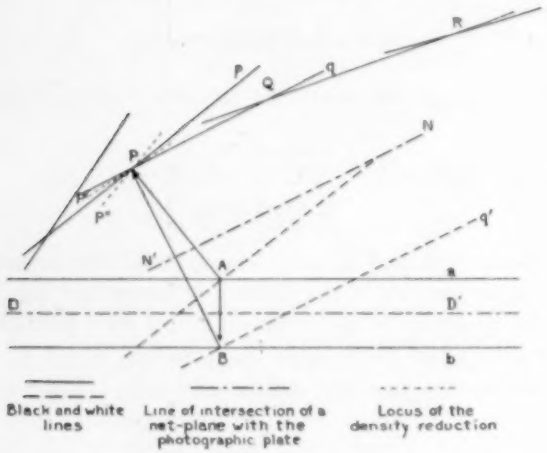

FIG. 4.

between them is usually large and consequently, the reflecting power of the disturbing net-plane becomes small.

4.

A qualitative investigation of the effect of the disturbance can be made in the following way. In Fig. 4, let DD' be the disturbing net-plane and P, one of the points of intersection of the Kikuchi lines. We shall assume, in accordance with the dynamical theory of electron diffraction, that the lines have finite breadth. Then we may expect that the intensity of the beam reflected from the direction given by A or B into P will have two maxima close to one another, separated by a narrow region of reduced density, as has been shown in a previous paper,[2] and studied experimentally by Kikuchi and Nakagawa[4] for the reflection of a beam by a cleavage plane. This reduction in density is due to the reflection of the beam by the plane DD' and the position of the minimum coincides approximately with the direction of the reflected beam which in its initial direction exactly satisfies Bragg's condition for the plane DD'. Now, Bragg's condition for DD' is satisfied by any point on a and b, and therefore there will be a locus of the minimum or density reduction corresponding to each and crossing p and q, respectively, in the neighborhood of P. The locus of the density reduction which intersects p in P may be either PP' or PP''. Making use of the fact that the directions of the incident and the reflected beams are related by $t_l = t_0 + 2\pi l$ and of the condition that the tangential components should be continuous at the surface, we can show by a simple calculation that the first situation occurs when the expression

$$D = [l_t - l_n(\alpha + 2\pi l_t)/\gamma_l]/[l_t - l_n(\alpha/\gamma)]$$

is positive at P and the second when it is negative, where α and γ are the tangential and normal components of the propagation vector of the incident beam; γ_l, the normal component of that of the reflected beam which is in the direction of P; and where l_t and l_n, respectively, are the components of l in the direction of α and γ. The sign of the normal components is taken so as to make γ_l positive.

In applying this to an intersection of two lines, two cases may be considered. In the first case the disturbing plane is the cleavage plane while in the second it is not. In the first case, D becomes positive for p and negative for q at P and further, as can be seen from a simple calculation, the locus of the density reduction coincides for the two lines. Thus, the appearance of the black lines at this point will be that shown in Fig. 3. The further fact that the branch near P''' (Fig. 3) becomes quite faint will be due to the dynamical interaction of the electrons with the crystal. The same will be true also for white curves, since, according to a calculation similar to that given in the previous paper, the extinction and absorption lines at P resemble one another in general features but are inverted in intensity. In the second case, when the disturbing plane is not a cleavage plane but a plane such as $(0\bar{1}1)$ or $(\bar{1}01)$ in Fig. 2, D is in general positive both for p and q at P and the behavior of the curve near this point is more complex than in the first case.

[4] S. Kikuchi and S. Nakagawa, Sci. Papers, Inst. Phys. and Chem. Res. **21**, 256 (1933).

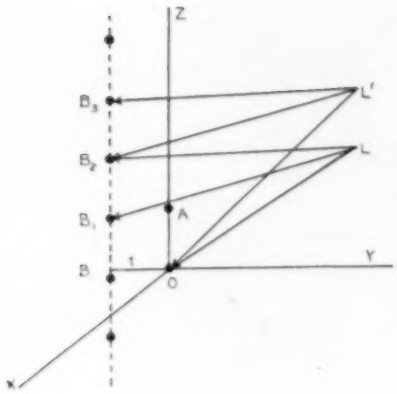

FIG. 5.

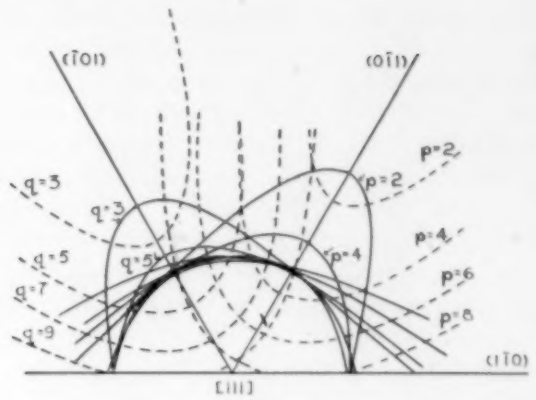

FIG. 6.

FORMATION OF PARABOLAS

5.

Let us now make some geometrical considerations of the formation of parabolas with the help of a reciprocal lattice. Take a series of lattice points B_1, B_2, B_3, $\cdots$ (Fig. 5) along a straight line and let LO, corresponding, for example, to P in Fig. 4, be the common emergent direction of the beams reflected by two net-planes B_1 and B_2. The disturbing plane, given by Eq. (3), is represented by A (Fig. 5). If we now alter the direction of the beam to be reflected by B_2 until it coincides with $L'O$, where it is reflected by two net-planes B_2 and B_3, the process corresponds to tracing out the line PQ from P to Q. By a series of segments such as PQ a kind of envelope $PQR\cdots$ is formed. As the points B_1, B_2, $\cdots O$ and A lie in one plane, the net-planes concerned contain a common zone axis perpendicular to this plane.

Now, because of the disturbance at the intersection P, Q, etc., the angles at these points are rounded with the result that the curve becomes almost continuous and approximates in its appearance an actual envelope defined as the locus of the ultimate intersections of a family of lines formed by varying the value of the parameter continuously; i.e., the envelope when the Kikuchi lines are supposed to lie continuously satisfying a certain geometrical condition necessary to form it. This condition may be satisfied by taking lattice points distributed continuously along B_1B_2. As a consequence, A is made to approach extremely near to O. The locus of the direction LO will be a cone, whose intersection with the photographic plate is the envelope.

Take the axes X, Y, Z as in Fig. 5 with the X axis in the direction of the common zone axis and the Z axis parallel to B_1B_2. Then the equation of the cone whose vertex is at O and whose generating line has the direction LO, is given by

$$k^2z^2+4\pi tky(x^2+y^2+z^2)^{\frac{1}{2}} - 4\pi^2t^2(x^2+y^2+z^2)=0, \quad (4)$$

where t is equal to OB, the length of the perpendicular drawn from O to B_1B_2 and k is the wave number (i.e., 2π divided by the wavelength). For high voltage cathode rays, we can take k large compared with πt. Further we shall assume the X axis to be approximately normal to the photographic plate as in most of the curves observed. Then, taking x large compared with y and z, and neglecting small quantities in Eq. (4), we obtain

$$k^2z^2+4\pi tkxy=4\pi^2t^2x^2. \quad (5)$$

When the x axis is perpendicular or nearly perpendicular to the plate we may replace x by a, the distance of the crystal from the plate, and the curve formed by the intersection of this cone with the plate becomes a parabola given by

$$k^2z^2+4\pi tkay=4\pi^2t^2a^2,$$

and coincides with the curve represented by Eq. (2) in the previous paper.

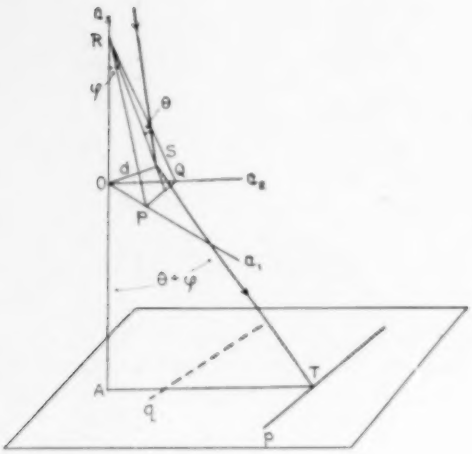

FIG. 7.

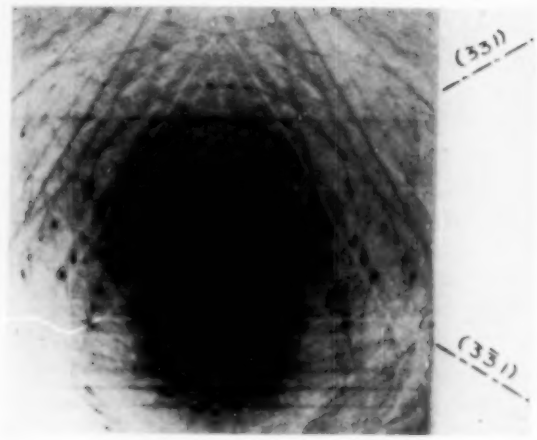

FIG. 8. Mica λ=0.056A (45 kv).

As an example we have in Fig. 2 a series of zone axes parallel to the $(0\bar{1}1)$ plane, having the indices $[p\ p+1\ p+1]$, such as [233], [455], [677], etc., and others, having indices $[q\ q+1\ q]$, parallel to the $(\bar{1}01)$ plane, as [343], [565], [787], etc., all making small angles with the [111] axis. In this case we obtain the series of parabolas shown in Fig. 6, in which the solid lines represent the black lines and the broken lines the white lines. The white curves, though observable in the original negative, will be difficult to see in the reproduction (Fig. 2).

CIRCLES

6.

In Fig. 2, besides the parabolas already described, there is observed a circle with its center at the intersecting point of the [111] axis with the photographic plate. This circle appears to be a sort of envelope of a family of parabolas. It will be seen that there are no black lines in the circle except those running radially. The circle will be taken as a kind of envelope of straight lines and gives the boundary within which black lines of a certain set of planes do not enter.

In Fig. 7, let $\mathfrak{a}_1$, $\mathfrak{a}_2$ and $\mathfrak{a}_3$ be three translations of the lattice, of which $\mathfrak{a}_3$ represents a special direction such as [111]. Further, let PQR be the net-plane which makes an angle φ with $\mathfrak{a}_3$ and has the indices (lmn). By reflection from this plane, a pair of black and white lines p and q will be formed on a photographic plate which we shall take, for simplicity, normal to $\mathfrak{a}_3$. Let A be the point of intersection of $\mathfrak{a}_3$ with the plate and T, the foot of the perpendicular drawn from A to the line p which lies farther from A, then the beam ST is determined by $\theta+\varphi$ where θ is the angle given by Bragg's condition $\lambda=2d\sin\theta$. From the figure we see that $\sin\varphi=nd/|\mathfrak{a}_3|$, therefore

$$\cos(\theta+\varphi)=\left(1-\frac{n^2d^2}{|\mathfrak{a}_3|^2}\right)^{\frac{1}{2}}\left(1-\frac{\lambda^2}{4d^2}\right)^{\frac{1}{2}}-\frac{n\lambda}{2|\mathfrak{a}_3|}.$$

If we take various net-planes having a common value for n, there is a minimum for $\theta+\varphi$. Considering l and m to vary continuously, it occurs at

$$d^2=\lambda|\mathfrak{a}_3|/2n \tag{6}$$

and

$$\cos(\theta+\varphi)=1-n\lambda/|\mathfrak{a}_3| \tag{7}$$

at this limit. Thus we see from Eq. (6) that the net-planes whose black lines approach this limit depend on the wavelength of the cathode rays and from Eq. (7), that the minimum of $\theta+\varphi$ is given by a right cone having OA as its axis, whose intersection with the photographic plate will be a circle. When $n=1$ the circle just coincides with that observed in Fig. 2. The radius of the circle is determined by $|\mathfrak{a}_3|$, n and the wavelength and for various values of n a number of concentric circles can be expected to appear. The arrangement of the lattice points on the plane parallel to $\mathfrak{a}_1$ and $\mathfrak{a}_2$ does not affect their

radii but may slightly affect the appearance of the circles.

As we can see in Fig. 2, the circle is quite continuous and is also isolated from the other lines. It is due to a large number of black lines concerned in its formation and the effect of the density reduction, which, in this case, arises from several net-planes having large reflecting powers, while in the case of a parabola, it arose from a single net-plane.

Another example of such circles can be seen in the pattern (Fig. 8) obtained by transmitting a beam of electrons through a thin sheet of mica. The center of the concentric circle is at the intersecting point of the $[\bar{1}03]$-axis, the axis parallel to the intersection of the (331)- and $(3\bar{3}1)$-planes with the photographic plate. Among the circles, those with large radii are quite continuous, but those with small radii look rather like polygons, as the black lines concerned in their formation are few in number.

Emslie has observed, in the paper already cited, a similar circle for stibnite and considered it to be due to the localizing of an electron's wave packet to the neighborhood of a single row of atoms. The radius of the circle due to the diffraction of such an electron coincides with that in our case. But this explanation, as in the case of parabolas, cannot account for the fact that some of the circles have many sudden breaks. As a matter of fact, we see by a close examination that even for the circle in Fig. 2, the radius of curvature is not exactly constant. Further, the value of the refractive index which Emslie measured from the contraction of the radius of the circle turned out too large but this we may expect from our theory as the contraction of the radius also will be caused by an effect related to the density reduction.

In conclusion the author wishes to express his sincere thanks to Professor S. Nishikawa for his kind guidance throughout this work.

MAY 15, 1935 PHYSICAL REVIEW VOLUME 47

Equation of a Wave in a Medium with Velocity a Function of Time

P. I. WOLD, *Union College, Schenectady*

(Received February 18, 1935)

The equation of a wave in a medium for which the velocity is a function of time is obtained. On purely physical considerations for the case of $v=v_0e^{-\alpha t}$ and a simple periodic oscillation at the source, the equation is $y=a\sin 2\pi\nu_0[t-(1/\alpha)\ln(1+(\alpha x/c)e^{-\alpha t})]$. From other considerations the differential equation obtained is $\ddot{y}+\alpha\dot{y}=c^2e^{-2\alpha t}y''$ which is satisfied by the equation above.

IN a recent article[1] the writer discussed the characteristics of a wave in a medium with the velocity decreasing slowly with time. It was shown that a wave once emitted would continue with a constant wavelength. The velocity function there considered was

$$v=c(1-\alpha t), \tag{1}$$

and it was shown that for an observer at a distance x from the source, there is a decrease in received frequency proportional to the distance to the source. In the case of light this means a redward shift and it was pointed out that one could thus account for the redward shift of light from nebulae without resorting to an expanding universe, the calculated value of α being 1.81×10^{-17} reciprocal seconds.

It has become desirable to find the form of the function $y=f(x, t)$ for a wave in such a medium and we shall take the velocity function as

$$v=ce^{-\alpha t}, \tag{2}$$

this v being more flexible mathematically than the linear function formerly used. Here again, as in any case where the velocity is a function of time and not of position, a wave once emitted continues with unchanged wavelength, but the wavelength as emitted at the source gradually changes as the velocity changes. The instan-

[1] Wold, Phys. Rev. **47**, 217 (1935).

taneous appearance of the wave train, when using Eq. (2) and giving α a large value, is shown in Fig. 1. The long waves were emitted first.

Take the origin of position at the source and the origin of time as that when the velocity is c.

FIG. 1. Instantaneous view of a wave in a medium with a velocity function $v=v_0e^{-\alpha t}$.

Then the wave front has traveled out a distance determined by t. Consider any point of the resulting wave train distant x from the source and let τ be the time that the element at x left the source. Then it has traveled outwards for the time $t-\tau$.

The simple periodic motion of oscillation at S is $y=a\sin 2\pi\nu_0 t$, where $2\pi\nu_0 t$ is the phase angle developed at the source since $t=0$. The motion at x is the same except that the phase angle is reduced by the number of radians in the wave standing between S and x. This may be expressed in terms of the number of waves standing in this space or in terms of the phase angle developed at the source since the element at x left the source. This phase angle will be $2\pi\nu_0(t-\tau)$. Thus the motion at x is

$$y=a\sin 2\pi\nu_0[t-(t-\tau)]=a\sin 2\pi\nu_0\tau. \quad (3)$$

Eq. (3) is to be looked upon as the fundamental expression for the motion at any point in the wave train, and is independent of the velocity function assumed.

In general, however, it is desirable to express τ in terms of the distance x, and this may be done if the velocity function is known. For the function (2)

$$x=\int_\tau^t ce^{-\alpha t}dt=(c/\alpha)[e^{-\alpha\tau}-e^{-\alpha t}].$$

Upon passing to antilogarithms we obtain

$$\tau=t-(1/\alpha)\ln(1+(\alpha x/c)e^{\alpha t}),$$

and (3) becomes

$$y=a\sin 2\pi\nu_0[t-(1/\alpha)\ln(1+(\alpha x/c)e^{\alpha t})] \quad (4)$$

for any position x and any time t. For a reflected wave or a wave traveling to the left the sign of the velocity is reversed and

$$y=a\sin 2\pi\nu_0[t-(1/\alpha)\ln(1-(\alpha x/c)e^{\alpha t})]. \quad (4')$$

If $\alpha=0$, these reduce to

$$y=a\sin 2\pi\nu_0(t\mp x/c), \quad (5)$$

the normal wave equation.

The frequency at any point is proportional to the velocity at that time as compared with the velocity at the source when the element of the wave at the point under consideration left the source. Thus $\nu=\nu_0e^{-\alpha(t-\tau)}$. For small values of α this becomes $\nu=\nu_0(1-\alpha x/c)$, whence

$$(\nu_0-\nu)/\nu_0=\alpha x/c, \quad (6)$$

showing a redward shift in the case of light which is proportional to the distance to the source. This is the Hubble-Humason law and the results are consistent with those in the article mentioned above. Obviously, this relation (6) may be transformed into one for wavelength in which it appears as $(\lambda-\lambda_0)/\lambda=\alpha x/c$.

DIFFERENTIAL EQUATION OF SUCH A WAVE

For a medium of constant velocity this is $\ddot{y}=c^2y''$, an equation which is derived fundamentally from two first order equations,

$$\partial V/\partial t=\beta\partial U/\partial x; \quad \partial U/\partial t=\gamma\partial V/\partial x, \quad (7)$$

in which V and U are two functions characteristic of the kind of system in which the wave is traveling. Thus for a string V might refer to the momentum and U to the elastic force resulting from the tension. β and γ are quantities which for the string are tension and reciprocal of density. If β and γ are constants elimination of U gives

$$\partial^2V/\partial t^2=\beta\gamma\partial^2V/\partial x^2, \quad (8)$$

and $\beta\gamma$ is the square of the velocity. (For a string $\beta\gamma=T/\rho$).

If β and γ are not constants the equation is more complicated. Treatment of the case has been found in which one of these (say tension) is a function of position but nowhere does the case seem to have been treated where β and/or γ are functions of time.

For concreteness let us consider the case of an electromagnetic wave. Maxwell's equations are

$$\epsilon\partial E/c\partial t=\text{curl } M, \quad -\mu\partial M/c\partial t=\text{curl } E. \quad (9)$$

Take a plane wave propagated in the x direction with electric component Y and magnetic component γ. Then $X=Z=\alpha=\beta=0$ and the equations above reduce to

$$\epsilon\partial Y/c\partial t=-\partial\gamma/\partial x; \quad -\mu\partial\gamma/c\partial t=\partial Y/\partial x. \quad (10)$$

These are of the form of the two first order equations above. If the velocity is a function of time it is probably because ϵ and μ vary. Let us assume the variation is such that $\epsilon=\epsilon_0e^{\alpha t}$ and $\mu=\mu_0e^{\alpha t}$. The equations then become

$$(\epsilon_0e^{\alpha t}/c)\partial Y/\partial t=-\partial\gamma/\partial x;$$

$$-(\mu_0e^{\alpha t}/c)\partial\gamma/\partial t=\partial Y/\partial x.$$

Elimination of γ and of Y, respectively, gives

$$\ddot{Y}+\alpha\dot{Y}=(c^2e^{-2\alpha t}/\mu_0\epsilon_0)\,Y'',$$

or
$$\ddot{Y}+\alpha\dot{Y}=v^2Y'' \quad (11)$$

and
$$\ddot{\gamma}+\alpha\dot{\gamma}=v^2\gamma'', \quad (12)$$

in which $v_0=c/(\mu_0\epsilon_0)^{\frac{1}{2}}$=phase velocity at $t=0$, and $v=v_0e^{-\alpha t}$ for other times. This is the velocity function assumed in finding Eq. (4), based on purely physical considerations. Substitution shows that (4) satisfies the differential equations. The symmetry of Eqs. (11) and (12) arises from the fact that we assumed the same time function for μ and ϵ.

While Eq. (4) is derived from purely physical considerations and satisfies (11), a solution by direct integration of (11) would be desirable.[2] Such a solution can be obtained as follows:[3]

Taking the velocity as a function of time according to $v(t)=ce^{-\alpha t}$, we may write (11) more explicitly as

$$\frac{\partial^2y(x,t)}{\partial t^2}+\alpha\frac{\partial y(x,t)}{\partial t}=c^2e^{-2\alpha t}\frac{\partial^2y(x,t)}{\partial x^2}. \quad (13)$$

To simplify, make the substitution

$$s=(c/\alpha)e^{-\alpha t}; \quad t=-(1/\alpha)\ln(\alpha/c)s,$$

whence $\partial^2y/\partial t^2=c^2e^{-2\alpha t}(\partial^2y/\partial s^2)+\alpha ce^{-\alpha t}(dy/\partial s)$.

Substitution in (13) gives

$$\partial^2y(x,s)/\partial s^2=\partial^2y(x,s)/\partial x^2. \quad (14)$$

This is the wave equation in a medium of constant unit velocity with respect to the parameter s, which is a decreasing function of time.

We are interested in that solution of this equation which represents a wave sent out from the origin, $x=0$, by a source of constant frequency and amplitude, represented by the function $y(0,t)=A\sin 2\pi\nu_0t$. In terms of the variable $s=(c/\alpha)e^{-\alpha t}$ this becomes

$$y(0,s)=-A\sin[(2\pi\nu_0/\alpha)\ln(\alpha/c)s].$$

The general solution of (14) is of the form $y(x,s)=f(s-x)+g(s+x)$.

The solution which fits the above initial condition is

$$y(x,s)=-\tfrac{1}{2}A(\sin[(2\pi\nu_0/\alpha)\ln(\alpha/c)(s-x)]+\sin[(2\pi\nu_0/\alpha)\ln(\alpha/c)(s+x)]).$$

In terms of t this becomes

$$y(x,t)=-\tfrac{1}{2}A(\sin[(2\pi\nu_0/\alpha)\ln(e^{-\alpha t}-\alpha x/c)]+\sin[(2\pi\nu_0/\alpha)\ln(e^{-\alpha t}+\alpha x/c)]). \quad (15)$$

[2] Gramatzki, in the Zeits f. Astrophys., Apr. 1, 87 (1934), has endeavored to treat this problem but goes astray in his first simplification where he takes $dt'=dt/\varphi(t)$. This means that he is introducing a variable time in which the unit of time is itself a function of time. His equations are probably correct for a wave in a medium in which the velocity is constant but the unit of time is varying. But in our problem, as stated above and as initially implied by Gramatzki, it is not the unit of time which is to vary but the velocity. That his work leads to an incorrect solution in his Eq. (5) so far as our problem is concerned, is indicated by the fact that it does not satisfy boundary conditions. Thus if in his Eq. (5) x is placed equal to zero it appears that the frequency is a function of time, decreasing steadily; also his frequency appears to be independent of x. Actually at $x=0$ the frequency is constant and at $x\neq0$ the frequency is different by an amount depending on x or, more strictly, on the time required for the wave to travel to x. In his article Gramatzki attempts a second solution of the problem and obtains his Eq. (23) which again fails to fulfill boundary conditions and is not in agreement with his Eq. (5). Gramatzki states that the changed frequency is given by $\nu=\nu_0(1-kt)$, which relationship is correct, and then calculates the value of k, obtaining a result in agreement with that of my article cited above. But this relation for changed frequency cannot be obtained from either of his Eqs. (5) or (23). Naturally, various discrepancies occur in his other conclusions.

[3] For this solution I am indebted to Mr. Augustus H. Fox, Dept. of Math., Union College.

The first term represents a wave traveling to the right with velocity $ce^{-\alpha t}$ and the second to the left with velocity $-ce^{-\alpha t}$. The first term readily reduces to

$$y=a \sin 2\pi\nu_0[t-(1/\alpha) \ln (1+(\alpha x/c)e^{\alpha t})]$$

in agreement with (4) and the second is in agreement with (4′).

In order to find the frequency of these waves at a point $x\neq 0$ we must find the change δ in t which will change the phase angle by 2π. For the first wave we have

$$2\pi\nu_0[t+\delta-(1/\alpha) \ln (1+(\alpha x/c)e^{\alpha(t+\delta)})]$$
$$=2\pi\nu_0[t-(1/\alpha) \ln (1+(\alpha x/c)e^{\alpha t})]+2\pi.$$

Transformations give

$$e^{-\alpha\delta}=e^{-\alpha/\nu_0}[1+(\alpha x/c)e^{\alpha t}-(\alpha x/c)e^{(\alpha t+\alpha/\nu_0)}]$$

or

$$\delta[\equiv 1/\nu]=1/\nu_0-(1/\alpha) \ln [1+(\alpha x/c)e^{\alpha t}(1-e^{\alpha/\nu_0})].$$

For small values of α this readily reduces to $(\nu_0-\nu)/\nu_0=\alpha x/c$ in agreement with (6).

It might seem that when dealing with such a medium one would obtain the appropriate differential equation by using the equation for constant velocity and inserting a variable velocity so the equation takes the form $\ddot{y}=c^2e^{-2\alpha t}y''$. The situation, however, is not as simple as this. By change of variables and their separation one finds the solution of the form,

$$y=(A \sin nx+B \cos nx)J_0(nc/\alpha)e^{-\alpha t}.$$

This solution, in which n is a constant of the nature $2\pi/\lambda$, involves a Bessel function of zero order and is the only place where t enters. This particular solution does not fit the boundary conditions in our problem, as is especially noticeable for $x=0$ at S. Nor is it easy to see how the above solution may be made to represent a monochromatic wave at $x=0$.

General Differential Equation

The treatment leading to Eqs. (11) and (12) has been for a special velocity function and for electromagnetic phenomena but one may now pass to a more general case, following a procedure analogous to that found in many treatises on wave motion in a medium of constant velocity in which the disturbance is taken as of the form $y=f(x-vt)$. Here the velocity is not constant and so vt must be replaced by $\int v dt$ and our wave function becomes $y=f(x-\int v dt)$.

Then $\quad \dot{y}=vf' \qquad y'=f'$

$$\ddot{y}=v^2f''+\dot{v}f' \qquad y''=f'',$$

$$\therefore \quad \ddot{y}-(\dot{v}/v)\dot{y}=v^2y'', \tag{16}$$

or $$\ddot{y}=v^2y''+vy' \tag{16′}$$

and either of these is the general differential equation of a wave in a medium with velocity a function of time, without regard to what that function may be.

If the velocity function is that of (1) then (16) and (16′) reduce, respectively, to

$$\ddot{y}+(\alpha/1-\alpha t)\dot{y}=v^2y''=c^2(1-\alpha t)^2y''$$

and $$\ddot{y}=v^2y''-\alpha v_0y'=c^2(1-\alpha t)^2y''-\alpha cy'.$$

If, on the other hand, the velocity function is that of (2), then (16) reduces readily to (11).

On the Nuclear Spins and Magnetic Moments of the Principal Isotopes of Potassium[1]

SIDNEY MILLMAN, *Columbia University*

(Received April 1, 1935)

The spin of the K^{39} nucleus and the hfs separation of the $^2S_{\frac{1}{2}}$ normal state were measured by the deflection of a beam of neutral atoms in a weak inhomogeneous magnetic field, produced by a system of parallel wires carrying current. To attain the required resolution narrow beams and long beam paths (141 cm) were used. The nuclear spin of K^{39} was found to be 3/2. The hfs separation, $\Delta\nu$, of the normal state was measured by the method of "zero moments," which utilizes the fact that the magnetic moment of the atoms in some of the magnetic levels vanishes at certain values of the magnetic field. A plot of the variation of intensity at the center of the pattern with respect to field yields distinct maxima at these fields. If the magnetic field is known the hfs separation can be deduced with accuracy. The value of $\Delta\nu$ was found to be 0.0152 ± 0.0006 cm^{-1}. Using the modified Goudsmit formula, one obtains the value of 0.39 for the nuclear magnetic moment (in units of $\mu_0/1838$). The resolution was sufficient to resolve a "peak" due to K^{41} by the method of "zero moments." The nuclear spin was found to be greater than 1/2, and the ratio of the magnetic moments μ_{41}/μ_{39} was found to be between the limits of 0.42 and 0.88 depending on the spin of K^{41}.

INTRODUCTION

THE two isotopes of potassium, K^{39} and K^{41}, have very small nuclear magnetic moments. For this reason spectral methods[2] used up to the present have failed to determine the spins of these nuclei. Until recently nothing was known of the hyperfine structure separation of the normal $^2S_{\frac{1}{2}}$ state of K^{39} other than the fact that it was small, with $\Delta\nu$ less than 0.02 cm^{-1}. However, the measurements of Loomis and Wood[3] on the alternating intensities of the band spectra of the K_2 molecule showed that the K^{39} nucleus must possess a spin other than zero. Concerning the corresponding properties of K^{41} no information was available. The present investigation had for its object the application of the methods of molecular beams to determine the nuclear spin of K^{39}, to measure the hyperfine separation of the normal state of K^{39} and to obtain information about the corresponding properties of K^{41}. These methods have already been applied with decisive results to determine the nuclear spins of sodium[4] and caesium.[5]

METHOD

The experimental method utilizes the fact that an alkali atom in the normal $^2S_{\frac{1}{2}}$ state and possessing nuclear spin i has some magnetic levels in which the moment of the atom becomes zero at definite values of the magnetic field. In such fields these atoms are not deflected in an inhomogeneous field. From the number of such levels and the values of the field at which they possess this property we can obtain both the spin of the nucleus and the hyperfine structure separation $\Delta\nu$ of the normal state.

The force on an atom in the normal $^2S_{\frac{1}{2}}$ state possessing nuclear angular momentum i, in units of $h/2\pi$, situated in an inhomogeneous magnetic field is given by.[6]

$$F_y=\pm\frac{2m/(2i+1)+x}{[1+(4m/(2i+1))x+x^2]^{\frac{1}{2}}}\mu_0\frac{\partial H}{\partial y}=f_m\mu_0\frac{\partial H}{\partial y}, \quad (1)$$

$$x=2\mu_0 H/hc\Delta\nu. \quad (2)$$

$\Delta\nu$ is the energy difference in wave numbers between the two states with total angular momentum $F=i+\frac{1}{2}$ and $F=i-\frac{1}{2}$, m is the total magnetic quantum number, the projection of F along H, and f_m is the effective magnetic moment

[1] A preliminary report on the spin and magnetic moment of K^{39} was submitted earlier. Millman, Fox and Rabi, Phys. Rev. **46**, 320 (1934).

[2] Schuler and Bruck, Zeits. f. Physik **58**, 735 (1929); Frisch, Physik. Zeits. Sowjetunion **1**, 302 (1932); Frisch, Physik. Zeits. Sowjetunion **4**, 557 (1933).

[3] Loomis and Wood, Phys. Rev. **38**, 854 (1931); Loomis, Phys. Rev. **38**, 2153 (1931).

[4] Rabi and Cohen, Phys. Rev. **46**, 707 (1934).

[5] Cohen, Phys. Rev. **46**, 713 (1934).

[6] Breit and Rabi, Phys. Rev. **38**, 2082 (1934).

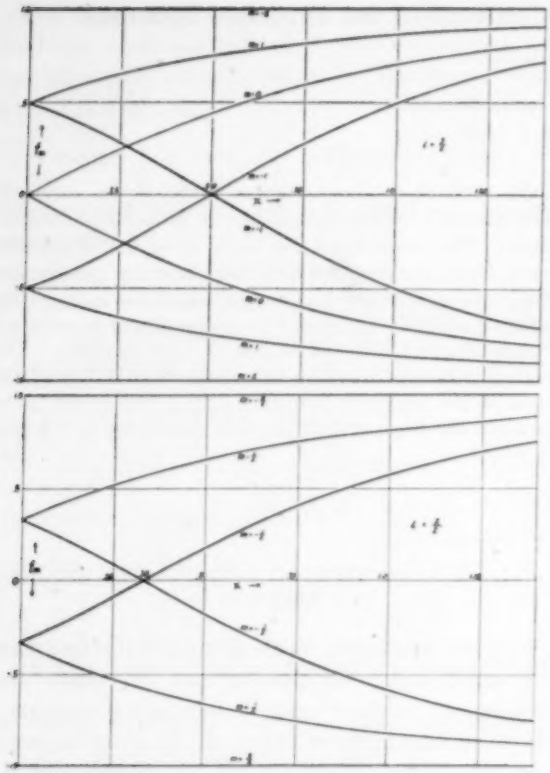

FIG. 1. Variation of effective magnetic moment, in units of μ_0 the Bohr magneton, of each magnetic level with $x=2\mu_0 H/hc\Delta\nu$ for $i=2/2$ and $i=3/2$.

of the atom (with quantum number m) in units of μ_0, the Bohr magneton.

For values of x much greater than 1 the f_m's approach the values ± 1, the same as for $i=0$ and thus all effects of nuclear spin are lost, to within the precision of experiments of this type. For potassium this occurs at fields as low as 300 gauss. Strong effects due to nuclear spin are obtained only in the region where x is less than 1. This is shown in Fig. 1 where the f_m's are plotted as a function of x for nuclear spins 2/2 and 3/2. In particular $f_m=0$ when

$$x=-2m/(2i+1), \quad [-(i-\tfrac{1}{2})\leqq m\leqq 0]. \quad (3)^*$$

When $i>\frac{1}{2}$ there are values of x other than zero for which Eq. (3) is satisfied. Thus for certain values of H atoms of magnetic quantum number m satisfying Eq. (3) will have zero moment. If a beam of potassium atoms is allowed to traverse an inhomogeneous magnetic field all atoms possessing a magnetic moment other than zero will be deflected while atoms with zero moment will not be deviated from their paths. Hence if we station our detector in the beam and increase the field beginning with zero the number of atoms arriving at the detector will decrease (since $\partial H/\partial y$ increases with increasing H) until we get to the region of the field where some states have zero moment (Eq. (3)) when the intensity will rise to a maximum and decrease again for higher values of the field.

For either of the two spins mentioned we get only one maximum at a field other than zero. For H zero the intensity is at a maximum for any spin, since there is no deflection of atoms of any state when $\partial H/\partial y=0$. Thus the mere determination of the number of maxima is not sufficient to define the spin. For example, one maximum implies a spin of either 2/2 or 3/2, two maxima, 4/2 or 5/2, etc. However when there are two or more maxima one can determine the spin from the relative values of the field at which these peaks occur. If there is only one peak we resort to analysis of the intensity distribution with respect to field at a position of zero deflection as well as to the analysis of the Stern Gerlach patterns at some definite value of the field.

In view of the known fact that $\Delta\nu$ of K^{39} is less than 0.02 cm^{-1} the region $x<1$ corresponds to a field of less than 200 gauss. Since it was quite possible that $\Delta\nu$ was considerably less than that amount the apparatus had to be designed to attain a considerable deflection in fields as low as 5 gauss.

The deflection in the y direction of an atom in an inhomogeneous magnetic field is given by

$$s_m=(f_m/2Mv^2)(l_1^2+2l_1l_2)\mu_0\partial H/\partial y, \quad (4)$$

where l_1 is the length of the magnetic field and l_2 is the distance between the end of the field and the detector. The deflection of an atom with kinetic energy kT is

$$s_{om}=(f_m/4kT)(l_1^2+2l_1l_2)\mu_0\partial H/\partial y. \quad (5)$$

* Relations (1) and (3) are true for the case of normal hyperfine splitting (magnetic moment in the direction of the spin vector). If the splitting is inverted (magnetic moment pointing in opposite direction to that of the spin) we must substitute $-m$ for m. This method cannot distinguish between the two cases.

For an undeflected beam of trapezoidal shape the intensity at any point in the deflection pattern is given by

$$I=\frac{I_0}{d-p}\frac{1}{2(2i+1)}\sum_m[(s+d)e^{-s\alpha_m/(s+d)} + |s-d|e^{-s\alpha_m/|s-d|}-(s+p)e^{-s\alpha_m/(s+p)} - |s-p|e^{-s\alpha_m/|s-p|}], \quad (6)$$

where I_0 is the intensity at the center of the undeflected beam with the field zero, $2d$ is the width of the lower base of the trapezoid, $2p$ that of the upper base, and s is the distance of the point from the center of the original beam. For $s=0$, Eq. (6) reduces to

$$\frac{I}{I_0}=\frac{1}{(d-p)(2i+1)}\sum_m[de^{-s\alpha_m/d}-pe^{-s\alpha_m/p}]. \quad (7)$$

It is clear from (7) that if in the region of a maximum the contribution to the intensity is to come mainly from the atoms of zero moment we must have s_α for the atoms with nonvanishing moments large compared to d. Since the value of the field is limited and it is impracticable to extend the ratio of gradient to field indefinitely and since it is difficult to work with slits less than 0.01 mm wide, recourse must be had to lengthening the beam to obtain the desired resolution.

Apparatus

A schematic diagram of the apparatus is shown in Fig. 2(A). The oven, A, is identical in design with that used by Rabi and Cohen.[4] It is supported by three steel pegs mounted on a dovetail slide so that the oven can be moved and accurately replaced. On the same slide is mounted the slit B, which can be used as a collimating slit. However, in this experiment it was used as a fore slit. The oven slit is about 0.013 mm wide and that of B about 0.2 mm. The distance between the oven slit and fore slit is 18.4 cm. The slit C, about 0.15 mm wide, separates the oven chamber from the receiving chamber, permitting a difference in pressure in the two chambers to exist during a run. The chambers are made of brass cylinder $4\frac{1}{2}''$ O.D. and $\frac{1}{8}''$ thick and are pumped out separately by Apiezon B oil diffusion pumps. Because of the gas coming out of the heated oven the pressure in this chamber is not much better than 2×10^{-6} mm while in the receiving chamber it is about 7×10^{-7} mm. The pressure in the oven chamber is measured with a McLeod gauge while that in the receiving end is measured with both a McLeod and an ionization gauge.

The collimating slit, D, is made movable by mounting it on a ground joint. The slit width was generally kept at 0.02 mm. The block E holding the field wires is made of duralumin. At the end nearest the collimating slit it is held in place by a knife-edge at the bottom and is pressed against another knife-edge at the back by means of screws. The block is made to pivot about this end by supporting the other end on round-headed screws against which it is held by springs. The motion toward or away from the beam is achieved by rotating one of the supporting screws through a ground joint. The distance between the oven slit and the detector, G, is 141 cm and between the oven and collimating slits is 31.1 cm. The length of the field is 61.5 cm and the field free distance is 46 cm. The beam is detected by the surface ionization method[7] with a one mil tungsten filament, G, mounted eccentrically on a ground joint. The positive ion current is collected by the plate H and amplified by an FP-54 electrometer through a resistance of 2×10^{10} ohms.

The inhomogeneous magnetic field is obtained from a system of parallel wires carrying current, as used by Rabi, Kellogg and Zacharias.[8] Fig. 2(B) shows a cross section of the duralumin block holding the wires. Here we have four wires instead of two. The outer wires are separated from the inner wires by mica strips and can be used separately. Thus when there is no current in the inner wires the field is exactly that used by R.K.Z. giving a ratio of $\partial H/\partial y$ to H of about 8 to 1 for the given diameter of the wires. If the inner wires are also used ratios as large as 11 to 1 and better homogeneity in H along the height of the beam are obtained. Fig. 3 gives a set of curves for both systems of conductors. For the four wire system I refers to the current in the outer wires (nearer the

[7] Taylor, Zeits. f. Physik **57**, 242 (1929).
[8] Rabi, Kellogg and Zacharias, Phys. Rev. **46**, 157 (1934).

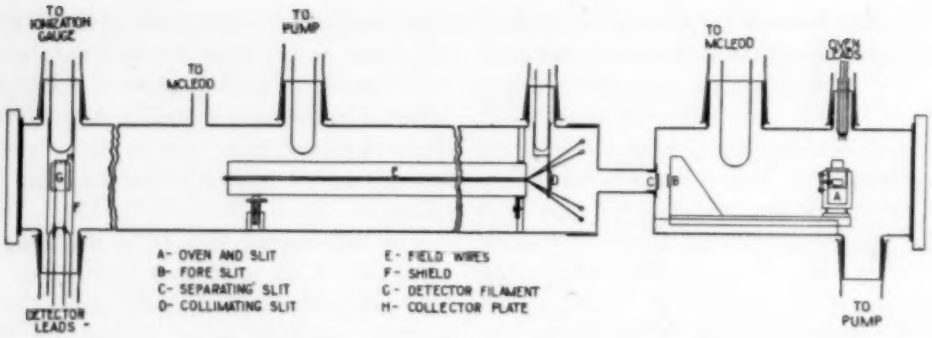

(A)

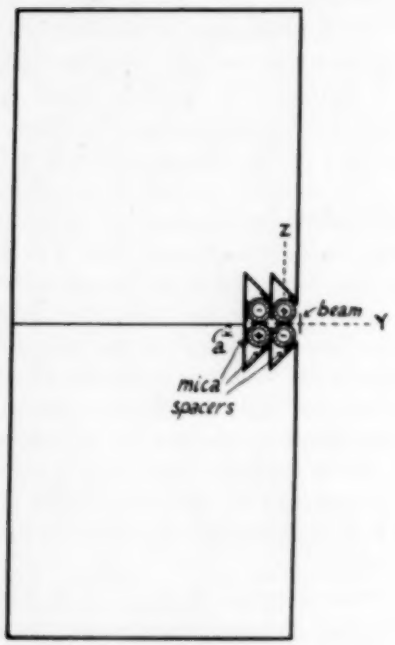

(B)

FIG. 2(A) Diagram of apparatus. (B) Cross section of field block showing wire arrangement. + and − indicate opposite directions of current.

beam). For the cases $y=1.2a$ and $y=1.3a$ the current in the inner wires is $2.0\times I$ while for $y=1.4a$ this current is $2.2\times I$. The four wires are so arranged that their centers form a square of side $2a$. The value of a is 0.124 cm. The height of the beam in the field is limited by stops at each end to 1 mm, and over this region H and $\partial H/\partial y$ in the two wire system are constant to about 1 percent. All wires are hollow permitting cooling by water.

Although the four wire system was used during the course of the experiments whenever additional resolving power was required and proved to be of great aid in finding the K^{41} peak, the experimental curves reported in this paper were obtained with the two wire system.

The distance of the beam from the wire surfaces is determined in the following manner: The edge of a slit jaw, used as a fiduciary mark is attached rigidly to the oven end of the duralumin block and with the aid of a microscope is set at any desired distance from the wire surfaces. A telescope is then set up with its axis parallel to the line determined by the fiduciary mark and the center of the fore slit B. With the cross hair set at the fiduciary mark the collimating slit is moved until the center of the slit coincides with the cross hair. This fixes the distance at the oven end. The distance at the detecting end is obtained by mounting a two mil tungsten filament, parallel to the collimating slit, at the desired distance from the wire surfaces. When the original undeflected beam is obtained the detector is set at the center of the beam and the field block is moved until the filament stops the beam. The filament is then burned away.

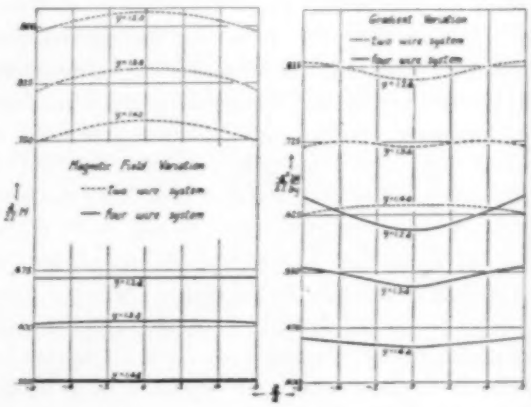

FIG. 3. Variation of magnetic field and gradient with position for two and four wire systems.

Procedure

A freshly-cut piece of potassium is placed in the oven and the system immediately evacuated. The oven temperature is raised at the rate of two degrees a minute to 325°C, reduced to about 300°C and stabilized. When conditions are steady an investigation of the undeflected beam is made by moving the detector in steps of about 0.02 mm and observing the corresponding beam intensity. The shape of the beam is in general in good agreement with that calculated from the slit widths and distances. The detector filament is then placed in the center of the beam and the intensities corresponding to different values of the applied magnetic field are observed.

A typical curve showing the variation of intensity at the center of the beam with respect to current in the field wires is shown in Fig. 4(A). At 63.3 amp. there is a fairly sharp peak having an intensity of 22.8 percent of that of the original undeflected beam. This ratio is accurately determined by taking alternate readings with field on and field off. The intensity at the region of 42 amp. is less than 3 percent. The irregularity in the curve at C is due to K^{41} as will be shown later. Fig. 4(B) is a plot of this region on a more suitable scale.

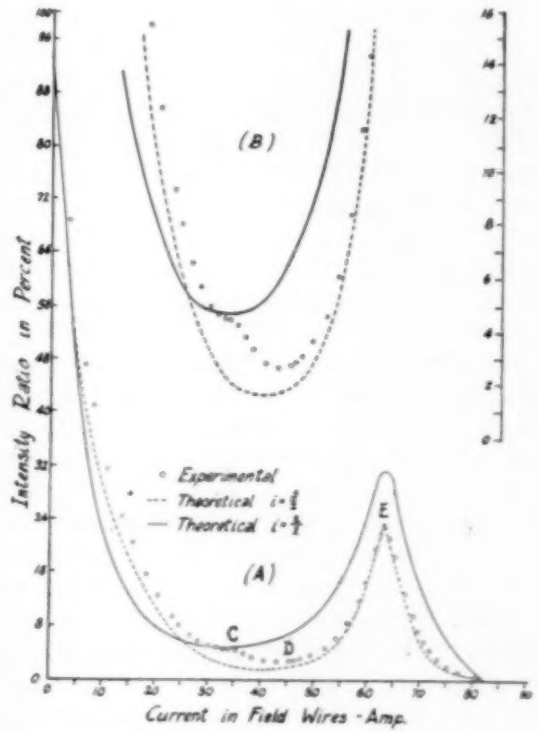

FIG. 4. (A) Variation of beam intensity with field at the position of zero deflection. 1 ampere = 1.29 gauss. (B) A portion of 4(A) with ordinates plotted to a larger scale to show the effect of K^{41} at C.

It is also of interest to obtain the deflection patterns for certain values of the field. This is done by keeping the current in the field wires constant and measuring the intensity at various points by moving the detector across the beam. Fig. 5 (full line) and Fig. 6 (circles) show deflection patterns taken in this manner.

Results

Nuclear spin of K^{39}

The smooth course of the curve of Fig. 4(A) excludes the possibility of a second peak of comparable size in the region of lower fields. From the theory of the experiment such a peak could occur only at values of the current equal to 31.6 amp. or 21.1 amp. Although the curve was carefully extended to above 200 amp. no other peak was found. Since K^{39} is present to the extent of over 90 percent these facts alone limit the spin of the K^{39} nucleus to either 2/2 or 3/2. To decide between the two possible values we resort to further analysis of the curves.

The theoretical value for the ratio I_w/I_0 of the intensity at the peak to that of the total beam intensity due to this isotope is $1/(2i+1)$, since there are in general $2(2i+1)$ different magnetic states of the atom, each equally probable, and the peak represents a place where two of these states have zero moment (Fig. 1). The deflection pattern at this value of the field is in fact a superposition of an undeflected beam of the same shape as the original beam, due to atoms with zero moment, on a deflected pattern due to the other components. This is clearly shown in Fig. 5. For a spin of 3/2, I_w/I_0 should be $\frac{1}{4}$ and for 2/2 the value for I_w/I_0 should be $\frac{1}{5}$. If we take the value 93.3 percent for the abundance of K^{39} as given by Brewer and Kueck[9] the intensity ratio at the maximum should be 23.3 percent for $i=3/2$ and 31.1 percent for $i=2/2$. The highest experimental ratio obtained is 22.8±0.4

[9] Brewer and Kueck, Phys. Rev. 46, 894 (1934).

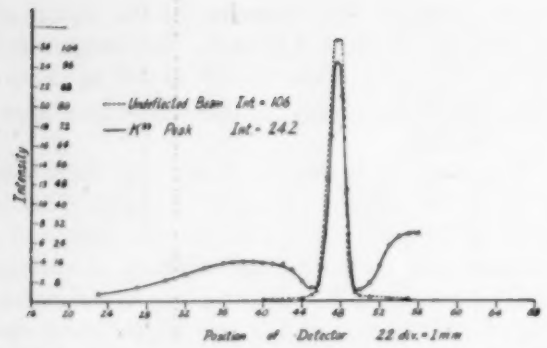

FIG. 5. Deflection pattern taken with field current equal to 63.3 amperes, the value at the peak at E, Fig. 4(A). The dotted curve is the beam with field off plotted to 1/4 the scale of the deflection pattern.

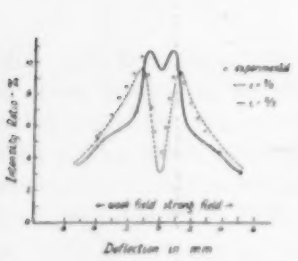

FIG. 6.

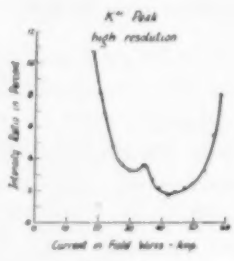

FIG. 7.

FIG. 6. Deflection pattern taken at field current corresponding to D of Fig. 4(A).
FIG. 7. Experimental curve as in Fig. 4 in region of K^{41} peak with high resolution.

percent, in good agreement with the theoretical ratio for a spin of 3/2 but not with the expected value for a spin of 2/2. Because of experimental errors in setting the field wires parallel to the beam by the method described above, a supplementary method must be employed to secure this result. The direction between the beam and field wires is varied in small steps by moving the collimating slit. At each stage the intensity at the peak is noted until the maximum ratio is obtained. This condition is easily reproducible. The value 0.228 was thus reproduced within the error stated in six distinct runs. Values lower than this ratio, ranging from 21 percent up, were obtained when the beam was not accurately parallel to the field wires.

Although different experimenters are not in agreement as to the abundance of K^{39}, Dempster[10] giving a value of 95 percent and Bainbridge[11] 92.6 percent, the differences are not of sufficient magnitude to weaken seriously the conclusions we draw from the intensity ratio at the peak.

Eqs. (1), (2), (5) and (7) will yield the intensities at points of zero deflection for various values of the current in the field wires if the relation between the parameter x and the current I is known. Since H is proportional to the current we may write $x=CI$. The position of the peak in the curve gives the proportionality factor C if the nuclear spin is known. For a spin of 3/2 the peak occurs at $x=\frac{1}{2}$ and for a spin of 2/2 the maximum is at $x=\frac{1}{3}$. Calculations are made by assuming each possibility in turn. A comparison between the calculated and observed curves is shown in Fig. 4. The calculated curves do not include the K^{41} isotope, i.e., the value of I/I_0 as calculated from Eq. (7) is multiplied by 93.3 percent, the assumed abundance of K^{39}. We see that the general shape of the experimental curve at the position of the peak as well as at the minimum region is in much better agreement with the calculated curve for a spin of 3/2 than with that for a spin of 2/2.

This method of deciding between the two spins is not particularly sensitive to errors in temperature, field gradient, or beam shape. Curves were calculated for both spins, with the individual s_{a_m}'s altered by ± 10 percent. It was found that although the intensity at any given value of the current changed, the shape of the curves changed very little, so that the calculated curves for $i=3/2$ were still in much better agreement with the experimental curve than those for $i=2/2$.

The deflection pattern taken at a field corresponding to point D in Fig. 4 offers another source of evidence for deciding between the two possible spins. Eqs. (1), (2), (5) and (6) can be applied to calculate the intensity at any distance from the center of the original pattern if the spin is known. There was no effort made in these experiments to obtain conditions such that the intensity calculations could be made with very high accuracy (accurate measurement of temperature, beam shape, etc.). We note in Fig. 6 that the general course of the experimental points bears little resemblance to the calculated curve for a spin of 2/2, but is in good agreement with the calculated curve for a spin of 3/2.

[10] Dempster, Phys. Rev. **20**, 631 (1932).
[11] Bainbridge, J. Frank. Inst. **212**, 317 (1931).

It should be mentioned that although K_2 molecules were looked for by the method of Lewis[12] no central peak greater than 0.4 percent of the total intensity was found at fields sufficiently high for the resolution of such a peak (120 gauss). This may be due to the following:

(1) Nonequilibrium conditions in the oven, due to temperature gradients between the oven slit and the interior, which would cause the dissociation of the molecules. This is the most likely reason since the oven heaters were closest to the slit.

(2) Because of the greater mass and larger cross section of the molecules they may have been scattered out of the beam to a far greater proportion than the atoms.

(3) The nuclear moment due to the molecular rotation[13] may have been sufficiently great to cause the molecules to be deflected.

Accordingly no corrections due to molecules have been made in any of the above calculations. However, even if one assumed that molecules were present to the extent found by Lewis (about 2 percent) they would have had no effect on the final results of these experiments.

$\Delta\nu$ of the $^2S_{\frac{1}{2}}$ state of K^{39}

With the value of the spin definitely fixed at 3/2, we may obtain at once the hyperfine structure separation $\Delta\nu$ of the normal $^2S_{\frac{1}{2}}$ state of K^{39} from Eq. (2). The value of the field at the peak is 81.5 gauss and therefore

$$\Delta\nu = 0.0152 \pm 0.0006 \text{ cm}^{-1}.$$

This is based on the determination of the distance of the beam from the field wires by the method described in the section under "Apparatus." In subsequent adjustment of parallelism of the beam to the wires the position of the beam with respect to the field wires is calculated from the measured value of the current at which the peak occurs.

The chief source of error is geometrical, incident to fixing the position of the beam relative to the field wires. The determination of $\Delta\nu$ is not affected by any errors in the measurement of temperature, field gradient, or beam shape. Neither does it depend on the assumption of Maxwellian distribution of velocities of the atoms in the beam. The value here reported is somewhat higher than the result 0.0147 cm^{-1} announced in the first report. The error in the latter determination was due to a shift in the collimating slit which was discovered when the apparatus was taken apart. In the subsequent experiments such a possibility was eliminated.

An independent measure of $\Delta\nu$ was obtained in the following manner. Sodium was substituted for potassium in the oven, and the peak located. Since the spin of sodium is the same as that of K^{39} the ratio of the value of the current at the peak for sodium to that of K^{39} is the same as the ratio of their respective $\Delta\nu$'s. With the value of 0.0583 for $\Delta\nu$ of sodium,[14] the value of 0.0151 was obtained for $\Delta\nu$ of K^{39}. The constancy of the geometrical factors was checked by sandwiching the sodium run between two potassium runs.

If we apply the formula of Goudsmit,[15] as modified by Fermi and Segrè,[16] for computing nuclear magnetic moments, using the value 3/2 for the spin of K^{39} and 0.0152 for $\Delta\nu$ we get

0.39 nuclear Bohr magnetons

for the magnetic moment of the K^{39} nucleus.

K^{41}

The experimental methods under consideration which have been applied to K^{39} are equally applicable, if sufficient resolution is obtained, to a mixture of isotopes. Since the value of the field at which the zero moments will occur for these isotopes will in general be different, one will obtain sets of peaks in a curve such as Fig. 4(A) corresponding to the different isotopes.[17] This is also true for a mixture of elements. In Fig. 4 the break in the curve at C can only be due to K^{41}. Under higher resolution, obtained by narrowing the slits to 0.012 mm, this break becomes a peak, as shown in Fig. 7, which is always found in the same place on the curve. This peak cannot be due to K^{39} because the intensity is too weak, and the peak is in the wrong position on the curve. It cannot be ascribed to contaminations by other alkali atoms since a pure

[12] Lewis, Zeits. f. Physik **69**, 786 (1931).
[13] Wick, Zeits. f. Physik **85**, 25 (1933); Estermann and Stern, Zeits. f. Physik **85**, 17 (1933).
[14] Granath and Van Atta, Phys. Rev. **44**, 935 (1933).
[15] Goudsmit, Phys. Rev. **43**, 636 (1933).
[16] Fermi and Segrè, Zeits. f. Physik **82**, 729 (1933).
[17] Rabi, Phys. Rev. **47**, 334 (1935).

tungsten surface at low temperature is capable of detecting only potassium, rubidium and caesium, and peaks due to rubidium and caesium cannot occur at such low field values. In fact the peak cannot be due to any impurities since there was no noticeable change in relative intensity after the oven had been heated for more than ten hours.

The height of the K^{41} peak is somewhat over 1 percent of the original beam. For such low intensities, it is difficult to apply the same considerations that have aided us in determining the spin of K^{39}. In the first place, due to insufficient resolution we cannot be certain that this is the only peak. Moreover, an accurate analysis of the course of the curve at the peak is not possible because of the presence of K^{39} to an extent which cannot be accurately calculated because of errors in the field gradient, temperature, and shape of original beam. However, we can state quite definitely that the spin of the K^{41} nucleus is greater than $\frac{1}{2}$, and that the ratio of the magnetic moment of the K^{41} nucleus to that of the K^{39} nucleus can be put between the limits

$$0.42 < \mu_{K^{41}}/\mu_{K^{39}} < 0.88,$$

depending on the spin.

Discussion

While this work was in progress, Jackson and Kuhn[18] succeeded in measuring the hyperfine structure separation of the resonance lines of K^{39} in absorption using a molecular beam to cut down the Doppler effect. The value which they calculated for $\Delta\nu$ of the normal state of K^{39} is 0.0152 cm^{-1}, in excellent agreement with our result for $\Delta\nu$. They did not succeed in determining the spin uniquely, but infer from their judgment of intensity of the hyperfine structure lines that the spin of the K^{39} nucleus is probably greater than 3/2. It is clear from our experiments that the spin of K^{39} cannot be greater than 3/2. It should be pointed out that this independent measure of $\Delta\nu$ from hyperfine structure may be used in our experiment as an additional source of evidence in deciding between a spin of 3/2 and 2/2. Inserting in Eq. (2) this value of $\Delta\nu$ and the value of the field at the peak we obtain at once the value of 0.50 for x at the peak and therefore $i = 3/2$.

The theory of our experiment depends on the cosine law of interaction between the angular momentum vectors of the nucleus and the external electrons. The value of $\Delta\nu$ which we obtain is a consequence of this assumption. The $\Delta\nu$ as measured by hyperfine structure is practically independent of this assumption. It is therefore interesting to note that the excellent agreement between the deflection and spectroscopic values for $\Delta\nu$, despite the fact that the magnetic moment of K^{39} is quite small, is strong evidence for the cosine law of interaction in the case of K^{39}.

In conclusion, the writer wishes to express his indebtedness to Professor I. I. Rabi for suggesting the problem and following these experiments with keen interest and helpful discussions, to Mr. Marvin Fox for his invaluable assistance throughout the course of the research, and to his other colleagues in the molecular beam laboratory for many helpful suggestions.

[18] Jackson and Kuhn, Proc. Roy. Soc. **A148**, 335 (1935).

Theory of Disintegration of Nuclei by Neutrons[1]

H. A. BETHE, *Cornell University*

(Received March 26, 1935)

The large probability of nuclear disintegration by slow neutrons as well as the large cross section for the elastic scattering of slow neutrons can be explained without any new assumption. Interaction between neutron and nucleus is assumed to be only present when the neutron is inside the nucleus or very near its boundary. The rate of change of the potential energy of the neutron at the boundary of the nucleus is important for the quantitative, but not for the qualitative results; in agreement with other data, it has been assumed that the potential drops to $1/e$ in a distance $1.5.10^{-13}$ cm (range of the forces between neutron and nucleus).

The large disintegration cross sections are due to two factors. The first is elementary: the cross section is inversely proportional to the neutron velocity, because a slow neutron stays longer in the nucleus. The second factor is $1/\sin^2\varphi_0$, where φ_0 is the phase of the neutron wave function at the nuclear boundary. This resonance factor explains the large differences between the cross sections of different elements. φ_0 cannot be predicted theoretically, but reasonable assumptions lead to agreement with experiment. The resonance factor occurs in all phenomena with slow neutrons; therefore large capture cross sections should always be accompanied by large elastic scattering. The explanation of the large neutron cross sections on the basis of ordinary wave mechanics makes one confident in the applicability of orthodox quantum theory in nuclear phenomena.

1. Elastic scattering. May be large for slow neutrons because of resonance. Magnitude is 5.10^{-24} cm² without, 10^{-22} and more with resonance. If present, large cross section persists up to neutron energies of 10,000 or 100,000 volts.

2. Capture with emission of γ-rays. Cross section large for slow netrons. About half the elastic scattering cross section for gas-kinetic energy. Cross section inversely proportional to neutron velocity. All capture effects observed should be due to admixtures of slow neutrons in the incident beam. Capture only possible, if unoccupied neutron level with angular momentum $l=1$ exists in the nucleus.

3. Disintegration with emission of α-particles. Very probable for slow neutrons if exothermic process, which is usually the case. Cross section for gas-kinetic neutrons and light nuclei 10^{-21} cm² without resonance, for $Z=11$ same cross sections as for fast neutrons (10^{-25} cm²). May be increased by resonance which may occur as well for neutrons as for α-particle. Cross section inversely proportional to neutron velocity up to neutron energies of some 100,000 volts, then cross section increases again because faster α-particles penetrate more easily through nuclear potential barrier. Disintegration by slow neutrons should stop at $Z\approx 16$, by fast ones at $Z\approx 27$, the latter in agreement with experiments.

4. Disintegration with emission of protons. Always endothermic, therefore impossible with slow neutrons. With fast neutrons, cross section $\approx 10^{-25}$ cm² up to $Z\approx 20$. Weak effects should be observable up to $Z=40$, in case of resonance even to 60.

5. Excitation of nucleus without capture of neutron or emission of particles. Should have cross section of the order 10^{-25} cm² independent of atomic number. Possible only for nuclei with suitable excited states and for fast neutrons.

1. INTRODUCTION

FERMI and his collaborators[2] have shown that neutrons, especially slow ones, are very effective in disintegrating nuclei. It is generally accepted that for the heavier nuclei the disintegration process consists in a simple capture of the neutron by the nucleus with the emission of a γ-ray. Indeed, it seems inconceivable that a heavy nucleus could emit a charged particle (proton or α-particle) if bombarded with neutrons, since the particle could never escape from the nucleus because of the potential barrier surrounding it (cf. paragraph 5 of this paper).

The cross sections for the capture of the neutron are surprisingly high, some of them amounting to 10^{-22} cm² and more for slow neutrons. On the basis of naïve considerations, one would expect cross sections of only about 10^{-25} cm². For, if the neutron hits the nucleus, the probability of its radiating is about 1 in 10,000 according to ordinary radiation theory; on the other hand, the (geometric) cross section

[1] This paper in its essential parts has been presented at the February Meeting of the American Physical Society, in place of a previous paper printed in the Abstracts of that meeting (Phys. Rev. **47**, 640 (1935)), which I had realized at the time of the meeting to be an unsuccessful attempt. Subsequently I received from Professor Fermi a manuscript of a paper submitted to the Royal Society, containing the same explanation of the large cross sections as the present paper.

Added in proof: Perrin and Elsasser (Comptes rendus **200**, 450 (1935)) came to the same conclusions concerning the large cross sections of slow neutrons; and an attempt in the same direction has been made by Beck and Horsley (Phys. Rev. **47**, 510 (1935)).

[2] E. Fermi, E. Amaldi, O. D'Agostino, F. Rasetti and E. Segrè, Proc. Roy. Soc. **A146**, 483 (1934).

of the nucleus is of the order 10^{-24} cm^2. The naïve theory thus gives a cross section about a million times too small.

We want to show in this paper that a straightforward application of wave mechanics leads to cross sections of just the right magnitude. Furthermore, long distance forces between neutron and nucleus are not required, it being assumed that the interaction is appreciable only when the neutron is inside the nucleus.

2. Wave Function of Slow Neutrons

Since the most interesting phenomena seem to occur with slow neutrons, we shall consider primarily neutrons with kinetic energies well below a million volts. For these neutrons, the de Broglie wavelength $2\pi\lambda$, *viz.*

$$\lambda=\frac{\hbar}{(2ME)^{\frac{1}{2}}}=\frac{4.54\cdot 10^{-10}}{E^{\frac{1}{2}}}\text{ cm}. \tag{1}$$

(E measured in volts) is large compared with the radius of the nucleus. The radius of a nucleus with medium atomic weight (about 100) being about 7.10^{-13} cm, our condition $\lambda>r_0$ is fulfilled for neutron energies below half a million volts.

Neutrons of a given angular momentum l pass the nucleus in general at a distance of the order $l\lambda$. For slow neutrons of, say, 1000 volts energy or less, there is therefore no chance of getting into the nucleus, if they have an angular momentum different from zero, since their distance of closest approach would be at least 30 times larger than the nuclear radius. Even if there is a resonance level for the neutron with $l=1$, it has no appreciable effect on the scattering or capture of slow neutrons (see Appendix 1). Therefore we need only consider the spherically symmetrical part of the wave function of the incident neutron, i.e., the part corresponding to $l=0$. The slow neutrons reaching the nucleus are consequently in an "s-state."

The wave function of the neutron at large distances from the nucleus can be written in the familiar form

$$\psi=(1/v^{\frac{1}{2}})e^{ikz}+\text{scattered wave},$$

ψ represents a stream of neutrons traveling in the z direction and is normalized per unit current, and

$$k=1/\lambda=Mv/\hbar=(2ME)^{\frac{1}{2}}/\hbar. \tag{2}$$

ψ can be expanded in spherical harmonics:

$$\psi=\frac{1}{v^{\frac{1}{2}}}\sum_{l=0}^{\infty}\frac{\psi_l(r)}{r}P_l(\vartheta), \tag{3}$$

r being the distance between nucleus and neutron. For $l\neq 0$, ψ_l has practically the same form far from the nucleus as if the neutron was entirely free, i.e., not influenced by the nucleus, for the reason given above. For $l=0$, the radial wave function satisfies the Schrödinger equation

$$d^2\psi_0/dr^2+2M/\hbar^2(E-V)\psi_0=0. \tag{4}$$

V is the potential energy of the neutron in the field of the nucleus.

Outside the nucleus, ($V=0$), the solution of (4) is

$$\psi_0=\sin(kr-\delta)/k. \tag{5}$$

It is properly normalized so as to fulfill (3). The phase shift δ determines the cross section for elastic scattering

$$\Phi_{el}=4\pi\sin^2\delta/k^2, \tag{6}$$

if, as we have supposed, only the partial wave $l=0$ contributes to the scattering.

Inside the nucleus, the neutron has a large negative potential energy V, of the order of some million volts. Its magnitude may be estimated from the binding energy of neutrons in the nucleus (cf. Appendix 2). From the number of neutrons present in the nucleus, one should expect the existence of 3 or 4 bound s-states for a neutron inside a medium-weight nucleus like, e.g., Ag. Correspondingly, the wave function of a neutron with small positive energy will oscillate several times inside the nucleus (3 to 5 complete oscillations for Ag). Therefore the wave function can be represented by the WKB (Wentzel-Kramers-Brillouin) solution:

$$\psi_0(r)=C(y(r))^{-1}\cos\varphi(r) \tag{7}$$

for $r<r_0$ (r_0 = radius of the nucleus). Here

$$y(r)=[2M(E-V(r))]^{\frac{1}{2}}/\hbar$$
$$\varphi(r)=\int^{r}y(\rho)d\rho. \tag{8}$$

At the boundary r_0 of the nucleus the potential V is known to drop rather suddenly to zero. We shall assume an *infinitely* sudden potential change from the value $-V_0$ inside the nucleus to zero. The influence of a gradual change of V is treated in Appendix 3. It does not change the results of the theory, but only the meaning of the constant λ_0 occurring in (11) and (14).

We have then merely to join the functions (5) and (7) together at the point r_0. The wave function and its derivative being continuous at r_0, we have

$$\begin{aligned} Cy(r_0)^{-\frac{1}{2}} \cos \varphi(r_0) &= k^{-1} \sin (kr_0 - \delta), \\ -Cy(r_0)^{+\frac{1}{2}} \sin \varphi(r_0) &= \quad \cos (kr_0 - \delta). \end{aligned} \tag{9}$$

Dividing the upper equation by the lower, we obtain

$$\operatorname{tg} (kr_0 - \delta) = -(k/y(r_0)) \operatorname{ctg} \varphi(r_0). \tag{10}$$

From (2) and (8) we see that for $k \ll y(r_0)$, i.e., slow neutrons, the right-hand side of (10) is small except for exceedingly large values of the ctg, consequently

$$\delta = k(\operatorname{ctg} \varphi(r_0)/y(r_0) + r_0) = k(\lambda_0 \operatorname{ctg} \varphi_0 + r_0) \tag{11}$$

with the abbreviations

$$\begin{aligned} &\lambda_0 = 1/y(r_0) = \hbar/(2MV_0)^{\frac{1}{2}}; \quad V_0 = |V(r_0)|; \\ &\varphi_0 = \varphi(r_0). \end{aligned} \tag{12}$$

In the special case when ctg φ_0 is very large, we have

$$\sin \delta = k(\lambda_0 \operatorname{ctg} \varphi_0 + r_0)/(1 + (k\lambda_0 \operatorname{ctg} \varphi_0)^2)^{\frac{1}{2}} \tag{11a}$$

when higher powers of kr_0 than the first are neglected.

The amplitude C of the wave function inside the nucleus can easily be obtained from (9), we have

$$1/C^2 = y(r_0) \sin^2 \varphi_0 + (k^2/y(r_0)) \cos^2 \varphi_0. \tag{13}$$

Since $k \ll y(r_0)$, the second term is negligible unless sin φ_0 is very small, in that case cos $\varphi_0 = 1$ and

$$1/C^2 = (1/\lambda_0)(\sin^2 \varphi_0 + E/V_0). \tag{14}$$

The wave function (5) is not normalized. The wave function normalized per unit energy[5] is

$$\psi_E = Ak^{\frac{1}{2}}\psi_0/r, \tag{15}$$

where

$$A = (\tfrac{1}{2}M)^{\frac{1}{2}}/\pi\hbar \tag{15a}$$

does not depend on the energy. Inside the nucleus,

$$\psi_E = ACk^{\frac{1}{2}}y^{-\frac{1}{2}} \cos \varphi/r. \tag{16}$$

It is convenient to separate the factors depending considerably on the energy, *viz.*, $Ck^{\frac{1}{2}}$, from the rest of the function by putting $\psi_E = Ck^{\frac{1}{2}}\psi_W$. Then

$$\psi_W = Ay^{-\frac{1}{2}} \cos \varphi/r \tag{17}$$

and

$$\psi_0 = rC\psi_W/A. \tag{18}$$

ψ_W changes only very slowly with the energy which makes it suitable for investigating the dependence of cross sections on E. Moreover, for large energies ψ_W becomes identical with the normalized wave function ψ_E, since for $E > V_0$ we have $k_0 = (2M)^{\frac{1}{2}}(E - V_0)^{\frac{1}{2}}/\hbar \approx k$ and therefore, according to (13), $C = 1/k^{\frac{1}{2}}$.

3. The Elastic Cross Section

Inserting (11) into (6), we obtain for the elastic cross section

$$\Phi_{el} = 4\pi(\lambda_0 \operatorname{ctg} \varphi_0 + r_0)^2 \tag{19}$$

with the abbreviations explained in (12).

If we had an accurate theory of the nucleus, we could determine λ_0 and φ_0 accurately. At present, we can only estimate them, which is fairly easy in the case of λ_0. As is shown in Appendix 3, λ_0 is connected with the range of the forces between nucleus and neutron, rather than with the potential energy inside the nucleus. Wigner has shown[6] that the forces between *proton* and neutron extend over a region of about 10^{-13} cm; this value follows from the observed mass defects of He^4 and H^2. The forces between a heavier nucleus and a neutron probably extend over a slightly larger distance, because the nucleus will become polarized under the influence of the neutron. We believe, therefore, that $l = 1.5 \cdot 10^{-13}$ cm is a fair estimate; this figure agrees well with the "apparent radius of the neutron" as derived by Rabi from the scat-

[5] Definition: $\int dr \psi_E \int dE' \psi_{E'} = 1$.
[6] E. Wigner, Phys. Rev. **43**, 252 (1932).

tering of fast neutrons.[7] Then, according to (80),

$$\lambda_0 = \tfrac{1}{2}\pi l = 2.4 \cdot 10^{-13} \text{ cm}. \qquad (20)$$

The corresponding V_0, calculated from (12), would be $V_0 = 3.4$ MV. We believe that λ_0 is not in error more than by a factor $\sqrt{2}$, and therefore the error introduced into the cross section is not more than a factor 2 one way or the other. λ_0 is only about one-third of the nuclear radius r_0.

The phase φ_0 cannot be estimated from pure theory. As we have already pointed out (above Eq. (7)), the wave function makes several oscillations inside the nucleus, so that φ_0 is of the order 2π. It is therefore impossible at present to predict φ_0 with an accuracy of the order $\pi/20$, which would be necessary to give a significant estimate for ctg φ_0. All we can say is that φ_0 is a constant characteristic for a given element, which is practically independent of the neutron energy. A change of about 150,000 volts in E is necessary to produce a change of one degree in φ_0 (cf. Appendix 2). The change of φ_0 with the number of protons and neutrons in the nucleus, may possibly be just regular enough so that large values of ctg φ_0 would be found preferably with neighboring elements. There seems indeed to be a slight indication of such an effect in the experiments (Rh, Ag and Cd all have large cross sections!). But φ_0 is probably not regular enough to allow *predictions* of large cross sections from the behavior of neighboring elements. Nor is it probable that the isotopes of the same element *all* have large cross sections, if one of them has: A change of only 2 percent would change φ_0 from $n\pi$ (n an integer) to $(n+1/25)\pi$, ctg φ_0 from ∞ to $25/\pi \approx 8$, and the cross section from infinity to the moderate value $50 \cdot 10^{-24}$ cm^2. The addition of a neutron to the nucleus will probably change φ_0 by more than 2 percent.

Therefore the only practicable procedure is to make a statistical study of all the experimental cross sections observed for various nuclei, and to compare the result with reasonable theoretical expectations. From the definition of φ_0 it is clear that any value of φ_0 between $-\pi/2$ and $+\pi/2$ (an additional integer multiple of π has no effect on the cross section) is *a priori* equally probable. Starting from this fact, we can easily calculate the "probable" distribution of cross sections.

Since the nuclear radius $r_0 = 7 \cdot 10^{-13}$ cm is about three times larger than our accepted value for λ_0 (Eq. (20)), the preponderant term in the cross section (19) is r_0 for the larger part of the possible values φ_0, *viz.*, for φ_0 between $-90°$ and $-18°$ and between $18°$ and $90°$ (ctg $18° = r_0/\lambda_0$). In both of these regions the cross section is of the order of magnitude $4\pi r_0^2 = 6 \cdot 10^{-24}$ cm^2, slightly smaller in the first, larger in the second region mentioned. If φ_0 is in the immediate neighborhood of $-18°$, the cross section is considerably smaller than the "hard sphere value" $4\pi r_0^2$, whereas for φ_0 near zero exceedingly large cross sections are obtained.

Table I gives the probabilities for various magnitudes of the cross section. With the assumed values of λ_0 and r_0, we have

$$\Phi_{el} = 0.7 \cdot 10^{-24} (\text{ctg } \varphi_0 + 3)^2. \qquad (21)$$

If we want to know, e.g., the probability for a cross section between 10 and 20×10^{-24} cm^2, we calculate first the values φ_0 corresponding to $\Phi = 10 \cdot 10^{-24}$, *viz.*, $+52.0°$ and $-8.4°$, and to $\Phi = 20 \cdot 10^{-24}$, *viz.*, $+23.0°$ and $-6.9°$. Hence we find that two intervals of φ_0, of 29.0° and 1.5° length, respectively, lead to the desired magnitude of Φ_{el}. The sum of the two intervals, 30.5°, corresponds to 17 percent of the total range available for φ_0, *viz.*, 180°. If we could study the cross section of each isotope of each element separately, we should find that 17 percent of all nuclei have cross sections for slow neutrons between 10 and 20×10^{-24} cm^2. Actually, almost all elements consist of several isotopes. If one of these has a large cross section, the other a small one, the large cross section will be measured. Therefore with natural elements the large cross sections should be more frequent, the small ones less frequent than for pure isotopes. The probable distribution of cross sections has been calculated (a) for elements containing two isotopes, in equal abundance, (b) for 4 isotopes. Case (a) is realized in most elements with odd atomic number, case (b) corresponds to the average even-numbered element. It has been assumed that the φ_0's of several isotopes have no relation to each other. It can be seen that the difference between 2-isotope and 4-isotope ele-

[7] Rabi, Phys. Rev. **43**, 838 (1933).

TABLE I. *Data on cross section.*

Range of cross section (units 10^{-24} cm²)	Corresponding ranges of φ_0		Probability for elements containing 1	2 isotopes	4	Ave. of 2 and 4	No. of elements among 27 investigated: expected	observed
0–2.5	-11.5 to $-42.1°$		17.0	6.3	1.1	3.7	1.0	2½†
2.5–5	-10.0 to -11.5	-42.1 to $-71.8°$	17.4	18.1	11.4	14.7	4.0	3½
5–10	-8.4 to -10.0	52.0 to 108.2*	32.1	34.7	35.2	35.0	9.5	9
10–20	-6.9 to -8.4	23.0 to 52.0	16.9	19.3	22.7	21.0	5.7	4
20–40	-5.4 to -6.9	12.4 to 23.0	6.7	8.0	11.3	9.7	2.6	3
40–100	-3.8 to -5.4	6.3 to 12.4	4.3	5.7	7.4	6.6	1.8	1
100–300	-2.4 to -3.8	3.2 to 6.3	2.5	3.4	4.7	4.0	1.1	2
over 300	-2.4 to $+3.2°$		3.1	4.4	6.2	5.3	1.5	2

* $-71.8°$ is equivalent to $+108.2°$.
† If an experimental cross section is just at the limit of two intervals, half an element has been attributed to each interval.

ments is not very great, only very small cross sections are more likely to be found with odd-number elements. Taking the average probability for even and odd elements, we have calculated how many of the 27 cross sections measured thus far should lie in each group. Most of the "observed" cross sections have been taken from recent experiments of Dunning and Pegram, whom we wish to thank for the communication of their data before publication.[8] Only elements with $Z>10$ have been included, because the lighter ones are apt to emit α-particles when bombarded with slow neutrons and have then much larger (inelastic) cross sections[9] (cf. paragraph 5). The agreement between experiment and theory is satisfactory, although there seem to be slightly more large cross sections. Part of this difference may be due to the fact that the experimental values include the capture cross section which might be of the same order of magnitude as the elastic one (paragraph 4).

We shall now discuss the physical meaning of the large cross sections: According to (19) the cross section is determined by the phase φ_0 with which the neutron wave ψ_0 leaves the nucleus; small phases φ_0 lead to large cross sections. For an "ordinary" value of φ_0 (not near zero), the wave function increases linearly outside the nucleus up to $r\approx\lambda$ when ψ_0 begins to oscillate. ψ_0 is therefore much larger at great distances r than inside the nucleus, and since its value outside is fixed by normalization, it is small inside. However, if φ_0 is zero or nearly so, the wave function leaves the nucleus with horizontal tangent, it does not increase outside, and is therefore comparatively very large in the interior of the nucleus. The neutron remains much longer inside the nucleus if $\varphi_0\approx 0$, and therefore all phenomena due to the nucleus—such as scattering, capture, disintegration—are much more intense. $\varphi_0=0$ means that the neutron has a virtual quantum level (more accurately: an s-level) in the nucleus with an energy near zero. The large cross sections may thus be called a resonance effect, but the "resonance" is very unsharp, since φ_0 changes only by 1° if the energy changes by about 150,000 volts. This makes the "resonance" such a frequent phenomenon.

If the cross section is large for small neutron energy, it remains fairly constant when the energy increases, until $4\pi\lambda^2$ ($2\pi\lambda$ = wavelength) becomes smaller than (19). The maximum energy up to which the cross section remains unchanged, is therefore

$$E_{\max}=\frac{\hbar^2}{2M\lambda^2_{\text{crit}}}=\frac{\hbar^2}{2M}\frac{4\pi}{\Phi_{el}}=\frac{2\cdot 6}{\Phi_{el}}\ \text{MV} \qquad (22)$$

if Φ_{el} is measured in units 10^{-24} cm². For higher energy, the cross section decreases as $4\pi\lambda^2$, i.e., proportional to $1/E$, until λ becomes of the order $r_0(E\approx\frac{1}{2}$ to 1 MV) when higher angular momenta begin to play a role.

4. Capture with Emission of γ-Rays

Since the incident slow neutrons which reach the nucleus are in an s-state (have angular momentum $l=0$), they can only make an optical

[8] Dunning, Pegram, Fink and Mitchell, Phys. Rev. **47**, 416 (1935).
[9] The elastic cross sections are smaller for light elements because of the smaller nuclear radii.

transition to a p-state. The capture of the neutron with emission of a γ-ray is therefore only possible if there is an unoccupied p-level for the neutron inside the nucleus. A nucleus which contains no such level cannot capture the neutron but only scatter it. This offers an explanation for the fact that some substances scatter slow neutrons considerably without absorbing them: e.g., slow neutrons penetrate through a paraffin sphere of 12 cm radius without being diminished measurably in intensity;[10] they have to travel about 3 meters in order to reach the sphere's surface, the mean free path for elastic scattering being about $\frac{1}{2}$ cm;[10] therefore the "mean free path" for absorption must be at least 1000 times larger than that for scattering, whereas for other substances the two cross sections are (for slow neutrons) of the same order of magnitude.[11] The obvious conclusion is that the nonabsorbing substances (in our case, H and C) have no neutron p-level.

[It should be noted, however, that it is probably a bad approximation to speak of the quantum states of the single particles in the nucleus, and that one should rather speak of the angular momentum of the nucleus as a whole. Then our selection rule reads: A neutron capture by a nucleus of angular momentum L is possible, if and only if the nucleus produced by the capture has a state with angular momentum L or $L\pm1$, whose energy is lower than that of the original nucleus plus a free neutron at rest. This selection rule is much less strict than the original rule for the neutron. A further restriction is, however, that the transition $L=0\rightarrow L'=0$ is, of course, forbidden: This is very important because many nuclei have no angular momentum. We shall therefore expect

(1) Capture is possible for many, but not for all nuclei.
(2) Impossibility of capture is most likely for nuclei having no angular momentum.]

The cross section for the capture of any particle with emission of radiation is[12]

$$\Phi_c=(4/3)(\omega^3/\hbar c^3)\,|\int\psi_n^*\mathbf{R}\psi d\tau|^2. \qquad (23)$$

ψ = wave function of incident particle (cf. (3)).
ψ_n = wave function of final (bound) state of particle.
$\omega=2\pi$ times frequency of emitted radiation $=(E-E_n)/\hbar$
$\mathbf{R}$ = electric moment associated with particle in the system of reference, where the center of gravity of the captured particle and the capturing system is at rest.

If we treat the nucleus as rigid, as we have always done so far, the coordinate of the nucleus with respect to the center of gravity of nucleus and neutron is $-\mathbf{r}/(M+1)$, where M is the atomic weight of the nucleus and $\mathbf{r}$ the neutron coordinate with respect to the nucleus. Therefore the electric moment of the whole system is

$$\mathbf{R}=-Ze\mathbf{r}/(M+1)=e'\mathbf{r}, \qquad (24)$$

where $e'=-eZ/(M+1)(=0.43e$ for Ag) (25)

can conveniently be called the effective charge of the neutron.

We express ψ in (23) in terms of ψ_W (17) with the help of (3) and (18):

$$\Phi_c=\frac{4}{3}\frac{\omega^3e'^2}{\hbar c^3}\frac{C^2}{A^2}\frac{1}{v}\left|\int\psi_n^*\mathbf{r}\psi_W d\tau\right|^2 \qquad (26)$$

and introduce the oscillator strength[13] corresponding to the transition from the state ψ_W to *one* of the p-states in the level n, namely, that one which is symmetrical round the z axis:

$$f_W=(2M/\hbar)\omega\,|\int\psi_{nz}^*z\psi_W d\tau|^2. \qquad (27)$$

Then, inserting C and A from (14) and (15a) and considering that transitions to each of the three p-states are possible:

$$\Phi_c=4\frac{e'^2}{\hbar c}\frac{\hbar^3\omega^2\pi^2}{M^2c^2v}\frac{\lambda_0}{\sin^2\varphi_0+E/V_0}f_W,$$

$$\Phi_c=4\pi^2\frac{e'^2}{\hbar c}\frac{\hbar\omega}{Mc^2}\frac{\lambda\lambda_0}{\sin^2\varphi_0+\lambda_0^2/\lambda^2}\hbar\omega f_W. \qquad (28)$$

Here $2\pi\lambda$ is the de Broglie wavelength of the neutron, λ_0 and φ_0 the characteristic quantities of the nuclear field defined in (12) and discussed in paragraph 3. Furthermore, according to (25),

$$\hbar c/e'^2=137/0.43^2=740. \qquad (29)$$

$\hbar\omega=-E_n$ is the binding energy of the neutron,

[10] All this according to experiments of Dunning and Pegram.
[11] Theoretically, see below.
[12] See, e.g. Handb. d. Physik **24** (1), p. 430, form. (38.11).
[13] Cf. e.g. Handb. d. Physik **24** (1), p. 431, form. (38.14).

which is, according to the observed mass defects for elements of medium atom weight, about 8 MV,[14] so that

$$Mc^2/\hbar\omega \approx 120. \tag{30}$$

Finally, f_W is a quantity of the dimension of a reciprocal energy. Moreover it is known that the total oscillator strength of all transitions starting from one level, say the level nz, is unity, and that the strong spectral lines ending at this level, extend over a frequency range of the order ω. Therefore we estimate[15]

$$\hbar\omega f_W = 1, \tag{31}$$

so that

$$\Phi_c \approx (\lambda\lambda_0/2300)[1/(\sin^2\varphi_0 + \lambda_0^2/\lambda^2)]. \tag{32}$$

For slow neutrons, unless φ_0 is unreasonably small, λ_0/λ may be neglected in comparison with $\sin\varphi_0$. Then the capture cross section is seen to increase with decreasing velocity as λ, i.e., as $1/v$. The slowest neutrons have the largest capture cross sections. Now the smallest velocity obtainable is gas-kinetic velocity, i.e.,

$$E = kT = 1/40 \text{ volt at room temperature,}$$
$$\lambda = 2.9 \cdot 10^{-9} \text{ cm.} \tag{33}$$

With the value (20) for λ_0, we have then

$$\Phi_c = 0.3 \cdot 10^{-24}/\sin^2\varphi_0. \tag{34}$$

The capture cross section becomes large if φ_0 is small, just as the elastic cross section. The reason for this "phase effect" has been explained at the end of paragraph 3. If φ_0 is small, we find from (34) and (21):

$$\Phi_{el}/\Phi_c \approx 2 \tag{35}$$

independent of φ_0. The ratio of the two cross sections should thus be independent[16] of their absolute magnitude, provided the cross sections are large, i.e., φ_0 small.

If the phase φ_0 is not small,

$$\Phi_{el}/\Phi_c = 2(\cos\varphi_0 + 3\sin\varphi_0)^2, \tag{36}$$

which is larger than (35). Therefore, if the elastic cross section is of the order of magnitude of the hard sphere value, the capture is less probable, even relative to the elastic scattering. The maximum of (36) is 10 times 2.

The capture cross section (32) decreases rapidly with increasing neutron velocity. Since the theory seems to be in agreement with experiment, if gas-kinetic energies are assumed for the neutrons, it seems reasonable actually to make this assumption. The effects observed with apparently fast neutrons should then be ascribed to a small admixture of slow neutrons which may be present in the neutron beam. We expect that the heavy elements cannot be made radioactive if the slow neutrons are carefully kept away. For 1 MV neutrons formula (32) would give a cross section of the order 5.10^{-29} cm^2.

5. Neutron-Produced Disintegrations with Emission of Charged Particles

Two kinds of disintegrations under this heading have been observed:

$$Z^M + n^1 \rightarrow (Z-1)^M + H^1, \tag{I}$$

$$Z^M + n^1 \rightarrow (Z-2)^{M-3} + He^4, \tag{II}$$

where Z^M denotes a nucleus with mass M and charge Z. Reaction (I) is found to occur, with fast neutrons ($E \sim 7$ MV), up to $Z = 30$, whereas process (II) stops at $Z = 27$.

a. Energy balance

Process (I) is always endothermic. For of the two isobars Z^M and $(Z-1)^M$, the former is known to be stable, so that the latter must disintegrate with β-emission

$$(Z-1)^M \rightarrow Z^M + \beta. \tag{III}$$

Since the masses of neutron and hydrogen atom are nearly equal, the energy absorbed in process (I) is just equal to that emitted in (III), i.e., to the energy liberated in the β-disintegration which is usually between 1 and 4 MV. Since very slow protons cannot escape from the nucleus, the minimum neutron energy required for the

[14] Here it has been assumed that the neutron is captured in the ground state, otherwise the capture cross section should be smaller.

[15] The actual value of f_W in a given case may easily be wrong by a factor 5 one way or the other. This uncertainty applies to all the formulae below.

[16] It should however be noted that there are irregular variations of the ratio Φ_c/Φ_{el} owing to different values of the oscillator strength f_W.

"proton-type disintegration" (I) is between 1 and 5 MV.

Process (II) is in general exothermic, because the neutron has a very high "internal" energy, which is set free in the process. For atoms of medium atomic weight, the packing fraction is known to change very little from element to element[17] and to be of the order $-1/1000$. Therefore the deviations of the masses of the particles occurring in process (II) from integral numbers in the O^{16}-scale are (in thousandths of mass units)[17a]

for the neutron	$+8.5$	α-particle	$+3.3$
nucleus Z_M	$-M$	nucleus Z_{M-3}	$-(M-3)$
initial particles	$8.5-M$	final part.	$6.3-M$

This leaves an energy balance of 2.2 thousandths of a mass unit, corresponding to about 2 MV. The "α-type" disintegration (II) can therefore be produced by *slow* neutrons, having practically no kinetic energy, at least with light nuclei. In fact, Chadwick, Taylor and Goldhaber[18] as well as Fermi and his collaborators have observed this type of disintegration with Li^6 and B^{10} and have in both cases found very large cross sections (10^{-21} cm^2).

b. Cross section, general

The cross section for the disintegration of a nucleus by a neutron with emission of an α-particle[19] is given by the well-known formula (Born theory)

$$\Phi_{dis}=(2\pi/\hbar)\,|\int\psi_{neut}\psi_{\alpha E}^{*} \times u(Z)u^{*}(Z-2)u^{*}(\alpha)\,V d\tau|^{2}, \quad (37)$$

where ψ_{neut} is the wave function (3) of the incident neutron, normalized per unit current, $\psi_{\alpha E}$ that of the α-particle, normalized per unit energy, $u(Z)$ is the wave function describing the internal motion of the particles in the original nucleus, $u(Z-2)$ and $u(\alpha)$ the same for final nucleus and α-particle, V is the total potential energy between all particles. We express ψ_{neut} by ψ_W (cf. (17), (3), (18)), and we introduce a function $\psi_{\alpha W}$ for the α-particle, which is exactly analogous to ψ_W for the neutron: Its value inside the nucleus varies slowly with the energy and it goes over into $\psi_{\alpha E}$ for high energy. It can easily be shown that

$$\psi_{\alpha E}=\psi_{\alpha W}/(4e^{2G}\sin^2\varphi_\alpha+\tfrac{1}{4}e^{-2G}\cos^2\varphi_\alpha)^{\frac{1}{2}}, \quad (38)$$

where e^{-2G} is the well-known penetrability of the potential barrier round the nucleus, *viz.*

$$G=((2M)^{\frac{1}{2}}/\hbar)\int(V-E)^{\frac{1}{2}}dr, \quad (39)$$

the integral extending over the region where the radicand is positive. φ_α is the phase of the α-particle wave function at the boundary of the nucleus.

Inserting (38) and (3), (18), (14) into (37), we obtain

$$\Phi_{dis}=\frac{2\pi}{\hbar}\frac{2\pi^2\hbar^2}{Mv}\frac{\lambda_0}{\sin^2\varphi_0+E/E_0} \times\frac{1}{4e^{2G}\sin^2\varphi_\alpha+\frac{1}{4}e^{-2G}\cos^2\varphi_\alpha} \times|\int\psi_W\psi_{\alpha W}^{*}u(Z)u^{*}(Z-2)u^{*}(\alpha)\,V d\tau|^{2} \quad (40)$$

or, if φ_0 and φ_α are not too small (not exact resonance),

$$\psi_{dis}=(\pi^2\lambda\lambda_0 e^{-2G}/\sin^2\varphi_0\sin^2\varphi_\alpha)I \quad \text{(neutron and } \alpha \text{ slow)} \quad (41)$$

where I stands for the integral in (40).

I is dimensionless, ψ_W and $\psi_{\alpha W}$ being normalized per unit energy. I should be rather smaller than unity, because the formation of the α-particle in the nucleus requires a rather serious rearrangement. The order of magnitude of I is determined by experiments with fast neutrons: if the neutron energy is a few million volts, $\lambda\lambda_0/\sin^2\varphi_0$ has to be replaced by r_0^2.[20] If the α-particle is fast enough to go over the top of the potential barrier, the factor $e^{-2G}/4\sin^2\varphi_\alpha$ has to be left out, so that for high energy of neutron and α-particle[21]

[17] Aston, *Mass Spectra and Isotopes*, 1933, pp. 106, 167.
[17a] H. A. Bethe, Phys. Rev. **47**, 633 (1935).
[18] J, Chadwick and Goldhaber, Nature **135**, 65 (1935); Taylor and Goldhaber, Nature **135**, 341 (1935).
[19] We speak for definiteness of α-particles, the theory is exactly similar for protons.

[20] The factor C^2 (cf. 18) has no longer the value $\lambda_0/\sin^2\varphi_0$ but is approximately λ (cf. 13). Besides, one has to consider that now neutron angular momenta up to $l=r_0/\lambda$ are effective, which introduces a factor $(r_0/\lambda)^2$.
[21] It should be noted, however, that the wave functions inside I change also, though slowly, with the energy of the particles. I in (42) (high energy) is therefore different from

$$\Phi_{dis}=4\pi^2 r_0^2 I. \qquad (E_{neutron}\text{ large, } E_\alpha\text{ large.}) \quad (42)$$

The measured cross sections for fast neutrons are of the order $0.3\cdot10^{-24}$ (fluorine, Fermi). The nuclear radius of F being about $4\cdot10^{-13}$, we have[22]

$$\pi^2 I\approx 1/2, \quad I\approx 1/60. \qquad (43)$$

c. Light nuclei, slow neutrons

If the nucleus is light and the gain in kinetic energy sufficiently large so that the α-particle can go over the top of the barrier even with neutron energy zero, we have to leave out $e^{-2G}/4\sin^2\varphi_a$ in (41) and find (cf. 43)

$$\Phi_{dis}=4\pi^2 I\lambda\lambda_0/\sin^2\varphi_0\approx 2\lambda\lambda_0/\sin^2\varphi_0.$$

(slow neutrons, fast α's.) (44)

The cross section increases in this case enormously with decreasing energy of the neutron, just as in the capture case. For gas-kinetic energy, we find (cf. (20), (23))[22]

$$\Phi_{dis}\approx 1300\cdot10^{-24}/\sin^2\varphi_0. \qquad (45)$$

The experimental cross sections of Li^6 and B^{10} for slow neutrons are of the order 10^{-21} cm^2. They can, therefore, be explained without assuming a "resonance effect" due to small φ_0. The greater *a priori* probability of disintegrations with emission of particles as against such with emission of γ-rays makes the cross section for the former process larger both for fast and slow neutrons.

d. Fast neutrons, heavy nuclei: potential barrier

We now want to discuss briefly the effect of the penetrability of the potential barrier surrounding the nucleus for charged particles. If the neutron is fast and the α-particle energy smaller than the top of the barrier, the cross section (42) has to be multiplied by the penetrability

$$P=e^{-2G}/4\sin^2\varphi_a. \text{ (fast neutrons, slow } \alpha\text{'s.)} \quad (46)$$

Leaving out for the present the resonance denominator $4\sin^2\varphi_a$, we have to discuss G. Assuming, as Gamow did, a large negative potential energy inside the nucleus ($r<r_0$) and the pure Coulomb potential $V=e^2Zz/r$ outside ($r>r_0$, $z=2$ for α-particle, 1 for proton), the integral $G(39)$ has the well-known value

$$G=\frac{2e^2Zz}{\hbar v}\left[\arccos\left(\frac{r_0}{r_1}\right)^{\frac12}-\left(\frac{r_0(r_1-r_0)}{r_1^2}\right)^{\frac12}\right], \quad (47)$$

where

$$r_1=e^2Zz/E \qquad (48)$$

is the distance of closest approach in the Coulomb field and v the velocity of the particle. We assume the nuclear radius to be proportional to $Z^{\frac13}$ which seems to be verified by experiment, then from Gamow's data on radioactive nuclei it follows that

$$r_0=1.9\cdot10^{-13}Z^{\frac13}\text{ cm}=\tfrac{2}{3}(e^2/mc^2)Z^{\frac13}. \qquad (49)$$

The height of the potential barrier is then

$$V_0=e^2Zz/r_0=(3/2)mc^2zZ^{\frac13}=0.75zZ^{\frac13}\text{ MV}. \quad (50)$$

To a given energy of the particle, there corresponds a critical nuclear charge Z_0 for which $V_0=E$, *viz.*,

$$Z_0=(2E/3zmc^2)^{\frac13}, \qquad (51)$$

the corresponding nuclear radius is

$$R=\left(\frac{2}{3}\right)^{\frac13}\frac{e^2}{mc^2}\left(\frac{E}{zmc^2}\right)^{\frac13}=1.55\left(\frac{E}{zmc^2}\right)^{\frac13}\cdot10^{-13} \quad (52)$$

If the particle of energy E falls on any nucleus having higher atomic number than the "critical" Z_0 we have $r_0=R(Z/Z_0)^{\frac13}$ and $r_1=RZ/Z_0$ and after slight reduction

$$G=\frac{4}{3^{\frac12}}\frac{e^2}{\hbar c}\left(\frac{M}{mz}\right)^{\frac12}\frac{E}{mc^2}\varphi(Z/Z_0)$$

$$=0.241\frac{E}{mc^2}\left(\frac{A}{z}\right)^{\frac12}\varphi(Z/Z_0), \quad (53)$$

where A is the atomic weight of the emitted particle and

$$\varphi(\zeta)=\zeta\arccos(\zeta^{-\frac13})-\zeta^{\frac13}(1-\zeta^{-\frac13})^{\frac12}. \quad (54)$$

For numerical calculations, it is still more convenient to use

$$G'=2\cdot{}^{10}\log e\cdot G=0.209\varphi(Z/Z_0)\frac{E}{mc^2}\left(\frac{A}{z}\right)^{\frac12}, \quad (55)$$

I in (41) (small energy), only the order of magnitude is the same. On the other hand, when the neutron energy changes, say, from 0 to 100,000 volts, I is very nearly constant.

[22] This estimate may, for a given case, be wrong by a factor 10 one way or the other. This uncertainty applies to the formulae (44) to (46).

so that $e^{-2G}=10^{-G'}$. Evaluation of (54) gives

for $Z/Z_0=$									
1.5	2.0	2.5	3	3.5	4	5	6	8	10
$0.209\varphi=$									
.026	.071	.125	.190	.259	.333	.490	.662	1.02	1.42

We are interested in the penetrability

(1) for α-particles produced by fast neutrons. The fastest neutrons emitted in appreciable number from the usually employed Be+radon source have experimentally[23] an energy of about 8 MV. Adding the 2 MV energy gained (in the average) in the α-type transformation (see above), and subtracting 1 MV for the energy of the recoil nucleus,[24] we find

$$E_\alpha=9 \text{ MV}, Z_0=14.6;$$

(2) for α-particles produced by slow neutrons; in the average,

$$E_\alpha=2 \text{ MV}, Z_0=1.53;$$

(3) for protons produced by fast neutrons. Assuming that the nucleus produced by this disintegration emits β-rays of 4 MV maximum energy, and taking $\frac{1}{2}$MV for the mass difference of the neutron and the hydrogen atom

$$E_p=4.5 \text{ MV}, Z_0=14.6.$$

The penetrabilities for these 3 cases are given for various nuclear charges in Table II. The nuclear charges refer to the nucleus *produced* by the disintegration. It is seen that the α-type disintegration by fast neutrons (9 MV α-particles) should begin to become less probable for Z larger than 20 and should be unobservable for $Z>27$, assuming that a penetrability of less than 1/10 makes the process unobservable and remembering that the initial nucleus has a charge by 2 higher than the nucleus produced. In Fermi's experiments, $Z=27$ (Co) is actually the heaviest nucleus found to emit α-particles under neutron bombardment, and the disintegrations of the α-type have only medium or weak intensity for $Z>20$, whereas most of the processes of the α-type found with lighter nuclei are "intense" in Fermi's nomenclature.

The heaviest nucleus for which *proton* emission under neutron bombardment has been established is Zn ($Z=30$) whereas we should expect weak effects of this type to persist up to nearly $Z=40$, and even higher atomic number if we take into account the possibility of resonance for the proton (factor $4\sin^2\varphi_a$ in the denominator of P, (46); any value for φ_a between $-90°$ and $+90°$ being equally probable). The proton penetrates the potential barrier easier because of its small mass, the energies (9 and 4.5 MV) being in the ratio of the respective charges.

e. Slow neutrons, comparatively heavy nuclei

When the penetrability of the potential barrier for the α-particle is disregarded, gas-kinetic neutrons are about 5000 times more effective in producing α-type disintegration than fast ones. According to Table II, the penetrability for 2 MV α-particles becomes 1/5000 when the nucleus produced has charge $Z=9$; therefore, with our assumption about the energy balance slow neutrons should be more effective than fast ones in producing α-type disintegration in all nuclei up to $Z=11$ (Na). A possible resonance for either neutron or α-particle would shift this limit to about $Z=16$ (S); the same would be true if the energy gained in the disintegration process was 3 instead of 2 MV.

Assuming the mass defects for all elements concerned to be correctly measured,[17a] the following α-type disintegrations should be more easily produced by slow than by fast neutrons: $N^{14}\rightarrow B^{11}(100)$, $F^{19}\rightarrow N^{16}$ [25](10), however, not: $C^{12}\rightarrow Be^{9}$, $Ne^{20}\rightarrow O^{17}$ and probably $O^{16}\rightarrow C^{13}$ which should be endothermic. The numbers in brackets give the probable increase of the cross section in going from fast to slow neutrons. For the heavier elements, the masses are not known accurately enough to predict the energy gain in the α-type disintegration; possibly the following transformations might be caused with high probability by slow neutrons: $Mg^{24}\rightarrow Ne^{21}$, $Mg^{25}\rightarrow Ne^{22}$, $Mg^{26}\rightarrow Ne^{23}$, $Al^{27}\rightarrow Na^{24}$, $Si^{28}\rightarrow Mg^{25}$, $P^{31}\rightarrow Al^{28}$, etc. The α-type disintegration caused by slow neutrons seems to provide a very good method for correlating masses of different nuclei. The kinetic energy of the projectile, the neutron, is known to be exactly zero (for purposes of atomic weight determination); consequently the α-

[23] Dunning, Phys. Rev. **45**, 586 (1934). Faster neutrons are reported as well but seem to be very rare indeed, and therefore are not likely to play an important part in causing disintegrations.

[24] True for Z of the order 20.

[25] The maximum energy of the β-rays emitted by N^{16} was assumed to be 6 MV, corresponding to an average energy of 2 MV as measured by Fermi.

TABLE II. *Reciprocal value of penetrability of potential barrier.*

$Z=$	5	7	10	15	20	25	30	40	50
α-particles									
9 MV	1	1	1	1	2.6	12	80	10^3	$4\cdot10^3$
2 MV	18	250	$2\cdot10^4$	$6\cdot10^7$	$6\cdot10^9$	$1.5\cdot10^{13}$	$4\cdot10^{16}$	10^{24}	10^{31}
protons									
4.5 MV	1	1	1	1	1.4	2.4	4.7	25	100

particles are homogeneous. The unambiguity of the energy determination is greatly increased by the fact that only very slow and very fast neutrons are effective in producing the α-type disintegration, but not neutrons of medium energy, say, a few hundred thousands of volts. When the neutron energy decreases from 5 MV, the first factor to change is the penetrability of the potential barrier for the α-particle. If this factor is small for neutron energy zero, it cannot be large for neutron energies of 1 MV. However when the neutron energy is reduced to 1000 volts or less, the cross section increases again because the neutron stays longer inside the nucleus.

The disintegration $F^{19}+n'\rightarrow N^{16}+He^4$ in particular, if it proves to be sufficiently exothermic to be possible with slow neutrons, seems to afford the most hope of determining the mass of the neutrino. For this purpose, the maximum energy of the β-rays emitted by N^{16} in the process $N^{16}\rightarrow O^{16}+e^-+n^0$ (n^0=neutrino) should be measured accurately, as well as the kinetic energies of the α-particles emitted in the production of N^{16}, and of those emitted in the process $F^{19}+H^1\rightarrow O^{16}+He^4$. Moreover, N^{16} seems to be the best nucleus known upon which to observe the recoil caused by β-disintegration;[26] if the maximum energy of the β-rays is 5 MV, which seems to be rather a lower limit, N^{16} should receive 800 volts recoil energy.

The disintegration group $Al^{27}+n^1\rightarrow Na^{24}+He^4$, $Na^{24}\rightarrow Mg^{24}+e^-+n^0$, $Al^{27}+H^1\rightarrow Mg^{24}+He^4$ would give an alternative way for the determination of the neutrino mass, but the first reaction of this group is less likely to occur with slow neutrons than the fluorine disintegration because of the high potential barrier of Na.

[26] Cf. H. Bethe and R. Peierls, Nature **133**, 532, 689 (1934).

APPENDIX 1. THE EFFECT OF SLOW NEUTRONS WITH NONVANISHING ANGULAR MOMENTUM $l\neq0$

For $l=1$, the wave function outside the nucleus is

$$\psi_1=\sin(kr+\delta_1)/k^2r-\cos(kr+\delta_1)/k. \quad (56)$$

Inside the nucleus ψ_1 has the same form as ψ_0, cf. (7), only with y having a different meaning. For convenience, we expand ψ in a power series in kr and δ:

$$\psi_1=\delta_1/k^2r+\tfrac{1}{3}kr^2+0(k^3r^4)+0(r\delta). \quad (57)$$

Neglecting all powers of δ and kr higher than the first, we find by joining the outside and inside wave functions together

$$\begin{aligned} C_1y(r_0)^{-\frac{1}{2}}\cos\varphi(r_0)&=\delta_1/k^2r+\tfrac{1}{3}kr^2,\\ -C_1y(r_0)^{+\frac{1}{2}}\sin\varphi(r_0)&=-\delta_1/k^2r^2+\tfrac{2}{3}kr, \end{aligned} \quad (58)$$

wherefrom

$$\begin{aligned} C_1&=\frac{kr_0(\lambda_1)^{\frac{1}{2}}}{(\lambda_1/r_0)\cos\varphi_1-\sin\varphi_1},\\ \delta_1&=\tfrac{1}{3}k^2r_0^3\frac{2(\lambda_1/r_0)\cos\varphi_1+\sin\varphi_1}{(\lambda_1/r_0)\cos\varphi_1-\sin\varphi_1}. \end{aligned} \quad (59)$$

Apart from the resonance denominator, δ_1 is smaller than the phase δ for $l=0$, given in (11), by a factor $(kr_0)^2$, the elastic scattering cross section therefore by a factor $(kr_0)^4=10^{-15}$ for gas-kinetic neutrons. C_1^2 is likewise smaller by a factor $(kr_0)^2=5\cdot10^{-7}$ than the corresponding quantity for $l=0$ (cf. (14)). To obtain, e.g., a capture cross section of only 10^{-25} cm² for neutrons of $E=kT$ and $l=1$, the phase φ_1 would have to lie in a region of $1/10°$ breadth near the value $\mathrm{tg}^{-1}(\lambda_1/r_0)$ which is very unlikely. It is

slightly better for higher energy, because all effects due to "p-neutrons" decrease with decreasing energy; the elastic scattering as E^2, the capture and α-type disintegration as $E^{\frac{1}{2}}$. There is just a chance that there might be an element which has no bound p-level for the neutron and therefore cannot capture s-neutrons, but for which incoming p-neutrons have a phase φ_1 within 1° of the "right" value $\mathrm{tg}^{-1}(\lambda_1/r_0)$: Such an element would capture p-neutrons of energies round 100,000 volt with a cross section of the order $3\cdot10^{-25}$ cm².

Appendix 2. Attempt to Determine the Potential Energy for Neutrons in the Nucleus[26a]

It is not likely that the approximation made in this paper, i.e., taking the nucleus as a rigid body and representing it by a potential field acting on the neutron, is really adequate. Anyhow, if it is made—and it is the only practicable approximation in many cases—it should be made consistently, and therefore the potential to be assumed is of interest.

We assume the potential to be constant, equal to $-V_0$, inside the nucleus, and treat the neutrons simply as a Fermi gas enclosed in a volume

$$\Omega=(4\pi/3)r_0^3.$$

Since $N=A-Z$ (A=atomic weight) neutrons are in the nucleus, their average kinetic energy is according to the Fermi statistics formula

$$E_0=\frac{3}{5}\frac{(2\pi\hbar)^2}{2M}\left(\frac{3N}{8\pi\Omega}\right)^{2/3}=\frac{3}{5}\frac{3^{4/3}\pi^{2/3}}{2^{7/3}}\frac{\hbar^2}{Mr_0^2}N^{2/3}. \quad (60)$$

Inserting for r_0 the value (49) and taking for N/Z the average value 1.25 (true for medium atomic weight), we find

$$E_0=2.39\left(\frac{3}{2}\right)^2\left(\frac{\hbar c}{e^2}\right)^2\frac{m}{M}mc^2(1.25)^{\frac{1}{3}}=24 \text{ MV}. \quad (61)$$

The binding energy is V_0-E_0, it has experimentally the value ~ 8 MV, which makes

$$V_0=32 \text{ MV}. \quad (62)$$

[26a] Similar calculations with similar results have been made by Van Vleck (Phys. Rev. in press) and Goudsmit (unpublished).

With this value for V_0, the phase φ_0 of the wave function of a neutron with energy E at the boundary r_0 of the nucleus becomes[26b]

$$\varphi_0=\frac{(2M)^{\frac{1}{2}}}{\hbar}(V_0+E)^{\frac{1}{2}}r_0-\frac{\pi}{2}$$

$$=\tfrac{2}{3}\sqrt{2}\frac{e^2}{\hbar c}\left(\frac{M}{m}\right)^{\frac{1}{2}}\left(\frac{V_0+E}{mc^2}\right)^{\frac{1}{2}}Z^{\frac{1}{3}}-\frac{\pi}{2}$$

$$=2.36Z^{\frac{1}{3}}(1+0.015E)-\tfrac{1}{2}\pi \quad (63)$$

if E is measured in million volts. For Ag($Z=47$)

$$\varphi_0=2.2\pi+0.04\pi E, \quad (64)$$

which means that the s-wave function makes $2\frac{1}{2}$ complete oscillations in the nucleus, and φ_0 changes by $1°=\pi/180$, if E changes by

$$1/(180\cdot0.04)=0.14 \text{ MV}.$$

Appendix 3. Effect of Gradual Decrease of Potential at the Boundary of the Nucleus

We represent the potential energy of the neutron at the boundary of the nucleus by the Eckart potential[27]

$$V=-V_0+V_0e^{2x/l}/(1+e^{2x/l})$$

$$=-V_0/(1+e^{2x/l}), \quad (65)$$

where $x=r-r_0$ and l is essentially the range of the forces between neutron and nucleus (V decreases, e.g., from $\frac{3}{4}V_0$ to $\frac{1}{4}V_0$ in a distance $1.1l$). Eckart has given the analytical form of the wave functions in the potential (65): If the wave function Ψ behaves like an outgoing wave e^{ikx} for large positive x (great distances from the nucleus), its value for large negative x (inside the nucleus) is

$$\Psi=a_1e^{ik_0x}+a_2e^{-ik_0x} \qquad (k_0=(2MV_0)^{\frac{1}{2}}/\hbar) \quad (66)$$

with
$$a_1^*=\frac{\Gamma(1+2i\beta)\Gamma(2i\alpha)}{\Gamma(1+i(\alpha+\beta))\Gamma(i(\alpha+\beta))},$$
$$a_2=\frac{\Gamma(1-2i\beta)\Gamma(2i\alpha)}{\Gamma(1+i(\alpha-\beta))\Gamma(i(\alpha-\beta))}, \quad (67)$$

[26b] From the definition (7), (8) it follows that $\varphi(r=0)=-\frac{1}{2}\pi$ if the potential is constant inside the nucleus.

[27] C. Eckart, Phys. Rev. **35**, 1303 (1930). We put Eckart's $B=0$, our l is Eckart's l divided by π, our $k=2\pi/\lambda'$, our $k_0=2\pi/\lambda$, our V_0=Eckart's A, our $E=W-A$.

where $\alpha=\frac{1}{2}k_0 l$; $\beta=\frac{1}{2}kl$. (68)

and the asterisk denotes the conjugate complex value.

From (66) it is easy to derive the asymptotic form for *large positive* x of a wave function whose behavior *inside* the nucleus is known to be (cf. (7))

$$\psi=C\cos(k_0x+\chi)/(k_0)^{\frac{1}{2}}. \tag{69}$$

The asymptotic form for large positive x is:

$$\psi=Re\frac{(a_1^*e^{ix}-a_2^*e^{-ix})C}{(|a_1|^2-|a_2|^2)(k_0)^{\frac{1}{2}}}e^{ikx}.$$

(Re = real part.) (70)

So far, the formulae are rigorous. We now make use of the fact that the energy of the neutron, and therefore β, is small. Neglecting higher powers of β than the first, we may write

$$a_1^*=a_0(1+(\kappa+i\lambda)\beta);\quad a_2=a_0(1-(\kappa+i\lambda)\beta) \tag{71}$$

$$\text{with } a_0=\Gamma(1)\Gamma(2i\alpha)/\Gamma(1+i\alpha)\Gamma(i\alpha)=ae^{i\gamma}, \tag{72}$$

where κ, λ, a and γ are supposed to be real. Then

$$|a_1|^2-|a_2|^2=4\kappa\beta a^2,$$

$$a_1^*e^{ix}-a_2^*e^{-ix}=2a[i\sin(\gamma+\chi+\lambda\beta)+\kappa\beta\cos(\gamma+\chi)], \tag{73}$$

and (70) goes over into

$$\psi=-\frac{2aC\sin(\gamma+\chi-\lambda\beta)}{4\kappa\beta a^2(k_0)^{\frac{1}{2}}}\times\sin(kx-\kappa\beta\operatorname{ctg}(\gamma+\chi)). \tag{74}$$

Evidently, we have to identify (cf. (5), (11), $x=r-r_0$!)

$$\gamma+\chi=\varphi_0 \tag{75}$$

$\delta=kr_0+\kappa\beta\operatorname{ctg}\varphi_0$, therefore (cf. (11)) $\kappa\beta=k\lambda_0$ and (cf. (68))

$$\lambda_0=\tfrac{1}{2}l\kappa, \tag{76}$$

and furthermore we have to put (cf. (5))

$$C\sin\varphi_0/2\kappa\beta a(k_0)^{\frac{1}{2}}=1/k,$$

$$C=l\kappa a(k_0)^{\frac{1}{2}}/\sin\varphi_0. \tag{77}$$

From the definition of κ, (71), we find, using the well-known formula[28] for $|\Gamma(1-ix)|$

$$\begin{aligned}2\kappa&=\lim_{\beta=0}\frac{d}{d\beta}\log|a_1|^2\\&=\lim_{\beta=0}\frac{d}{d\beta}\log\left(\frac{\beta\sinh^2\pi(\alpha+\beta)}{\alpha\sinh 2\pi\beta\sinh 2\pi\alpha}\right)\\&=\lim_{\beta=0}\left(\frac{1}{\beta}-\frac{2\pi}{\operatorname{tgh}2\pi\beta}+\frac{2\pi}{\operatorname{tgh}\pi(\alpha+\beta)}\right)=\frac{2\pi}{\operatorname{tgh}\pi\alpha}.\end{aligned} \tag{78}$$

Inserting this into (76), we have

$$\lambda_0=(\pi/2)(l/\operatorname{tgh}\pi\alpha). \tag{79}$$

For rapid changes of potential, or more accurately, if l is small compared with the wavelength $\hbar/(2MV_0)^{\frac{1}{2}}$ of the particles inside the potential field, α is small (cf. 68) and (79) goes over into (12), *viz.*

$$\lambda_0=1/k_0=\hbar/(2MV_0)^{\frac{1}{2}}.$$

In our case, however, l is assumed to be 1.5×10^{-13} cm (cf. paragraph 3), whereas $\hbar/(2MV_0)^{\frac{1}{2}}=1.0\cdot10^{-13}$ with $V_0=32$ MV. Therefore, $\pi\alpha=2.36$ and $\operatorname{tgh}\pi\alpha=0.982$, so that practically

$$\lambda_0=\tfrac{1}{2}\pi l. \tag{80}$$

To evaluate (77), we calculate

$$\begin{aligned}a^2&=\lim_{\beta=0}|a_1|^2=\frac{\sinh^2\pi\alpha}{2\pi\alpha\sinh 2\pi\alpha}=\frac{\operatorname{tgh}\pi\alpha}{4\pi\alpha}\\C&=l\left(\frac{\pi}{4\alpha\operatorname{tgh}\pi\alpha}\right)^{\frac{1}{2}}\frac{(k_0)^{\frac{1}{2}}}{\sin\varphi_0}=\frac{(\pi l/2\operatorname{tgh}\pi\alpha)^{\frac{1}{2}}}{\sin\varphi_0}\end{aligned} \tag{81}$$

which is exactly formula (14) with λ_0 given by (79).

[28] Jahnke-Emde, *Table of Functions*, p. 89.

Angular Momentum, Mass-Center and the Inverse Square Law in Special Relativity

J. L. SYNGE, *Department of Applied Mathematics, University of Toronto*

(Received December 17, 1934)

It is assumed that the interaction of two particles takes place by means of streams of elementary impulses traveling with the velocity of light c, an impulse of energy W having a momentum W/c. The momentum-energy 4-vector of a complete system and a skew-symmetric angular momentum tensor are defined in such a way that they are constants for the system, and the mass-center of the system is defined in such a way that it travels with uniform velocity relative to a Galilean frame. The formulae are similar to those of Newtonian mechanics. The two-body problem is discussed, and it is shown that for particles with constant proper masses and relative velocity small compared with c, the inverse square law is a consequence of the mechanical laws of conservation. The whole theory is relativistically invariant.

1. INTRODUCTION

WE are well accustomed to the two methods of describing physical phenomena—the discrete and the continuous, or, in other words, the corpuscular method and the method of the field. Each has its domain of usefulness, and attempts to mix the two methods are usually fraught with difficulties. Thus the general theory of relativity is essentially a field theory: if we attempt to introduce a gravitating particle, we find singularities in the field. Maxwell's theory is a field theory: if we attempt to speak of a point electron we encounter the difficulty of infinite energy. It is true that this difficulty is avoided in the Born-Infeld theory,[1] but other difficulties due to nonlinearity are formidable obstacles to its application.

To be consistent, it would appear that in a theory which regards matter as composed of particles and electromagnetic radiation as composed of photons, all other vehicles of interaction should also be treated as discrete. If the momentum and energy of a field of electromagnetic radiation may be adequately represented by a stream of discrete photons, why should not a similar discrete description be available for an electromagnetic field which is not a field of radiation? A field of radiation is theoretically characterized by the conditions that the electric and magnetic vectors are *precisely* equal and perpendicular. If a field changes continuously into a field of radiation, it is inconsistent to suppose that the discrete character is completely absent from the field until the moment when these conditions are exactly fulfilled.

The purpose of this paper is to present some results of the assumption of discrete interaction between particles. Taking a lesson from two historical facts, we shall not attempt to link the theory with electromagnetic field theory. The first of these facts is the great success of Newton's third law, which has been generally regarded (at least in the days prior to relativity) as of universal validity, without regard to the nature of the forces of reaction. Secondly, although the special theory of relativity with its mechanical laws emerged from electromagnetic theory, those mechanical laws are now regarded as more firmly established than the electromagnetic theory from which they grew. Thus Einstein[2] recently expressed the view that the mechanical laws of conservation are more fundamental than electromagnetic field theory, a view confirmed by the work of Born and Infeld,[1] for they have modified the field equations but left the laws of conservation unchanged in form.

The theory to be presented is relativistically invariant in the sense of the special theory of relativity. It is purely mechanical, in the sense that it deals only with momentum and energy and their conservation. The usual relativistic definitions of momentum and energy of a particle are adopted. It is assumed that energy is propagated through space in straight lines with the fundamental velocity c, and that it possesses momentum in accordance with the now widely accepted hypothesis[3]

[1] M. Born and L. Infeld, Proc. Roy. Soc. **A144**, 425 (1934).

[2] A. Einstein, Willard Gibbs Lecture, Pittsburgh, 1934.

[3] M. Planck, Physik. Zeits. **9**, 828 (1908).

$$\mu_\alpha = l_\alpha W/c, \quad (\alpha = 1, 2, 3), \qquad (1.1)$$

where μ_α are the components of momentum, l_α the direction cosines of the line of propagation, and W the energy. The only extension of this familiar idea found necessary is the conception that W may be negative, (1.1) still holding.

When two particles interact, streams of energy flow in both senses between them. As a convenient language, but without any further physical implication, we shall refer to a portion of energy in transit as an elementary impulse.[4] When the elementary impulses strike the particles or are emitted by them, momentum and energy, in the relativistic sense, are conserved. This idea of the exchange of energy (and consequently momentum) between particles by means of elementary impulses traveling with the velocity of light is the most immediate and natural relativistic generalization of Newton's third law. In the present theory the idea of "force" plays no essential part: it is only introduced at a later stage to facilitate comparison with classical theory.

To realize the relativistic invariance of this theory of interaction, it is useful to consider the space-time picture of two interacting particles (Fig. 1). AA' and BB' are the world-lines of the particles: the connecting lines represent the world-lines of elementary impulses (geodesic null-lines), the arrows indicating senses of propagation. It follows from (1.1) that the momentum-energy 4-vector of an elementary impulse lies on its world-line, but in the case of attraction (for which, as we shall see, $W<0$) the sense is opposed to that of propagation.

Applying the methods described above to any complete system of interacting particles (that is, a system free from external influences), we find in §2 that the angular momentum of the system is a skew-symmetric tensor with constant components. The concept of angular momentum is applied to define the mass-center. The mass-center of a complete system has a straight world-line (corresponding to uniform motion in a straight line with constant velocity); when the

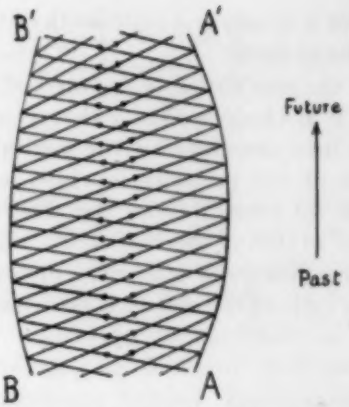

FIG. 1. Space-time picture of two interacting particles. AA', BB' are world-lines of the two particles. Connecting lines are the world-lines of elementary impulses.

frame of reference is chosen so as to reduce the mass-center to rest, three of the components of the angular momentum relative to the mass-center vanish, and the other three components take the classical form, with relativistic momentum substituted for classical momentum and with the momentum of the elementary impulses included. For such a frame of reference the mass-center of the system is given by the usual formula, mass being replaced by energy, and the elementary impulses being included.

But the most remarkable deduction from the purely mechanical principles of the present theory is the inverse square law of attraction or repulsion for a system consisting of two interacting particles with constant proper masses, having a relative velocity small compared with that of light. This fundamental law has never been deduced before from purely mechanical principles. In Newtonian gravitation this law is a definite postulate, in the general theory of relativity and in electrodynamics it is a deduction from partial differential field equations which are not contained in the mechanical laws. Moreover, the system is self-contained: there is no question of the radiation of energy from it.

Too much should not be claimed however for the present theory. It is not satisfactory when applied to the motion of a planet about a massive nucleus (one-body or Kepler problem). When the argument is pushed to a higher degree of approximation (in a calculation not included in the present paper), a rotation of perihelion is

[4] For a statistical development of the theory of the energy tensor of a continuous medium, based on this idea, see J. L. Synge, Trans. Roy. Soc. Canada, Section III, 28, 127 (1934).

found, but it is only one-eighteenth of the correct astronomical value.

As for the application of the method to atomic physics, it is obvious that a theory which does not take into consideration the intrinsic angular momenta of the particles involved is not adequate. In its present form, the theory is to be compared to that of the Bohr atom, but with the satisfactory feature of relativistic invariance even when the ratio of the masses is not assumed to be infinite. A relativistically invariant treatment of the two-body problem has proved very difficult. Sommerfeld[5] treated approximately the case where the two particles described circles about the mass-center, but the method cannot be extended to the case of elliptical orbits. Using the retarded potential, Darwin[6] developed a Lagrangian and a Hamiltonian for the two-body problem, but was careful to retain only terms of the order $1/c^2$, to avoid the awkward question of the theoretical radiation of energy from an accelerated electron. Darwin's results have been used in modern quantum theory by Breit.[7] Attempts to treat the atomic two-body problem by the method of the retarded potential are necessarily defective by reason of the radiation of energy, implied by that theory, and inconsistent with quantum theory. Indeed Bohr's initial success[8] was due to his complete neglect of the electromagnetic field except insofar as it supplied a Coulomb field for the electron. Sommerfeld's work, referred to above, was an attempt to extend that idea to the two-body problem. But here the two-body problem differs essentially from the one-body problem when relativistic invariance is considered. When the nucleus is regarded as infinitely massive, it defines a privileged Galilean frame of reference, and a Coulomb field relative to that privileged frame may be postulated without doing violence to relativistic invariance. But when the ratio of the masses is finite, field theory gives no privileged frame of reference, and it is impossible to formulate a law of interaction based on the Coulomb law. Some of the difficulties of the situation have been discussed by Frenkel.[9]

In view of these difficulties experienced in the application of more usual methods, the method of the present paper may be worthy of consideration on three grounds:

(1) It gives a relativistically invariant definition of angular momentum, such that the angular momentum of a complete system is conserved.

(2) It gives a relativistically invariant definition of mass-center, such that the mass-center of a complete system moves in a straight line with constant velocity.

(3) It gives a relativistically invariant treatment of the two-body problem, with the inverse square law deduced as a consequence of mechanical conservation laws.

2. Momentum, Energy, Angular Momentum and Mass-Center of a System

The laws of conservation of linear and angular momentum for systems of particles in Newtonian mechanics depend on Newton's third law. We proceed to develop these ideas in relativity, employing the idea of elementary impulses. Intrinsic angular momenta of the particles are not taken into consideration. It is not necessary to assume that the proper masses of the particles are constant.

We shall use Latin subscripts for the range 1, 2, 3, 4 and Greek for the range 1, 2, 3 with the usual summation convention. We shall employ a general Galilean reference system, x_ρ being rectangular Cartesians and $x_4 = ict$.

The system of particles to be discussed is supposed free from external influences. We may call such a system *complete*. The space-time picture consists of the world-lines of the particles and the null world-lines of the elementary impulses passing between them. It is conceptually simplest to regard the impulses as discrete, although we may obviously pass in the limit to the case of continuous streams. The world-lines of particles and impulses will consist of straight portions between collisions of particles with elementary impulses, with sudden changes of direction at these collisions.

Associated with each event on the world-line of a dynamical element (particle or impulse) there is a momentum-energy 4-vector M_r which lies on the world-line. The components M_r

[5] A. Sommerfeld, *Sitz. math. phys. Kl. K.B. Akad. d. Wiss. zu München* (1916), p. 140.
[6] C. G. Darwin, Phil. Mag. **39**, 527 (1920).
[7] G. Breit, Phys. Rev. **34**, 553 (1929).
[8] N. Bohr, Phil. Mag. **26**, 1 (1913).
[9] J. Frenkel, *Lehrbuch der Elektrodynamik*, Bd. 1 (Berlin, 1926), pp. 352–353.

remain constant as we pass along the world-line between collisions. At a collision the law of conservation gives

$$\sum M_r = \sum M_r', \tag{2.1}$$

the summation on the left being the sum of the momentum-energy 4-vectors of the elements involved in the collision just before the collision, and that on the right the corresponding sum after the collision.

Let us draw across space-time a 3-space S (Fig. 2). It may conveniently be taken to be $x_4 = \text{const.}$, but this is not necessary. *We define the momentum-energy 4-vector of the system to be*

$$X_r = \sum_i M_r^{(i)}, \tag{2.2}$$

the summation being taken over all the events where world-lines are cut by S. It might appear that X_r depended on the choice of S, but that is not the case. If we displace S, X_r certainly does not vary as long as S in its variation does not pass across a collision. If it passes from S to S' across a collision C (Fig. 2), X_r remains unaltered on account of (2.1). Thus X_r is independent of S. *Thus the momentum-energy 4-vector of a complete system is constant.* It is a free (unlocalized) 4-vector.

Let x_r be the coordinates of an event on the world-line of a dynamical element, M_r being the momentum-energy 4-vector. *We define the angular momentum of the element with respect to an arbitrary base-event* ξ_r *to be the skew-symmetric tensor*[10]

$$Y_{rs}(\xi) = (x_r - \xi_r) M_s - (x_s - \xi_s) M_r. \tag{2.3}$$

We note that Y_{rs} is not changed by a variation of x_r along the world-line between collisions, the increments in x_r being proportional to M_r. Further, a displacement of ξ_r parallel to M_r does not alter Y_{rs}.

Drawing, as before, a 3-space S across space-time, *we define the angular momentum of a system with respect to an arbitrary base-event* ξ_r *to be*

$$Y_{rs}(\xi) = \sum_i [(x_r^{(i)} - \xi_r) M_s^{(i)} - (x_s^{(i)} - \xi_s) M_r^{(i)}], \tag{2.4}$$

[10] Cf. J. Frenkel, reference 9, where, however, the absence of an equivalent to Newton's third law hinders the useful development of the idea.

FIG. 2.

the summation extending over all events $x_r^{(i)}$ *at which* S *cuts world-lines,* $M_r^{(i)}$ *being the momentum-energy 4-vector at* $x_r^{(i)}$. It is easy to see that Y_{rs} is independent of the choice of S. Y_{rs} certainly remains unaltered as we vary S without crossing a collision. When S crosses a collision C as in Fig. 2, the values of the $x_r^{(i)}$ involved are the same as the x_r of the collision, so that the part of Y_{rs} involved in the collision is

$$(x_r - \xi_r) \sum_i M_s^{(i)} - (x_s - \xi_s) \sum_i M_r^{(i)}, \tag{2.5}$$

the summations extending over all the elements involved in the collision. It follows immediately from (2.1) that this is unchanged by the collision. *Thus the angular momentum of a complete system is constant:* the value of $Y_{rs}(\xi)$ of course depends on the choice of ξ_r. However, we may write

$$Y_{rs}(\xi) = \sum_i (x_r^{(i)} M_s^{(i)} - x_s^{(i)} M_r^{(i)}) - \xi_r X_s + \xi_s X_r, \tag{2.6}$$

and therefore a displacement of ξ_r parallel to X_r leaves Y_{rs} unaltered.

We now define the *mass-center* as follows: *the world-line of the mass-center of a complete system consists of those events* ξ_r *such that when* ξ_r *is used as a base for the measurement of angular momentum we have*

$$Y_{rs}(\xi) X_s = 0. \tag{2.7}$$

To see that such events exist, let us choose our reference system with its time-axis in the direction of X_r: then

$$X_\rho = 0, \tag{2.8}$$

and (2.7) reduce to

$$Y_{\rho 4}(\xi) = 0, \tag{2.9}$$

the equation for $r = 4$ being identically satisfied on account of the skew-symmetry of Y_{rs}. Using the general form (2.6), (2.9) gives

$$\xi_\rho = \sum_i (x_\rho^{(i)} M_4^{(i)} - x_4^{(i)} M_\rho^{(i)}) / X_4; \tag{2.10}$$

thus ξ_4 remains indeterminate, and (*2.10*) *are the equations of the world-line of the mass-center of the system for a frame of reference in which the momentum of the system is zero. Referred to a general Galilean frame, the mass-center has a uniform velocity.*

Referring again to a frame in which the mass-center is at rest, the observer may conveniently take S to be $x_4 = \text{const.}$, his instantaneous space. Then, since

$$\sum_i M_\rho^{(i)} = X_\rho = 0, \tag{2.11}$$

the coordinates of the mass-center are given by

$$\xi_\rho = \sum_i x_\rho^{(i)} M_4^{(i)} / \sum_i M_4^{(i)}. \tag{2.12}$$

For any dynamical element the momentum-energy 4-vector has components

$$M_\alpha = \mu_\alpha / c, \quad M_4 = iW/c^2, \tag{2.13}$$

where μ_α is the momentum 3-vector and W the energy. For a particle we have

$$\mu_\alpha = m_0 \gamma u_\alpha, \quad W = m_0 \gamma c^2, \quad \gamma = (1 - u^2/c^2)^{-\frac{1}{2}}, \tag{2.14}$$

m_0 being the proper mass and u_α the velocity. Thus *relative to a frame of reference in which the mass-center is at rest, the position of the mass-center is given by*

$$\xi_\rho = \sum_i x_\rho^{(i)} W^{(i)} / \sum_i W^{(i)}, \tag{2.15}$$

where the summation extends over all the dynamical elements in existence at any specified time, $x_\rho^{(i)}$ being the coordinates and $W^{(i)}$ the energy of the element.

This is of course the Newtonian formula, energy replacing mass as we might expect. But it is to be remembered that (2.15) holds only for a reference system in which the mass-center is at rest.

In treating the two-body problem for small relative velocity, we shall see that the total energy of the elementary impulses is of the same order as the Newtonian kinetic energy ($\frac{1}{2}m_0 u^2$) of the particles, and therefore small in comparison with their relativistic energy ($m_0 \gamma c^2$). In that case we may get a first approximation to the position of the mass-center by substituting the proper masses of the particles for the energies in (2.15), and omitting terms corresponding to elementary impulses.

It is interesting to note that this theory provides us with the seven dynamical quantities usually associated with a dynamical system, three components of momentum, energy, and three components of angular momentum relative to the mass-center. The first four are given by the components X_r. There are six components of angular momentum as given by (2.4) : but when the mass-center is base, these are connected by (2.7) which are actually three in number, on account of the identity

$$Y_{r\alpha}(\xi) X_r X_\alpha = 0. \tag{2.16}$$

Let us now write down *the components of angular momentum relative to the mass-center when the frame of reference is chosen to reduce the mass-center to rest.* Let us take the mass-center for origin. Of the six components, three vanish by (2.9), that is

$$Y_{\rho 4}(0) = 0\,; \tag{2.17}$$

the other three are, by (2.6) and (2.8),

$$Y_{\rho\sigma}(0) = \sum_i (x_\rho^{(i)} M_\sigma^{(i)} - x_\sigma^{(i)} M_\rho^{(i)}). \tag{2.18}$$

By (2.13) this may also be written

$$c\,Y_{\rho\sigma}(0) = \sum_i (x_\rho^{(i)} \mu_\sigma^{(i)} - x_\sigma^{(i)} \mu_\rho^{(i)}), \tag{2.19}$$

which is the Newtonian formula, except that the contributions from elementary impulses are to be included in the summation. In the case of the two-body problem it will be seen that these last are small compared with the contributions from the particles.

3. A Mechanical Proof of the Inverse Square Law in the Two-Body Problem

Consider two interacting particles, A and B. As shown in §2, the mass-center of the system describes a straight line with constant velocity in any Galilean reference system. Let us choose our reference system so that the mass-center is at rest at the origin. Since, by (2.15), the position of the mass-center depends not only on the particles but also on the energy in transit between

them, we cannot conclude that the line AB passes accurately through the mass-center.

We shall now assume that the velocities of the particles are small compared with that of light. Let m_0, m_0' be the proper masses of A, B, respectively. We shall not at present assume them to be constant but only that their fractional increments are of the order u^2/c^2, where u is the velocity of either. This means that we admit the possibility of variations in intrinsic energy (m_0c^2) comparable with the Newtonian kinetic energy.

Consider the particles at some instant t: let their distance apart be r. Let τ be the short time required by light to cover this distance, so that

$$\tau = r/c. \tag{3.1}$$

Terms of the order u^2/c^2 being neglected, the momentum of A is m_0u_α, and its increment in the short interval $(t, t+\tau)$ is

$$m_0(du_\alpha/dt)\tau = m_0f_\alpha\tau, \tag{3.2}$$

where f_α is the acceleration of A. But this increment in momentum is due to

(i) elementary impulses received from B during the interval τ;

(ii) elementary impulses expelled towards B during the interval τ.

Denoting the momenta of these two sets of impulses by μ_α, μ_α', respectively, we have by the conservation of momentum

$$\mu_\alpha = m_0f_\alpha\tau + \mu_\alpha'. \tag{3.3}$$

Let l_α be the direction cosines of the instantaneous position of BA. The lines along which the elementary impulses move are very close to BA, and we may write, as in (1.1),

$$\mu_\alpha = l_\alpha W/c, \quad \mu_\alpha' = -l_\alpha W'/c, \tag{3.4}$$

where W is the total energy of the impulses (i) and W' the total energy of the impulses (ii). Thus, by virtue of (3.1), (3.3) gives

$$l_\alpha(W+W') = m_0f_\alpha\tau c = m_0f_\alpha r. \tag{3.5}$$

In (3.1) we deliberately chose the interval τ so that all the impulses destined to strike A during the interval τ (and no others) are already on their way from B at time t. Their total energy is W. Also the total energy of the impulses on their way from A to B at time t is approximately the same as the total energy of the impulses expelled from A during the interval τ, that is, W'. *Hence the total energy E of impulses in transit at time t is*

$$E = W + W'. \tag{3.6}$$

Thus (3.5) may be written

$$l_\alpha E = m_0f_\alpha r. \tag{3.7}$$

When we consider the motion of B, we have an equation of the same form

$$l_\alpha' E = m_0'f_\alpha' r, \tag{3.8}$$

where l_α' are the direction cosines of the instantaneous position of AB, so that $l_\alpha' = -l_\alpha$.

Therefore the acceleration vectors of the particles lie on the instantaneous position of the line AB, directed away from one another if E is positive and towards one another if E is negative. We shall denote by f, f' the algebraic values of the accelerations, positive when outward, negative when inward. Then (3.7), (3.8) give

$$E = m_0fr = m_0'f'r. \tag{3.9}$$

The energy E in transit is therefore small in comparison with the relativistic energies of the particles m_0c^2, $m_0'c^2$. Hence to our order of approximation (2.15) gives for the coordinates of the mass-center

$$\xi_\alpha = (m_0x_\alpha + m_0'x_\alpha')/(m_0+m_0'), \tag{3.10}$$

where x_α, x_α' are the coordinates of the particles. But this point is the origin, and so

$$m_0x_\alpha + m_0'x_\alpha' = 0, \tag{3.11}$$

which shows that to our order of approximation the line AB passes through the mass-center. Let ρ, ρ' denote the distances of the particles from the mass-center: then

$$\rho = rm_0'/(m_0+m_0'), \quad \rho' = rm_0/(m_0+m_0'), \tag{3.12}$$

and (3.9) gives

$$\begin{aligned} E &= f\rho(m_0/m_0')(m_0+m_0') \\ &= f'\rho'(m_0'/m_0)(m_0+m_0'). \end{aligned} \tag{3.13}$$

As a consequence of our basic hypotheses, the total energy of the system is conserved. This

consists of the energies of the particles and the energy E in transit. The energy of A is accurately

$$m_0c^2(1-u^2/c^2)^{-\frac{1}{2}}, \tag{3.14}$$

and approximately

$$m_0c^2+\tfrac{1}{2}m_0u^2, \tag{3.15}$$

and consequently throughout the motion we have the conservation of energy expressed in the form

$$m_0c^2+\tfrac{1}{2}m_0u^2+m_0'c^2+\tfrac{1}{2}m_0'u'^2+E=\text{const.} \tag{3.16}$$

Differentiation of (3.11) leads to

$$m_0u=m_0'u', \tag{3.17}$$

and thus, by virtue of (3.13), (3.16) may be written

$$m_0c^2+m_0'c^2+(m_0/m_0')(m_0+m_0')(\tfrac{1}{2}u^2+f\rho) =\text{const.} \tag{3.18}$$

Since the acceleration of A is central, we have also

$$\rho^2d\theta/dt=h, \tag{3.19}$$

a constant, θ being the polar angle.

We have now the two equations of motion (3.18) and (3.19). The first two terms in (3.18) represent the sum of the intrinsic energies of the particles. As long as these are supposed variable the motion remains indeterminate. This measure of generality has been retained in the argument in order to show that the law of the inverse square is not deducible by the present method when the intrinsic energies of the particles are variable. Thus there is no implication of this law in the case where the particles are atoms, for example. The theory leaves a considerable measure of indeterminacy in such cases.

Let us now confine our attention to the case where the proper masses are constant, or the proper energies are so nearly constant that their variations are small in comparison with the Newtonian kinetic energies. The former assumption applies to the proton-electron combination and the latter to the sun-planet combination. Then (3.18) gives

$$\tfrac{1}{2}u^2+f\rho=C, \tag{3.20}$$

a constant. The rest of the reasoning is simple, being merely an inversion of familiar arguments. We have by (3.19)

$$\left.\begin{aligned} f&=d^2\rho/dt^2-\rho(d\theta/dt)^2=d^2\rho/dt^2-h^2\rho^{-3},\\ u^2&=(d\rho/dt)^2+\rho^2(d\theta/dt)^2=(d\rho/dt)^2+h^2\rho^{-2},\end{aligned}\right\} \tag{3.21}$$

and so, passing along the orbit,

$$d(\tfrac{1}{2}u^2)=(d^2\rho/dt^2-h^2\rho^{-3})d\rho=fd\rho. \tag{3.22}$$

Thus (3.20) may be written

$$\tfrac{1}{2}u^2+\rho d(\tfrac{1}{2}u^2)/d\rho=C, \tag{3.23}$$

and hence

$$\tfrac{1}{2}\rho u^2=C\rho-D, \tag{3.24}$$

where D is a constant. Substituting in (3.20), we obtain

$$f=D/\rho^2=k/(m_0r^2), \tag{3.25}$$

where k is a constant. By (3.9) the acceleration of B is

$$f'=k/(m_0'r^2), \tag{3.26}$$

and the energy E in transit, the *potential energy* of Newtonian mechanics, is

$$E=k/r. \tag{3.27}$$

Unlike Newtonian potential energy, this is *not* indeterminate to within an additive constant.

To sum up: *when two particles of constant proper masses move under their mutual interaction with relative velocity small compared with that of light, their motion relative to the mass-center is identical to a first approximation with that of the Newtonian two-body problem when the law of force is that of the inverse square.*

We may call

$$F=m_0f=m_0'f'=k/r^2 \tag{3.28}$$

the "repulsive force" between the particles: we would therefore put $k=ee'$ in the case of particles carrying charges e, e', and $k=-Gm_0m_0'$ in the case of gravitation, G being the constant of gravitation.

4. Discussion

It will be noticed that the present theory combines some of the features of "action at a distance" and "action through a medium." Action at a distance has appeared objectionable to some on vague philosophical grounds, but it

receives its death-blow from the theory of relativity, since the idea of an absolute simultaneity is implicit in it. On the other hand, action through a medium fails to deal satisfactorily with the mechanics of particles. There is also an aesthetic objection to treating kinetic energy as corpuscular and potential energy as continuously distributed. The present method succeeds in localizing the potential energy in space, and at the same time making it corpuscular like kinetic energy. But the fact that it makes the law of the inverse square a deduction instead of a supplementary hypothesis is probably the most remarkable feature.

The law of the inverse square is usually associated with the fact that space is three-dimensional, and that the surface area of a sphere consequently varies as the square of the radius. That has nothing whatever to do with the present theory; our argument may be outlined as follows, supposing for simplicity that B is massive and the interaction repulsive. There are two effects at work as A recedes from B. First, as the distance increases, the impulses arrive less frequently at A: this makes the momentum received per unit time vary as $1/r$. Secondly, the impulses become weaker as they impart energy to A: this produces another factor $1/r$, and the combination of the two effects gives the inverse square law.

Hyperfine Structure Formulae for the Configuration d^2s

Application to $5d^26s\ {}^4F$ States of La I*

M. F. CRAWFORD, *Department of Physics, University of Wisconsin*

(Received March 22, 1935)

Hfs interval factor formulae for the states of d^2s are derived by the method of Breit and Wills. The formulae for intermediate coupling are expressed in two forms: one involving the coefficients C's, the other the coefficients K's, corresponding to the representation of the functions of the states in intermediate coupling as a linear combination of the (jj) and the (LS) functions, respectively. The (LS)←→(jj) transformation matrices as well as the interval factor formulae for (LS) and (jj) coupling are also given. As the coefficients are determined from the empirical multiplet separations, the energy matrices in both (LS) and (jj) coupling are listed. The theory is applied to the $5d^26s\ {}^4F$ states of La I and consistently accounts for the relative hfs separations of these states. The values obtained for the interaction constants of the $6s$ and $5d$ electrons are 0.119 and 0.0039 cm^{-1}, respectively. The nuclear g-factor computed from these is $g(\mathrm{I})=0.71$. The corresponding value of the nuclear magnetic moment is 2.5 nuclear magnetons.

I. INTRODUCTION

BREIT and Wills[1] extended the relativistic theory of hyperfine structure[2] to intermediate coupling and derived the interval factor formulae for several important types of configurations. A number of other configurations, types with an unpaired s electron which usually give rise to measurable hyperfine separations, merit consideration. The configuration d^2s is frequently encountered in the spectra of the elements with partially filled d shells. As the data on the nuclear magnetic moments of these elements are meager, it is of some importance to treat d^2s by the same method; particularly since by so doing one obtains the interval factors of the states individually rather than the sum of the interval factors of all states with the same J, and is thus able to evaluate the nuclear magnetic moment when the hyperfine separations of only a few states are known. Hyperfine structure formulae for d^2s are presented in this paper and applied to the observed structures of the $5d^26s\ {}^4F$ states of La I.

II. WAVE FUNCTIONS AND INTERVAL FACTOR FORMULAE IN INTERMEDIATE COUPLING

The configuration d^2s gives rise to sixteen states: two with $J=9/2$, three with $J=7/2$, four with $J=5/2$, four with $J=3/2$, and three with $J=1/2$. As the relativistic treatment of hyperfine structure must be made via (jj) coupling, the configuration will be considered first in this coupling. The functions representing the states in (jj) coupling can be conveniently thought of as arising from the coupling of the states of d^2 with an s electron. The states of d^2 are given in Table I. They are designated by

TABLE I. *States of* d^2.

$(j_1, j_2)=$	(5/2, 5/2),			(5/2, 3/2),				(3/2, 3/2)	
Resultant $J=$	4	2	0,	4	3	2	1,	2	0
Symbol	ψ^4	ψ^2	ψ^0	φ^4	φ^3	φ^2	φ^1	χ^2	χ^0

Greek letters with their J values indicated by superscripts.

The calculations can be made expediently by using eigenfunctions for a given magnetic quantum number. These functions of d^2 states will be represented by the state symbols with the magnetic quantum number m added as a subscript. It is necessary in the calculation to express the two-election functions in terms of the one-electron functions, which for a given j and m will be represented by symbols of the type $(j)_m$. The two-electron functions for the states with $m=J$, expressed in terms of the one-electron functions, are given here. The functions for other values of m can readily be obtained from these by the method of Gray and Wills.[3]

* This research was carried out during the tenure of a Royal Society of Canada Fellowship.

[1] G. Breit and L. A. Wills, Phys. Rev. **44**, 470 (1933).

[2] G. Breit, Phys. Rev. **35**, 1447 (1930); **38**, 463 (1931); G. Racah, Zeits. f. Physik **71**, 431 (1931); E. Fermi and E. Segrè, Zeits. f. Physik **82**, 729 (1933).

[3] N. Gray and L. A. Wills, Phys. Rev. **38**, 248 (1931).

(5 2, 5/2) Sub-group.

$\psi_4{}^4=(1/\sqrt{2})[(5/2)_{5/2},\ (5/2)_{3/2}]$.

$\psi_2{}^2=((5/14)^{\frac{1}{2}}1/\sqrt{2})[(5/2)_{5/2},\ (5/2)_{-\frac{1}{2}}]-((9/14)^{\frac{1}{2}}1/\sqrt{2})[(5/2)_{3/2},\ (5/2)_{\frac{1}{2}}]$.

$\psi_0{}^0=(1/\sqrt{3}\cdot 1/\sqrt{2})[(5/2)_{5/2},\ (5/2)_{-5/2}]-(1/\sqrt{3}\cdot 1/\sqrt{2})[(5/2)_{3/2},\ (5/2)_{-3/2}]$
$+(1/\sqrt{3}\cdot 1/\sqrt{2})[(5/2)_{\frac{1}{2}},\ (5/2)_{-\frac{1}{2}}]$.

(5/2, 3/2) Sub-group.

$\varphi_4{}^4=(1/\sqrt{2})[(5/2)_{5/2},\ (3/2)_{3/2}]$.

$\varphi_3{}^3=((3/8)^{\frac{1}{2}}1/\sqrt{2})[(5/2)_{3/2},\ (3/2)_{3/2}]-((5/8)^{\frac{1}{2}}1/\sqrt{2})[(5/2)_{5/2},\ (3/2)_{\frac{1}{2}}]$.

$\varphi_2{}^2=((10/21)^{\frac{1}{2}}1/\sqrt{2})[(5/2)_{5/2},\ (3/2)_{-\frac{1}{2}}]-((8/21)^{\frac{1}{2}}1/\sqrt{2})[(5/2)_{3/2},\ (3/2)_{\frac{1}{2}}]$
$+((3/21)^{\frac{1}{2}}1/\sqrt{2})[(5/2)_{\frac{1}{2}},\ (3/2)_{3/2}]$.

$\varphi_1{}^1=((10/20)^{\frac{1}{2}}1/\sqrt{2})[(5/2)_{5/2},\ (3/2)_{-3/2}]-((6/20)^{\frac{1}{2}}1/\sqrt{2})[(5/2)_{3/2},\ (3/2)_{-\frac{1}{2}}]$
$+((3/20)^{\frac{1}{2}}1/\sqrt{2})[(5/2)_{\frac{1}{2}},\ (3/2)_{\frac{1}{2}}]-((1/20)^{\frac{1}{2}}1/\sqrt{2})[(5/2)_{-\frac{1}{2}},\ (3/2)_{3/2}]$.

(3/2, 3/2) Sub-group.

$\chi_2{}^2=(1/\sqrt{2})[(3/2)_{3/2},\ (3/2)_{\frac{1}{2}}]$.

$\chi_0{}^0=(1/\sqrt{2}\cdot 1/\sqrt{2})[(3/2)_{\frac{1}{2}},\ (3/2)_{-\frac{1}{2}}]-(1/\sqrt{2}\cdot 1/\sqrt{2})[(3/2)_{3/2},\ (3/2)_{-3/2}]$.

Each square bracket in the preceding equations is an abbreviation for the determinant representation of a two-electron function as a combination of products of two one-electron functions.

The states of d^2s will now be considered. The functions of the s electron will be symbolized by s_m (as $j=\frac{1}{2}$ always it need not be specified). They can be combined with the functions for the d^2 states without paying attention to symmetry.

$J=9/2$. The functions representing the two states with $J=9/2$, $m=9/2$ in (jj) coupling can be written

$$\mathrm{I}=s_{\frac{1}{2}}\psi_4{}^4,\quad \mathrm{II}=s_{\frac{1}{2}}\varphi_4{}^4. \tag{1}$$

The function representing a state with $J=9/2$, $m=9/2$ in intermediate coupling, symbolically written $(9/2)_{9/2}$, then is

$$(9/2)_{9/2}=C_1\mathrm{I}+C_2\mathrm{II}, \tag{2}$$

where C_1 and C_2 are numerical coefficients whose squares sum to unity. The interval factor formula obtained from this function by the procedure of Breit and Wills[1] is

$$9/2\cdot A(J=9/2)=1/2\cdot a_s(C_1{}^2+C_2{}^2)+a'(4C_1{}^2+5/2\cdot C_2{}^2)+3/2\cdot a''C_2{}^2+4C_1C_2a'''. \tag{3}$$

a_s, a', a'', a''' represent the hyperfine structure interaction or coupling constants as in the paper of Breit and Wills. Eq. (3) is the general expression for the interval factors of the states with $J=9/2$ in intermediate coupling. The expression involves the coefficients C_1 and C_2, and there is a different set of these for each of the two states.

$J=7/2$. The functions representing the three states with $J=7/2$, $m=7/2$ in (jj) coupling are

$$\mathrm{I}=(8/9)^{\frac{1}{2}}s_{-\frac{1}{2}}\psi_4{}^4-1/\sqrt{9}\cdot s_{\frac{1}{2}}\psi_3{}^4,\quad \mathrm{II}=(8/9)^{\frac{1}{2}}s_{-\frac{1}{2}}\varphi_4{}^4-1/\sqrt{9}\cdot s_{\frac{1}{2}}\varphi_3{}^4,\quad \mathrm{III}=s_{\frac{1}{2}}\varphi_3{}^3. \tag{4}$$

In intermediate coupling the general function for a state with $J=7/2$, $m=7/2$ is

$$(7/2)_{7/2}=C_1I+C_2\mathrm{II}+C_3\mathrm{III}. \tag{5}$$

From this we obtain

$$7/2\cdot A(J=7/2)=a_s(-7/18\cdot C_1^2-7/18\cdot C_2^2+1/2\cdot C_3^2)+a'(35/9\cdot C_1^2+175/72\cdot C_2^2+17/8\cdot C_3^2 +\sqrt{15}/12\cdot C_2C_3)+a''(35/24\cdot C_2^2+7/8\cdot C_3^2-\sqrt{15}/12\cdot C_2C_3)+a'''(35/9\cdot C_1C_2+2(5/12)^{\frac{1}{2}}\cdot C_1C_3). \quad (6)$$

J=5/2. The functions representing the four states with $J=5/2$, $m=5/2$ in (jj) coupling are

$$\mathrm{I}=s_1\psi_2^2, \quad \mathrm{II}=(6/7)^{\frac{1}{2}}s_{-1}\varphi_3^3-(1/7)^{\frac{1}{2}}s_1\varphi_2^3, \quad \mathrm{III}=s_1\varphi_2^2, \quad \mathrm{IV}=s_1\chi_2^2. \quad (7)$$

In intermediate coupling the general function is

$$(5/2)_{5/2}=C_1\mathrm{I}+C_2\mathrm{II}+C_3\mathrm{III}+C_4\mathrm{IV}. \quad (8)$$

From this we obtain

$$5/2\cdot A(J=5/2)=a_s(\tfrac{1}{2}C_1^2-5/14\cdot C_2^2+\tfrac{1}{2}C_3^2+\tfrac{1}{2}C_4^2)+a'(2C_1^2+85/42\cdot C_2^2+11/6\cdot C_3^2 +16/21\sqrt{2}\cdot C_2C_3)+a''(5/6\cdot C_2^2+\tfrac{1}{6}C_3^2+2C_4^2-16/21\sqrt{2}\cdot C_2C_3) +a'''(-4/7\cdot C_1C_2+4\sqrt{2}\cdot C_1C_3+8/\sqrt{21}\cdot C_2C_4-14(2/21)^{\frac{1}{2}}C_3C_4). \quad (9)$$

J=3/2. The functions for the four states with $J=3/2$, $m=3/2$ in (jj) coupling are:

$$\mathrm{I}=2/\sqrt{5}\cdot s_{-1}\psi_2^2-1/\sqrt{5}\cdot s_1\psi_1^2, \quad \mathrm{II}=2/\sqrt{5}\cdot s_{-1}\varphi_2^2-1/\sqrt{5}\cdot s_1\varphi_1^2, \quad \mathrm{III}=s_1\varphi_1^1,$$
$$\mathrm{IV}=2/\sqrt{5}\cdot s_{-1}\chi_2^2-1/\sqrt{5}\cdot s_1\chi_1^2. \quad (10)$$

In intermediate coupling the general function is

$$(3/2)_{3/2}=C_1\mathrm{I}+C_2\mathrm{II}+C_3\mathrm{III}+C_4\mathrm{IV}. \quad (11)$$

From this we obtain

$$3/2\cdot A(J=3/2)=a_s(-3/10\cdot C_1^2-3/10\cdot C_2^2+\tfrac{1}{2}C_3^2-3/10\cdot C_4^2)+a'(9/5\cdot C_1^2+33/20\cdot C_2^2 +7/4\cdot C_3^2-3\sqrt{7}/10\cdot C_2C_3)+a''(3/20\cdot C_2^2-\tfrac{3}{4}C_3^2+9/5\cdot C_4^2+3\sqrt{7}/10\cdot C_2C_3) +a'''(18\sqrt{2}/5\cdot C_1C_2-2\sqrt{14}/5\cdot C_1C_3-3\sqrt{42}/5\cdot C_2C_4+\sqrt{6}/5\cdot C_3C_4). \quad (12)$$

J=1/2. The functions for the three states with $J=\frac{1}{2}$, $m=\frac{1}{2}$ in (jj) coupling are

$$\mathrm{I}=s_1\psi_0^0, \quad \mathrm{II}=(2/3)^{\frac{1}{2}}s_{-1}\varphi_1^1-1/\sqrt{3}\cdot s_1\varphi_0^1, \quad \mathrm{III}=s_1\chi_0^0. \quad (13)$$

The general function in intermediate coupling is

$$(1/2)_{\frac{1}{2}}=C_1\mathrm{I}+C_2\mathrm{II}+C_3\mathrm{III}. \quad (14)$$

From this we obtain

$$\tfrac{1}{2}A(J=\tfrac{1}{2})=a_s(\tfrac{1}{2}C_1^2-\tfrac{1}{6}C_2^2+\tfrac{1}{2}C_3^2)+7/6\cdot C_2^2a'-\tfrac{1}{2}C_2^2a''+a'''(20/3\sqrt{5}\cdot C_1C_2+2(10/3)^{\frac{1}{2}}\cdot C_2C_3). \quad (15)$$

III. Interval Factor Formulae in (jj) and (LS) Coupling, and the (jj)—(LS) Transformation Matrices

The interval factors of the states in (jj) coupling can be obtained directly from the preceding formulae. Consider the states with $J=9/2$. It is obvious that for one of these states in (jj) coupling $C_1=1$, $C_2=0$; and for the other $C_1=0$, $C_2=1$. The substitution of these values in Eq. (3) gives the following expressions for the (jj) interval factors.

J=9/2. Sub-group.

$$(5/2,\ 5/2,\ \tfrac{1}{2}): \quad A(J=9/2)=1/9\cdot a_s+8/9\cdot a'.$$
$$(5/2,\ 3/2,\ \tfrac{1}{2}): \quad A(J=9/2)=1/9\cdot a_s+5/9\cdot a'+\tfrac{1}{3}\cdot a''. \quad (16)$$

Similarly for the other states we get:

$J=7/2$. *Sub-group.*

$$\begin{aligned}
(5/2,\,5/2,\,\tfrac{1}{2}):&\quad A(J=7/2)=-1/9\cdot a_s+10/9\cdot a'.\\
(5/2,\,3/2;\,j=4;\,\tfrac{1}{2}):&\quad A(J=7/2)=-1/9\cdot a_s+25/36\cdot a'+5/12\cdot a''.\\
(5/2,\,3/2;\,j=3;\,\tfrac{1}{2}):&\quad A(J=7/2)=1/7\cdot a_s+17/28\cdot a'+\tfrac{1}{4}a''.
\end{aligned}\tag{17}$$

$J=5/2$. *Sub-group.*

$$\begin{aligned}
(5/2,\,5/2,\,\tfrac{1}{2}):&\quad A(J=5/2)=\tfrac{1}{5}a_s+4/5\cdot a'.\\
(5/2,\,3/2;\,j=3;\,1/2):&\quad A(J=5/2)=-1/7\cdot a_s+17/21\cdot a'+1/3\cdot a''.\\
(5/2,\,3/2;\,j=2;\,\tfrac{1}{2}):&\quad A(J=5/2)=\tfrac{1}{5}a_s+11/15\cdot a'+1/15\cdot a''.\\
(3/2,\,3/2,\,\tfrac{1}{2}):&\quad A(J=5/2)=\tfrac{1}{5}a_s+4/5\cdot a''.
\end{aligned}\tag{18}$$

$J=3/2$. *Sub-group.*

$$\begin{aligned}
(5/2,\,5/2,\,\tfrac{1}{2}):&\quad A(J=3/2)=-\tfrac{1}{5}a_s+6/5\cdot a'.\\
(5/2,\,3/2;\,j=2;\,\tfrac{1}{2}):&\quad A(J=3/2)=-\tfrac{1}{5}a_s+11/10\cdot a'+1/10\cdot a''.\\
(5/2,\,3/2;\,j=1;\,\tfrac{1}{2}):&\quad A(J=3/2)=\tfrac{1}{5}a_s+7/6\cdot a'-\tfrac{1}{2}a''.\\
(3/2,\,3/2,\,\tfrac{1}{2}):&\quad A(J=3/2)=-\tfrac{1}{5}a_s+6/5\cdot a''.
\end{aligned}\tag{19}$$

$J=1/2$. *Sub-group.*

$$\begin{aligned}
(5/2,\,5/2,\,\tfrac{1}{2}):&\quad A(J=\tfrac{1}{2})=a_s.\\
(5/2,\,3/2,\,\tfrac{1}{2}):&\quad A(J=\tfrac{1}{2})=-\tfrac{1}{3}a_s+7/3\cdot a'-a''.\\
(3/2,\,3/2,\,\tfrac{1}{2}):&\quad A(J=\tfrac{1}{2})=a_s.
\end{aligned}\tag{20}$$

TABLE II. *Transformation matrices,* (jj)–(LS).

$J=9/2$.	$s\psi^4$	$s\varphi^4$
$^4F_{9/2}$	$2/\sqrt{5}$	$1/\sqrt{5}$
$^2G_{9/2}$	$-1/\sqrt{5}$	$2/\sqrt{5}$

$J=7/2$.	$s\psi^4$	$s\varphi^4$	$s\varphi^3$
$^4F_{7/2}$	$1/\sqrt{5}$	$\tfrac{1}{2}\sqrt{5}$	$\sqrt{3/2}$
$^2G_{7/2}$	$1/\sqrt{5}$	$-2/\sqrt{5}$	0
$^2F_{7/2}$	$3/\sqrt{15}$	$3/2\sqrt{15}$	$-\tfrac{1}{2}$

$J=5/2$.	$s\psi^3$	$s\varphi^3$	$s\varphi^2$	$s\chi^2$
$^4F_{5/2}$	$2/5\sqrt{5}$	$-5/3\sqrt{5}$	$-8\sqrt{2}/15\sqrt{5}$	$-4\sqrt{21}/15\sqrt{5}$
$^2F_{5/2}$	$1/5$	$\tfrac{1}{3}$	$-4\sqrt{2}/15$	$-2\sqrt{21}/15$
$^2D_{5/2}$	$6/5\sqrt{3}$	0	$-\sqrt{6}/5$	$\sqrt{21}/5\sqrt{3}$
$^4P_{5/2}$	$4\sqrt{7}/5\sqrt{10}$	0	$3\sqrt{7}/5\sqrt{5}$	$-\sqrt{6}/5\sqrt{5}$

$J=3/2$.	$s\psi^2$	$s\varphi^2$	$s\varphi^1$	$s\chi^2$
$^4F_{3/2}$	$3/5\sqrt{5}$	$-4\sqrt{2}/5\sqrt{3}$	0	$-2\sqrt{21}/5\sqrt{5}$
$^2D_{3/2}$	$2\sqrt{3}/5$	$-\sqrt{6}/5$	0	$\sqrt{7}/5$
$^4P_{3/2}$	$2\sqrt{21}/15\sqrt{5}$	$\sqrt{21}/5\sqrt{10}$	$-5\sqrt{3}/3\sqrt{10}$	$-1/5\sqrt{5}$
$^2P_{3/2}$	$2\sqrt{7}/5\sqrt{3}$	$\sqrt{21}/5\sqrt{2}$	$1/\sqrt{6}$	$-1/5$

$J=1/2$.	$s\psi^0$	$s\varphi^1$	$s\chi^1$
$^4P_{1/2}$	$2/\sqrt{15}$	$1/\sqrt{3}$	$\sqrt{2}/\sqrt{5}$
$^2P_{1/2}$	$\sqrt{2}/\sqrt{15}$	$-\sqrt{2}/\sqrt{3}$	$1/\sqrt{5}$
$^2S_{1/2}$	$\sqrt{3}/\sqrt{5}$	0	$-\sqrt{2}/\sqrt{5}$

The interval factors of the states in (LS) coupling can be obtained from Eqs. (3, 6, 9, 12, 15) by using the (jj)–(LS) transformation matrices. These matrices are given in Table II.

The interval factors of the states in (LS) coupling, obtained by substituting the appropriate coefficients from the transformation matrices in Eqs. (3, 6, 9, 12, 15), are

$$\begin{aligned}
A(^4F_{9/2})&=1/9\cdot a_s+37/45\cdot a'+1/15\cdot a''+16/45\cdot a'''\leqq 1/9\cdot a_s+40/63\cdot a_d.\\
A(^2G_{9/2})&=1/9\cdot a_s+28/45\cdot a'+4/15\cdot a''-16/45\cdot a'''\leqq 1/9\cdot a_s+8/9\cdot a_d.\\
A(^4F_{7/2})&=5/63\cdot a_s+46/63\cdot a'+4/21\cdot a''+16/63\cdot a'''\leqq 5/63\cdot a_s+344/441\cdot a_d.\\
A(^2G_{7/2})&=-1/9\cdot a_s+7/9\cdot a'+\tfrac{1}{3}\cdot a''-4/9\cdot a'''\leqq -1/9\cdot a_s+10/9\cdot a_d.\\
A(^2F_{7/2})&=-1/21\cdot a_s+19/21\cdot a'+1/7\cdot a''+4/21\cdot a'''\leqq -1/21\cdot a_s+122/147\cdot a_d.\\
A(^4F_{5/2})&=1/105\cdot a_s+1609/2625\cdot a'+991/2625\cdot a''-368/2625\cdot a'''\leqq 1/105\cdot a_s+1272/1225\cdot a_d.
\end{aligned}\tag{21}$$

* Eqs. (21) continued on next page.

$$A(^2F_{5/2})=1/21\cdot a_s+232/525\cdot a'+268/525\cdot a''-464/525\cdot a'''\leqq 1/21\cdot a_s+296/245\cdot a_d.$$

$$A(^2D_{5/2})=\tfrac{1}{5}a_s+14/25\cdot a'+6/25\cdot a''-8/25\cdot a'''\leqq \tfrac{1}{5}a_s+4/5\cdot a_d.$$

$$A(^4P_{5/2})=\tfrac{1}{5}a_s+91/125\cdot a'+9/125\cdot a''+168/125\cdot a'''\leqq \tfrac{1}{5}a_s+12/25\cdot a_d.$$

$$A(^4F_{3/2})=-\tfrac{1}{5}a_s+46/125\cdot a'+104/125\cdot a''-192/125\cdot a'''\leqq -\tfrac{1}{5}a_s+304/175\cdot a_d.$$

$$A(^2D_{3/2})=-\tfrac{1}{5}a_s+42/50\cdot a'+18/50\cdot a''-24/50\cdot a'''\leqq -\tfrac{1}{5}a_s+6/5\cdot a_d.$$

$$A(^4P_{3/2})=11/45\cdot a_s+1456/1125\cdot a'-606/1125\cdot a''+688/1125\cdot a'''\leqq 11/45\cdot a_s-8/225\cdot a_d.$$

$$A(^2P_{3/2})=-1/9\cdot a_s+434/450\cdot a'+66/450\cdot a''+632/450\cdot a'''\leqq -1/9\cdot a_s+34/45\cdot a_d.$$

$$A(^4P_{1})=5/9\cdot a_s+7/9\cdot a'-\tfrac{1}{3}a''+40/9\cdot a'''\leqq 5/9\cdot a_s-4/9\cdot a_d.$$

$$A(^2P_{1})=1/9\cdot a_s+14/9\cdot a'-\tfrac{2}{3}a''-40/9\cdot a'''\leqq 1/9\cdot a_s+4/9\cdot a_d.$$

$$A(^2S_{\frac{1}{2}})=a_s.$$

The relativistic corrections for a d type electron are usually quite small and frequently can be neglected. In this nonrelativistic approximation a', a'', a''' can be expressed in terms of a_d as follows:

$$a'=24/35\cdot a_d,\quad a''=8/5\cdot a_d,\quad a'''=-1/10\cdot a_d, \tag{22}$$

where $a_d=2g\mu_0^2(\overline{r^{-3}})$. The second simplified expression given above for each interval factor in (LS) coupling is obtained by using these nonrelativistic approximations for the a's.

IV. Interval Factors in Intermediate Coupling Expressed in Terms of the Coefficients, K's, of the Transformation Relating the Intermediate to the (LS) States

When the coupling in a configuration tends towards (LS) it is convenient for the application of the theory to have the interval factors expressed in terms of the coefficients, K's, that relate the intermediate states to the (LS) states. The interval factors can be readily converted into this form by making use of the (jj)–(LS) transformation matrices. In terms of the K's the interval factors are:

$$\begin{aligned}9/2\cdot A(J=9/2)=&\tfrac{1}{2}a_s(K_1^2+K_2^2)+a'(37/10\cdot K_1^2+14/5\cdot K_2^2-6/5\cdot K_1K_2)\\&+a''(3/10\cdot K_1^2+6/5\cdot K_2^2+6/5\cdot K_1K_2)+4a'''(\tfrac{2}{5}K_1^2-\tfrac{2}{5}K_2^2+\tfrac{3}{5}K_1K_2).\end{aligned} \tag{23}$$

$$\begin{aligned}7/2\cdot A(J=7/2)=&a_s(5/18\cdot K_1^2-7/18\cdot K_2^2-\tfrac{1}{6}K_3^2-8\sqrt{3}/18\cdot K_1K_3)+a'(23/9\cdot K_1^2+49/18\cdot K_2^2\\&+57/18\cdot K_3^2+\tfrac{1}{3}K_1K_2+7/3\sqrt{3}\cdot K_1K_3+2/\sqrt{3}\cdot K_2K_3)+a''(\tfrac{2}{3}K_1^2+7/6\cdot K_2^2\\&+\tfrac{1}{2}K_3^2-\tfrac{1}{3}K_1K_2-1/\sqrt{3}\cdot K_1K_3-2/\sqrt{3}\cdot K_2K_3)+a'''(8/9\cdot K_1^2-14/9\cdot K_2^2\\&+\tfrac{2}{3}K_3^2-\tfrac{2}{3}K_1K_2+10/3\sqrt{3}\cdot K_1K_3-4/\sqrt{3}\cdot K_2K_3).\end{aligned} \tag{24}$$

$$\begin{aligned}5/2\cdot A(J=5/2)=&a_s(1/42\cdot K_1^2+5/42\cdot K_2^2+\tfrac{1}{2}K_3^2+\tfrac{1}{2}K_4^2+40/21\sqrt{5}\cdot K_1K_2)\\&+a'(1609/1050\cdot K_1^2+116/105\cdot K_2^2+7/5\cdot K_3^2+91/50\cdot K_4^2-46/15\sqrt{5}\cdot K_1K_2\\&+176/35\sqrt{15}\cdot K_1K_3-64\sqrt{7}/175\sqrt{2}\cdot K_1K_4+64\sqrt{3}/105\cdot K_2K_3\\&-4\sqrt{14}/35\sqrt{5}\cdot K_2K_4+\sqrt{42}/5\sqrt{5}\cdot K_3K_4)+a''(991/1050\cdot K_1^2+134/105\cdot K_2^2\\&+\tfrac{3}{5}K_3^2+9/50\cdot K_4^2+122/105\sqrt{5}\cdot K_1K_2-176\sqrt{3}/105\sqrt{5}\cdot K_1K_3\\&+64\sqrt{7}/175\sqrt{2}\cdot K_1K_4-64\sqrt{3}/105\cdot K_2K_3+4\sqrt{14}/35\sqrt{5}\cdot K_2K_4-\sqrt{42}/5\sqrt{5}\cdot K_3K_4)\\&+a'''(-184/525\cdot K_1^2-232/105\cdot K_2^2-4/5\cdot K_3^2+84/25\cdot K_4^2\\&-556/105\sqrt{5}\cdot K_1K_2-352\sqrt{3}/105\sqrt{5}\cdot K_1K_3+64\sqrt{14}/175\cdot K_1K_4\\&-128\sqrt{3}/105\cdot K_2K_3+8\sqrt{14}/35\sqrt{5}\cdot K_2K_4-2\sqrt{42}/5\sqrt{5}\cdot K_3K_4).\end{aligned} \tag{25}$$

$$3/2\cdot A(J=3/2)=a_s(-3/10\cdot K_1^2-3/10\cdot K_2^2+11/30\cdot K_3^2-\tfrac{1}{6}K_4^2-4/3\sqrt{5}\cdot K_3K_4)$$
$$+a'(69/125\cdot K_1^2+63/50\cdot K_2^2+728/375\cdot K_3^2+217/150\cdot K_4^2$$
$$+48\sqrt{3}/25\sqrt{5}\cdot K_1K_2-16\sqrt{21}/125\cdot K_1K_3-4\sqrt{21}/25\sqrt{5}\cdot K_1K_4$$
$$-3\sqrt{7}/25\sqrt{5}\cdot K_2K_3+6\sqrt{7}/25\cdot K_2K_4+49/75\sqrt{5}\cdot K_3K_4)+a''(156/125\cdot K_1^2$$
$$+27/50\cdot K_2^2-101/125\cdot K_3^2+11/50\cdot K_4^2-48\sqrt{3}/25\sqrt{5}\cdot K_1K_2$$
$$+16\sqrt{21}/125\cdot K_1K_3+4\sqrt{21}/25\sqrt{5}\cdot K_1K_4+3\sqrt{7}/25\sqrt{5}\cdot K_2K_3$$
$$-6\sqrt{7}/25\cdot K_2K_4+17/25\sqrt{5}\cdot K_3K_4)+a'''(-288/125\cdot K_1^2-18/25\cdot K_2^2$$
$$+344/375\cdot K_3^2+316/150\cdot K_4^2-96\sqrt{3}/25\sqrt{5}\cdot K_1K_2+32\sqrt{21}/125\cdot K_1K_3$$
$$+8\sqrt{21}/25\sqrt{5}\cdot K_1K_4+6\sqrt{7}/25\sqrt{5}\cdot K_2K_3-12\sqrt{7}/25\cdot K_2K_4+502/75\sqrt{5}\cdot K_3K_4). \quad (26)$$

$$\tfrac{1}{2}A(J=\tfrac{1}{2})=a_s(5/18\cdot K_1^2+1/18\cdot K_2^2+\tfrac{1}{2}K_3^2+4\sqrt{2}/9\cdot K_1K_2)+a'(7/18\cdot K_1^2+7/9\cdot K_2^2$$
$$-7\sqrt{2}/9\cdot K_1K_2)+a''(-\tfrac{1}{6}K_1^2-\tfrac{1}{3}K_2^2+\sqrt{2}/3\cdot K_1K_2)$$
$$+a'''(20/9\cdot K_1^2-20/9\cdot K_2^2-10\sqrt{2}/9\cdot K_1K_2). \quad (27)$$

V. Energy Matrices in (*LS*) and (*jj*) Coupling

The coefficients, *C*'s, *K*'s, that appear in the interval factor formulae are obtainable from the empirical energies of the states of the configuration. To evaluate the coefficients from the energies the energy matrices are required, preferably for both (*LS*) and (*jj*) coupling to correspond to the two forms of the interval factor formulae. Condon and Shortley[4] have worked out the electrostatic energies of the d^2s states in (*LS*) coupling. The magnetic energies can readily be worked out in (*jj*) coupling. The complete energy matrices in both (*LS*) and (*jj*) coupling can be formed from these by using the (*jj*)—(*LS*) transformation matrices. The energy matrices in (*LS*) coupling are given in Table III. The $^4F_{9/2}$ state was chosen as the energy datum level. The (*jj*) energy matrices are given in Table IV. The energies here are referred to $s\psi^4(J=9/2)$ as the datum level.

The energy matrices of d^2s are somewhat too complicated to give explicit formulae for the determination of the coefficients. They are obtained more easily from the matrices by successive approximations to the secular equations.

The coefficients determined from the empirical energies can be checked by computing the Landé *g* factors from the coefficients and comparing them with the empirical *g*'s. The *g*'s can be computed most easily *via* (*LS*) coupling since the matrices for the *g*'s of the (*LS*) states are diagonal. Thus the *g* of a state with a given *J* in intermediate coupling is given by $\sum_i g_i K_i^2$ summed over all the (*LS*) states with the given *J*. The g_i's are the *g* factors of the (*LS*) states and the K_i's are the coefficients in the linear combination that expresses the function of the intermediate state in terms of the functions of the (*LS*) states.

VI. Application to $5d^26s\ ^4F$ of La I

Anderson[5] has measured the hyperfine structures of the $5d^26s\ ^4F$ states of La I, and from their separations has evaluated the magnetic moment of the lanthanum nucleus. There are two limitations in his computation: First, he considers that the coupling is strictly (*LS*), and second, he neglects the interactions of the spins of the *d* electrons with the magnetic nucleus. He points out that his treatment is only approximate and that it does not give a very consistent explanation of the relative magnitudes of the hyperfine separations of the ^4F states. It is evident that his experimental data should be treated more rigorously before one can rely on the nuclear magnetic moment derived from them. The preceding theory is applied in this section to Anderson's data.

We determine the coefficients from the em-

[4] E. U. Condon and G. H. Shortley, Phys. Rev. **37**, 1025 (1931).

[5] O. E. Anderson, Phys. Rev. **46**, 473 (1934).

TABLE III. *Energy matrices, (LS) coupling.*

States	$^4F_{9/2}$	$^2G_{9/2}$	$^4F_{7/2}$	$^2G_{7/2}$	$^2F_{7/2}$	$^4F_{5/2}$	$^2F_{5/2}$	$^2D_{5/2}$	$^4P_{5/2}$	$^4F_{3/2}$	$^2D_{3/2}$	$^4P_{3/2}$	$^2P_{3/2}$	$^4P_{1/2}$	$^2P_{1/2}$	$^2S_{1/2}$
$^4F_{9/2}$	0															
$^2G_{9/2}$	$-a$	$12F_2+10F_4$ $+G_2-3a/2$														
$^4F_{7/2}$			$-3a/2$													
$^2G_{7/2}$			$\frac{1}{2}a$	$12F_2+10F_4$ $+G_2-3a/2$												
$^2F_{7/2}$			$a\sqrt{3}/2$	$a\sqrt{3}/2$	$3G_2-\frac{1}{2}a$											
$^4F_{5/2}$						$-8a/3$	$-a\sqrt{5}/3$	$4a/\sqrt{15}$	0							
$^2F_{5/2}$						$-a\sqrt{5}/3$	$3G_2-17a/6$	$2a/\sqrt{3}$	0							
$^2D_{5/2}$						$4a/\sqrt{15}$	$2a/\sqrt{3}$	$5F_2+45F_4$ $+G_2-3a/2$	$a\sqrt{21}/\sqrt{10}$							
$^4P_{5/2}$						0	0	$a\sqrt{21}/\sqrt{10}$	$15F_2-75F_4-a$							
$^4F_{3/2}$										$-7a/2$	$2a\sqrt{3}/\sqrt{5}$	0	$a\sqrt{7}/2$			
$^2D_{3/2}$										$2a\sqrt{3}/\sqrt{5}$	$5F_2+45F_4$ $+G_2-3a/2$	$a\sqrt{7}/2\sqrt{5}$	$a\sqrt{5}/6$			
$^4P_{3/2}$										0	$a\sqrt{7}/2\sqrt{5}$	$15F_2-75F_4-11a/6$	$15F_2-75F_4$ $+3G_2-7a/6$			
$^2P_{3/2}$										0	$a\sqrt{5}/6$	$a\sqrt{5}/6$				
$^4P_{1/2}$														$15F_2-75F_4-a\sqrt{2}/6$	$2a$	
$^2P_{1/2}$														$-a\sqrt{2}/6$	$\sqrt{2}a$	
$^2S_{1/2}$														$2a$	$22F_2+135F_4$ $+G_2-3a/2$	

pirical energies. Russell and Meggers[6] have identified all the states of $5d^26s$ of La I except ^2S. Their term values relative to $^4F_{9/2}$ are given in Table V. As the coupling in this configuration approaches (LS) we use the (LS) energy matrices and determine the coefficients by successive approximations to the secular equations. The first step is the evaluation of the parameters, F_2, F_4, G_2, $\bar{a}$, from the empirical term values. The sum of the diagonal terms of the energy matrix for the states with a given J is equal in any coupling to the sum of the roots (energy values) of the secular equation for these states. This fact is made use of. For each J matrix the mean of the diagonal terms is taken and equated to the mean of the empirical term values of the states involved. The resulting relation for each J matrix is then subtracted from the corresponding relation for each of the other matrices. In general this procedure gives a sufficient number of equations to evaluate the parameters.

In the present case, however, some judgment must be used in applying this procedure. As $^2S_{\frac{1}{2}}$ has not been identified, the mean for the states with $J=\frac{1}{2}$ cannot be used. Further there is a possibility that the two groups of states with $J=5/2$ and $3/2$ are appreciably perturbed by the $^2D_{3/2,\ 5/2}$ of the adjacent $5d6s^2$ configuration. Thus one hesitates to use the differences obtained by subtracting the mean of either of these two groups from the means of the unperturbed groups. However, according to theory[7] one expects that the perturbation by $5d6s^2$ will displace the means of the $J=5/2$ states and $J=3/2$ states about equally in the same direction. Thus the relation obtained by taking the difference between the means of these two groups should be fairly reliable. Actually in forming this difference the $5d6s^2\ ^2D$ states were included and five diagonal terms used in the $J=5/2$ and $J=3/2$ matrices. The electrostatic components in the diagonal terms of the $5d6s^2\ ^2D$ states cancel out when the difference is taken; the magnetic parts do not, but as $\bar{a}$ is assumed the same for both configurations no additional parameters are introduced. The inclusion of the $5d6s^2\ ^2D$ states gives values of the parameters

[6] H. N. Russell and W. F. Meggers, Bur. Standards J. Research **9**, 625 (1932).
[7] C. W. Ufford, Phys. Rev. **44**, 732 (1933).

TABLE IV. *Energy matrices, (jj) coupling.*

$J=9/2$.	$I=s\psi^4$	$II=s\varphi^4$
I	0	$-24F_2/5-4F_4-2G_2/5$
II	$-24F_2/5-4F_4-2G_2/5$,	$36F_2/5+6F_4+3G_2/5-5\bar{a}/2$

$J=7/2$.	$I=s\psi^4$	$II=s\varphi^4$	$III=s\varphi^3$
I	$9G_2/5$,	$-24F_2/5-4F_4+G_2/2$,	$-3G_2\sqrt{3/2}\sqrt{5}$
II	$-24F_2/5-4F_4+G_2/2$,	$36F_2/5+6F_4+21G_2/20-5\bar{a}/2$,	$-3G_2\sqrt{3/4}\sqrt{5}$
III	$-3G_2\sqrt{3/2}\sqrt{5}$,	$-3G_2\sqrt{3/4}\sqrt{5}$,	$-12F_2/5-2F_4+11G_2/20-5\bar{a}/2$

$J=5/2$.	$I=s\psi^2$	$II=s\varphi^2$	$III=s\varphi^2$	$IV=s\chi^2$
I	$168F_2/25-14F_4+2G_2/5$,	$2G_2/5$,	$\sqrt{2}(96F_2/25-36F_4-2G_2/5)$,	$\sqrt{21}(-2F_2/25+6F_4)$
II	$2G_2/5$,	$-12F_2/5-2F_4+17G_2/15-5\bar{a}/2$,	$-8G_2\sqrt{2}/15$,	$-4G_2\sqrt{21}/15$
III	$\sqrt{2}(96F_2/25-36F_4-2G_2/5)$,	$-8G_2\sqrt{2}/15$,	$159F_2/25-29F_4+7G_2/15-5\bar{a}/2$,	$\sqrt{42}(-14F_2/25+G_2/15)$
IV	$\sqrt{21}(-2F_2/25+6F_4)$,	$-4G_2\sqrt{21}/15$,	$\sqrt{42}(-14F_2/25+G_2/15)$,	$-7F_2/25+7F_4+6G_2/5-5\bar{a}$

$J=3/2$.	$I=s\psi^2$	$II=s\varphi^2$	$III=s\varphi^2$	$IV=s\chi^2$
I	$168F_2/25-14F_4+7G_2/5$,	$\sqrt{2}(96F_2/25-36F_4+3G_2/5)$,	$G_2\sqrt{14}/5$,	$\sqrt{21}(-2F_2/25+6F_4)$
II	$\sqrt{2}(96F_2/25-36F_4+3G_2/5)$,	$159F_2/25-29F_4+13G_2/10-5\bar{a}/2$,	$3G_2\sqrt{7}/10$,	$\sqrt{42}(-14F_2/25-G_2/10)$
III	$G_2\sqrt{14}/5$,	$3G_2\sqrt{7}/10$,	$63F_2/5-77F_4+3G_2/10-5\bar{a}/2$,	$-G_2\sqrt{3}/5\sqrt{2}$
IV	$\sqrt{21}(-2F_2/25+6F_4)$,	$\sqrt{42}(-14F_2/25-G_2/10)$,	$-G_2\sqrt{3}/5\sqrt{2}$,	$-7F_2/25+7F_4+G_2/5-5\bar{a}$

$J=1/2$.	$I=s\psi^2$	$II=s\varphi^2$	$III=s\chi^2$
I	$84F_2/5+49F_4+4G_2/5$,	$-2G_2/\sqrt{5}$,	$-7F_2\sqrt{6}/5-42F_4\sqrt{6}$
II	$-2G_2/\sqrt{5}$,	$63F_2/5-77F_4+9G_2/5-5\bar{a}/2$,	$-G_2(6/5)$
III	$-7F_2\sqrt{6}/5-42F_4\sqrt{6}$,	$-G_2(6/5)$,	$91F_2/5+91F_4+6G_2/5-5\bar{a}$

only slightly different from those obtained when these states are not included. A second relation can be obtained from the difference of the means of the $J=9/2$ and $J=7/2$ groups; and a third from the secular equation for the $J=9/2$ states. A fourth relation is needed for the complete determination of the four parameters. This could be obtained from the secular equation for the states with $J=7/2$. But it is equally good to express F_2, F_4, G_2 in terms of $\bar{a}$ by means of the three relations discussed above, then by trial find the value of $\bar{a}$ that gives the best agreement between the theoretically predicted and the observed term values.

We obtain by the above procedure the following expressions for the three parameters in terms of $\bar{a}$:

$$\begin{aligned} 6G_2&=4\bar{a}-1/5798\cdot\bar{a}^2+6692.\\ 70F_4&=4375-7/6\cdot\bar{a}-5/34788\cdot\bar{a}^2. \qquad (28)\\ 42F_2&=14202+7/2\cdot\bar{a}-5/11596\cdot\bar{a}^2. \end{aligned}$$

The term values predicted by putting $\bar{a}=400$ cm^{-1}, which gives $G_2=1377$, $F_2=370$, $F_4=56$, are in good agreement with the empirical term values except for the ^4P states which are much higher than predicted (see Table V). The poor agreement for the ^4P states cannot be attributed to perturbation by $5d6s^2$, since according to Ufford[7] $^2D_{3/2,\,5/2}$ are the only states of $5d^26s$ affected by the interaction between the two configurations. A perturbation of the ^2D states would indirectly affect $^4P_{3/2,\,5/2}$, but the effect should be a second order one. The fact that $^4P_{\frac{1}{2}}$ also is much higher than predicted further indicates that perturbation by $5d6s^2$ is not primarily responsible for this discrepancy. Similar anomalies for ^4P states of d^3s configurations of other spectra have been found.[4] The $5d^26s$ term values, except for the ^4P states, then are consistent with the theory of multiplet structure. Thus, as there are no nondiagonal elements between the ^4F and the ^4P states in the (LS) energy matrices, one expects the preceding theory to give a consistent interpretation of the hyperfine structures of the ^4F states when the values of the parameters given above are used in the energy matrices.

The coefficients, K's, for the ^4F states can be determined from the energy matrices with the values of the parameters inserted by successive

TABLE V. *Comparison of predicted and empirical term values of $5d^26s$ states.*

State	Position re. $^4F_{9/2}$	Position calc. $\bar{a}=400$ cm^{-1}	State	Position re. $^4F_{9/2}$	Position calc. $\bar{a}=400$ cm^{-1}
$^4F_{5/2}$	-1453 cm^{-1}	-1459 cm^{-1}	$^4P_{5/2}$	3558 cm^{-1}	904 cm^{-1}
$^4F_{3/2}$	-1112	-1117	$^2D_{3/2}$	4325	4600
$^4F_{7/2}$	-627	-630	$^2D_{5/2}$	5062	5322
$^4F_{9/2}$	0	0	$^2P_{1/2}$	4923	4627
$^2F_{5/2}$	2890	2922	$^2P_{3/2}$	5598	5650
$^2F_{7/2}$	3930	3893	$^2G_{9/2}$	5798	5798
$^4P_{1/2}$	3110	410	$^2G_{7/2}$	5839	5842
$^4P_{3/2}$	3369	650	$^2S_{1/2}$	——	16414

approximations to the secular equations. They are

$$
\begin{aligned}
{}^4F_{9/2}:\quad & K_1=0.9976, && K_1^2=0.9952;\\
& K_2=0.0693, && K_2^2=0.0048.\\
{}^4F_{7/2}:\quad & K_1=0.9966, && K_1^2=0.9932;\\
& K_2=-0.0313, && K_2^2=0.00098;\\
& K_3=-0.0762, && K_3^2=0.0058.\\
{}^4F_{5/2}:\quad & K_1=0.9951, && K_1^2=0.9903;\\
& K_2=0.0730, && K_2^2=0.00533;\\
& K_3=-0.0664, && K_3^2=0.00441; \quad K_4=0.\\
{}^4F_{3/2}:\quad & K_1=0.9955, && K_1^2=0.9911;\\
& K_2=-0.0946, && K_2^2=0.00894;\\
& K_3=K_4=0.
\end{aligned}
$$

The relativistic corrections for a $5d$ electron of La I, for which the effective nuclear charge is certainly less than 50, are very small and can be neglected. Thus for this application a', a'', a''' can be expressed in terms of a_d by Eq. (22). When these substitutions are made and the values of the K's listed above are inserted in Eqs. (23, 24, 25, 26) the following formulae for the interval factors of the ${}^4F$ states are obtained. They are equated on the right to Anderson's experimentally determined interval factors.

$$
\begin{aligned}
A({}^4F_{9/2})&=0.1111a_s+0.6508a_d\\
&=0.01571\ \text{cm}^{-1},\\
A({}^4F_{7/2})&=0.09514a_s+0.7864a_d\\
&=0.01464\ \text{cm}^{-1},\\
A({}^4F_{5/2})&=0.03531a_s+1.0705a_d\\
&=0.00900\ \text{cm}^{-1},\\
A({}^4F_{3/2})&=-0.2000a_s+1.7988a_d\\
&=-0.01667\ \text{cm}^{-1}.
\end{aligned}
\tag{29}
$$

There are four equations in a_s and a_d, so we can solve for each and test the solution for consistency. Solving for a_s and a_d from the first and last equations of (29), which are the least sensitive to coupling changes, we obtain $a_s=0.1185\ \text{cm}^{-1}$, $a_d=0.00391\ \text{cm}^{-1}$. Substituting these values in the second and third equations of (29) we calculate $A({}^4F_{7/2})=0.0143$, observed 0.0146; $A({}^4F_{5/2})=0.0084$, observed 0.0090. Anderson gives the probable error of his most reliable interval factor as 5 percent. Thus we see that the preceding theory gives a consistent interpretation of the hyperfine separations of the ${}^4F$ states.

It is instructive to contrast the formulae for the interval factors of the ${}^4F$ states in strict (LS) coupling with the formulae (29) which take into account the actual coupling conditions. The interval factors in strict (LS) coupling are by Eqs. (21),

$$
\begin{aligned}
A({}^4F_{9/2})&=0.1111a_s+0.6349a_d,\\
A({}^4F_{7/2})&=0.07937a_s+0.7800a_d,\\
A({}^4F_{5/2})&=0.00952a_s+1.0384a_d,\\
A({}^4F_{3/2})&=-0.2000a_s+1.7371a_d.
\end{aligned}
\tag{30}
$$

Comparing (29) and (30), it is evident that $A({}^4F_{9/2})$ and $A({}^4F_{3/2})$ are not overly sensitive to departure from strict (LS) coupling; $A({}^4F_{7/2})$ is more sensitive, and $A({}^4F_{5/2})$ is very sensitive. This comparison shows that one should be very careful in using (LS) interval factor formulae for states dependent on coupling even though the multiplet structure indicates that the coupling is close to (LS).

The nuclear magnetic moment of lanthanum can be calculated from the values of a_s and a_d. The nuclear g factor is computed from the interaction constant of an s electron by the formula[8]

$$
g(I)=\frac{3}{8}\,\frac{a_s}{R\alpha^2}\,\frac{n^3_{\text{eff.}}}{Z_i Z_0^2}\,\frac{1838}{K(\tfrac{1}{2},Z_i)}.
$$

For our case $a_s=0.119\ \text{cm}^{-1}$, $n_{\text{eff.}}=1.60$, $Z_i=57$, $Z_0=1$, $R\alpha^2=5.82$, $K(\tfrac{1}{2},Z_i)=1.43$. The substitution of these values in the above equation gives $g(\text{I})=0.71$. A reliable value of $g(\text{I})$ cannot be readily obtained from a_d since first, a_d is very small, and second, it is difficult to estimate the value of Z_i that should be used for a $5d$ electron in the $5d^26s$ configuration. However, the substitution of $g(I)=0.71$, $a_d=0.0039\ \text{cm}^{-1}$, $\Delta\nu=1000\ \text{cm}^{-1}$ in the formula for a non-s electron[8] gives, on solving for Z_i, $Z_i=40$. This appears to be a reasonable value, indicating that $g(\text{I})=0.71$ is consistent with $a_d=0.0039$. The nuclear spin

[8] S. Goudsmit, Phys. Rev. **43**, 636 (1933); E. Fermi and E. Segrè, Zeits. f. Physik **82**, 729 (1933).

of lanthanum is 7/2, hence the nuclear magnetic moment as determined by this analysis is 2.5 nuclear magnetons. This is in fair agreement with the value 2.8 nuclear magnetons determined from La III hyperfine structures by the writer and N. S. Grace.[9]

[9] M. F. Crawford and N. S. Grace, Phys. Rev. **47**, 536 (1935).

This investigation was carried out under the supervision of Professor G. Breit, and I wish to thank him for the invaluable advice and assistance so freely given. I also take this opportunity to acknowledge the award of a Fellowship by the Royal Society of Canada, and to thank the University of Wisconsin and the Department of Physics for the privilege of working here.

MAY 15, 1935 PHYSICAL REVIEW VOLUME 47

Can Quantum-Mechanical Description of Physical Reality Be Considered Complete?

A. EINSTEIN, B. PODOLSKY AND N. ROSEN, *Institute for Advanced Study, Princeton, New Jersey*

(Received March 25, 1935)

In a complete theory there is an element corresponding to each element of reality. A sufficient condition for the reality of a physical quantity is the possibility of predicting it with certainty, without disturbing the system. In quantum mechanics in the case of two physical quantities described by non-commuting operators, the knowledge of one precludes the knowledge of the other. Then either (1) the description of reality given by the wave function in quantum mechanics is not complete or (2) these two quantities cannot have simultaneous reality. Consideration of the problem of making predictions concerning a system on the basis of measurements made on another system that had previously interacted with it leads to the result that if (1) is false then (2) is also false. One is thus led to conclude that the description of reality as given by a wave function is not complete.

1.

ANY serious consideration of a physical theory must take into account the distinction between the objective reality, which is independent of any theory, and the physical concepts with which the theory operates. These concepts are intended to correspond with the objective reality, and by means of these concepts we picture this reality to ourselves.

In attempting to judge the success of a physical theory, we may ask ourselves two questions: (1) "Is the theory correct?" and (2) "Is the description given by the theory complete?" It is only in the case in which positive answers may be given to both of these questions, that the concepts of the theory may be said to be satisfactory. The correctness of the theory is judged by the degree of agreement between the conclusions of the theory and human experience. This experience, which alone enables us to make inferences about reality, in physics takes the form of experiment and measurement. It is the second question that we wish to consider here, as applied to quantum mechanics.

Whatever the meaning assigned to the term *complete*, the following requirement for a complete theory seems to be a necessary one: *every element of the physical reality must have a counterpart in the physical theory*. We shall call this the condition of completeness. The second question is thus easily answered, as soon as we are able to decide what are the elements of the physical reality.

The elements of the physical reality cannot be determined by *a priori* philosophical considerations, but must be found by an appeal to results of experiments and measurements. A comprehensive definition of reality is, however, unnecessary for our purpose. We shall be satisfied with the following criterion, which we regard as reasonable. *If, without in any way disturbing a system, we can predict with certainty (i.e., with probability equal to unity) the value of a physical quantity, then there exists an element of physical reality corresponding to this physical quantity.* It seems to us that this criterion, while far from exhausting all possible ways of recognizing a physical reality, at least provides us with one

such way, whenever the conditions set down in it occur. Regarded not as a necessary, but merely as a sufficient, condition of reality, this criterion is in agreement with classical as well as quantum-mechanical ideas of reality.

To illustrate the ideas involved let us consider the quantum-mechanical description of the behavior of a particle having a single degree of freedom. The fundamental concept of the theory is the concept of *state*, which is supposed to be completely characterized by the wave function ψ, which is a function of the variables chosen to describe the particle's behavior. Corresponding to each physically observable quantity A there is an operator, which may be designated by the same letter.

If ψ is an eigenfunction of the operator A, that is, if

$$\psi' \equiv A\psi = a\psi, \tag{1}$$

where a is a number, then the physical quantity A has with certainty the value a whenever the particle is in the state given by ψ. In accordance with our criterion of reality, for a particle in the state given by ψ for which Eq. (1) holds, there is an element of physical reality corresponding to the physical quantity A. Let, for example,

$$\psi = e^{(2\pi i/h)p_0 x}, \tag{2}$$

where h is Planck's constant, p_0 is some constant number, and x the independent variable. Since the operator corresponding to the momentum of the particle is

$$p = (h/2\pi i)\partial/\partial x, \tag{3}$$

we obtain

$$\psi' = p\psi = (h/2\pi i)\partial\psi/\partial x = p_0\psi. \tag{4}$$

Thus, in the state given by Eq. (2), the momentum has certainly the value p_0. It thus has meaning to say that the momentum of the particle in the state given by Eq. (2) is real.

On the other hand if Eq. (1) does not hold, we can no longer speak of the physical quantity A having a particular value. This is the case, for example, with the coordinate of the particle. The operator corresponding to it, say q, is the operator of multiplication by the independent variable. Thus,

$$q\psi = x\psi \neq a\psi. \tag{5}$$

In accordance with quantum mechanics we can only say that the relative probability that a measurement of the coordinate will give a result lying between a and b is

$$P(a, b) = \int_a^b \bar{\psi}\psi dx = \int_a^b dx = b - a. \tag{6}$$

Since this probability is independent of a, but depends only upon the difference $b-a$, we see that all values of the coordinate are equally probable.

A definite value of the coordinate, for a particle in the state given by Eq. (2), is thus not predictable, but may be obtained only by a direct measurement. Such a measurement however disturbs the particle and thus alters its state. After the coordinate is determined, the particle will no longer be in the state given by Eq. (2). The usual conclusion from this in quantum mechanics is that *when the momentum of a particle is known, its coordinate has no physical reality.*

More generally, it is shown in quantum mechanics that, if the operators corresponding to two physical quantities, say A and B, do not commute, that is, if $AB \neq BA$, then the precise knowledge of one of them precludes such a knowledge of the other. Furthermore, any attempt to determine the latter experimentally will alter the state of the system in such a way as to destroy the knowledge of the first.

From this follows that either (1) *the quantum-mechanical description of reality given by the wave function is not complete* or (2) *when the operators corresponding to two physical quantities do not commute the two quantities cannot have simultaneous reality.* For if both of them had simultaneous reality—and thus definite values—these values would enter into the complete description, according to the condition of completeness. If then the wave function provided such a complete description of reality, it would contain these values; these would then be predictable. This not being the case, we are left with the alternatives stated.

In quantum mechanics it is usually assumed that the wave function *does* contain a complete description of the physical reality of the system in the state to which it corresponds. At first

sight this assumption is entirely reasonable, for the information obtainable from a wave function seems to correspond exactly to what can be measured without altering the state of the system. We shall show, however, that this assumption, together with the criterion of reality given above, leads to a contradiction.

2.

For this purpose let us suppose that we have two systems, I and II, which we permit to interact from the time $t=0$ to $t=T$, after which time we suppose that there is no longer any interaction between the two parts. We suppose further that the states of the two systems before $t=0$ were known. We can then calculate with the help of Schrödinger's equation the state of the combined system I+II at any subsequent time; in particular, for any $t>T$. Let us designate the corresponding wave function by Ψ. We cannot, however, calculate the state in which either one of the two systems is left after the interaction. This, according to quantum mechanics, can be done only with the help of further measurements, by a process known as the *reduction of the wave packet*. Let us consider the essentials of this process.

Let $a_1, a_2, a_3, \cdots$ be the eigenvalues of some physical quantity A pertaining to system I and $u_1(x_1), u_2(x_1), u_3(x_1), \cdots$ the corresponding eigenfunctions, where x_1 stands for the variables used to describe the first system. Then Ψ, considered as a function of x_1, can be expressed as

$$\Psi(x_1, x_2) = \sum_{n=1}^{\infty} \psi_n(x_2) u_n(x_1), \tag{7}$$

where x_2 stands for the variables used to describe the second system. Here $\psi_n(x_2)$ are to be regarded merely as the coefficients of the expansion of Ψ into a series of orthogonal functions $u_n(x_1)$. Suppose now that the quantity A is measured and it is found that it has the value a_k. It is then concluded that after the measurement the first system is left in the state given by the wave function $u_k(x_1)$, and that the second system is left in the state given by the wave function $\psi_k(x_2)$. This is the process of reduction of the wave packet; the wave packet given by the infinite series (7) is reduced to a single term $\psi_k(x_2)u_k(x_1)$.

The set of functions $u_n(x_1)$ is determined by the choice of the physical quantity A. If, instead of this, we had chosen another quantity, say B, having the eigenvalues $b_1, b_2, b_3, \cdots$ and eigenfunctions $v_1(x_1), v_2(x_1), v_3(x_1), \cdots$ we should have obtained, instead of Eq. (7), the expansion

$$\Psi(x_1, x_2) = \sum_{s=1}^{\infty} \varphi_s(x_2) v_s(x_1), \tag{8}$$

where φ_s's are the new coefficients. If now the quantity B is measured and is found to have the value b_r, we conclude that after the measurement the first system is left in the state given by $v_r(x_1)$ and the second system is left in the state given by $\varphi_r(x_2)$.

We see therefore that, as a consequence of two different measurements performed upon the first system, the second system may be left in states with two different wave functions. On the other hand, since at the time of measurement the two systems no longer interact, no real change can take place in the second system in consequence of anything that may be done to the first system. This is, of course, merely a statement of what is meant by the absence of an interaction between the two systems. Thus, *it is possible to assign two different wave functions* (in our example ψ_k and φ_r) *to the same reality* (the second system after the interaction with the first).

Now, it may happen that the two wave functions, ψ_k and φ_r, are eigenfunctions of two noncommuting operators corresponding to some physical quantities P and Q, respectively. That this may actually be the case can best be shown by an example. Let us suppose that the two systems are two particles, and that

$$\Psi(x_1, x_2) = \int_{-\infty}^{\infty} e^{(2\pi i/h)(x_1 - x_2 + x_0)p} dp, \tag{9}$$

where x_0 is some constant. Let A be the momentum of the first particle; then, as we have seen in Eq. (4), its eigenfunctions will be

$$u_p(x_1) = e^{(2\pi i/h)px_1} \tag{10}$$

corresponding to the eigenvalue p. Since we have here the case of a continuous spectrum, Eq. (7) will now be written

$$\Psi(x_1, x_2) = \int_{-\infty}^{\infty} \psi_p(x_2) u_p(x_1) dp, \tag{11}$$

where

$$\psi_p(x_2) = e^{-(2\pi i/h)(x_2 - x_0)p}. \tag{12}$$

This ψ_p however is the eigenfunction of the operator

$$P = (h/2\pi i)\partial/\partial x_2, \tag{13}$$

corresponding to the eigenvalue $-p$ of the momentum of the second particle. On the other hand, if B is the coordinate of the first particle, it has for eigenfunctions

$$v_x(x_1) = \delta(x_1 - x), \tag{14}$$

corresponding to the eigenvalue x, where $\delta(x_1 - x)$ is the well-known Dirac delta-function. Eq. (8) in this case becomes

$$\Psi(x_1, x_2) = \int_{-\infty}^{\infty} \varphi_x(x_2) v_x(x_1) dx, \tag{15}$$

where

$$\varphi_x(x_2) = \int_{-\infty}^{\infty} e^{(2\pi i/h)(x - x_2 + x_0)p} dp$$

$$= h\delta(x - x_2 + x_0). \tag{16}$$

This φ_x, however, is the eigenfunction of the operator

$$Q = x_2 \tag{17}$$

corresponding to the eigenvalue $x + x_0$ of the coordinate of the second particle. Since

$$PQ - QP = h/2\pi i, \tag{18}$$

we have shown that it is in general possible for ψ_k and φ_r to be eigenfunctions of two noncommuting operators, corresponding to physical quantities.

Returning now to the general case contemplated in Eqs. (7) and (8), we assume that ψ_k and φ_r are indeed eigenfunctions of some noncommuting operators P and Q, corresponding to the eigenvalues p_k and q_r, respectively. Thus, by measuring either A or B we are in a position to predict with certainty, and without in any way disturbing the second system, either the value of the quantity P (that is p_k) or the value of the quantity Q (that is q_r). In accordance with our criterion of reality, in the first case we must consider the quantity P as being an element of reality, in the second case the quantity Q is an element of reality. But, as we have seen, both wave functions ψ_k and φ_r belong to the same reality.

Previously we proved that either (1) the quantum-mechanical description of reality given by the wave function is not complete or (2) when the operators corresponding to two physical quantities do not commute the two quantities cannot have simultaneous reality. Starting then with the assumption that the wave function does give a complete description of the physical reality, we arrived at the conclusion that two physical quantities, with noncommuting operators, can have simultaneous reality. Thus the negation of (1) leads to the negation of the only other alternative (2). We are thus forced to conclude that the quantum-mechanical description of physical reality given by wave functions is not complete.

One could object to this conclusion on the grounds that our criterion of reality is not sufficiently restrictive. Indeed, one would not arrive at our conclusion if one insisted that two or more physical quantities can be regarded as simultaneous elements of reality *only when they can be simultaneously measured or predicted*. On this point of view, since either one or the other, but not both simultaneously, of the quantities P and Q can be predicted, they are not simultaneously real. This makes the reality of P and Q depend upon the process of measurement carried out on the first system, which does not disturb the second system in any way. No reasonable definition of reality could be expected to permit this.

While we have thus shown that the wave function does not provide a complete description of the physical reality, we left open the question of whether or not such a description exists. We believe, however, that such a theory is possible.

LETTERS TO THE EDITOR

Prompt publication of brief reports of important discoveries in physics may be secured by addressing them to this department. Closing dates for this department are, for the first issue of the month, the twentieth of the preceding month; for the second issue, the fifth of the month. The Board of Editors does not hold itself responsible for the opinions expressed by the correspondents.

Electrocoupling of Vibrating Quartz Plates

Let x_1, x_2, x_3, respectively, represent the coordinates x, y', z' of a Cartesian system which is formed by rotating the Cartesian system x, y, z through an angle θ about its X axis. Similarly, let u_1, u_2 and u_3 represent the displacements u, v' and w' of the notation of Love.[1] One can derive, following Mason,[2] expressions for the displacements and resonance frequencies of three idealized shear modes of vibration. These expressions are, briefly

$$u_i = A_{ij} \sin \alpha_i x_i \cos \alpha_j x_j \cos \omega t, \quad (1)$$

$$u_j = A_{ij}(\alpha_i/\alpha_j) \cos \alpha_i x_i \sin \alpha_j x_j \cos \omega t,$$

$$f_{ijmn} = C_{ij}(m^2/a_i^2 + n^2/a_j^2)^{\frac{1}{2}}, \quad (2)$$

in which the three pairs of i and j are $i=1$, $j=2$; $i=1$, $j=3$; $i=2$, $j=3$; and in which m and n are integers associated with the mnth harmonic of the frequency series f_{ijmn}. The $y'z'$-shear mode of Mason[3] is obtained by choosing $i=2$ and $j=3$. The following observations were made upon the xy' and xz'-shear modes which are obtained, respectively, by setting $i=1$, $j=2$ and $i=1$, $j=3$ in (1) and (2).

The crystal plates of Table I are specially oriented

TABLE I. *Crystal plates.*

Crystal	$\theta°$	x(mm)	y'(mm)	z'(mm)	(f_{1111}	f_{1311}	f_{1331}) kc/sec.
190	−58.5	7.867	6.960	3.545	419.0	386.5	556.3
191	−58.0	7.867	6.961	3.543	420.0	387.0	556.3
192	−57.5	7.867	6.962	3.544	418.7	386.5	556.3

Y'-cuts of the type described by Lack, Willard and Fair[4] and may therefore be characterized by the angle θ of orientation.[5] The convention as to the sign of θ is here the opposite of that of Mason. At least two surfaces of each of these optically flawless plates were plane polished. These crystals were first placed, one at a time, between electrodes which were connected inductively or directly to a Hartley oscillator. The vibrational patterns were observed in the simple interferometer[6] and the resonance frequencies f_{ijmn} (Table I) recorded. In the neighborhood of these frequencies the crystals showed only one resonant response.

In attempting to compare more closely the vibrational patterns of the three plates by placing the three plates together in the simple interferometer and driving them through common electrode arrangements, the following noteworthy phenomenon was discovered: *When two or more piezoelectric plates, possessing like resonance frequencies and vibrational patterns, are driven through common electrode arrangements, the resonant responses are no longer those which are characteristic of each plate. Instead, they are characteristic of the plates as a group and are formed by the "electrocoupling" of the mechanical modes of one plate with the mechanical modes of the other plates.*

In the series connection of Fig. 1 the three plates resonated in the cases of f_{1311} and f_{1331} in unison at 386.5

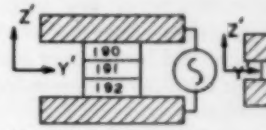

FIG. 1. Series connection.

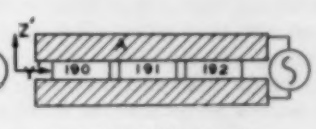

FIG. 2. Parallel connection.

kc/sec. and 556.3 kc/sec., respectively. The combination behaved as one plate. In f_{1311} the plates tended to resonate separately, each at *two* nearby frequencies. The vibrational patterns associated with these two frequencies were slightly different from the pattern associated with the single frequency f_{1311} listed in Table I.

In the parallel connection of Fig. 2 the plates tended, in the case of f_{1331}, to resonate separately, each at two frequencies in the neighborhood of 556.3 kc/sec. In the cases of f_{1111} and f_{1311} the crystals tended to resonate each at a different or at two different frequencies, depending upon which of the various Z' faces were placed in contact with the electrode A.

The behavior of two plates in these electrical connections is similar to the described behavior of three plates.

Only a few of the observations which have been made are here presented, but these are sufficient to prove that when two or more crystal plates are connected electrically, their resonant responses may be radically complicated by the electrocoupling of the various mechanical modes of vibration. A follow-up study of this interesting and important phenomenon cannot be made at this time by the writers.

We wish to point out that this phenomenon should find practical application in electrical wave filters employing quartz plates as elements. Thus, filter combinations of two or more plates may pass a wider (or perhaps narrower) frequency band than that passed by a single plate filter. A variety of different modes of vibration of quartz plates can be employed in many possible filter circuit arrangements. A richer variety of resonant responses thus becomes possible.

HAROLD OSTERBERG
JOHN W. COOKSON

Department of Physics,
University of Wisconsin,
March 19, 1935.

[1] Love, *Mathematical Theory of Elasticity*, 1920, p. 35.
[2] Mason, Bell Sys. Tech. J. 13, 447 (1934).
[3] Reference 2, p. 448.
[4] Lack, Willard and Fair, Bell Sys. Tech. J. 13, 456 (1934).
[5] Mason, Bell Sys. Tech. J. 13, 450 (1934).
[6] H. Osterberg, J. O. S. A. 23, 34 (1933).

Gamma-Rays from the Disintegration of Beryllium by Deuterons and Protons

Beryllium Bombarded with Deuterons

It was found in this laboratory that beryllium bombarded by deuterons gives a large yield of neutrons,[1] and, later, that the neutrons were accompanied by gamma-rays in about equal numbers, having an absorption coefficient corresponding to about 0.7 MEV quantum energy.[2] More recently we have investigated the same gamma-radiation by means of a cloud chamber and verified the existence of a very strong component of about 0.7 MEV, and have found additional, but weaker, lines up to 4 MEV. Bonner and Brubaker[3] have investigated the energy spectrum of the neutrons emitted under the same conditions, and have made some attempt at correlating the differences in energy of neutron groups with the observed gamma-rays.

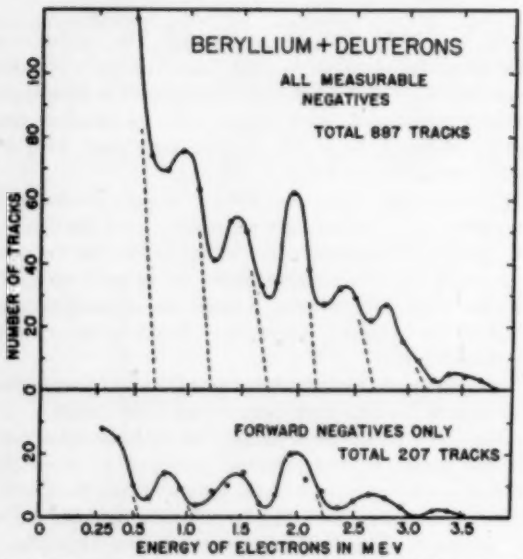

FIG. 1. Energy spectra of negative electrons ejected from the glass wall of the cloud chamber by the gamma-radiation from beryllium bombarded with deuterons.

Fig. 1 shows the energy spectra of electrons obtained by measuring the curvature of tracks in a 1000 gauss magnetic field, from 1200 cloud-chamber photographs. The source of the recoil electrons was the glass wall of the cloud chamber, which has a thickness corresponding to roughly 2 MEV stopping power for electrons in this region of energy. The radiation was obtained from beryllium metal bombarded with about 80 microamperes of deuterons at 700 kv. The upper curve in Fig. 1 includes all measurable tracks, without regard to direction. However, to meet the specification of measurability a track must lie approximately in the plane of the chamber: for example, if it is visible for 2/3 the diameter of the chamber it necessarily makes an angle less than 7.5° with the horizontal. The lower curve in Fig. 1 is composed only of tracks which make angles less than 7.5° with the direction of the incident quantum, in both the horizontal and the vertical planes. This, as is to be expected, gives fewer tracks, but greater resolution, and gives a more accurate determination of the gamma-ray energies, especially at the lower end of the scale. The two curves are in agreement as to the essential features of the spectrum, and indicate gamma-ray lines at about 0.8, 1.3, 2.0, 2.5, 2.9, 3.3, and 4.0 MEV. In accordance with the theory of Compton collisions we have added 0.2 to 0.25 MEV to the values of the intercepts in the electron spectra to obtain the corresponding gamma-ray energies. It is not certain, on the basis of intensity, that the 4.0 MEV line is not due to protons, since protons cannot be eliminated entirely from the beam.

The gamma-ray lines we have found correspond to the strongest lines indicated by differences in energy of neutron groups found by Bonner and Brubaker, but they have found indications of a number of additional lines. The natural explanation of this is that the resolving power of our method is sufficient to reveal only the strong lines. The agreement, both as to energy groups and total numbers, of neutrons and gamma-rays suggests that they arise from the same reaction, namely, $Be^9+H^2 \rightarrow B^{10}+n^1+\gamma$.

Beryllium Bombarded with Protons

Fig. 2 shows similar energy spectra of recoil electrons due to the radiation from beryllium bombarded with protons.

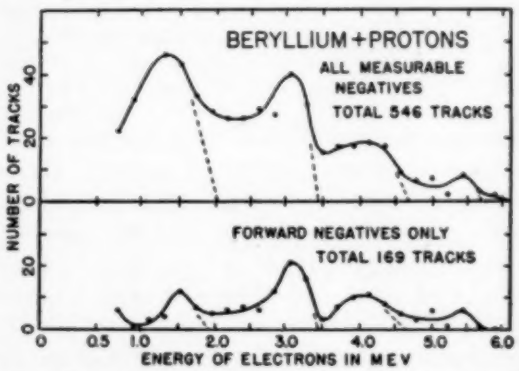

FIG. 2. Energy spectra of negative electron ejected from the glass wall of the cloud chamber by the gamma-radiation from beryllium bombarded with protons.

Here are represented 3400 photographs, taken at 900 kv, 80 microamperes proton current, and 1500 gauss magnetic field. The lines indicated are 2.2, 3.7, 4.8 and 6.0 MEV. Although the total intensity of this gamma-radiation is much smaller than that due to deuteron bombardment, the difference in the character of the spectra eliminates any suspicion of deuteron contamination.

The upper energy limit of the gamma-radiation is so high that it seems possible to account for it only on the basis of a radiative capture process, namely, $Be^9+H^1 \rightarrow B^{10}+\gamma$, provided we assume a stable mass for Be^9. The emission of an alpha-particle, for example, would lead to a much lower estimate for the maximum gamma-ray energy available. Although the upper limit of energy is not very definite, because of the small number of tracks, it can be used to obtain a lower limit for the mass of Be^9 referred to $B^{10}=10.0135$, with $H^1=1.0078$. It gives $Be^9>9.0117$, assuming that the proton energy corresponding to maxi-

mum probability of capture is 500 kv. Using Bethe's values[4] for B^{10} and H^1 we obtain $Be^9 > 9.0124$.

Voltage Excitation Curve

We have determined the yield of gamma-rays as a function of proton bombarding voltage in the range 200 to 800 kv, by means of an ionization chamber. Because of the low intensity of the effect, it was necessary to use a thick target. The effect began rather abruptly at 450 kv and continued to increase to 800 kv. This may mean, if the reaction postulated above is correct, that the first maximum in the probability for proton capture occurs when the proton energy is in the neighborhood of 0.5 MEV.

H. R. Crane
L. A. Delsasso
W. A. Fowler
C. C. Lauritsen

Kellogg Radiation Laboratory,
California Institute of Technology,
April 30, 1935.

[1] Crane, Lauritsen and Soltan, Phys. Rev. **44**, 692 (1933).
[2] Crane and Lauritsen, Phys. Rev. **45**, 226 (1934); (see correction in Phys. Rev. **45**, 493 (1934)).
[3] Bonner and Brubaker, Phys. Rev., June 1, 1935 (in press).
[4] Bethe, Phys. Rev. **47**, 633 (1935).

Alternating Intensities in the Spectrum of P_2

The nuclear spin quantum number I for phosphorus was found to be 1/2 by Miss Ashley,[1] who studied the alternating intensities in the $^1\Sigma$, $^1\Sigma$ bands of P_2. Although her work proved definitely that an alternation ratio of 2 ($I=1$) or lower was out of the question, it seemed desirable to have a direct measurement of this ratio to see if any discrepancy occurs similar to that observed by Aars[2] for fluorine. Aars found a ratio varying between 3.4 and 5.5 in different bands, although the highest value predicted theoretically is 3.0, for $I=\frac{1}{2}$.

The phosphorus bands were excited in a sealed-off quartz tube containing pure phosphorus and helium at 20 mm pressure. Power was supplied through external electrodes connected to a 5 kw power-oscillator giving a wavelength of 45 m. The spectrum was photographed in the second order of the 21-ft. grating, with a step-weakener directly in front of the plate so that the band lines themselves constituted the calibration marks. The weakener had seven steps of different thicknesses of platinum sputtered on a quartz plate, and the transmissions of the steps were determined as a function of wavelength by a monochromator and quartz vacuum phoelectric cell connected to a Wynn-Williams bridge amplifier. The peak intensities of the lines were measured, and the continuous background subtracted in each case. On plotting these intensities on a logarithmic scale, two parallel curves were obtained, and the displacement required to make the curve for the weaker lines (even K) coincide with that for the stronger gave the ratio of alternating intensities. The results of measurements on five different bands are summarized in Table I, data from two different plates being given for the 5,21 and 6,22 bands.

Table I.

Bands	Lines used	g_e/g_o
5,21	$P(56)+R(68)$ to $P(66)+R(78)$	3.5 ± 0.2
	$P(47)+R(59)$ to $P(66)+R(78)$	3.4 ± 0.2
6,22	$P(5)+R(17)$ to $P(47)+R(59)$	3.0 ± 0.2
	$P(21)+R(33)$ to $P(56)+R(68)$	3.0 ± 0.1
9,28	$P(47)$ to $P(65)$	3.0 ± 0.1
	$R(61)$ to $R(77)$	3.0 ± 0.6
9,29	$P(47)$ to $P(65)$	2.9 ± 0.2
	$R(61)$ to $R(79)$	2.8 ± 0.4
10,31	$P(41)$ to $P(59)$	2.9 ± 0.1

The deviation of g_e/g_o from the expected value of 3.0 in the 5,21 band may be due to the presence of lines from a faint underlying band, or it may result from the fact that this band shows much stronger perturbations than the others which were studied. It seems hardly possible to invoke the quenching mechanism proposed by Aars to explain his results, since in the present case the fairly high pressure of helium would serve to maintain a normal distribution of molecules among the rotational states.[3] This may account for the better agreement with theory shown by the above results.

F. A. Jenkins

Department of Physics,
University of California,
April 17, 1935.

[1] Muriel Ashley, Phys. Rev. **44**, 919 (1933).
[2] J. Aars, Zeits. f. Physik **79**, 122 (1932).
[3] O. Oldenberg, Phys. Rev. **46**, 210 (1934).

Arcs in Inert Gases—III

Several previous reports[1] have shown that a stable arc discharge of low amperage (5 to 10 amperes) between metal electrodes of high purity cannot be maintained under ordinary conditions in argon gas and in some of the other inert gases, provided the gases are first highly purified. In discussion of these earlier results, several arc authorities have suggested that the phenomenon might be one which occurs only in low current arcs and would probably disappear when higher currents flowed upon short circuiting of the electrodes. In a current investigation[2] of the metallurgical properties of pure iron welds made in argon, it is found on the contrary that a stable arc discharge cannot be maintained even across a gap one millimeter long, with open circuit voltages up to 60 volts and with short circuit amperages up to 120 amperes. If the open circuit voltage is increased to 62 to 64 volts or if the short circuit current is increased to 150 amperes, an arc discharge can be maintained for several seconds. If the open circuit voltage is increased to 65 to 70 volts or the short circuit amperage increased to 170 amperes, a stable arc discharge can be maintained indefinitely. These tests were carried out in argon gas of 99.5 percent purity. The electrode wires were of carefully cleaned pure iron in one case and of carefully cleaned steel wire in the other. The wires were one-eighth inch in diameter. In each case a plate of the same material was used as the opposite electrode.

The above phenomenon occurs with the welding electrode either as anode or as cathode. If the welding wire is not carefully cleaned of all drawing compound (a lime and ferrous sulphate film), the phenomenon of unstable arcing is not obtained at all. Thus it is shown that the non-arcing phenomenon reported previously for low current arcs obtains in high current welding arcs also.

The crater under the welding arc in air likewise has come to be considered an inherent characteristic of the arc. Upon this crater formation depends the penetration into and joining of the parts being welded. With argon of 99.0 percent purity or greater, there is a complete absence of crater formation in the base metal or previous weld deposit, and a resulting complete lack of penetration into, and fusion of, the parts being welded. Thus, another of the basic and essential features of the commercial arc welding process, namely, crater formation and penetration, is shown to be not an inherent characteristic of the iron arc, but fortunately is one which appears when arc welds are made in air.

A complete and detailed account of the experimental conditions of these tests, including certain important metallurgical aspects, will be published shortly.

Altogether it appears that fundamentally the high current arc is something quite different from that to which we have become accustomed by observing the arc between steel electrodes operated in air for welding.

GILBERT E. DOAN*
WILLIAM C. SCHULTE†

Lehigh University,
March 26, 1935.

* Associate Professor of Metallurgy, and † Engineering Foundation Research Fellow, respectively, at Lehigh University.

[1] G. E. Doan and J. L. Myer, Phys. Rev. **40**, 36 (1932); G. E. Doan and A. M. Thorne, Phys. Rev. **46**, 49 (1934).

[2] The investigation is sponsored by The Engineering Foundation of New York City.

Proceedings of the American Physical Society

MINUTES OF THE WASHINGTON MEETING, APRIL 25–27, 1935

THE 198th regular meeting of the American Physical Society was held in Washington, D. C. at the Bureau of Standards on Thursday and Friday, April 25 and 26, and at the National Academy of Sciences on Saturday, April 27, 1935. There were three parallel sessions for the reading of ten-minute contributed papers on Thursday morning and afternoon and Friday morning and afternoon, and two parallel sessions on Saturday morning and afternoon. The presiding officers were R. W. Wood, President of the Society, F. K. Richtmyer, Vice President, H. L. Curtis, W. E. Forsythe, W. D. Harkins, Bernhard Kurrelmeyer, W. F. Meggers, L. B. Tuckerman and C. W. Ufford. The attendance at the meeting was about five hundred.

The Society held a dinner at the Raleigh Hotel on Friday evening with two hundred and seventy present. The President, R. W. Wood, presided and the after-dinner speakers were K. K. Darrow, R. Ladenburg, F. K. Richtmyer and J. H. Van Vleck.

Meeting of the Council. At its meeting held on Thursday, April 25, 1935, the Council adopted the following minute in memory of Professor M. I. Pupin:

On receiving the Secretary's report of the death, on March 12, 1935, of Michael Idvorsky Pupin, Professor Emeritus of Electromechanics in Columbia University, the Council ordered that it be recorded in the Minutes of this meeting that Professor Pupin was one of the founders of the American Physical Society, one of that small group of young physicists who in 1899 had the vision to foresee the coming development of physics on this continent, and the zeal to create an organization to further it: and that he was one of the most distinguished of the Fellows of this Society, having a record of high accomplishments in science and its applications, and exerting an influence enhanced by the strength and charm of a rare personality.

Two candidates were transferred from membership to fellowship and thirty-two candidates were elected to membership. *Transferred from membership to fellowship:* Otto Glasser and Carl W. Miller. *Elected to membership:* Lucien V. Alexis, Charles P. Baker, L. V. Berkner, William H. Bessey, Walter C. Bosch, H. Brinkman, Carroll W. Bryant, Henry A. Carlock, Alfred H. Cash, Eugene F. Coleman, Charles A. Coulson, George A. Fink, Gertrude Fleming, Hobert W. French, Jr., John T. S. Fung, Frank Genevese, Ivan A. Getting, Thomas T. Goldsmith, John M. Ide, Ernest M. Lyman, Stuart T. Martin, W. H. McCorkle, Daniel J. McHugh, Edward E. Minor, Jr., Lloyd P. Morris, Lothar Nordheim, Charles H. Shaw, Herbert M. Strong, Th. J. ter Horst, Alfred Traeger, Walter Wallin, and Harold Washburn.

The regular scientific program of the Society consisted of one hundred and forty-six papers of which numbers 36, 63 and 98 were read by title. The abstracts of these papers are given in the following pages. An *Author Index* will be found at the end.

HAROLD W. WEBB, *Acting Secretary*

ABSTRACTS

1. Variation of Small-Ion Production Near the Earth's Surface. A. G. MCNISH AND G. R. WAIT, *Carnegie Institution of Washington, Department of Terrestrial Magnetism.* —Measurements of small-ion production in a thin-walled, closed vessel during 1933 and 1934, at Washington, D. C., demonstrate the existence of a regular diurnal variation in the production-rate. A maximum occurs around sunrise and a minimum shortly before sunset, on fair-weather days. The form of the variation is similar to the inverse of the daily temperature-curve and is therefore interpreted as due to a diminution of the radium-emanation content, in the lower region of the atmosphere, through scattering by convection currents. Contrary to popular beliefs there is no apparent connection between the rate of small-ion production and changes in the barometric pressure. In addition to the regular variations there are saltatory variations, ion-production being unusually high or unusually low for one or more hours at a time, which have not been associated with any meteorological phenomenon. These saltatory variations are distinct from the increase

in ion-production accompanying thunderstorms previously reported.[1]

[1] Mon. Weath. Rev. 62, 1–4 (1934).

2. The Distinction Between Langevin Ions and Dust-Particles in the Atmosphere. G. R. WAIT, *Carnegie Institution of Washington, Department of Terrestrial Magnetism.*—It is commonly believed that the Langevin ions (mobility about 1/3000 cm per sec. per volt per cm) of the atmosphere are electrically charged dust-particles. The fact that these ions do not exist in a gas from which all dust has been filtered has contributed to this belief. Two sets of experimental results are in agreement in showing that the Langevin ions of the atmosphere are not dust-particles. (1) These ions are condensation-nuclei, whereas ordinary dust-particles do not act as centers for condensation as has been shown by previous experiments. (2) These ions diminish greatly in number during times of dust-storms. The diminution in number is interpreted to mean that the dust-particles, through combination with the condensation-nuclei, remove them from the air. Through the process of filtering, the condensation-nuclei are removed from the air as well as the dust-particles, thus accounting for the absence of Langevin ions in filtered air.

3. The Annual and Diurnal Variations of Ions in Urban Communities. A. P. GAGGE, *John B. Pierce Foundation and Yale University.*—The results of daily ion counts at 9 A.M. and 24-hour counts taken once a month are given for the year from February, 1934, to February, 1935, at a station located in the center of New Haven City. The counts for both positive and negative ions are presented for four threshold mobilities, *viz.*: 0.07, 0.017, 0.0014, and 0.0006 cm per second, volt per cm. The number of ions were determined by hand on a counter of the Zeleny type, made at Frankfurt, Germany. Analysis of the mobility spectrum shows there to be only two finite mobility values, the usual small ions and the large, Langevin ions. The mobilities for the latter ions were found to be 0.0007 for the positive and 0.0005 for the negative. The number of positive ions of the small-ion group showed a rise for the summer months over that of the winter months. On the other hand, the number of negative ions in the small-ion group decreased during the summer months. In the large-ion group there is a minimum for both signs in July and a maximum in January. The diurnal variation for the ions of both signs of the small-ion group shows a single small maximum at 4 P.M. (E.S.T.) and a minimum at 3 A.M., for the year around. For the large-ions the diurnal variation has a maximum at 7 A.M. and at 7 P.M., for the winter months, while the second maximum becomes less distinct for the summer months.

4. The Electricity of Rain and Thunderstorms. ROSS GUNN, *Naval Research Laboratory, Washington, D. C.*—Rain.—It is shown that the unusually diverse electrical properties of rain may be correlated by assuming that each elementary water droplet and the surrounding ionized water vapor constitute a concentration cell of some 60 millivolts potential difference. The electrical charge on the droplet is therefore proportional to its radius and can be shown to be positive if the drop is evaporating and negative if it is condensing. The elementary droplets grow by association into large drops and build up charges of the order of 1/50 e.s.u. which discharge by conduction in a time of the order of 10^3 seconds. The calculated values are in excellent agreement with those observed. Thunderstorms.—It is shown that, in the presence of a rapidly rising current of air and the formation of raindrops greater than a critical size, separation of charge takes place. The ions (usually positive) are swept to great heights while the rain (usually negative initially) falls. Both charge distributions discharge, but at different rates, leaving a usually negative free charge in the rain formation zone which, in turn, induces a usually positive charge on the earth. The electrical distributions in a typical thunderstorm are quantitatively calculated from physical data and excellent agreement is obtained with observation in regard to the potential difference, electric field, electric moment, charging current, recovery time and the charges precipitated on rain. The maintenance of the earth's charge may be attributed to precipitation by rain under special conditions or possibly to systematic convection induced either by great natural barriers or by heat released in special regions by volcanic action.

5. A Mobile Radio Research Laboratory. H. SELVIDGE AND HARRY ROWE MIMNO, *Harvard University.*—A mobile research unit, recently constructed by the Cruft Laboratory, extends the scope of present fundamental research on ultra-high frequency radio propagation, ground wave propagation, scattering and ionosphere refraction. All experimental apparatus is mounted on relay racks, which form an integral part of a special steel body built on a Packard chassis. Partial heat and sound insulation and electrical shielding are provided. All equipment can be operated either from internal power sources in the truck or from external alternating current. The apparatus initially installed includes: (a) a novel ultra-high frequency receiver operating on three channels between 1 and 6 meters; (b) a superheterodyne receiver covering the range from 10 to 550 meters; (c) cathode-ray monitor equipment; (d) a low-power 5-meter transmitter; (e) a 200-watt crystal-controlled transmitter, operating on any of eight channels between 17 and 85 meters. Either transmitter can be operated with code, voice or pulse modulation. The main transmitter is also designed so that it can deliver a two-phase radiofrequency output for use in new Kennelly-Heaviside layer polarization experiments. Additional equipment can be added or substituted quickly. The new power unit will supplement two trailers which have been employed previously.

6. Recording of Ionosphere Echoes at Non-Vertical Incidence. PAUL B. KING, JR. AND HARRY ROWE MIMNO, *Harvard University.*—Continuous recording apparatus, used in tracing rapid changes in the ionosphere, must maintain exact synchronism with a modulating device at the associated transmitting station. In previous experiments synchronization has been obtained by operating

60-cycle motors on a common power network. The transmitters and receivers have usually been located in the same metropolitan area and the waves returned to earth after reflection at practically normal incidence. By simultaneous measurements at a distance it should be possible to secure additional information regarding vertical distribution of ionization, horizontal extent of ionic clouds, directional effects produced by the earth's field and the extent of ground-wave propagation under various soil conditions. Self-synchronizing sweep circuits have been tested but for best results the synchronizing device should be independent of the echo pattern which is being observed. In a trial installation we have used unattended motor-driven automatic apparatus, mounted in an automobile trailer, at a point 40 miles from the Cruft Laboratory. To extend the range beyond the reliable limit of the 60-cycle power network we have recently constructed a portable crystal-controlled thyratron inverter which maintains synchronism with the absolute frequency standard at the laboratory. The frequency drift has been reduced below 0.0001 percent per hour.

7. The Exact Measurement of Electron Tube Coefficients. ROGER W. HICKMAN AND FREDERICK V. HUNT, *Harvard University.*—The analysis of the conventional bridge circuits (Chaffee, *Thermionic Vacuum Tubes*) for the measurement of electron tube coefficients has been extended to include the effect of grid current and tube and battery capacitances. It has been found that the addition of an auxiliary capacitance bridge to the usual circuits permits annulment of the quadrature component of voltage introduced into the detector circuit by the tube capacitances. In every case in which one or more of the tube capacitances form one arm of the auxiliary bridge the conditions of balance show the expression for the tube coefficient to be independent of the capacitances of the auxiliary bridge. If all the tube capacitances are considered it appears that a single balancing condenser in the auxiliary bridge will always suffice to give an exact null balance, although the expression for the tube coefficient may contain a correction factor, usually negligible, involving the capacitances. This capacitance balancing method has been applied to circuits suitable for measuring both positive and negative values of the plate and grid coefficients and the exact expressions for the coefficients are given under the general condition that electron current flow to both grid and plate.

8. A New Type Radio Transmitter for Short Waves.[1] RONOLD KING, *Lafayette College.*—The directional properties of the loop type antenna are incorporated in a new form of radiator of electromagnetic waves. The device combines in a single compact unit, a multi-oscillator and a directional antenna system. The circuit, construction and properties of an ultra-short wave transmitter of this type operating at a carrier frequency of 170 megacycles are described, and a working model is displayed. The condition for oscillation and the frequency equation are briefly discussed; the formula for the radiation resistance is given. The solution of the equations for the electromagnetic field is outlined for the wave zone; it is shown that a good approximation of the field is that of the magnetic dipole. Several modifications in the form of the device and their effect on its characteristics are considered, together with possible applications in the field of short wave radio transmission.

[1] The mathematical treatment has been sent to the Philosophical Magazine of London under the title, *A Loop Transmitter.*

9. The Spectrum of Carbon Deuteride. ANDREW MCKELLAR AND CHARLES A. BRADLEY, JR., National Research Fellows, *Massachusetts Institute of Technology.*—Bands due to the CD molecule with heads at λ4307 and λ3865 have been photographed using a 21-foot grating and also in the first order of the Institute's 35-foot 30,000 lines per inch grating. They were obtained both by means of a hollow cathode discharge in C_2D_2 and by burning C_2D_2 in an excess of oxygen. The bands correspond to the $^2\Delta$, $^2\Pi$CH band with head at λ4315 and the $^2\Sigma$, $^2\Pi$CH band with head at λ3871. The band at λ3865 has been measured. It is found that the normal $^2\Pi$ state is almost pure Case *b*, being much more nearly so than the analogous state of CH. This is made manifest by the fact that the R_1 and R_2, the P_1 and P_2 and the Q_1 and Q_2 branches are coalesced to form an apparent three branch band. It is only for $K \leq 3$ that, on the 35-foot grating plate, branch lines can be resolved into very narrow doublets. From term differences the constants B_0' and B_0'' for this band have been calculated as 6.88 and 7.70, respectively. The corresponding constants for CH when multiplied by ρ^2 give 6.80 and 7.65. The agreement is about as good as might be expected since the relation $\rho^2 = B^i/B$ holds strictly only for B_e^i/B_e and not for B_e^i/B_e.

10. The Methane Content of the Giant Planet Atmospheres. ARTHUR ADEL, *University of Michigan,* AND V. M. SLIPHER, *Lowell Observatory.* (*Introduced by D. M. Dennison.*)—The identification of more than forty vibration-rotation absorption bands in the photographic region of the spectra of Jupiter, Saturn, Uranus and Neptune as due to the methane molecule is ample evidence of the vast amounts of this gas present in the atmospheres of the Giant planets. The most outstanding and penetrating harmonic sequence of bands in the planetary spectrum is $n\nu_3$. This sequence extends to $7\nu_3$ (543$\mu\mu$) in the spectra of Jupiter and Saturn, to $8\nu_3$ (486$\mu\mu$) in the spectrum of Uranus, and to $9\nu_3$ (442$\mu\mu$) in the spectrum of Neptune. The quantities of methane present in the absorbing layers of the planets (the layers penetrated by sunlight before it is scattered back into interplanetary space) can be determined from the path-lengths required to display these sequence limits in the laboratory. Path-lengths of sufficient magnitude were used to photograph down to and including $7\nu_3$, thus providing a direct estimate of the methane content of the absorbing layers of Jupiter and Saturn. The methane concentrations in the absorbing layers of Uranus and Neptune were secured through extrapolation along a curve which was obtained by plotting a characteristic of the sequence $n\nu_3$ against n. Preliminary values for the absorbing layer depths are:

Jupiter — $\frac{1}{2}$ Mile-Atmosphere
Saturn — $\frac{1}{4}$ Mile-Atmosphere
Uranus — 4 Mile-Atmospheres
Neptune—25 Mile-Atmospheres.

These values yield the following absorbing layer methane contents:

Jupiter — 8×10^{16} tons
Saturn — 6×10^{16} tons
Uranus — $8^{+}\times10^{16}$ tons
Neptune—60×10^{16} tons.

11. On the Intensity Formulas for $^1\Sigma^+-{}^1\Sigma^-$ Transitions in Band Spectra. R. D. PRESENT AND J. H. VAN VLECK, *Harvard University.*—G. Herzberg has recently studied certain faint absorption bands in O_2 which show Q branches ($\Delta K=0$) but not the customary P and R branches ($\Delta K=\pm1$). These bands he attributes on the basis of the configuration theory to a transition $^3\Sigma_g^--{}^3\Sigma_u^+$. Such transitions are forbidden by the usual selection rules and have hitherto not been observed. There exist two alternative explanations for the occurrence of these bands: (1) spin-orbit interaction, (2) rotational distortion. Both of these effects would cause the Σ states to assume some of the characteristics of Π states; consequently the forbidden bands would appear with small intensity. For the case of spin-orbit interaction the intensities have been calculated in case (a) and transformed to case (b) where the theory predicts twelve branches with $\Delta K=\pm2,0$ provided the J structure is resolved. When this structure is unresolved we find that transitions with $\Delta K=0$ should be more intense than transitions with $\Delta K=\pm2$ in the ratios: 6 : 1 when $K=\infty$, 5 : 1 for $K=5$ and 4 : 1 for $K=1$. In view of the faintness of the observed bands this appears to be sufficient to account for the absence of branches with $\Delta K\neq0$. With rotational distortion, calculations show that only Q branches will occur. With spin-orbit interaction the intensities vary approximately as the first power of K, while for rotational distortion they increase asymptotically as K^3. Further experiments are needed to decide between the two explanations.

12. Transfer of Rotational Energy. FOSTER F. RIEKE, *Harvard University. (Introduced by O. Oldenberg.)*—HgH bands are emitted when a mixture consisting of traces of Hg vapor and H_2 and a few mm of N_2 is irradiated with the Hg 2537 line. Their appearance is known to be a consequence of two reactions involving metastable Hg atoms: (1) formation of HgH in its normal electronic state and (2) excitation. In the interval between these processes, and between successive excitations, the HgH makes thousands of collisions with normal N_2 molecules. The interval between processes, and therefore the number of collisions, is inversely proportional to the concentration of excited atoms and can be increased by reducing the intensity of the exciting radiation. Experiments show that the rotational temperature, always greatly in excess of the temperature of the gas, decreases with decreasing intensity of the primary light. Additional experiments show that the phenomenon is not caused by self-absorption of the low-rotation lines; and moreover it is not to be explained by the influence of higher states of Hg excited by successive absorptions. The result may be interpreted as evidence of extremely slow decay of rotation of HgH in collisions with N_2. Other experiments indicate that the principal source of excess rotation is not the formation process, as Beutler and Rabinowitch assumed, but transfer of vibrational or electronic energy into rotation during the lifetime of the excited molecule.

13. The Far Ultraviolet Absorption Spectra and Ionization Potentials of H_2S, CS_2 and SO_2. W. C. PRICE, *The Johns Hopkins University.*—A new absorption spectrum has been found in H_2S in the region below 1650A. The rotational structure of a few of the bands has been resolved. They have P, Q and R branches and are shaded towards the red. Their structure indicates that the moment of inertia is not changed by more than a few percent by the excitation. The bands with possibly one or two exceptions are all due to the vibrationless electronic transitions of a non-bonding electron. Three Rydberg series going to a limit of 84,420 cm^{-1} and one going to a limit of 84,510 cm^{-1} were found in the bands. Up to 15 members were found for one series. The ionization potentials of H_2S can thus be given as 10.414 ± 0.002 and 10.425 ± 0.003 volts. Absorption spectra of CS_2 and SO_2 have been found in the region 2300–1000A. These consist of various sets of long vibrational progressions which widen out to either side with increasing pressure. A consideration of the bands indicates that they both go to ionization potentials around 10.3 volts. In the case of SO_2 however, there is a much stronger set of bands starting around 1350A. These are probably the bands which go to the observed ionization potential at 13 volts.

14. A Spectroscopic Investigation of Chemical Reactions of OH in the Electric Discharge. A. A. FROST AND O. OLDENBERG, *Harvard University.*—Through light absorption as observed with the aid of the 21-ft. grating, relative concentrations of OH may be measured. OH produced by the electric discharge through H_2O vapor has a lifetime of the order of $\frac{1}{4}$ of a second. Measurements of the OH concentration as a function of the time after interruption of the discharge and as a function of the total pressure indicate that the chief process by which OH disappears is the three-body process $OH+OH+M\rightarrow H_2O_2+M$.

15. Extension of the Absorption Spectrum of the Hydrogen Molecule. JOHN J. HOPFIELD, *Libby-Owens-Ford Glass Co.*—Using the continuous spectrum of helium as a background, discrete absorption lines (bands) have been observed in H_2 at low pressures as far as 738A. Some bands belong to the $A-D$ system already reported and the rest belong to new systems. Some of these bands extend into the region above the ionization potential of H_2 (15.9 v), that is, into the region of vibration in the normal electronic state of the hydrogen molecule ion. Apparently they are the higher vibration states of band systems of H_2 which begin below this ionization limit. This lends further evidence in support of the correctness of the above value of the ionizing potential of the molecule. The $A-D$ band system has already been described. An alternative interpretation has been suggested by Richardson in his recent book.

His interpretation does not seem to fit the absorption data if normal spectral behavior is the rule in the case. No new vibration bands of this system are evident to change the vibrational analysis that had already been given by the author. The $A-D$ band system, one of the strongest in the spectrum of the hydrogen molecule, seems therefore to remain unclassified in the present scheme of H_2.

16. Effect of Visible Light upon the Ultraviolet Fluorescence of Various Compounds Previously Irradiated with Roentgen or Gamma-Rays. OTTO GLASSER AND I. E. BEASLEY, *Cleveland Clinic Foundation.*—The ultraviolet fluorescence of sodium chloride, potassium chloride, sodium bromide, rocksalt and fluorite crystals following their exposure to roentgen or gamma-radiation is conspicuously increased if the irradiated compounds are exposed to visible light. Intensity and quality of the emitted ultraviolet radiation was measured with a photoelectric Geiger-Müller counter tube equipped with a cadmium electrode and a quartz window. The half-life of induced ultraviolet fluorescence ranges from a few minutes to several days depending upon the intensity and duration of exposure to the primary radiation and the subsequent exposure to visible light. Spectrographic examination in the case of sodium chloride shows that the emitted radiation has one maximum in the neighborhood of 2450A.

17. Optical Properties of Lithium Fluoride in the Schumann Region. EDWIN G. SCHNEIDER, *Harvard University.*—Vacuum spectrograph measurements on artificially produced lithium fluoride crystals have been made to determine the absorption, reflecting power and index of refraction in the extreme ultraviolet. The absorption coefficient and reflecting power were determined by photographic measurement of the transmission of several thicknesses of lithium fluoride taken from the same crystal. For this reason the term reflecting power includes all surface mechanisms acting to remove light from the transmitted beam. A comparison of the measurements on polished and on cleavage surfaces shows very nearly the same values for reflection. These values are considerably higher than the theoretical curve for short wavelengths, but approach this curve for longer wavelengths. This discrepancy is similar to that found by W. M. Powell (Phys. Rev. **45**, 154 (1934)) for fluorite. The absorption coefficient for the best crystal was found to increase slowly from 0.3 per cm at 1600A to 1.0 per cm near 1200A. Below this point it increases rapidly. The refractive index was determined by the method of minimum deviation. In the near ultraviolet the values obtained are in complete agreement with those of Z. Gyulai (Zeits. f. Physik **46**, 80 (1927)). At 1130A the index has increased to 1.70.

18. The Electro-Optical Kerr Effect in NH_3, N_2 and O_2. WILLIAM M. BREAZEALE, *University of Virginia.* (*Introduced by J. W. Beams.*)—Absolute values for the Kerr constant of anhydrous ammonia, nitrogen and oxygen have been determined. The apparatus used was an improved form of that first developed by Stevenson and Beams (Phys. Rev. **38**, 133 (1931)). NH_3 and N_2 were measured directly, but the fire hazard prevented doing this with O_2. Instead the Kerr constant was determined for a mixture of N_2 and O_2 and the value for O_2 deduced from this and the known value for N_2. Measurements in NH_3 were made using wavelengths of 6500A and 5750A, pressures from 13 to 30 atmospheres and temperatures from 40 to 80°C. In N_2 and O_2 the wavelength used was 6500A, pressures in the neighborhood of 100 atmospheres and temperatures from 20 to 65°C. The absolute value of the Kerr constant B reduced to 6500A and N. P. T. is for NH_3 $(62.6\pm1.8)10^{-12}$, for N_2 $(4.60\pm0.10)10^{-12}$ and for O_2 $(6.94\pm0.30)\ 10^{-12}$. These values are in agreement with the predictions of the Langevin-Born theory.

19. Diffuse Infrared Transmission of Solids. J. D. HARDY AND CARL MUSCHENHEIM, *New York Hospital.*—In the course of experiments on the total amount of infrared energy transmitted through human skin it was found necessary to develop a method for measuring the energy scattered when Lambert's law was not obeyed. Angstrom's law of scattering was found to fit the experimental data and a simple integration method was used to determine the total energy transmitted. Such materials as ground glass, white bond paper, and human epidermis were examined. The method was tested by measuring the transmission of a piece of glass before and after grinding. It was found that the two were in satisfactory agreement; the glass after grinding transmitting about 5 percent less than before. Layers of skin as thin as 0.03 mm were found to have strong absorption maxima due to water; upon drying the skin, the bands due to the organic linkages became apparent.

20. Color Temperature Scale of the Nela Laboratories. W. E. FORSYTHE, *Incandescent Lamp Department, General Electric Company, Nela Park.*—The color temperature scale for the laboratories at Nela Park has been maintained by a number of tungsten lamps which had been color matched against carbon tube and various platinum wound porcelain black bodies. The platinum wound furnaces were operated at temperatures between 1300 and 1828°K and the carbon tube furnace between 1600 and 2600°K. Above 2600°K the color temperatures were determined by indirect methods, making use of several hollow tungsten tube black bodies used by Dr. A. G. Worthing[1] in measuring the emissivity of tungsten. About a year ago the National Bureau of Standards[2] announced the establishment of a new color temperature scale. To check our color temperature scale with this new scale, a number of tungsten lamps were sent to the Bureau with the request that these lamps be color matched with their standards. It was found that our temperature scale was about 26° low at 2400°K and about 26° low at 2800°K. Since it does not seem that the incandescent lamps used to maintain this scale have changed in the past 10 years, this 26° deviation indicates a real difference between the two scales.

[1] Phys. Rev. **10**, 377 (1917).
[2] B.S. Jour. Res. **12**, 527 (1934).

21. Molar Polarization of Nitrogen and Argon by Displacement Interferometry. CLARENCE E. BENNETT, *University of Maine.*—(Experimental data obtained at Massachusetts Institute of Technology.) An improved displacement interferometer suitable for precise measurements of dispersion in gases over ranges of pressure and temperature was described about a year ago.[1] At that time it was pointed out that for pure nitrogen, because of a strictly linear variation of fringe displacement with pressure up to 14.145 atmospheres, it was possible to calculate simultaneously the Cauchy dispersion constants A and B corresponding to N.T.P. conditions and infinite wavelength. $A-1=0.002932$ and $B=1.637\times10^{-14}$ to 0.1 percent. More recently, the pressure readings in these nitrogen experiments have been reduced to corresponding density values by a Keyes type equation of state.[2] $p=RT/(v-\beta e^{-\alpha/v})-A/(v+b)^2$. As a result, it now becomes possible to state that the Lorentz-Lorenz relation is valid to one part in fifteen hundred for densities up to 0.01656 gram/cc. Furthermore, the molar polarization is found to be 4.369 ± 0.003. Also, similar observations and calculations have been made for argon of purity known to exceed 99.8 percent, over a range of densities from zero to 0.03342 gram/cc (18.482 atmos.) involving two different temperatures. Although the fringe displacements deviate slightly from linearity with pressure in this case, they are linear with density to less than one part in one thousand. Therefore the Cauchy dispersion constants A and B for N.T.P. conditions and infinite wavelength are obtainable with a precision approaching that in the case of nitrogen. The values are: $A-1=0.0002771$ and $B=1.478\times10^{-14}$. Also, the Lorentz-Lorenz relation is strictly followed (the average deviation being less than 0.2 percent), and the molar polarization is found to be 4.136 ± 0.010. Preliminary calculations on CO_2 data over the density range from zero to 0.03839 gram/cc indicate that the Lorentz-Lorenz equation is not followed.

[1] Phys. Rev. **45**, 3 (1934).
[2] Proc. Nat. Acad. Sci. **3**, 323 (1917).

22. Theory of Photoelasticity. HANS MUELLER, *Massachusetts Institute of Technology.*—Elastic deformations cause birefringence because they produce anisotropy of (1) the Lorentz forces, (2) the Coulomb forces in ionic crystals and (3) the atomic polarizabilities. For D-lattices and amorphous solids the photoelasticity due to the first two effects is calculated from Ewald-Born's lattice potentials. Comparison with experimental data shows that in most cases the third effect is predominant. For pressure the anisotropy of the atomic refractions always causes negative birefringence. Positive birefringence occurs only if the first two effects give a large positive contribution. This is the case for highly refractive glasses, for ZnS, CaF_2 and CsCl for pressure normal to an octahedral face, and for crystals of the type NaCl if the pressure is normal to a cube face and if the ratio of the refractions of the anion and cation is less than 10. In some cases this ratio can be calculated from the photoelastic constant p_{44}. Diamond and zincblende show a large photoelastic effect for pressure normal to a cube face because the first and third effects give both negative birefringence. The optical anisotropy produced by pressure is larger for anions than for cations. Hydrostatic pressure decreases the refractions.

23. Quantum Theory of Metallic Reflection. L. I. SCHIFF AND L. H. THOMAS, *Ohio State University.*—In the classical (Drude) theory of the reflection and refraction of light at a metallic surface, the component of electric intensity perpendicular to the surface is discontinuous there, the remaining components of the field vectors being continuous. In a more detailed description the interaction of the light with the metal is expressed as scattering by the conduction electrons according to quantum theory. Those components of the field vectors which were continuous in the classical theory retain very approximately their values in that theory. The electric intensity perpendicular to the surface, though given approximately elsewhere by the classical theory, fluctuates widely within a few electron wavelengths of the surface. If this fluctuating field is used to calculate the surface photoelectric effect by Mitchell's method (K. Mitchell, Proc. Roy. Soc. **A146**, 442 (1934)), the agreement of his result for a clean potassium surface with observation seems to be improved. No calculations have been made for sensitized surfaces, but arguments based on the use of the Drude form seem to be precarious.

24. The Half-Lives of Potassium, Rubidium, Neodymium and Samarium. ARTHUR E. RUARK AND KARL H. FUSSLER, *University of North Carolina.*—The long apparent half-lives of K, Rb and Nd are in striking disagreement with theory. To relieve this discrepancy, at least in part, the suggestion has often been made that their activities are due to isotopes of small abundance, having half-lives small in comparison with the apparent ones. This paper shows that the active fractions have half-lives longer than 10^8 years; the same is true for the alpha-rayer Sm. It is pointed out that these activities may be caused by small radioactive fractions of well-known isotopes; RaD and stable Pb 210 constitute a similar case. Data are presented which show that it is possible for the active portions of Nd and Sm to be genetically connected.

25. The Hollow Cathode as an Ion Source. P. GERALD KRUGER AND B. T. DARLING, *University of Illinois.*—A Paschen hollow cathode has been set up in a way similar to that used in a vertical type lamp for the excitation of spectra. Various sized holes were made in the bottom of the cathode and an electrode, at 1000 v negative potential, placed a few mm from the bottom, to see what magnitude of positive ion current could be drawn from the cathode. A pressure of about 100 bars of He gas was maintained in the lamp and the cathode glow excited by a 700 v d.c. potential. Table I shows the order of magnitude of ion currents which can be obtained. Apparently the ion current is directly proportional to the lamp current and the area of the hole in the cathode. The total power used in the experiment so far has been 350 watts. No ion current is observed when the accelerator voltage is applied

TABLE I. *Positive Ion Current from Hollow Cathode.*

AREA OF HOLE CM²	ION CURRENT MICROAMP.	LAMP CURRENT AMP.	ACCELERATION POTENTIAL VOLTS	ION CURRENT PER CM² PER 0.5 AMP. LAMP CURRENT M.A.
1.64×10^{-3}	5	.50	1000	3.0
6.7	18	.50	1000	2.7
22.8	60	.50	1000	2.7
43.8	65	.25	1000	3.0
43.8	110	.40	1000	3.1

to the accelerator electrode and there is a zero current through the lamp.

26. Electrostatic Generator with Small Vertical Clearance. WILLARD H. BENNETT, *Ohio State University.*—In order to obtain the highest possible voltage on an electrostatic generator in a room with a ceiling twelve feet high, the collecting surface for charge at high voltage is supported by ropes at 20° with the horizontal. This exposes smooth surfaces having a maximum radius of curvature towards the nearest grounded surfaces (above and below) and also avoids having dielectric surfaces in the gap. Tests on the generator show that both of these points of design are important.

27. A High Current Ion Source. E. S. LAMAR AND E. W. SAMSON, *Massachusetts Institute of Technology.*—Since the capillary ion source described by Tuve, Dahl and Van Atta (Phys. Rev. **46**, 1027 (1934)) was a decided advance over previous types, it seemed desirable to investigate its possibilities further. In the present source, as in theirs, the arc runs through an $\frac{1}{8}$ inch capillary in a stainless steel block. The essential modifications are the use of glass insulation for cathode and anode, and elimination of the auxiliary electrode for drawing ions out of the arc. The ions simply drift through a 1.18 mm outlet tapered to a 45° edge. The ranges of current, voltage and gas pressure in the arc were 0.1 to 3.5A, 80 to 100v, and 0.04 to 0.6 mm. The ion current is approximately proportional to arc current when the outlet is tapered, and depends little on pressure, but varies greatly with outlet shape and gas purity. A 1.92a. arc current gave 4.2 milliamperes, which converged into a 12 mm beam at 8 cm from the outlet when 10 kv was applied to a 2.5 cm focusing electrode placed at a distance of 4 cm. Two groups of secondaries were produced by positive ions striking the collectors, one group roughly independent of voltage, the other rising sharply at 8 kv.

28. The Efficiency of the Tube Counter. SELBY M. SKINNER, *Columbia University.*—The efficiency of counting ionizing particles by the tube counter is investigated, taking account of the electrical behavior of the counter, and the random nature of the arrival of the particles. Expressions are obtained for the efficiency of counting, the number of particles counted per unit time (n), and the average recovery time, in terms of the number of particles arriving per unit time (n_0), the time constant of the counter, and one other parameter, d, which is constant for a given counter. Methods for measuring d (which for most counters lies between 1.3 and 5) are indicated. The efficiency of counting decreases with an increase of n_0, rapidly at first, then more slowly, so as to have the asymptotic value $1/d$. The determination of n_0 from n is discussed.

29. Characteristics of Geiger-Müller Counters Filled with Different Gases. C. L. HAINES, *Bartol Research Foundation.*—Nine counters of the metal-glass type were made, having oxidized copper cylinders 1 cm in diameter and 3 cm long. Tungsten wires of 3 mils diameter were put into one group of three, of 5 mils into another, and of 10 mils into the third. Air, hydrogen, oxygen, argon (oxygen-free) and argon-oxygen mixtures in the approximate proportions 94 percent A and 6 percent O_2 and 99 percent A and 1 percent O_2 were used at pressures from 1 to 100 mm of Hg. Starting voltage *vs.* pressure was measured for each gas and each wire size. A crossing of the three curves for each gas is shown; indicating that the starting voltage is lower for the larger wire, at low pressures, than for the smaller wire. The starting and breakdown voltages were determined when the counter resistor was only 10^6 ohms, and the difference between these two voltages taken as a measure of the operating range of the counter. Counting rate *vs.* pressure was also measured for each gas, using a constant radioactive source. Werner's equation (Zeits. f. Physik **90**, 384 (1934)) is shown to fit the data well for the pure gases and fairly well for the argon-oxygen mixtures, but not so well in the case of air.

30. New Methods for the Detection of Minute Quantities of Thorium in Common Materials. ROBLEY D. EVANS,* *Massachusetts Institute of Technology,* GLADYS D. FINNEY, ARTHUR F. KIP AND RAYMOND MUGELE, *University of California.*—Advances in geophysical radioactivity and in age measurements on meteorites, igneous rocks and other common materials await development of precision technique for the determination of minute traces of thorium and its radioactive products. Our experimental results show the Th emanation-flow-technique to be inherently inefficient, as the emanating power of liquid specimens may vary and is at best only about 0.6. We have therefore developed four new methods for thorium detection based on (1) vacuum-tube-electrometer counting of all alpha-rays emitted from smooth surfaces of solids, such as polished rocks, (2) counting of all alpha-rays emitted from powdered specimens, such as finely ground rocks or chemically prepared precipitates, (3) counting of ThC′ alpha-rays only, after exclusion of all shorter rays by absorbers placed over solid or powdered sources, (4) detection of the feeble gamma-rays emitted by larger sources, using very sensitive screen-cathode γ-ray tube-counters. Methods 1, 2, 4 require corrections for radiations due to the uranium series, and these are based on accurate radium analyses. Method 3 reaches the Th series directly. Method 2 gives a direct measure of the rate of production of helium, when very thin sources are used. Methods 2, 3, 4 may be referred to internally standardized sources, but Method 1 cannot, and is, moreover, subject to difficulties due to the escape of traces of emanation from the source. We find it least

reliable for routine work. Analyses of a suite of Sierra Nevada igneous intrusive rocks showed that Methods 2 and 4 are most suitable and give mutually consistent results. They also indicate that the ratio of Th/U is higher than previously supposed and that therefore thorium determinations are even more important to geophysics than had been previously supposed.

* National Research Fellow, University of California, 1932–1934.

31. Theories of Ion Condensation. DONALD H. LOUGHRIDGE, *University of Washington*.—The very great importance of cloud expansion photography in the field of nuclear investigations has brought sharply to the front a need for suitable correlation of physical and chemical properties of liquids and their suitability for ion condensation. Results obtained on minimum expansion ratios for alpha-ray track condensation, in a large number of organic vapors, are compared on the basis of the original Thomson theory and the new one of Volmer and Flood, with good agreement in most cases on the latter basis. The radii assumed for these calculations are taken from the best experimental values for the cases available. The effect of the size of the chamber on the assumption of adiabatic expansion, by considering the effects of heat conductivity, is plotted.

32. The Raman Spectra and the Latent Heat of Fusion of Nonassociated Substances. C. J. PHILLIPS, *Corning Glass Works*. (*Introduced by J. T. Littleton.*)—The relationship

$$\lambda = mNhc/JML_f = m(2.845\times10^{-1})/ML_f,$$

where $m=1, 2\cdots$, N=Avogadro's number, h=Planck's constant, c=velocity of light, J=Joule's equivalent, M=molecular weight, and L_f=latent heat of fusion, is applied to thirty-eight organic and inorganic substances in the crystalline and liquid states. The wavelengths calculated in this way are found to agree quite closely with the observed infrared absorption bands. For each substance a Raman shift can be found which is equal to the calculated frequency, both being expressed in wave numbers. In all but five cases, the calculated Raman shifts lie within the range 350 cm^{-1} to 1600 cm^{-1}, although the molecular weights vary in a 6 to 1 ratio and the latent heats of fusion in a 21 to 1 ratio. The relationship apparently holds only for nonassociated substances. There are remarkable similarities between the calculated values for various homologous compounds. It is suggested that in glass the SiO_2 group may vibrate independently, at least to a certain extent.

33. The Complete Raman Spectrum of Heavy Chloroform. R. W. WOOD, *The Johns Hopkins University*, AND D. H. RANK, *Pennsylvania State College*.—The complete Raman spectrum of heavy chloroform has been photographed. Two distinct isotope effects were found and the calculations agree well with the observations. The 3318 frequency difference is shifted to 2256. The probable error is one wave number.

34. Diffraction Gratings for Use in the Far Infrared. A. H. PFUND AND J. A. SANDERSON, *The Johns Hopkins University*.—Glass halftone plates (Levy screens), the surfaces of which consist of alternate polished bars and etched grooves, have been silvered chemically and used as diffraction gratings in the far infrared: 25μ–100μ. The surfaces of the gratings have been prepared as follows: (1) the entire surface of the halftone plate was silvered, (2) the polished surfaces were silvered and the grooves filled with $CaSO_4$, which is black in the far infrared. No great differences in the behavior of the two types have been found. From 75 to 100 orders of the green mercury line can be seen on one side of the central image in the spectrum formed by these gratings as compared with about 20 visible orders in the spectrum formed by a wire grating. This indicates that the resolving power of the halftone plates should exceed that of wire gratings. By using filters of paraffin and black paper, energies measured in the central image are about one-fifth as great as the energy obtained by reflection from a silver mirror. Large radiometer deflections up to wavelength 100μ have been obtained. This work indicates that although the energy obtained from the halftone plates is not as great as that from echelettes, the resolving power is comparable to that of the echelette. The gratings are easily prepared; the cost is quite nominal.

35. Powder Filters for the Infrared. R. BOWLING BARNES, R. ROBERT BRATTAIN AND R. S. FIRESTONE, *Princeton University*.—The infrared transmission of thin layers of finely divided crystals of uniform particle sizes has been measured. Such layers are found to be opaque to radiations where $\lambda \ll \rho$, where ρ is the average diameter of the particles, and transparent to radiations where $\lambda \gg \rho$. If a characteristic frequency of the crystal lies in the region of opacity a sharp maximum of transmission is found upon the short wavelength side of this absorption band. Pfund has studied filters of this type. The use of such filters enables one to obtain very sharp monochromatic bands of infrared radiation. The explanation of the behavior of such powder filters lies in the fact that in regions where $\lambda \ll \rho$, the waves are refracted by the relatively large particles and emerge from the layer in random directions giving rise to an apparent opacity. In the region where $\lambda \gg \rho$ the particles are too small to act as refracting centers, and the only intensity loss is by scattering. At some point on the short wavelength side of the crystal frequency, the refractive index becomes equal to 1, and no refraction takes place. Hence the sharp transmission maximum. The true absorption of the crystal helps sharpen this maximum. It will be recognized that the origin of the sharp transmission band is the well-known Christiansen filter effect.

36. The Infrared Spectrum of GeH_4. WENDELL B. STEWARD AND HARALD H. NIELSEN, *Ohio State University*.—The absorption spectrum of GeH_4 in the infrared has been investigated with a prism spectrometer to 13.0μ, and bands, enumerated in the order of their intensities, have been located at 12.0μ (833 cm^{-1}), 4.7μ (2125 cm^{-1}), 3.3μ (3031 cm^{-1}), 3.4μ (2923 cm^{-1}), 6.0μ (1666 cm^{-1}) and 2.2μ

(4545 cm^{-1}). The regions at 3.3μ and 4.7μ have been measured under higher dispersion using an echelette grating ruled with 3600 lines per inch, in second order, and an echelette grating ruled with 4800 lines per inch in first order, respectively. The 3.3μ region consists of at least two overlapping bands and has only incompletely been resolved. The 4.7μ region consists of a single band with a very strong Q branch converging toward lower frequencies. The individual lines in the P and R branches are quite well resolved and give evidence of a more complex structure. The spacing between the principal peaks appears to be about 4.8 cm^{-1}. By analogy to the spectrum of methane the bands given above are identified respectively as ν_4, ν_3, $\nu_2+\nu_4$, $\nu_1+\nu_4$, $2\nu_4$ and $2\nu_3$.

37. The Infrared Absorption Spectrum of MgO. R. Robert Brattain, R. Bowling Barnes and Frederick Seitz, *Princeton University.*—By using plates, ranging in thickness from 0.075 mm to 3.05 mm cleaved from large single crystals of MgO, the infrared absorption spectrum of this substance has been studied. The absorption spectrum of this cubic crystal was found to consist of several prominent peaks and additional fine structure. An explanation of this is being sought on the basis of the three-dimensional lattice theory, in which harmonic and anharmonic terms are taken into account. Additional experiments are being performed to check preliminary results of the theory.

38. The Absorption of the Acetylenes in the Photographic Infrared. Charles A. Bradley, Jr. and Andrew McKellar, National Research Fellows, *Massachusetts Institute of Technology.*—By using an absorbing column 9 meters long of over 90 percent pure C_2D_2 at a pressure of 85 cm, no absorption bands were observed in the region 7000–11,700A. Inasmuch as it can be calculated on the basis of the vibrational assignments of the C_2H_2 bands taken in conjunction with the predicted frequencies for C_2D_2 that several bands should be present in this region under the above conditions, the lack of absorption is somewhat surprising. Possible causes of this unexpected behavior are discussed. A new faint absorption band of C_2H_2 was photographed in the first order of a 21-foot grating. For this an absorbing column of 7.5 meters in length at 90 cm pressure was required. The band's origin occurs at 12,720 cm^{-1} (7859A). It may arise from the combination $\nu_1+3\nu_2+2\nu_3$ which should occur (using Herzberg and Spinks' constants) at 12,708 cm^{-1}. We are indebted to Professors H. C. Urey and J. E. Zanetti of Columbia University for the D_2O and specially prepared CaC_2 used in generating the C_2D_2 and to Professor E. F. Barker of the University of Michigan for testing the purity of a sample of the gas.

39. The Infrared Absorption Spectra of Acetic Acid and Acetic Anhydride. E. K. Plyler and E. S. Barr, *University of North Carolina.*—Acetic acid and acetic anhydride show bands in the regions of 1.9, 2.3, 2.5 and 2.8μ. There is a slight variation in position and intensity but the two spectra are similar. In the region of 5.5μ there is an intense band in the acetic anhydride spectrum. When water is present acetic acid has a strong band at 5.7μ. A study of the intensities of these two bands made it possible to determine the time of formation of acetic acid from the anhydride and water. When 1 mole of water and 1 mole of anhydride were kept at 70°C, 50 percent of the anhydride had reacted in 45 minutes. At 26°C the change required approximately 12 hrs. Other factors being constant, increasing the mole fraction of water increases the rate of reaction, and decreasing the mole fraction of water decreases the rate of reaction.

40. The Production of Very Small Electric Currents. George J. Mueller, *Cornell University.*—Through improvements in construction and an extension of its range, the device for producing small electric currents of known magnitude described by Smith[1] has been developed into an exceedingly useful and reliable laboratory instrument. Experiments indicate that the device is convenient as a source of small known quantities of both positive and negative charge. Some unusual results of a careful study of expected tube constants as determined from electrode dimensions and experimentally determined values as well as constructional details and associated apparatus are described.

[1] L. P. Smith, *A Device for Obtaining Very Small Electric Currents of Known Magnitude*, R. S. I. **2**, 237 (1931).

41. A Rotating Coil Alternating-Current Potentiometer. Walter C. Michels and Barbara Raines, *Bryn Mawr College.*—An apparatus of high voltage and current sensitivities for the measurement of low frequency alternating currents has been constructed. The small potential difference to be measured is opposed to a sinusoidal electromotive force generated by a coil rotating in the magnetic field of a set of Helmholtz coils. The rotating coil is driven by a synchronous motor and the amplitude and phase of the opposing electromotive force can be varied by control of the Helmholtz coil currents. The detecting instrument is a three-stage amplifier supplying a tuned vibration galvanometer. Sensitivities of the order of 10^{-6} volt/mm or 10^{-14} ampere/mm are obtainable. Since the amplifier is used only as a null instrument, difficulties due to nonlinearity do not arise.

42. The Use of Thermionic Vacuum Tubes for Voltage Control. Chas. R. Larkin, *Lehigh University.*—The use of thermionic vacuum tubes to maintain a constant high potential supply for Geiger-Müller counters and ionization chambers is now quite common. Johnson and Street[1] devised two such circuits, and following them several modifications have been published. Under certain conditions some of these circuits may develop a seriously large damped oscillation which is not controlled by the regulator tube and which is not detected by a d.c. meter in the output. A study of these fluctuations in the various regulators has been made and is here presented. Several simple methods are available for reducing or eliminating them in the output. The overall control characteristics of the several circuits are compared and data on their

performance are given. A modified two-tube circuit having better characteristics than any so far examined, is described.

[1] J. C. Street and T. H. Johnson, J. Frank. Inst. 214, 155 (1932).

43. On the Nature of the Barrier Plane in the Cuprous-Oxide Photovoltaic Cell. JAMES W. BALLARD, *University of Pittsburgh*, AND E. D. WILSON, *Westinghouse Electric and Mfg. Co.*—Two possible internal structures of cuprous-oxide photovoltaic cells are considered, one in which the semi-transparent metal is either in intimate contact with the oxide or at most separated from it by a short gap, and one in which the semi-transparent metal is separated from the oxide by a polarized layer. Potential energy diagrams, representing approximately the potential energy of an electron in these two assumed structures, are drawn and transmission coefficients are calculated and plotted for incident light of wavelength range from 4000A to 6500A. Experimental results, obtained by means of "synthetic cells" purposely constructed to emphasize one or the other structure, are presented and discussed. Both theoretical and experimental evidence indicates the second postulated structure is more likely to explain the photovoltaic effect.

44. On the Peculiarities of Dielectric Constant *versus* Pressure Curves for Vapors. J. D. STRANATHAN, *University of Kansas.*—Deviation from linearity of the curve of $(K-1)/(K+2)$ *versus* pressure for many vapors has been attributed to various causes, most generally to a conductivity effect. The author finds in the case of water vapor, which gives an unusually large deviation, that the break is definitely not due to conductivity. Data show definitely that it is due to adsorption on the insulator surfaces and the consequent increase in polarization contributed by these additional molecules. This has been shown experimentally by changing markedly the adsorbing surface without changing the conductivity. In all probability the same phenomenon is responsible for the smaller deviations shown by other vapors.

45. The Variation of Thermal e.m.f. with Magnetization and Temperature. F. WOODBRIDGE CONSTANT, *Duke University.*—The variation of the e.m.f. of a thermocouple when one of the metals is magnetized was first discovered by William Thomson in the case of iron and nickel. This means that a couple may be formed entirely of one material provided the magnetization is not the same throughout. In spite of the many investigations of this effect since Thomson's the results are conflicting and the conclusions confusing. This attempt has been made first to summarize previous work, and second to repeat measurements of the effect on as many different ferromagnetic metals as possible when under exactly the same conditions in order that the resulting data might be more available for interpretation. Fe, Ni, Co and permalloy were tested by comparison of the ferromagnetic metal first unmagnetized and then magnetized in a uniform magnetic field against copper. There are indications of a connection between this effect, the change of length in a magnetic field and crystal structure which is of interest regarding theories of ferromagnetism.

46. The Establishment and Destruction of Superconductivity at Radiofrequency. R. B. SCOTT, F. B. SILSBEE AND F. G. BRICKWEDDE, *National Bureau of Standards.*—A tin wire 0.022 cm in diameter was supplied simultaneously with direct current and with alternating current of 200 kilocycles per second and of such value that the circular magnetic field in the outer layers exceeded the critical value at one crest of each cycle but was less than critical at the other crest. If the resistance of the material followed these pulsations it would be expected that the flow of the alternating current would produce between the ends of the specimen a drop of potential of distorted wave form containing a strong component of double frequency. Such a double-frequency component of the expected value was found. It varied with the temperature and the magnitudes of the components of current in the manner to be expected. It may be concluded that the mechanism of superconduction can come into action or be destroyed within a few microseconds by a sufficiently large magnetic field.

47. A New Phenomenon in the Superconducting Transition of Tin and Tantalum. F. B. SILSBEE, F. G. BRICKWEDDE AND R. B. SCOTT, *National Bureau of Standards.*—The effect of combinations of the variables, temperature, transverse magnetic field and specimen current, on the resistance in the transition range was investigated. The most characteristic effect, noted when the current is large (several thousand amp./cm^2), is that the passage from the superconducting to the normal resisting condition is accompanied by a spontaneous increase in resistance, occupying several seconds, followed by a slower return. This transient resistance is sometimes 75 percent of the normal. After such an effect has occurred, it will not occur again when the same conditions are reestablished after a short interval. The combination of variables at which this effect occurs is, however, definite if the time interval is long enough or if the specimen has been cooled to a low temperature. The effect occurs in two tantalum specimens at approximately the same (apparent) current density. The tin wire requires about 50 percent greater current density. For tin $H=2I/r$ connects, approximately, with specimen radius the currents and fields which acting alone (1) restore a given fraction of the normal resistance and (2) initiate the spontaneous rise. For tantalum the currents required were only 3 to 4 percent of the calculated values.

48. Free Path and Thermoelectric Effects. L. W. NORDHEIM, *Purdue University.* (*Introduced by K. Lark-Horovitz.*)—A general expression for the mean free path of electrons in metals is derived. This expression is valid for high temperatures and for any spherically symmetrical but otherwise arbitrary distribution of eigenvalues. The formulae for the resistance and the thermoelectric phenomena can be obtained in a simple manner for any model of the interaction between the electrons and the ionic lattice. The method is applied to derive relations between changes

in the resistance and thermoforce produced by foreign atoms or by distortions. The agreement with the experimental material is fairly good.

49. Atomic Weights Derived from Nuclear Transmutations. H. A. BETHE, *Cornell University.*—Simple stability considerations require for Be^9 an atomic weight <9.0124 as compared with the mass spectroscopic value 9.0154. Similarly, the excited state of the C nucleus, 5.5 MV above the ground level, should disintegrate into 3 α-particles before a γ-ray could be emitted, if $C^{12}>12.0013$ (Aston: 12.0036). On the other hand, excited O^{16} (5.6 MV energy) should disintegrate into C+He, if $C^{12}<12.0028$. These limits are irreconcilable unless it is assumed that the mass of He^4 referred to O^{16} is much too small. This follows also from the energy balance of nuclear transformations: It agrees perfectly with Bainbridge's mass values for H, He, Li; transmutations of "heavier nuclei" (Be, B, C) into one another agree reasonably well, whereas all transmutations of heavier nuclei into light ones give much less energy than expected. All stability difficulties can be solved, and all energy balances made to agree perfectly, if He^4 is assumed to be 3.0 ± 0.7 parts in 10,000 heavier than hitherto assumed. This correction applies also to H and Li, whose weights have been measured with respect to He. The weights of the heavier atoms are not very much changed. Some atomic weights derived purely from transmutation data are: $n^1=1.0085$, $H^1=1.00807$, $He^4=4.0033$, $Be^9=9.0135$, $B^{10}=10.0146$, $B^{11}=11.0111$, $C^{12}=12.0037$, $N^{14}=14.0076$, if $O^{16}=16.0000$. The probable error does not exceed 1 MV in any case.

50. Interaction Between Deuterons and Alpha-Particles. ERNEST POLLARD AND HENRY MARGENAU, *Yale University.*—In a continuation of experiments recently described to this society (New York meeting, Feb. 23, 1935) we have investigated the anomalous scattering of alpha-particles in deuterium for energies near which it first becomes effective; and also the angular variation of the yield of scattered particles for two different velocities of the incident alpha-particle. In each case the recoil deuterons were counted. In the first experiments we found that if the range of the alpha-particle is increased from 1.5 to 2.3 cm, the simple rise in yield of recoil deuterons (as expected from comparison experiments with protons) is not found. Instead there is a rise followed by a drop and a second rise which continues smoothly for higher ranges. We suggest that this maximum is due to resonance with an energy level in the nucleus of $_3Li^6$. The angular scattering experiments show a rapid fall in yield as the angle increases. For low velocities the results agree with Taylor's theory as well as the values found by Chadwick and Bieler do. At higher velocities the agreement is not satisfactory.

51. A Correlation of Nuclear Disintegration Processes. M. STANLEY LIVINGSTON, *Cornell University,* AND ROBLEY D. EVANS, *Massachusetts Institute of Technology.*—Bombardment of known elements by energetic alphas, deuterons, protons, neutrons and photons has already led to more than 150 reported modes of artificial nuclear transmutation. Each of the established nuclear reactions, including the 47 cases of natural radioactivity, may, however, be classified under one of 14 generalized type reactions. Compact and readily visualizable charts showing all these 200 or more reactions are presented. Each known isotope is represented by a square on a diagram. With atomic number Z as abscissa, and isotopic weight A plotted in terms of $(A-2Z)$ as ordinates, a simple and orderly arrangement results. A series of straight lines connecting nuclear species then serves to completely portray any reaction. By virtue of their geometrical identity the type reactions stand out with great clarity. Similarly, such matters as the distinction between the artificially radioactive elements which emit positrons and those which emit electrons become sharply significant and general rules for the creation and behavior of new nuclear species may be formulated. When backed by simple mass-energy calculations, the charts facilitate the prediction or verification of new reactions, and suggest the direction for systematic nuclear investigations. Supplementary charts depicting type reactions in a greatly simplified symbolical form will also be shown.

52. Low Voltage Disintegration of Lithium with Lithium. C. A. WHITMER AND M. L. POOL, *The Ohio State University.*—The lithium source consisted of a cylindrical steel boiler which had a narrow slit opening at one end and was heated electrically to about 700°C. From the slit a ribbon of atomic lithium issued and passed between two electrodes across which a violent disruptive discharge took place. The lithium ions of various charges then were drawn by an auxiliary voltage into the region of the main acceleration potential of about 120 kv. This potential was obtained by rectifying and smoothing the output of a transformer. It was necessary for the disintegration products to pass through a window of aluminum foil of 2 cm air equivalent before striking a zinc sulphide screen. With a lithium target alpha-particle scintillations were observed at the rate of about one per minute. When the source was adjusted for a less favorable production of multiply charged lithium ions, no appreciable results were obtained. LiOH and LiOD targets gave a somewhat larger alpha-particle count than a pure lithium target; while a beryllium target gave no results. A delayed activity was observed in the zinc sulphide screen indicating perhaps that neutrons as well as alpha-particles are products of the disintegration process.

53. Nuclear Chemistry and the Scattering of Protons in Collisions with Neutrons. DAVID M. GANS AND WILLIAM D. HARKINS, *University of Chicago.*—In 1933 the writers with Dr. Newson discovered a new isotope of nitrogen of mass 16, produced from fluorine by bombardment by neutrons. It was assumed that this nitrogen would be radioactive and would emit a negative electron to form oxygen 16. This has been confirmed by Fermi. A study of the mechanics of nuclear collisions from the relativistic standpoint showed that in nuclear collisions disintegration in no case occurs unless the projectile is captured. Obviously this does not need to hold at the extraordinary energy values of cosmic rays. The scattering of neutrons

and protons in their mutual collisions is of fundamental importance in the determination of the nature of the proton and the neutron and their relationship to the positive and negative electron. There is a possibility of an exchange reaction. Experiments on scattering will be described. These exhibit relations which depart from those to be expected for elastic spheres.

54. Absorption and Velocity of Slow Neutrons. J. R. DUNNING, G. B. PEGRAM, G. A. FINK AND D. P. MITCHELL, *Columbia University.*—The question of whether "slow" neutrons approximate ordinary thermal velocities was first studied by Fermi, using artificial radioactivity, with apparently negative results. Using the particles ejected by the slow neutrons from Li, with an ionization-chamber amplifier system as a detector, we have investigated the effect of varying the temperature, from about 95° to 373°K of a cylindrical vessel of water containing a Rn–Be neutron source, on the number of disintegrations produced in Li, and on the absorption coefficient of Cd for these slowed-down neutrons. Three separate experiments gave increases of ionization chamber counts due mostly to Li disintegrations, of 10, 4 and 9 percent, respectively, for "cold" neutrons as compared to "hot" neutrons. Cd absorption of "cold" neutrons measured about 6 percent greater than that of "hot" neutrons. The number of particles counted was so large that the probable statistical error would be less than 2 percent. Certain experimental factors still being investigated make it uncertain how definitely these results indicate thermal equilibrium. The absorption curve of slow neutrons in Cd appears to be completely exponential within experimental limits.

55. Neutron Effects in a Photographic Emulsion. DONALD W. MUELLER AND HENRY A. BARTON, *Princeton University.*—We are investigating the neutrons arising from 100 kv encounters between deuterium nuclei. The neutrons pass through a lead screen to stop charged particles and soft x-rays originating at the target. They then enter a photographic emulsion producing recoil protons and nuclear reactions. Numerous proton and alpha-particle tracks in the developed emulsions are readily observed by means of a binocular microscope with eyepiece half-stops affording stereoscopic vision. A 100 power N.a. 1.3 fluorite oil-immersion objective is used with full aperture illumination. By means of an eyepiece scale and a vertical micrometer, three coordinates are obtainable for any grain. The density of these tracks decreases with distance from the target, being on one plate 40 per sq. mm at a distance of 2 mm. We investigate only those tracks having both ends within the emulsion because only then is the range as well as the orientation determinable. With range and linear grain density known, the data of Blau and Wambacher (Akad. wissens. Vienna, Sitz. ber. **143**, 284 (1934)) enable us to distinguish between α-particle and proton tracks and, in the proton case, the direction of travel. We are proceeding to investigate the energy of the neutrons from the above source. A surprising number of α-particles have been observed which we can only account for as products of interactions between the neutrons and atoms in the emulsion.

56. Collisions of Alpha-Particles with Neon Nuclei. WILLIAM W. EATON, *Yale University.* (*Introduced by A. F. Kovarik.*)—Pure neon was introduced into a Wilson cloud chamber of the piston type, and a large number of photographs taken of the tracks of alpha-particles from a Th C+C′ active deposit source placed outside the chamber. By a system of mirrors, two photographs are taken at right angles on a single motion picture film through a single lens, the image planes being slightly inclined so that all regions of the chamber are in focus. The collisions have been studied by replacing the film in the camera, illuminating and reconstructing the complete forks in space by suitable inclination of a white screen. A device for the rapid and convenient determination of the actual plane of collision is described. The screen is then replaced by photographic paper, and prints taken, which are subsequently analyzed. Calculation of the velocities and measurement of the ranges of the recoil nuclei enable the construction of a range velocity curve. This curve is discussed and compared with Feather's fluorine curve. A number of apparently elastic high energy collisions have been obtained, which are discussed, and examples of these are shown, together with an illustration of the method of recombination of the forks in their original sizes.

57. The Energies of the Beta-Rays and Positrons Emitted by Various Artificially Produced Radioactive Substances. FRANZ N. D. KURIE (National Research Fellow), J. R. RICHARDSON AND H. C. PAXTON, *University of California.*—The energy distribution curves of the β-rays and positrons from radioactive substances produced by deuteron bombardment have been determined from measurements of the curvature of the tracks due to them in a Wilson cloud chamber traversed by a magnetic field. The following table gives our provisional values of the maximum energies together with values of the half-lives as evaluated by others.

Substances	E_{max}	*Half-Life*
$N^{13}+$	1.35 MV	11 min.
$Na^{24}-$	1.45 MV	15.5 hours
$P^{30}-$	1.85 MV	17.5 days
$Cl^{28}-$	4.5 MV	37 min.
$K^{42}-$	2.3 MV	13.5 hours

There is some evidence, as yet unverified, that there are two separate groups of β-rays from radio-chlorine. The two groups found by Cockcroft, Gilbert and Walton in carbon are not found. The data are considered in the light of the Fermi theory and their bearing on the Sargent relation is discussed.

58. An Analysis of the Data on Radioactivity Induced by Neutron Bombardment. CALVIN N. WARFIELD, *Woman's College of the University of North Carolina.*—Acting upon a suggestion of A. E. Ruark a study was made of the literature and the following generalizations were drawn: (1) Plotting atomic number (Z) against mass number (M) minus Z to represent the transmutations, an orderliness is apparent; (2) $M-Z$ is an even number for each of the 29 known parent isotopes; (3) Z is odd for the 19 parent isotopes which are activated by simple capture or by capture and emission of an alpha-particle, whereas in 8

of the 10 cases in which protons are emitted Z is even; (4) present data indicate that every parent isotope except K 41 is the most abundant natural isotope of the element; (5) all final isotopes resulting from the beta-emission are known stable isotopes; (6) all known final stable isotopes of atomic number less than 30 are the most abundant of the natural isotopes; (7) among the final stable isotopes are found 6 of elements which compose over 90 percent of the earth's crust; and (8) five of these six are activated by capture and emission of a proton, the final stable isotope thereby being identical with the parent isotope, whereas the other (oxygen 16) has not been found to be activated.

59. Propagation of Elastic Waves in Lake Ice. A. P. CRARY, MAURICE EWING AND E. B. DOUGLAS, *Lehigh University.*—Elastic waves were produced in ice on a frozen lake by the explosion of blasting caps and were recorded by electric seismographs. Three components of motion were recorded at distances of 400 to 2000 ft. The magnification of the instruments was determined and the amplitudes and phase relations of the various components of motion were obtained. Longitudinal, transverse and flexural waves were observed and for each type of wave the motion was maximum in its proper plane.

60. Dispersion in Flexural Waves in Lake Ice. MAURICE EWING, A. P. CRARY AND E. B. DOUGLAS, *Lehigh University.*—In an experiment similar to the one described in the above abstract, the vertical component of motion was measured by three seismographs placed at different points along the path of a train of flexural waves. By this procedure it was possible to follow individual crests over considerable distances and to determine group and phase velocities.

61. The Vacuum Centrifuge. E. G. PICKELS, *University of Virginia. (Introduced by J. W. Beams.)*—Recent developments have greatly improved the efficiency and operating characteristics of the ultracentrifuge reported previously (Pickels and Beams, Phys. Rev. **47**, 336 (1935)). The starting and stopping of the vacuum rotor has been simplified by the introduction of a new flat bearing type of turbine which is separately supported and driven by two sets of air jets. A larger wire is used for transmitting power from the turbine to the rotor. Other improvements deal with bearings, lubrication, temperature control and arrangements for photographic work. An air pressure of only 15 to 20 lbs./in.^{2} is needed for obtaining ordinarily used forces of several hundred thousand gravity with $3\frac{1}{2}$ inch rotors. With a pressure of 50 lbs./in.^{2}, a simple duralumin rotor of this size, especially shaped for high speeds, was exploded at 156,000 revolutions per minute with the attendant centrifugal force of over 1,200,000 gravity. Photographs of molecular sedimentations in an observational centrifuge demonstrate the possibilities of the apparatus in molecular weight determinations. Good separations of molecules have also been obtained with a newly developed continuous-feed type of centrifuge of 33 cc capacity. Keeping the vacuum chamber at the vapor pressure of the solution being treated reduces frictional effects and prevents evaporation.

62. The Measurement of Young's Modulus in Rocks by a New Dynamical Method. JOHN IDE, *Cruft Laboratory, Harvard University. (Introduced by G. W. Pierce.)*—This paper describes a method for determination of Young's modulus for any rigid substance obtainable in rod form. The modulus is computed from the natural longitudinal frequency of the specimen, which is set into vibration by simple electrostatic traction. The test bar forms one plate of an electrical condenser. The other plate is fixed, and separated from the bar by a thin sheet of dielectric. A nonconducting specimen may be driven by cementing tin foil to one end. An alternating voltage of variable frequency combined with a polarizing voltage is connected to the condenser thus formed. The rod vibrates when its characteristic frequencies resonate with the driving voltage. This vibration can be detected by ear, or by amplifying the piezoelectric voltage set up across a small Rochelle salt crystal in contact with the rod. Dynamic values of E were obtained for the series of rock specimens measured statically by Zisman. Agreement is good for compact rocks like diabase, while dynamic E is higher than static E for granite, gneiss and other rocks. The dynamic values for Quincy granite and Sudbury norite agree with those obtained by Leet from explosion wave velocities in the same rocks.

63. Surface Pressures and Potentials of Monomolecular Films of Long Molecules: Hydroxy-Decanoic Acid Polymers. WILLIAM D. HARKINS, EVERETT F. CARMAN AND HERMAN E. RIES, JR., *University of Chicago.*—Remarkable relations are exhibited by films of linear polymers of the formula $HO[(CH_2)_9COO]_xH$ with molecular weights to 25,200 as prepared by Drs. Carothers and van Natta. The molecules lie flat on the surface and exhibit the following characteristics for the condensed films at 3 dynes per cm of pressure: (1) Thickness 4.5A; (2) distance between centers of adjacent chains approximately the same as the thickness of the film; (3) apparent vertical cross section of the molecules 20 sq. A, or about the same as the horizontal cross section of molecules oriented vertically; (4) compressibility very large, independent of molecular weight and of value 0.045 per dyne; (5) the surface potential increases 13 percent less rapidly with pressure than the density of the film; (6) at zero pressure the molecular area is very large (10,400 sq. A) for the molecules of molecular weight 25,200.

64. The Heat-Flow Calorimetric Method. W. P. WHITE, *Geophysical Laboratory, Carnegie Institution.*—This method belongs to the group where the heat is known and the temperature change produced by it is to be found. Since 1900 the heat has been more often produced electrically, but the older heat-flow method, where the heat passes directly from the warmer surrounding walls to the calorimeter, still has advantages. In the modern form of this method these walls are usually heated electrically, giving continuous runs over wide temperature ranges very simply. The whole procedure is really elementary, but the precision has sometimes been so low that an investigation seemed worth while. The chief difficulty has usually been

lack of uniformity in the surrounding temperature, which falsifies the thermal head measurement on which knowing the heat depends. A precision of at least 0.02° in this measurement will usually be necessary for 1 per mille final precision. Stirred baths can give this; well-distributed heaters alone usually not. Convection greatly complicates the heat determination; it can be practically eliminated by making the air gap small, say 5 mm. To obtain the precision made possible by the above features the heat-conducting partitions inside the calorimeter and the thermels must be more effective than they have sometimes needed to be.

65. The Coefficient of Linear Expansion for Stretched Rubber Bands at Room Temperatures. MILTON L. BRAUN, *Catawba College.*—A number of vulcanized rubber bands of the same composition were suspended so as to support respective loads of 350, 550, 750 and 1000 g. The lengths of the bands at plus and minus room temperature deviations from 27.0°C were observed from day to day. The coefficient of expansion, $\alpha=(\Delta l/\Delta t)/l_{27}$, was found to vary with time and with load. It has been shown that the length of a loaded band varies continuously with time,[1] but this phenomenon is insufficient to account for the change with time in the coefficient. That is to say, $\Delta l/\Delta t$, as well as l_{27}, varies with time but not in the same manner. For the first three loads $|\alpha|$ decreased both with time and with load, the range being -0.00244 at the first time-region of about 20 days (with an elongation of 207 percent), to -0.000435 at 6 months (when the elongation was 589 percent). For the kilogram load, however, α was found to increase instead of decrease with time, its numerical value being more than 10 percent greater in the neighborhood of 3 months than at 3 weeks, and more than 30 percent greater at 6 months, the increase in the coefficient being about ten times that of the corresponding increase in elongation. The coefficient seems to be independent of the sign of Δt.

[1] M. L. Braun, *The Extensibility of a Rubber Band as a Function of Time*, paper presented at the sixth annual meeting of the Society of Rheology, Philadelphia, October 19, 1934.

66. Scattering of Alkali Atoms in Various Gases. S. ROSIN, *Columbia University.*—The investigation previously reported of the scattering of narrow atomic beams of sodium and potassium in the several gases employed, has been extended to include the remaining alkalis. With geometrical conditions such that changes in the direction of motion of the beam atoms of more than one minute of arc were counted as collisions, the mean free paths of the different alkali atoms in the various gases were determined. Table I gives the effective collision radii thus calculated.

TABLE I. *Collision radii in Angstroms.*

Gas	Lithium	Sodium	Potassium	Rubidium	Caesium
H_2	6.21	7.01	7.47	7.38	7.54
D_2	6.32	7.62	8.54	8.24	8.34
He	5.82	6.44	7.25	6.96	7.18
Ne	6.18	8.24	9.10	9.23	9.56
A	9.83	11.3	13.6	13.5	13.45

Interesting results of the extended investigations include the disappearance of the difference in collision radius of hydrogen and deuterium when lithium is employed as the parent beam, and the constancy within experimental error (5 percent) of the collision radii of the heavier alkalis with each of the gases employed. Another result of the experiment is that the beam after passing through the scattering gas has the same form as the original unscattered beam. This implies that the total collision cross section is finite, in agreement with quantum theory, but in sharp disagreement with classical prediction.

67. Deep Terms in Ions of the Isoelectronic Sequence Cl I to Mn IX. S. G. WEISSBERG AND P. GERALD KRUGER, *University of Illinois.*—The $3p^5\ ^2P^0_{3/2\ 1/2}$ deepest terms of this sequence combined with $3p^44s\ ^2P_{3/2\ 1/2}$ to give a very strong characteristic P^0P multiplet. With the aid of constant second difference graphs, of the displacement of radiated frequencies (Kruger and Shoupp, Phys. Rev. **46**, 124 (1934)), it has been possible to identify the P^0P multiplet of Ca IV from E. Ekefors (Inaugural Dissertation, Verlagsbuchhandlung Julius Springer in Berlin, 1931) and of Ti VI and Mn IX from data on our spectrograms, which were taken with a twenty-one foot grazing incidence vacuum spectrograph. Table I gives the value of the deepest term as computed from the $(v/R)^{\frac{1}{2}}$ law and the corresponding value of the ionization potential in volts. The values in parentheses are interpolated. The radiated frequencies of the lines identified as the P^0P multiplets are given in Table II.

TABLE I. *Values of deep terms and ionization potentials.*

Ion	$3p^5\ ^2P_{3/2}$ cm^{-1}	Ion. potential (volts)	First diff. (volts)	Second diff. (volts)
Cl I	104,991	12.952		
			14.76	
Ar II	224,721	27.722		4.1
			18.8	
K III	377,000	46.5		4.4
			23.2	
Ca IV	565,000	69.7		4.1
			27.3	
Sc V	(786,400)	97.0		4.0
			31.3	
Ti VI	1,040,000	128.3		3.9
			35.2	
V VII	(1,325,000)	163.5		4.0
			38.0	
Cr VIII	(1,640,000)	202.		4.0
			42.0	
Mn IX	1,983,000	245.		

TABLE II. *Radiated frequencies of the P^0P multiplet.*

	$^2P^0_{1/2}-{}^2P_{3/2}$	$^2P^0_{1/2}-{}^2P_{1/2}$	$^2P^0_{3/2}-{}^2P_{3/2}$	$^2P^0_{3/2}-{}^2P_{1/2}$
Ca IV	(4?) 295,135	(4) 297,129	(5) 298,201	(0) 300,175
Ti VI	(2) 496,758	(8) 500,608	(30) 502,566	(2) 506,436
Mn IX	(881,700)	(4) 889,585	(7) 892,498	(900,383)

68. Hyperfine Structure of Y II Lines. C. N. CHALLACOMBE AND P. GERALD KRUGER, *University of Illinois.*—The yttrium spectrum has been excited in a water-cooled hollow cathode lamp of the vertical type by using argon as the exciting gas. The lines of the $4d^2\ ^3F_{432}-4d5p\ ^3D_{321}$ multiplet have been examined for hyperfine structure with a Fabry-Perot etalon inserted between the collimating lens and the prisms of a three-prism Steinheil spectrograph. A separation of 3, 4, 5, 8, 10, 12, 20 and 40 mm has been used

between the etalon plates. From the observed components it is possible to deduce the hyperfine term splittings as shown in Table I. The splitting of the terms $^3D_1$ and $^3F_2$

TABLE I. *Hyperfine term splitting in terms of Y II.*

Term	Splitting (cm^{-1})	Term	Splitting (cm^{-1})
$^3D_3$	+1.15	$^3F_4$	+1.18
$^3D_2$	+0.23	$^3F_3$	+0.38
$^3D_1$	(−0.67)?	$^3F_2$	(−1.05)?

are only estimates since the weakest hfs component for this transition has not been found. The data do indicate, however, that the hfs terms are inverted for $^3D_1$ and $^3F_2$. A value of the nuclear moment $i=\frac{1}{2}h/2\pi$ is in agreement with these data.

69. Wavelength Measurements in the Spectra of the Neodymium Arc and the Standard Pfund Iron Arc. GEORGE R. HARRISON AND WILLIAM W. BARTLETT, *Massachusetts Institute of Technology.*—Over 100 spectrograms have been taken on 2×20-inch plates in the region 6000–2200A, at dispersions averaging 0.4A/mm and resolution of about 200,000. Highly purified neodymium oxide from two sources (Hilger Rolla and Hilger Prandtl) was burned in silver and in graphite arcs, and a standard Pfund iron arc spectrum was superposed. The plates are being measured with hand setting but automatic wavelength reduction and recording on the Institute's automatic plate measuring engine (Harrison, Phys. Rev. **45**, 760 (1934)). The International Secondary Iron Standards are being used, and a redetermination is being made of the tertiary iron standards, particularly of the weaker lines, in terms of these. The internal consistency of the neodymium wavelengths, and the fits found in a tentative quadratic array of Nd II terms, indicate that most of the lines are being measured correctly to 0.001A. It is expected that the entire set of plates will be measured several times with automatic setting.

70. Atomic Absorption Spectra of the Rare Earths. FRED W. PAUL, *Massachusetts Institute of Technology.* (*Introduced by George R. Harrison.*)—A modified King electric furnace, charged with various rare earth oxides, has been used to observe the absorption spectra of cerium, neodymium, samarium, europium, dysprosium, holmium, thulium, and ytterbium in the region 9000 to 2900A, with a concave grating giving dispersion of 2.5A/mm. 550 lines have been observed in the absorption spectrum of Ce between 3500 and 8900A, and in Sm 880 lines have been observed between 2900 and 8300A. More than 300 lines have been identified as arising from Nd, and as many from Tm. Eu and Yb give rise to very simple absorption spectra, and impurities of either in other substances are very evident in absorption. Only the strongest lines of Dy and Ho have been observed in absorption. In general the absorption spectra confirm the line types as given by King's temperature classification in that, of those lines which are absorbed, the Class I lines are absorbed much more strongly than Class II lines, which are in turn stronger than Class III lines; and give additional data in that only those lines of each class which involve the lowest levels appear in absorption. The data obtained are being used in the laboratory program of analysis of rare earth spectra.

71. The Spectra of Phosphorus, P II, P III, P IV. HOWARD A. ROBINSON, *Massachusetts Institute of Technology.*—Spectrograms have been taken using a Geissler tube discharge in phosphorus vapor from 500A to 7000A. The present analyses summarized in Bacher and Goudsmit are substantially confirmed. A fairly complete set of singlets has been found in P II together with intercombinations and a few high series terms in the triplet system. Most of the remaining doublets predicted by the Hund theory have been located in P III together with possible intercombinations. Some changes are suggested in the higher series terms. A few new levels have been located in P IV. In this spectrum the intercombinations are fairly numerous and show that Bowen's estimate for the low $3s3p\,^3P$ term is too high by 326 cm^{-1}.

72. An Extension of the Thallium II Spectrum. CECIL ELLIS AND RALPH A. SAWYER, *University of Michigan.*—The spectrum of Tl from the hollow cathode discharge tube has been photographed in the region from 600A to 9200A. Knowledge of the first spark spectrum has been extended by the classification of 150 new lines of from moderate to strong intensities, which locate 26 new levels and also fill in missing transitions in the existing system. The new terms include members up to $n=11$ of the s, p and d series, the first two members of the g series, as well as 5 new odd levels which probably belong to the $5d^96s^26p$ configuration. Large hyperfine structure was observed in many of the new lines which, while not accurately investigated, appears to agree with known hfs separations in this spectrum.

73. The Spectra of Argon and Krypton in the Extreme Ultraviolet. J. C. BOYCE, *Massachusetts Institute of Technology.*—Continuing the investigation of rare gas spectra with the Carnegie Institution of Washington vacuum spectrograph located in this laboratory, considerable extensions have been made in the extreme ultraviolet spectra of argon and of krypton. Revisions have been made in the limit assignments of the terms in de Bruin's analysis of A II. A number of triplet terms have been added to those already known for A III and the low odd term and most of the intermediate even terms of the doublet system of A IV have been discovered. Additional confirmation is thus obtained for the identification of the nebular lines λ4711.4 and λ4740.2 as due to the nebular type of forbidden transition in A IV. Two multiplets of A V have been found. In krypton 31 additional extreme ultraviolet lines from Kr II have been identified bringing to 82 the total number of known lines in this region assigned to this spectrum. 138 lines of Kr III have been identified in collaboration with C. J. Humphreys' analysis of the longer wavelength range of the third spectrum of this gas.

74. The Third Spectrum of Krypton. C. J. HUMPHREYS, *Massachusetts Institute of Technology.*—The spectrum char-

acteristic of the Kr^{++} ion has been selected from the various krypton spectra excited in a Geissler tube discharge. The distinction between lines of Kr III or higher spark spectra and those of Kr II is based on the partial or complete suppression of the former by inductance in the discharge circuit. Wavelength measurements, based mainly upon observations with the Rowland grating at the Bureau of Standards, extend from λ2100 to λ7400. A total of 369 lines has been classified arising from 88 levels of Kr III. The low states of Kr^{++} are ^3P, ^1D and ^1S, due to the $4s^24p^4$ configuration. The higher excited states are built upon the ^4S, ^2D and ^2P states of Kr^{+++} by the addition of *ns*, *np* or *nd* to the normal $4s^24p^3$ configuration. All but 8 of the 76 levels comprising the first excited states have been found. The connection between these and the low states has been established by use of J. C. Boyce's extreme ultraviolet data. Numerous inter-limit combinations have permitted precise evaluation of relative term values. Calculations based on the $4p^3(^4S)ns^3S^0$, and $4p^3(^4S)nd^3D^0$ and $^5D^0$, series have led to an estimated value of 298,020 cm^{-1} for the lowest $4p^4(^4S)^3P_2$ level, corresponding to an ionization potential of 36.8 volts.

75. Production and Absorption of Cosmic-Ray Showers. R. H. WOODWARD AND J. C. STREET, *Harvard University.*—A group of Geiger-Müller counters has been arranged to investigate the production of showers. A slight modification of this arrangement has been used to measure directly the absorption of the shower particles. The shower production curve for lead obtained with this arrangement is in agreement with similar data reported by numerous observers but the directly observed absorption of the shower particles is quite different from the usual assumption that these particles have a penetrating power of about 1.5 cm of lead (thickness for maximum observed number of showers). The shower particles are absorbed approximately exponentially and fall to one-third value in three mm of lead. Using this absorption coefficient for shower particles and the observed rate of shower production, we have corrected for self-absorption of shower particles in the scattering material to obtain the true (or total) rate of shower production. The derivative of this rate of production with respect to the thickness is presumably proportional to the intensity of the shower producing radiation. It is found that the intensity of the producing radiation rises to a peak at one cm of lead two or three times its initial value and then decreases approximately exponentially attaining the initial value at about seven cm.

76. On the Longitude Effect of Cosmic Radiation. M. S. VALLARTA, *Massachusetts Institute of Technology.*—If the equivalent magnetic dipole describing the earth's magnetic field at large distances is placed at the magnetic center of the earth as calculated by Schmidt, instead of at the center of the geoid, then the theory of the latitude and azimuthal effects developed by Lemaitre and Vallarta also accounts for the longitude effect found by Clay, Van Alphen and Hooft and, independently, by Millikan and Neher. Further, if the distribution function of magnetically deflectable particles capable of reaching the tropical belt is substantially an exponentially decreasing function of their energy, the theory agrees quantitatively with experiment; except for the measurements made by Millikan and Neher on the steamer lane from Honolulu to Sydney-Melbourne.

77. The Corpuscular Theory of the Cosmic Rays. W. F. G. SWANN, *Bartol Research Foundation.*—An exponential law of absorption results from the assumption that the measured intensity is that of secondaries which perpetuate the directions of the primaries and are produced all along the paths thereof in amounts proportional to the primary energies. It is maintained that this approximation provides the component of the radiation which, by analysis of the absorption curves, represents the greater part of the measured intensity. The incorporation of principles which cause the range or intensity of production of secondaries, and so the rate of absorption of energy per unit length of primary path, to increase with energy less rapidly than linearly gives a softening of the individual rays with decrease of energy such as is necessary to account for the variation of east-west asymmetry with altitude and latitude. The assumption of a range of energies in the rays entering the atmosphere, necessary for the latitude and directional effects, then provides for the story of hardening in passage through the atmosphere. The assumption that the production of the secondaries in lead increases with primary energy more rapidly than linearly serves, in its development, to correlate a variety of phenomena concerning the effect of altitude, latitude, and direction of primary rays, in the production of showers.

78. A Study of Oxygen Isotopes. WALKER BLEAKNEY AND J. A. HIPPLE, JR., *Princeton University.*—During the last year over a hundred samples of oxygen have been analyzed with the mass spectrograph. All the values for the ratio $O^{16} : O^{18}$ cluster around the number 500. These samples came from a variety of sources prepared in a number of different ways. A few came from meteorites. Samples of commercial oxygen were found to vary in isotopic concentration from tank to tank. This suggests that refinements of some of our atomic weight determinations would have little meaning without an isotopic analysis at the same time. The fractionation of the oxygen isotopes produced by the electrolysis of water was measured and found to be about 1.01. This result is in good agreement with the recent work of Johnson but disagrees with the earlier work of Washburn and the Bureau of Standards group.

79. The Production of Helium of Mass Three? H. D. SMYTH, G. P. HARNWELL, W. BLEAKNEY AND W. W. LOZIER, *Princeton University.*—In letters to the *Physical Review* last summer we reported evidence for the production of helium of mass three by impact of canal rays of deuterium in deuterium. Mass spectrograph analyses of the treated samples showed ions of mass three appearing at an ionization potential approximately that of helium. Further evidence was the detection of helium lines in the spectrum of a sample of the treated gas. Doubt has now

been cast on interpretation of the mass spectrograph evidence by experiments on the rate of diffusion of the gas producing the mass three peak. It has been found to diffuse more slowly than ordinary helium. Another explanation of the mass three ion is to assume it a secondary product of ionization of heavy methane (CH_2D_2 or CH_3D) present as a small impurity. This had been considered at the time of the original experiments but discarded as of negligible probability. A study of ionization processes in methane made this winter in our laboratory shows the explanation hardly possible. The spectroscopic results remain entirely unexplained. Consequently we find ourselves in the position of having apparently good evidence both for and against the production of helium three in these experiments. Since we are progressing out of the dilemma very slowly we feel we should report the present state of the problem unsatisfactory though it be.

80. The Hyperfine Structure and Nuclear Magnetic Moment of Caesium. R. K. STRANATHAN AND L. P. GRANATH, *New York University.*—The hyperfine structure of the lines λλ8761, 4593, 4555, 3889 and 3877 in the arc spectrum of caesium has been investigated using a Fabry-Perot etalon. The $g(I)$ values were calculated from Goudsmit's formulas, using Z_i values for the P states as obtained from fine structure data. (Table I.) The interval for the

TABLE I.

State	Interval factor	Percent error	Z_i	$g(I)$
$6^2S_{\frac{1}{2}}$	0.0767	0.2	55	0.76
$6^2P_{\frac{1}{2}}$	0.00925	3.	49	0.68
$7^2P_{\frac{1}{2}}$	0.00331	4.	49	0.75
$8^2P_{\frac{1}{2}}$	0.0017	20.	48	0.86

$6^2P_{\frac{1}{2}}$ level was measured directly, while the separations for the unresolved $7^2P_{\frac{1}{2}}$ and $8^2P_{\frac{1}{2}}$ states were obtained from the difference between the doublet separations of the two lines involved in each case. The $g(I)$ values calculated from the P states agree within the limits of experimental error. The experimental error in the interval factor for the $6^2S_{\frac{1}{2}}$ state is extremely small; however it is unlikely that the theoretical formula is as accurate for this state. The $g(I)$ value appears to be 0.72.

81. Nuclear Spin and Magnetic Moment of Li^7. M. FOX, S. MILLMAN AND I. I. RABI, *Columbia University.*—The nuclear spin and hfs separation, $\Delta\nu$, of the normal $^2S_{\frac{1}{2}}$ state of Li^7 has been determined by the method of neutral atomic beams previously applied to determine similar properties of K^{39}. The value obtained for the spin is 3/2, in units of $h/2\pi$, in agreement with the results from hyperfine structure and alternating intensities in band spectra, but not with the results of Ladenburg and Levy. The value of $\Delta\nu$ was found to be 0.0262 cm^{-1}. Using the modified Goudsmit formula we obtain a value of 3.14 nuclear magnetons for the magnetic moment of the Li^7 nucleus. The value for the nuclear magnetic moment obtained by Granath from work on hyperfine structure lines of singly ionized lithium, using the theory of Breit and Doerman, is 3.29. Although the difference between the two values is somewhat greater than the experimental error, it is strikingly good in view of the theoretical foundation of the modified Goudsmit formula. The question whether this difference between the two values of the nuclear magnetic moment is real must await further theoretical consideration.

82. On the Nuclear Spin and Magnetic Moment of K^{41}. S. MILLMAN, M. FOX AND I. I. RABI, *Columbia University.*—In the course of the work on K^{39} previously reported (Phys. Rev. **46**, 320 (1934)) sufficient resolution was obtained to resolve a peak due to K^{41} by the method of "zero moments" (Phys. Rev. **46**, 707 (1934); **47**, 334 (1935)). The existence of this peak proves that the nuclear spin of K^{41} is greater than 1/2, in units of $h/2\pi$. From the value of the field at which this peak occurs we can place the ratio of the nuclear magnetic moment of K^{41} to that of K^{39} between the limits of 0.42 and 0.88 depending on the spin of K^{41}.

83. The Production of X-Radiation by Very Fast Electrons. EDWIN MCMILLAN, *University of California.*—The theoretical calculation by Bethe and Heitler[1] of the rate of production of radiation by fast electrons indicates that this becomes a very probable process at energies of several million volts. The availability of strong sources of artificially radioactive substances has made it possible to test the prediction experimentally. Active phosphorus (P^{32}) gives beta-particles with a maximum energy of 1.8 mv, and no gamma-rays, and has a very long half-life; it is therefore admirably suited for this experiment. The radiation emitted when these beta-particles are stopped by paraffin, aluminum and lead was observed by an electroscope. The intensity of the radiation from lead corresponds to about one quantum per 25 beta-particles; it is absorbed to about 1/4 in 1 mm of lead and to 1/8 in 2 mm of lead. The intensity of the radiation when the beta-particles are stopped in aluminum and paraffin is respectively 1/6 and 1/12 as great as in lead, being thus proportional to the atomic number as required by the theory. Chlorine activated by deuteron bombardment gives an active body with very energetic (4.5 mv) beta-particles, but these are accompanied by gamma-rays (about 1/4 quantum per disintegration) increasing the difficulty of studying the secondary radiations. It is possible to show, however, that they are 2 or 3 times as intense as those produced by the phosphorus beta-particles, and considerably harder.

[1] Bethe and Heitler, Proc. Roy. Soc. **A146**, 83 (1934).

84. Oscillographic Study of Overvolted Discharges. J. W. FLOWERS, *University of Virginia.* (*Introduced by J. W. Beams.*)—The initiation of discharges in effectively ion-free gases (Phys. Rev. **46**, 338 (1934)) has been studied by means of an oscillograph using a time resolving power of about 6×10^{-9} sec. per mm on the film. The potential is applied in a few hundredths of a microsecond to a sphere gap (also point and plane) in an inclosure containing dry, dust-free air. Under these conditions potentials of more

than 10 times static breakdown values can be applied. For potentials much exceeding this the breakdown occurs immediately on reaching a value where field emission might be expected. For values slightly less than this time lags as long as a half microsecond are observed. When the discharge occurs at these high field strengths the rate of fall of potential in the initial stages is very much faster than for ordinary breakdown. The breakdown potential for spherical electrodes has been traced from atmospheric pressure down to the vacuum spark stage and found to be relatively independent of the pressure until the electron mean free path has reached a value comparable to the electrode spacing. It is believed that these discharges are initiated by field emission.

85. Electrical Conductance of Short Cold-Metal Gaps in Air. ROBERT E. FEARON, *University of Pittsburgh.* (*Introduced by E. Hutchisson.*)—The conductance of sphere-plane gaps, or their equivalent, for potentials between 0.0001 volt and two volts was determined in air at atmospheric pressure for gap widths between 5000A and 100A. Radii of curvature for the spherical electrodes were 7 meters, 14 cm and 25 microns. Appreciable conduction for gaps of the type used appears to be caused by a layer of fine dust between the surfaces and by imperfections in them. Results obtained with intermediate radius of curvature of the spherical electrode were more erratic than those obtained with a spherical electrode of very large radius of curvature. Since the area of close approach is larger in the latter case, this result is to be expected if the conductance is caused by the total effect of a large number of dust particles. The increasing abruptness of the change of conduction with respect to gap width for curves representing successive experiments indicates the eventual formation of conducting prominences on the surfaces during the course of the experiments. This occurrence is more marked for electrodes of smaller radius of curvature.

86. A Cloud Chamber Study of the Initiation of Ionization in Spark Discharge. CHARLES D. BRADLEY, *University of Virginia.*—Using the method described recently for photographing the initial ionization in spark discharge (Bradley and Snoddy, Phys. Rev. **47**, 541 (1935)), a study of the initiation of ionization between a small sphere and a plane in a cloud chamber has been made with the electrodes irradiated with the ultraviolet radiation from an iron arc. A short potential impulse of less than 10^{-7} sec. duration is applied to the electrodes at the end of the expansion of the chamber and the resulting ionization photographed. Discharges requiring a maximum field intensity of the order of 10^6 volts/cm to start during this impulse, without irradiation, are started by maximum fields of the order of 5×10^4 volts/cm with the electrodes irradiated. This starting potential is not markedly affected by whether the small electrode is the anode or the cathode during the impulse. However, photographs of the ion distribution show that the propagation of ionization is faster when the small electrode is the anode. This propagation may therefore determine the real time lag of discharges in nonuniform fields.

87. Products of Ionization in Methane. J. A. HIPPLE, JR. AND WALKER BLEAKNEY, *Princeton University.*—An investigation has been made of the ionization products in methane by the usual mass-spectrographic method. The following ions have been observed: CH_4^+, CH_3^+, CH_2^+, CH^+, C^+, H_2^+ and H^+. Pressure, electron current and pumping speed variations show that all of these are primary products with the exception of H_2^+ which was too small to study. The H_2^+ is approximately 1/10,000 the size of the CH_4^+ peak and is possibly an impurity. The ionization probability curves that have been obtained are of the usual shape. The percentage of the total ionization due to each ion is independent of the pressure over a wide range and independent of the electron velocity from 30 to 100 volts. Using argon for calibration appearance potentials for CH_4^+, CH_3^+, CH_2^+, CH^+, C^+, H^+, have been observed at 13.7, 14.7, 15.7, 23, 27 and 31 volts, respectively. The use of Ne, CO and H_2 for calibration yields values in substantial agreement with the above. No negative or doubly-charged ions have so far been observed. A preliminary analysis of CD_4 and CHD_3 reveals characteristics similar to those outlined above for CH_4.

88. Ionization of Neon and Argon by Singly Charged Magnesium Ions. J. C. MOUZON AND NEWELL H. SMITH, *Duke University.*—The efficiency of ionization (the number of electrons ejected per initial positive ion per cm path per mm pressure) by singly charged magnesium ions is compared with that of singly charged sodium ions to obtain further information on the parts played by mass and electron configuration in the ionization process. The efficiency of the former is about 60 percent of that of the latter in both gases. Data on the mean free path of magnesium and sodium ions in the two gases must be had before a quantitative comparison of the results can be made. If one assumes the mean free path of magnesium ions greater than that of sodium ions, the results indicate that the chance of ionization on a single impact may be approximately the same for both ions.

89. New Measurements on the Lifetimes of Excited States in Neon. EUGENE W. PIKE, *Scott Paper Co., Chester, Pa.*—Penning has shown that illumination of a Townsend discharge in neon with light from a positive column in neon reduces the concentration of excited atoms in the former discharge. From his data, the quantitative relation of the concentration to the illumination intensity is derived directly. This relation also can be deduced from existing data on line contours, line intensities, etc., and a comparison yields these values for the mean lifetime of excited atoms in pure neon; $s_3(^3P_2)$ metastable state, 1/(500×pressure in mm Hg); mean of s_2 and s_4 resonance states, 1/(15,000×pressure). Comparison values by absorption methods for the metastable state are: 1/(1100 ×pressure) and 1/(125×pressure). Weizel has suggested that inelastic collisions between two atoms are essentially transitions between electronic levels of the quasi-molecule formed of the two impacting atoms, and that the usual quantum rules apply. On this basis, metastable neon atoms can return to the normal state only by direct

radiative transitions during collision. The "coupling broadened" resonance lines of Langmuir and Found also find theoretical backing.

90. The Diffraction of Electrons by Thin Films of Iron Oxides and Hydrates. NEWBERN SMITH, *University of Pennsylvania.* (*Introduced by Raymond Morgan.*)—Diffraction patterns have been obtained by the transmission of electrons through thin films of iron oxide and of ferric oxide monohydrate. The films removed electrolytically from iron heated in air had the crystal structure common to both ferrosic oxide (Fe_3O_4) and ferromagnetic ferric oxide (γ-Fe_2O_3). The evidence indicates that the oxide was probably Fe_3O_4. This disagrees with U. R. Evans, who believed the films to be of nonmagnetic ferric oxide (α-Fe_2O_3). The crystals in the films were at least 200A on a side, and showed no preferred orientation. The films of ferric oxide hydrate were prepared by the action of ammonia on the surfaces of solutions of iron salts. The patterns of the γ-hydrate (γ-FeOOH) films showed the presence of some oxide, and the diffuseness of the rings indicated peculiarities of crystal structure. The dehydration of these films gave films of γ-Fe_2O_3, with a lattice constant somewhat larger than that of the γ-Fe_2O_3 obtained by the oxidation of the Fe_3O_4 films, and with crystals of colloidal dimensions ($\sim$20A). On heating, these crystals grew to over 200A before the γ-Fe_2O_3 changed into the rhombohedral α-Fe_2O_3. The α-hydrate films were normal in structure, and gave α-Fe_2O_3 on dehydration.

91. The Spectra of Helium by High Frequency Excitation. MAX PETERSEN AND HOWARD CARL, *Lehigh University.*—The spectra of helium, atomic and molecular, have been studied under a variety of conditions of pressure, purity and electrical excitation to ascertain whether the enhancement of certain singlet lines, notably λ5015A, is accompanied by any similar behavior of the singlet molecular spectrum. The helium was excited in a quartz tube 5 cm in diameter, 75 cm long. It was continuously circulated for purification through a chabazite trap and a misch-metal arc chamber. Excitation, by various electrical power sources, was always through external electrodes, usually using the "electrostatic" field. The relative enhancement of λ5015 was found to depend less on the high frequency of the excitation than on other conditions of the discharge, similarly the singlet band spectrum and the continuous. A survey of the variously observed spectra seems to indicate that in the band spectrum of helium there is not such a diversity of excitation functions as Hanle found in the atomic terms.

92. Extension of the Rh I-Like Isoelectronic Sequence to the Spectrum of Ag III. W. P. GILBERT, *Cornell University.*—The vacuum spark spectrum of silver has been photographed and measured in the region 500 to 2600A. To assist in the identification of Ag III lines, the spectrum of silver from the hollow cathode discharge in an atmosphere of helium was photographed in the same region. A spark gap placed in series with the Schüler tube served to bring out the Ag III lines in the spectrum of the discharge. With the already reported separation of 4607 cm^{-1} for the ground state, $4d^9\ ^3D_{3\frac{1}{2},\ 4}$, as a basis and by employing the above method of distinguishing the radiations, it has been possible to establish 55 terms originating from the $4d^9$, $4d^85s$, and $4d^85p$ configurations and to classify a total of 257 lines. Approximate term values have been obtained by extrapolation of a Moseley diagram for the elements of this sequence. The value obtained for the lowest state of Ag III with respect to the $4d^9\ ^2F_4$ state of Ag IV is 291,250 cm^{-1}, which corresponds to an ionization potential of 35.9 volts.

93. The Energy Levels of the Rare Gas Configurations. C. L. BARTBERGER, *Allegheny College.* (*Introduced by C. W. Ufford.*)—The energy levels of the $n'p^5np$ configuration of the rare gases were calculated for low values of n from the secular equations involving the electrostatic and spin-orbit interactions. For these low values of n, the electrostatic interaction between the levels having different levels of the ionic doublet as parents becomes appreciable. The radial integral parameters were found from the observed levels by a graphical method. The results obtained in this way agree with observed values on the average about as do the levels found recently by Shortley for the $2p^5\,3p$ configuration of neon. In some cases the absolute magnitudes of the errors are small enough so that it is hoped to obtain reliable values for the transition probabilities.

94. Zeeman Effect in Diatomic Molecular States Having L-Uncoupling. JULIAN K. KNIPP, *Harvard University.*—A theoretical investigation has been made of the behavior of Zeeman levels in molecular states intermediate between Hund's case b' and case d', which are the limiting cases in the passage from a state in which the orbital angular momentum of the electrons is quantized along the axis of figure of the molecule to one in which it is quantized along the axis of rotation of the nuclei. Zeeman patterns for the $3d$ and $4d$ complexes ($L=2$) of the helium molecule have been calculated and curves obtained for the variation of the overall widths with K, the rotational quantum number. For small K the energies are near the case b' values, but as K increases a breaking away occurs which results in their approaching the case d' energies. When the state in the limiting case d' has the electronic angular momentum quantized anti-parallel to the nuclear rotation, a crossing over of the magnetic energy curves takes place with the passage through a state in which the molecule is relatively insensitive to the field. This crossing over occurs between K equal to 4 and 8 for the Δ states of the helium molecule considered (magnetic field 30,000 gauss). For the state correlated to the limiting case of zero component along the axis of rotation, a crossing and recrossing can take place.

95. Orbital Valency According to an Extended Heitler-London Method. GERTRUD NORDHEIM, *Purdue University.* (*Introduced by K. Lark-Horovitz.*)—An extension of the Heitler-London theory of chemical bond is developed so as to take into account not only the ground states but

also the lowest excited states of the composing atoms (their excitation energies included). It can be shown that possible molecular states of the same symmetry-character (arising from different atomic terms) may interact strongly. In this way the concept of orbital valency and the different behavior of the ground states of diatomic molecules, which are not necessarily those of lowest multiplicity (triplet terms of C_2 and O_2), can be satisfactorily described. The directional properties of valency in polyatomic molecules (f.i. tetrahedral structure of CH_4, the rigidity of the double bond) can also be explained by this combination method considering the degeneration of the atomic P and D levels.

96. The Normal Helium Atom. J. H. BARTLETT, JR., J. J. GIBBONS, JR. AND C. G. DUNN, *University of Illinois.*—It is proposed to test the goodness of approximate wave functions by means of a least-squares criterion. A root-mean-square energy deviation is defined, and calculated to be 3.5 volts for the six-term function of Hylleraas (Zeits. f. Physik **54**, 347 (1929)). It can be proved that there is no series in ascending powers of the variables r_1, r_2, and r_{12} which is a formal solution of the Schrödinger equation. It is possible, however, to find formal solutions for the region $r_1<r_2$ (and similarly for $r_1>r_2$) which are series in descending powers of r_2 and in ascending powers of $z=\cos\theta$, where θ is the angle between r_1 and r_2.

97. Intramolecular Forces Between Bound Atoms. WM. ALTAR, *The Pennsylvania State College.* (*Introduced by William R. Ham.*)—The analytic method of Lennard-Jones and Pike (Trans. Faraday Soc. **30**, 830 (1934)) is extended and refined. Particularly, a study is made of the forces acting between the two CH_2Cl groups in 1,2-dichloroethane, and between the CHCl groups in dichloroethylene. The presence of repulsive forces between bound Cl atoms at distances as large as 4.4A is established, which is at variance with current views though well in line with theoretically derived curves for the potential of interatomic interaction. It is shown how this result can be coordinated with seemingly conflicting evidence obtained from the thermal equilibrium ratio r of the two isomers of dichloroethylene (63 percent cis at 300°C). This is done by discussing the temperature variation of r which one must expect when considering the differences between the entropies, rotational and vibrational, of the two isomeric forms; the zero-point energy of each form, particularly, constitutes an important contribution to the respective heat of formation, and is apparently considerably larger for the transform of dichloroethylene.

98. Gravitational and Electromagnetic Mass in the Born-Infeld Electrodynamics. B. HOFFMANN, *University of Rochester.*—In the general spherically symmetric field of the Born-Infeld theory, the gravitational part contains an integration constant m in the form $-2m/r$. This leads to an infinity at $r=0$. If it is postulated that only fields that are nowhere infinite are allowed, the constant m must be taken as zero: It is shown that this makes the gravitational mass of the electron correspond to its electromagnetic mass, and that this implies that the gravitational mass cannot be negative, which is not the case in the usual relativity theory. The alternative Born-Infeld field equations may be considered in the light of the above postulate. It turns out that the $G\neq 0$ field equations permit the existence of isolated magnetic poles, while the $G=0$ field equations, since they would lead to an infinity in the field of such a pole, deny that such a pole can exist.

99. Extra Negative Term in the Incoherent Part of the Diffuse Scattering from Neon-Like Crystals. G. E. M. JAUNCEY AND J. H. DEMING, *Washington University.*—Using the technique developed by Jauncey and Claus (Phys. Rev. **46**, 941 (1934)) we have measured S values for NaF for primary rays whose spectral distribution showed a maximum at $\lambda=0.48$A. The results for various scattering angles were: 17°, 0.94 (0.96, 1.09); 20°, 1.07 (1.04, 1.15); 25°, 1.11 (1.12, 1.20); 30°, 1.12 (1.12, 1.17); 40°, 1.09 (1.10, 1.12); 55°, 1.04 (1.05); 90°, 0.91 (0.93). The quantum-mechanical values including the Waller-Hartree extra negative term are shown as the first number in parenthesis, the second number (where there is such) not including this negative term. The inclusion of the negative term brings better agreement between the theoretical and experimental values. Measurements on the diffuse scattering from MgO are now in progress.

100. The Effect of Target Temperature on the Wavelengths of Soft X-Rays from Metals. PAUL MCCORKLE AND CHARLES B. BAZZONI, *University of Pennsylvania.*—Chalklin reported a small change in the wavelengths of soft x-rays from Ta and W with change of target temperature. We have repeated this work and have extended it to other metals. In order to eliminate some possible sources of error, a camera shutter was designed so that the spectra from hot and cold targets could be photographed on the same plate. No changes were made in cathode, anode, or camera during the entire exposure. The target was heated by electron emission and the temperature was increased from about 200°C to 900°C. A water-cooled target support prevented thermal expansion. Since the two spectra were on the same plate, a shift of 0.2A could have been detected by inspection. No such shift was found for Ta, W, Mo or Pt.

101. Ruled Grating Measurements of X-Ray Wavelengths. J. A. BEARDEN, *Johns Hopkins University.*—A plane grating ruled with 100 lines per mm and 75 mm long has been used in a double crystal ionization spectrometer for measuring the wavelength of the copper $K\alpha_1$ line. The ruled grating was placed between the two "perfect" calcite crystals which were in the (1+1) position. This arrangement places the reflected and diffracted beams in the (1−1) position and the direct $K\alpha_1$ line in the (1+1). Thus the two most important angular measurements were made with very narrow lines. The diffracted α_1 and α_2 lines were 14″ wide at half maximum, and were separated about 45″. The correction for the overlapping of the lines amounted to about 0.5″. Four carefully calibrated microscopes read the precision circle. Since two lines, ten

minutes apart, were read in each microscope, eight angular readings were obtained for each individual setting of the circle. Different parts of the circle were used in order to eliminate any effects due to possible erratic rulings on the circle. The average of all the results gave $\lambda = 1.5406$A which is 0.253 percent greater than the best crystal measurements. The average of the photographic ruled grating measurements of the author gives 0.247 percent when compared to the same crystal values.

102. Comments on the Coster-Kronig Theory of a New Type of Auger Effect. F. R. HIRSH, JR. AND F. K. RICHTMYER, *Cornell University.*—Coster and Kronig's theory (Physica **2**, 13 (1935)) of the origin of certain L series satellites, by a new type of Auger effect, accounts for their presence by an ionization of the $M_{IV, V}$ shell caused by the radiationless transition $L_{III} \rightarrow L_I$. The atom is then doubly ionized, with $M_{IV, V}$ and L_{III} electrons lacking. Satellites result from a subsequent single electron transition. According to this theory, ionization of the $M_{IV, V}$ shell by the radiationless transition $L_{III} \rightarrow L_I$ should cease at $Z = 50$. Experimentally it has been shown that the satellites of $L\alpha_1$, $(L_{III}M_V)$, and the satellites of $L\beta_2$, $(L_{III}N_V)$, extend to $Z = 53$ *and then cease*. One might similarly account for the satellites of $L\beta_1$, $(L_{II}M_{IV})$, by assuming $M_{IV, V}$ ionization to be caused by the radiationless transition $L_{II} \rightarrow L_I$. Coster and Kronig mention that this Auger ionization is possible below $Z = 40$ but is impossible above. Coster has however shown that the $L\beta_1$ satellites exend from $Z = 29$ to $Z = 51$. A study of the intensities of these satellites over their entire range is needed to decide whether the Coster-Kronig theory applies. The Coster-Kronig theory fails to account for the satellites of $L\gamma_1$, $(L_{II}N_{IV})$. It also cannot account for the satellites of $L\gamma_{2, 3}$, $(L_IN_{II, III})$. A radiationless transition is impossible in this case.

103. The Auger Effect for Au (79) and the Origin of Certain *L*-Satellites in X-Ray Spectra. E. RAMBERG AND F. K. RICHTMYER,[1] *Cornell University.*—Calculations of Auger transition probabilities reported at the New York meeting have been extended considerably and make possible a more detailed comparison between predicted and observed natural energy level widths. The Auger effect is found to explain the main features of the apparently anomalous variation of the natural widths with the total and azimuthal quantum numbers of the states considered. Furthermore results are given of roughly quantitative calculations of the positions and relative intensities of the $L\alpha$ and $L\beta_2$ satellites of gold on the basis of the hypothesis for their origin recently advanced by Coster and Kronig.

[1] Grateful acknowledgment is made to the American Philosophical Society of a grant-in-aid of this research. F. K. R.

104. X-Ray Line Widths: Correction for Finite Resolving Power of Crystals. LYMAN G. PARRATT, National Research Fellow, AND LLOYD P. SMITH, *Cornell University.*—A study of the widths of several x-ray lines using 14 different pairs of crystals on a two-crystal spectrometer leads to the following conclusions: (1) The width of the $(1, -1)$ curve is *not* an adequate criterion for the resolving power of the crystals. (2) The uncertainties of the crystal contributions depend upon the magnitude of the width of the parallel position curve as well as upon the ratio of the widths of the curves in the parallel and anti-parallel positions. (3) Etching a given pair of crystals may or may not increase the resolving power. (4) The shapes of the single calcite crystal diffraction patterns vary for a given wavelength as indicated by different $(1, -1)$ curve shapes. (5) The different measured degrees of asymmetry of the Ti $K\alpha_1$ line in various orders of reflection indicate that the single crystal patterns of calcite are asymmetrical as predicted by theory. (6) A correlation exists between percent reflection and effective resolving power of crystals having the same $(1, -1)$ widths. (7) A correction formula for obtaining a true x-ray line width may be applied for crystals of high percent reflections in first and second orders providing the ratio of widths $(n, -n)/(n, +n)$ is not greater than about 0.2 for Mo $K\alpha_1$ or 0.1 for Ti $K\alpha_1$.

105. Ionization of Liquids by X-Rays. LAURISTON S. TAYLOR AND FRED L. MOHLER, *National Bureau of Standards.*—Continuing studies reported last year,[1] measurements have been made on the ionization of carbon bisulphide, ligroin, tetrahydronapthalene and various mixtures of the three. To minimize absorption and scattering corrections the ionization chamber consisted of parallel grids of fine aluminum wires separated by fused quartz disks having a 2-cm hole in the center. The ionization current extrapolated to infinite field was proportional to the grid separations in the range 0.5 to 2.5 mm. Precise determination of effective field strengths was complicated by the presence of space charge or dielectric absorption in the liquid. This charge builds up slowly, not reaching a steady value for many minutes, at least, after application of the field. The magnitude of the difference between the applied and effective field is obtained in two ways—(1) by the difference between the initial ion current at zero time and the final steady state current, and (2) by direct measurement of the residual potential difference between the grids after the applied field is removed. After exposure to strong x-rays, the residual potential amounted to the order of 2700 volts when the applied field had been 60 kv/cm.

[1] F. L. Mohler and L. S. Taylor, Bur. Standards J. Research 13, 659 (1934).

106. A Simple Device for Producing Very Small Unidirectional Currents. G. FAILLA, *Memorial Hospital.*—For the measurement of ionization currents a null method is most desirable. This, however, necessitates the production of a "balancing" current of the same magnitude as the unknown current by such means as will permit its evaluation from simple measurements of related quantities. The device consists of a rotating condenser (simply a small insulated metal cylinder) with an excentric pin which makes contact first with a source of potential and then with the ionization chamber producing the current to be balanced. Other conditions remaining constant, the uni-

directional current thus produced is proportional, respectively, to the applied voltage and to the speed. The device has been used in conjunction with an FP-54 tube with floating grid and no trouble has been encountered from the intermittent contacts even at low speeds (250 r.p.m.). Readings are easily reproducible. This scheme makes possible the construction of simple and reliable integrating dosimeters for x-rays and ultraviolet light. For this purpose the applied voltage is maintained constant (standard cell) and the speed is varied according to the variations in the intensity of radiation. The total number of revolutions of the condenser is proportional to the dose.

107. A Study of the Crystal Structure of Heat-Treated Tungsten Filaments. R. P. BIEN, *Massachusetts Institute of Technology.*—Straight tungsten filaments have been examined after various heat treatments. Microphotographs of the cross sections and longitudinal sections were made showing the crystal sizes, while x-ray and goniometer measurements were made to show crystal orientation and surface facets. Well aged tungsten filaments all showed very large crystals extending across the entire diameter of the filament. Their lengths varied from two or three cm down to about a tenth cm. This result applied to filaments flashed for a short time at 3100°K and higher, or aged some hours at 2600°K without higher temperature treatment. Optical reflections from well aged 10 mil filaments showed distinct facets when viewed with light at normal incidence perpendicular to the axis of the filament. The predominant reflecting surfaces seem to be the (110) and (211) planes of a crystal oriented with a (110) plane normal to the filament axis. The fact that all Richardson plots so far reported on well aged filaments are perfectly straight lines would indicate that either the work functions of these two surfaces in presence of a strong field are identical, or emission from the (110) planes is so much greater than that from the (211) planes that the latter contribution may be neglected over the observed temperature range.

108. Thermionic Emission from Tungsten with Weak Accelerating Fields. W. B. NOTTINGHAM, *Massachusetts Institute of Technology.*—The thermionic emission from a well aged 3 mil tungsten filament of the G.E. 218 type has been studied as a function of the temperature, over the range 1218°K to 1973°K, and the surface field for values between zero and 64,000 volts per cm. For fields greater than 2000 volts per cm, the observed currents when plotted as $\log I$ *vs.* $V^{\frac{1}{2}}/T$ (where V = voltage and T = temperature) are accurately represented by the straight line given by the Schottky mirror image theory. A "zero field" Richardson plot obtained by extrapolating the mirror image lines to zero, yielded an $A = 60$ amp. per cm^2 per degree^2 and $b_0 = 52{,}400°$ in exact agreement with Dushman's values. The true values of emission current at zero field were less than those obtained by extrapolation by 53 percent at 1218°K and 34 percent at 1848°K. Space charge effects definitely distort the results at zero field for temperatures above 1840°K. The surface excess theory of Tonks would suggest that a decrease of 25 to 30 percent should be expected, but this theory cannot account for the above temperature effect. Bien's work on the crystal structure of tungsten shows promise of explaining this if there is a difference in work function of 0.5 to 1.0 volt between the 110 and the 211 facets giving rise to local contact potential fields between facets.

109. Dependence on Applied Field of Thermionic Constants for Thoriated Tungsten. A. ROSE, *Cornell University. (Introduced by L. P. Smith.)*—Data are presented for the variation of slope of Richardson plot with applied field, for stages of activation ranging from a flashed surface to maximum activity. An analysis is made of the variation of slope of Richardson plot in terms of a square array patch theory. The size of patch remains roughly constant at 3×10^{-4} cm during activation. The contact potential between patches increases from 0.8 volt for low activity to 1.4 volts near 0.5 monatomic layer and decreases to 0.4 volt for maximum activity. Analysis of data for a thoriated tungsten surface, bombarded and contaminated with alkali atoms, shows an increase in contact potential difference between patches to 2.4 volts. Insofar as the log of the intercept may be related to the change in slope, they are proportional, the constant of proportionality not changing seriously with state of activation.

110. Sputtering of Thorium and Barium from Tungsten. L. R. KOLLER, *General Electric Company.*—Measurements have been made of the sputtering of thorium from tungsten in neon, argon and mercury at pressures of the order of 1 mm. Thoriated filaments were bombarded with ions of known velocity, and surface conditions were determined by thermionic emission measurements. Values were obtained for the number of ions required to remove an atom of thorium from the surface of cold tungsten, at ion velocities between 25 and 70 volts. For 40 volt ions the values were:

6×10^3 ions per atom for neon
1×10^4 " " " " mercury
2×10^4 " " " " argon.

Measurements were also made of the sputtering of barium from tungsten. Sputtering was observed for ions of as low velocity as 12 volts. At 18 volts in neon the value was 3×10^2 ions per atom. Relative values for sputtering, as a function of voltage, were also determined for an oxide coated cathode. A method is suggested for determining the cathode fall by means of the rate of sputtering.

111. The Velocity Distribution of Electrons in Gas Discharge Problems. PHILIP M. MORSE, W. P. ALLIS AND E. S. LAMAR, *Massachusetts Institute of Technology.*—The method used by Langevin and Lorentz to determine the behavior of electrons colliding with elastic spheres has been extended to take into account the angle distribution and loss of energy of the electrons scattered from actual atoms. The detailed balancing of momentum and energy results in differential equations giving the dependence of the distribution function on the coordinates and on the components of the velocity. These equations have been

solved in two simple cases. One case is that of a homogeneous beam of electrons, of energy ϵ_0, shot into a field-free space, where they lose energy to the gas atoms by elastic collisions. The distribution function depends on s, the distance along the beam measured in mean free paths, and on t, the average number of collisions an electron has had before its energy decreases from ϵ_0 to ϵ. It is found that the distribution function is not Maxwellian, but depends on a solution of an equation in s and t having the form of the heat equation, which can be solved subject to suitable boundary conditions. These solutions have been tested experimentally, and a quantitative check is obtained. The other case considered is that of the behavior of electrons in a uniform electric field, where the distribution function is independent of position. The field is assumed to be small enough so that the number of inelastic collisions is small compared to the number of elastic ones. The distribution is found to be proportional to $\exp(-\epsilon^2/a^2)$, instead of to $\exp(-\epsilon/\epsilon)$, as is the case in the Maxwell distribution, when the electrons are in thermal equilibrium with the gas atoms. The average energy of the electrons, the drift current, the number of ions created, etc., can be computed as a function of the field strength.

112. The Force at the Anchored Cathode Spot. LEWI TONKS, *General Electric Company.*—The force exerted by a cathode spot anchored as a cathode line (C.L.) along a meniscus edge at a Mo surface has been measured in three different ways. The depression of the meniscus edge with increasing current density gave the value 22.6 dynes/amp. for the total average force exerted normal to the Hg surface. An anchor suspended in Hg from a pendulum gave the value 20.2 dynes/amp. for the same force increased by any pressure against the exposed part of the anchor. This was independent of the area of anchor exposed, so that the latter component was negligible at distances greater than 2 mm from the C.L. A torsion pendulum tube containing Hg with a trace of Mg gave 31 dynes/amp. This large value is not understood. All values lie below the 40 dynes amp.$^{-1}$ from Kobel's measurements on an unanchored confined spot. Cathode force measurements establish a numerical relation between electron temperature, T, in the cathode plasma and the fraction of current, f, at the cathode carried by electrons. For 20 dynes/amp. this is $(1-f)T^{\frac{1}{2}} \sim 20/2.74 = 7.3$ so that if $T = 20{,}000°\text{K}$, $f \sim 0.95$.

113. The Photoelectric Threshold of Uranium, Calcium and Thorium Treated with Limited Amounts of Oxygen. H. C. RENTSCHLER AND D. E. HENRY, *Westinghouse Lamp Company.*—At the meeting of the Optical Society, February 23, 1935, we reported a shift in the photoelectric threshold toward the longer wavelength when a surface of pure thorium is allowed to react with a small amount of oxygen. Uranium and calcium are found to possess this same property. The photoelectric work functions for these oxygen treated surfaces agree remarkably well with the thermionic work functions obtained by Dushman (Phys. Rev. **21**, 626 (1923)) for activated tungsten filaments containing oxides of these same metals. The amount of oxygen required for best results depends upon the area and thickness of the active coating. The threshold shift is definitely obtained before the interaction with the oxygen is complete. Excessive amounts of oxygen again completely destroy the photoelectric activity in all cases.

114. Stepwise Fluorescence in Mercury Vapor; the 3650 Line. LOUIS A. TURNER, *Princeton University.*—This paper presents modifications of E. Gaviola's theoretical treatment of the experiments of R. W. Wood and of himself on stepwise fluorescence (Phil. Mag. 6 (1928)). No new experimental results are given. They showed that if the intensity of the exciting light of all wavelengths be changed by a factor, f, the intensity of 3650 in fluorescence varies as f^3 and the intensities of many other lines vary as f^2. From this result, with equations for the steady state, one can conclude: (1) That the $^3P_2$ metastable atoms are destroyed principally by collisions rather than by absorption of radiation; (2) that the concentration of $^3P_0$ metastable atoms is probably proportional to that of $^3P_1$ atoms; (3) that the $^3S_1$ atoms can be produced by absorption of both 4358 and 4047 to a comparable extent. Wood found that the addition of nitrogen produces either a decrease or an increase of the intensity of the 3650 line according to whether 4047 and 4358 are present in the exciting light or not. This result can be accounted for on the plausible hypothesis that collisions with nitrogen molecules effect interchanges of atoms among the $^3D_3$, $^3D_2$ and $^3D_1$ states as well as decrease the concentration of the $^3P_2$ atoms. The intensity of the 3650 line at the higher pressures of nitrogen is greater than Gaviola's theory predicts. This additional effect accounts for the discrepancy.

115. Quenching of Cadmium Resonance Radiation (3261) by N_2, CO and CH_4. HARRY C. LIPSON AND ALLAN C. G. MITCHELL, *New York University.*—The quenching of Cd resonance radiation (3261) has been extended to include the gases CO, N_2 and CH_4. The method used is the same as that previously described.[1] On plotting the reciprocal of the quenching (τZ_Q) against the pressure of the foreign gas a straight line results for all gases measured to date. The values of $\sigma^2_Q \times 10^{16}$, computed in the usual manner from the curves, are: H_2, 0.67; CO, 0.14; N_2, 0.02; CH_4, 0.012. The energy difference between the excited (5^3P_1) and the metastable (5^3P_0) states is 0.07 volt, a quantity of the order of magnitude of the thermal kinetic energy of the molecules at the temperature used (210°C). It seems probable that the process in the case of N_2 and CH_4 is a transfer of the atoms to the metastable state with a resulting increase in the translational energy of the N_2 or CH_4 molecule. In the case of CO the Cd atom is probably returned to the normal state, the excess energy going into vibrational energy of the CO molecule. In the case of hydrogen there are two possibilities: (1) the formation of CdH+H and (2) a process similar to that in CO.

[1] H. C. Lipson and A. C. G. Mitchell, Abstract New York Meeting, 1935.

116. The Crystal Structure of Ammonium Chlorobromoiodide. R. C. L. MOONEY, *Newcomb College, Tulane*

University.—The crystal structure of ammonium chlorobromoiodide has been determined by x-ray methods, and accurate data concerning the complex anion group obtained. The crystal is orthorhombic. The unit cell, containing four molecules, has the following dimensions: $a=6.14$A; $b=8.58$A; $c=10.03$A. The space group is $Pmcn$(V_h^{16}). The halogen positions were found by intensity considerations, while the ammonium positions were located by means of a two-dimensional Fourier series calculation of electron density. The parameters, which give good agreement between observed intensities and calculated structure amplitudes, are as follows:

	$2\pi x$	$2\pi y$	$2\pi z$
NH_4	90°	10°	131°
Cl	90°	135°	65°
I	90°	202°	135°
Br	90°	265°	203°

Thus the atoms all lie in planes which are perpendicular to the x-axis and separated by a distance $a/2$. The halogen atoms are associated in a strictly linear group, the iodine lying at the center. The distance between the iodine and bromine atoms in a group agrees closely with the sum of the atomic radii of iodine and bromine as found in I_2 and Br_2 from band spectra. The separation between I and Cl is slightly larger than the value given for the ICl molecule. The ammonium atom is coordinated with four chlorines at a distance of 3.34A; four bromines at a distance of 3.63A; and two iodines at a distance of 3.79A.

117. Fourier Analyses of X-Ray Patterns of Phosphorus. N. S. GINGRICH AND RALPH HULTGREN,* *Massachusetts Institute of Technology.*—A Fourier analysis of the x-ray powder patterns of four samples of phosphorus has been made. Black crystalline, black "amorphous," red crystalline, and red "amorphous" samples of phosphorus were used, and diffraction patterns were obtained by means of Mo $K\alpha$ x-rays, monochromatized by reflection from a rocksalt crystal. From these patterns, the distribution of atoms about any one atom was determined with the aid of a Coradi analyzer. In all four cases, the number of nearest neighbors is three, at a distance of 2.28A, in agreement with the accepted radius of 1.10A for the phosphorus atom, and the threefold coordination expected in a covalent structure. The number of next nearest neighbors is approximately twelve and they are at about 3.6A in all four cases. The number and positions of more remote neighbors are less definite, but they appear to be different for the various samples. In the case of crystalline black phosphorus, the atomic distribution curve has led to a complete structure determination.

* National Research Fellow.

118. The Crystal Structure of Black Phosphorus. RALPH HULTGREN* AND B. E. WARREN, *Massachusetts Institute of Technology.*—The rhombohedral structure of black phosphorus reported in the literature by Linck and Jung gives improbable interatomic distances. The set of lines they report does not agree with the lines we obtained from five different samples. These lines cannot be fitted to a lattice of high symmetry. Preferred orientation of some of the lines indicates a layer structure, agreeing with the graphite-like properties of the material. Using this fact and the results of the Fourier analysis reported earlier, we were able to derive a structure which has a side centered orthorhombic cell of the following dimensions: $a=3.31$A, $b=4.38$A and $c=10.50$A. The first 42 lines of the cell fit the accurately determined interplanar spacings. The cell has 8 atoms, which gives a calculated density of 2.69 g/cc in place of the experimental 2.70 g/cc. The space group is V_h^{15}—$Bmab$ and the two parameters of the eight atomic positions occupied can be determined from line intensities, giving excellent agreement. The structure consists of double layers 5.25A apart. Each atom is surrounded by three neighbors at 2.18A with bond angles slightly larger than in the arsenic structure. The latter structure is not quite so dense, which is probably the reason the high pressure form of phosphorus prefers the black phosphorus structure.

* National Research Fellow.

119. The X-Ray Analysis of Amorphous Rubber. G. L. SIMARD AND B. E. WARREN *Massachusetts Institute of Technology.*—The x-ray scattering curve for unstretched rubber is obtained with Cu $K\alpha$ and Mo $K\alpha$ radiation. To eliminate background correction a vacuum camera is used, and the radiation is monochromatized by NaCl reflection. A typical amorphous pattern is obtained showing three distinct peaks. By the usual method of Fourier analysis, a distribution curve is obtained giving the average number of carbon atoms to be found at any distance from a given carbon atom. The first peak in the distribution curve occurs at 1.5A and contains 2.0 carbon atoms. The second peak is at 2.6A and has an area corresponding to about 3.5 carbon atoms. As the peak is not sharply defined on the outer side, this number represents second nearest neighbors and others beyond. The results are in good agreement with the usual chain molecule. The strong inner peak observed in the diffraction patterns of unstretched rubber is due to a slight excess distribution at about 5.0A.

120. The X-Ray Analysis of Vitreous B_2O_3. B. E. WARREN AND O. MORNINGSTAR, *Massachusetts Institute of Technology.*—The x-ray scattering curve for vitreous B_2O_3 is obtained in a vacuum camera with Cu $K\alpha$ and Mo $K\alpha$ radiation monochromatized by crystal reflection. The sample was in the form of a cylindrical rod. The glass gives a typical amorphous pattern showing four distinct peaks. The method of Fourier analysis is readily extended to the case of a material containing more than one kind of atom, by setting each atomic scattering factor $f_m=Z_m f_0$ where Z is the atomic number and f_0 is a weighted average scattering factor per electron. The distribution curve which is obtained shows strong peaks at 1.4A and 2.38A. The first is due to the B—O distance and the second to the O—O distance. Both the distances and the areas under the peaks indicate a triangular coordination with each boron bonded to three oxygens and each oxygen to two borons.

121. Slip, Twinning and Cleavage in Silicon Ferrite (4.17 percent Si). CHARLES S. BARRETT, *Carnegie Institute of Technology*.—The crystallography of the deformation process was determined in five single crystals cut from sheets of commercial silicon iron containing 4.17 percent Si. Each crystal was mounted and polished and its orientation determined by stereographic projection of back reflection Laue photographs. Each crystal used was free from distortion and lineage; its orientation was determined from 50 or 100 sharp spots with an accuracy of $\pm 0.5°$. Deformation markings on the polished surface were photographed at 100 diameters and plotted on the projection. As expected from previous results, repeated bending causes cleavage on cube planes, {100}, and hammer blows cause twinning (Neumann bands) on icositetrahedral planes, {112}. Slip produced by slow inhomogeneous deformation at 20°C, however, does not occur by the mechanisms proposed by Gough, or Taylor, or Fahrenhorst and Schmid for α-iron; the slip lines are generally straight instead of wavy as in α-iron, and slip occurs *only* on rhombic dodecahedral planes, {110}. These are preliminary results in a general study by the Metals Research Laboratory of the effect of alloy composition and temperature on the deformation process in iron.

122. New Lines in the *K* Series Spectrum of Tungsten. J. C. HUDSON AND H. G. VOGT, *Harvard University*, AND A. H. ARMSTRONG, *Wellesley College*.—A re-examination of the K series x-ray spectrum of tungsten has been carried out with a high dispersion spectrograph in which the dispersion is 0.5 X.U. per mm. The Bragg focusing arrangement is used with a distance from slit to crystal of 615 cm. The crystal is oscillated through 30 minutes of arc by means of a cam so that the entire K spectrum is secured with one exposure. The regular diagram lines appear on the photographic plate though the delta doublet is not separated appearing as a single line. The separation of δ and γ_1 is 0.96 X.U. and lying between these two lines is a very faint new line of wavelength 178.6 X.U. which apparently results from a $N_{IV,V}-K$ transition. Between γ_2 and β_1 are two faint lines of wavelength 179.9 X.U. and 182.8 X.U., respectively. The first cannot be assigned to any transition in tungsten but agrees well with the $K\alpha_1$ line of gold. The second line agrees well with the $M_{IV}-K$ transition in tungsten. Both of the new tungsten lines are very faint compared to the regular diagram lines.

123. Interaction of Nuclear Particles. LLOYD A. YOUNG, *Carnegie Institute of Technology*.—Heisenberg's assumption concerning nuclear binding was that the main effect arose from a proton-neutron attraction. Majorana, in an important contribution, showed that this attractive force could not be like classical forces but had to be of an exchange nature. The amended theory predicts certain nuclear properties in a qualitative way but is unsatisfactory in others. First, the magnitude of the Majorana proton-neutron interaction, as determined from mass-defects of heavy nuclei, is too large to explain the small mass-defect of the deuteron. Second, the theory predicts too large a value for the ratio Z/A. Finally, a theory based on proton-neutron interactions alone (plus eventually Coulomb forces) cannot explain the striking odd-and-even number properties of nuclei. In the present work the effects of proton-proton and neutron-neutron forces of the Majorana type are considered. We are led to assume that every nuclear particle interacts with every other nuclear particle in the Majorana sense. The new attack resolves the above difficulties satisfactorily, giving values for the parameters of the interaction, mass-defects, nuclear radii, etc. Finally it gives a very simple explanation of odd-and-even nuclear properties.

124. Neutron-Proton Interaction and the Binding Energies of the Hydrogen and Helium Isotopes. EUGENE FEENBERG, *Harvard University*.—In the present state of nuclear theory it is reasonable to assume, for particles bound in the same nucleus, that the neutron-proton interaction operator can be represented fairly well by a potential function $J(r)$. Taking $J(r)$ to have the form $Ae^{-\alpha r^2}$, which is well adapted to the discussion of the three and four body problems, A and α have been determined to fit the binding energies of the deuteron and the alpha-particle. The results are roughly $A=170mc^2$, $1/\alpha^{\frac{1}{2}}=1.3\times10^{-13}$ cm, with both the Wigner and Majorana theories. The computed binding energy of H^3 has the value $12.7mc^2$ (Wigner) or $11.2mc^2$ (Majorana), not very far below the experimental value of $16.0\pm1.7(?)mc^2$. The two theories appear to be about equally good. It may be that also in the case of free particles the interaction operator can be represented by a potential $J'(r)$. Because the conditions of binding and of scattering are so different there is no reason to expect J and J' to be identical. The inequalities $J'<J$ and $\partial J'/\partial W<0$ (W—kinetic energy) should hold if some part of the potential results from a polarization of each particle in the field of the other or from a high frequency exchange process such as that suggested by Heisenberg. For slow neutrons a thirty-percent *decrease* in the magnitude of the interaction in going from binding to free particles yields an *increase* in the scattering cross section against protons of several hundred percent over the value given by J. This larger value is required by recent measurements. The rapid fall of the experimental cross section with increasing W requires that J' decrease steadily as W is made larger.

125. Energy Levels of Light Nuclei. GUIDO BECK, *University of Kansas*. (*Introduced by H. W. Webb.*)—The theoretical analysis of the experiments on the anomalous scattering of alpha-particles which recently has been given by P. Wenzel and L. H. Horsley shows that it is possible to determine the quantum numbers of the virtual energy levels of light nuclei. The virtual energy levels investigated fit nicely in a simple picture for the structure of light nuclei which can be schematically represented by a potential hole of variable depth. This picture holds if one assumes that—at least in light nuclei—every pair of neutrons and protons is bound in an intranuclear alpha-particle. This view is strongly supported by the mass defects. No unambiguous conclusions can so far be reached on the nuclear spins but it can be shown that several

levels of slightly different energy and of low spin values play a role in the structure of light nuclei.

126. The Interaction Between a Neutron and a Proton. L. H. THOMAS, *Ohio State University.*—It has been suggested (E. Wigner, Zeits. f. Physik **83**, 253 (1933)) that the interaction between a neutron and a proton can be regarded as described by a singularity of the wave function in their configuration space where their positions coincide, of such a nature as to give the observed mass defect of H^2. A function has been found which makes the expression for the energy in the corresponding variation problem for H^3 arbitrarily large and negative, provided that there is no compensating repulsion between the two neutrons. Subject to this provision, the above suggestion seems to be untenable; in fact a lower limit to the distance below which a neutron and a proton are effectively in interaction may be deduced.

127. A Nuclear Model. WILLIAM V. HOUSTON, *California Institute of Technology.*—If a nucleus is treated as composed of alpha-particles, protons and neutrons, the forces between the particles can be crudely approximated as attractions proportional to the distance. This approximation has the great advantage of giving a problem which is soluble as an n-body problem. By assuming force constants of a reasonable order of magnitude it is possible to account for the general trends of nuclear binding energies. The instability of Be^8 and the stability of C^{12} composed of two and three alpha-particles, respectively, is understandable. A limitation on the number of neutrons which are bound to a given number of alpha-particles can be imposed from energetic considerations by the application of the Pauli exclusion principle to the neutrons among themselves. Alpha-particle radioactivity does not appear in the model because only attractive forces are considered. This property could be added by some sort of repulsion between the alpha-particles or some sort of exclusion principle. The model gives the correct magnitude for the excited levels of C^{12} and O^{16}, but does not give the large number of close levels observed in the radioactive elements. These can perhaps be included by slight modifications of the forces.

128. The Electronic Structure of Diamond. GEORGE E. KIMBALL, National Research Fellow, *Massachusetts Institute of Technology.*—The quantum-mechanical methods of Wigner, Seitz and Slater have been applied to the structure of the diamond. The lattice eigenfunctions were approximated by linear combinations of $2s$ and $2p$ functions of carbon. It is found that the $2s$ level splits into two energy bands in the lattice. One of these bands keeps its s-like character as the interatomic distance is decreased. Its energy shows a strong minimum in the neighborhood of the observed carbon-carbon distance. The other band shows a slight maximum in energy and then a minimum, again near the observed carbon-carbon distance. The corresponding eigenfunctions lose their s characteristics and become p-like. The $2p$ level splits into six bands, two following the course of the $2s$ bands, the other four being repulsive. The number of available electrons is just sufficient to fill the two $2s$ bands and the two low $2p$ bands. The large gap in energy between the highest filled band and the lowest empty level explains the absence of electrical conductivity.

129. The Electronic Structure of Copper. HARRY M. KRUTTER, *Massachusetts Institute of Technology. (Introduced by J. C. Slater.)*—The method of Wigner, Seitz and Slater has been applied to the calculation of the energy levels and wave functions of the electrons in the face-centered copper lattice, assuming a spherically symmetric field about each atom, and making the functions continuous at the midpoints between nearest neighbors. As a first approximation the Cu^+ potential field of Hartree was used for the s, p and f states. A correction for the $4s$ electron was used in the study of the $3d$ electrons. Calculations of the energy bands on this basis show a strong overlapping of the $3d$ band with the $4s$ band. The minimum of the $4s$ energy band comes approximately at the correct interatomic distance for copper. Results of the calculation of energy as a function of momentum, which can only be solved simply in the 100, 110 and 111 directions, show that the eleven electrons $3d^{10}4s$ fall into six bands, five of which are filled, leaving one electron in the unfilled band, accounting for the conductivity of copper. This electron cannot be said to be either an s or d electron but is built up of s, p and d wave functions. In the 100 direction this electron behaves roughly as a free electron.

130. On the Reduction of Space Groups. FREDERICK SEITZ, *Princeton University.*—The connection between group theory and quantum mechanics has proved to be of considerable service in the development of the theory of the solid state, and in this work the range of reduced groups has been extended to include the 230 space groups. Though it has been found practical to develop no more than a scheme by means of which the reduction may be carried through, this scheme is entirely convenient and may be applied to any given group. Among a number of definite applications of these results, one of the most outstanding, at present, is concerned with an investigation of the discontinuities of the energy of the electron waves in metals when the energy is regarded as a function of the wave number vector. These discontinuities appear at the so-called Brillouin zones, and are connected with the partial removal of a degeneracy which obtains for waves going with vectors not on a zone. The results for a body-centered lattice of the type met with in simple metals are being determined at present.

131. Ionization Balance of the Atmosphere Near the Earth's Surface. G. R. WAIT, *Carnegie Institution of Washington, Department of Terrestrial Magnetism.*—The number of small, molecular ions in a gas depends upon the ratio of rate of production to that of destruction. Small-ion destruction-rate in the lower layers of the atmosphere is due principally to the presence of larger ions and uncharged particles, the number of which varies considerably and systematically through the day. The rate of small-ion

production in the lower atmosphere also undergoes large and systematic variations through the day, as shown in the preceding paper. This observed rate of production provides a check on any calculated rate of production, based on the number of small ions in the atmosphere and the number of larger particles present acting to destroy them. Observations in Washington, D. C., during the past year have provided data for making comparisons between calculated and observed rates of production. It is found, contrary to prevailing opinion, that the large or Langevin ion does not play a predominant role as a remover of small ions. The intermediate ion, having a mobility of about 0.07 cm per sec. per volt per cm, due to its much larger combination-coefficient, plays an equally important part in the removal of small ions from the lower atmosphere.

(To be called for immediately following paper No. 8.)

132. Effect of Cosmic-Ray Energy Upon Stoss Production. W. F. G. SWANN AND D. B. COWIE, *Bartol Research Foundation.*—The fact that the intensity of Stoss and shower production increases with altitude much more rapidly than does the cosmic radiation intensity itself leads one of us to the view that the intensity of Stoss production was a rapidly increasing function of the energy of the primary cosmic rays. If such is the case, Stoss production per unit intensity of primary, by primary rays which are limited to a vertical direction, should be much larger than the corresponding quantity for primary rays limited to directions in the neighborhood of 45°, since the latter rays have travelled a much greater thickness of atmosphere. To test this conclusion we set up an apparatus comprised of a one-inch thick iron sphere suitably arranged as a Stoss measuring ionization chamber. One set of counters was placed vertically above and another was placed vertically below the center, and the two were used as a double coincidence set. Coincidences between this counter discharge and Stösse produced serve to indicate which Stösse were produced by the vertical rays determined by the counter system. An exactly similar pair of counters arranged at 45° to the vertical gave the information for this direction also. The experiments show that while over a period of 48 hours the number of counts obtained by the vertical and 45° counters was in the ratio of 2.7 to 1, the corresponding number of Stösse (involving more than 1.5×10^4 ions) was in the ratio of 12 to 1, which result confirms the conclusion cited above.

(To be called for immediately following paper No. 83.)

133. Observations on the Townsend Discharge in Neon. EUGENE W. PIKE, *Scott Paper Co., Chester, Pa.*—The potential V_T across a self-maintaining Townsend discharge in neon is sensitive to illumination of the discharge with light from a positive column discharge in neon. The relationship of this change (ΔV_T) in V_T to gas pressure, gas purity, and electrode geometry has been investigated in detail. Although ΔV_T is enormously sensitive to traces of foreign gases in the neon, in the purest possible neon it is very small ($\approx$1 volt), negative, and practically independent of pressure and electrode geometry. A tentative interpretation in terms of atomic processes yields the following major information:

(a) The *motion* of neon resonance radiation in neon at a few mm Hg pressure is essentially in straight lines.

(b) Slow neon metastable atoms radiate their excitation energy on striking a metal surface; this radiation is emitted isotropically, including into the metal.

The first conclusion is supported by the observation of Langmuir and others that the resonance lines from a positive column discharge in neon were transmitted rectilinearly for considerable distances in unexcited neon, and finds a tentative explanation in the theory of the excited neon molecule.

(To be called for immediately following paper No. 90.)

134. Refraction of the Copper $K\beta$ Line by a Diamond Prism. J. A. BEARDEN, *Johns Hopkins University.*—Precision measurements of the index of refraction of x-rays may be used as a means of determining x-ray wavelengths. Since the method of correcting for the electronic binding is unsatisfactory in some details it is best to use a prism of very low atomic number in which the effect will be very small. A diamond prism fulfills all requirements better than any other substance. Photographic refraction measurements of the copper $K\beta$ line have been made using a 90 degree edge of a diamond block 9 mm$\times$9 mm $\times$3 mm. Two surfaces were polished optically flat and a very perfect edge was obtained. However, absorption was so low that it was not necessary to allow any part of the x-ray beam to strike the edge of the prism. The gold faced slits were 0.003 mm wide and were 430 mm apart. The prism to plate distance was 1908 mm. The exposure time was varied from 3 to 12 hours. The result from 25 of the best plates gives $\delta=[9.224\pm.001]\times10^{-6}$. This gives λ Cu $K\beta=1.3924$A which is 0.26 percent greater than the best crystal values. Thus the refraction measurements are in complete accord with the ruled grating results.

(To be called for immediately following paper No. 106.)

135. Propagation of Explosion Condensation Through Air. L. THOMPSON, *Naval Proving Ground.*—An empirical study of the velocity and intensity functions as affected by quantity of explosive detonated and by distance from the center of the pulse at the instant of disintegration. The unit of distance is taken as a representative length from the center to the boundary of the explosive. The experimental work employs a set of piezoelectric pressure gauges of Rochelle salt to obtain velocity and pressure data, recording by oscillograph.

136. The Formation of Electron Pairs by Internal Conversion of Gamma-Radiation. MORRIS E. ROSE AND GEORGE E. UHLENBECK, *University of Michigan.*—The production of an electron and positron by the spherical wave emitted from a nucleus has been considered on the basis of the rigorous theory and by certain approximate methods. Regarding the nucleus as a Hertzian oscillator, both the dipole and quadripole radiation is treated. The approximate methods, which may be classified according to which of a certain set of parameters (the momenta of the particles, $Z/137$, and eventually the ratio of these) are to

be considered small compared to unity, form a consistent scheme. Since the completion of the work there has appeared the rigorous treatment of the problem by Hulme and Jaeger (Proc. Roy. Soc. **A148**, 708 (1935)). In view of the labor involved in the numerical computations which this theory necessitates, it is of advantage to consider the results of the approximate methods so far as these are reliable. It is found that the differential and total internal conversion coefficients are given quite accurately by the use of nonrelativistic wave functions for gamma-ray energies up to about 2MEV. For greater energies the Born approximation may be used to give the total conversion coefficient within 25 percent or better.

137. Resolution of the ND_3 Bands at 13.5μ. M. V. MIGEOTTE* AND E. F. BARKER, *University of Michigan.*—The low frequency parallel vibration of ND_3 gives rise to a pair of bands in the neighborhood of 13.5μ. The two components are slightly separated because of the double minimum in the potential energy with respect to the coordinate along the axis of symmetry. These bands have been observed and completely resolved using a sample of very pure deutero-ammonia supplied by Professor Taylor of Princeton University. The separation of the two component vibrations is much less than the line interval in the rotational structure; consequently the lines in the positive and negative branches appear in pairs and may be properly assigned without difficulty. The maxima of the two zero branches lie at 745.0 cm^{-1} and 748.5 cm^{-1}, but the band centers are 745.5 and 749.2 as indicated by the rotation series. The interval between them, 3.7 cm^{-1}, is considerably larger than that predicted, in first approximation, from the potential function adjusted to yield the separation observed in NH_3. Both component bands have the same line interval, $2B = 10.25$ cm^{-1} from which the moment of inertia with respect to an axis through the centroid and normal to the symmetry axis is immediately obtained, $A = 5.40 \times 10^{-40}$. The corresponding value for NH_3 is 2.80×10^{-40} and a comparison of these two determines the dimensions of the molecular pyramid. The computed distance between hydrogen atoms is $a = 1.59 \times 10^{-8}$ cm, and the displacement of the nitrogen atom from the hydrogen plane is $h = 0.413 \times 10^{-8}$ cm.

* C. R. B. Fellow.

138. Band System of TiCl. ALLAN E. PARKER AND ALICE H. PARKER, *Columbia University.*—An analysis has been made of a band system due to TiCl. The band system which is four-headed extends from 4340A to 3730A and degrades to the violet. The $\Delta_v = 0, \pm 1, +2$ sequences are observed. From the analysis the following constants are obtained $\nu_{head}^{(-1,-1)} = 23{,}875.8$ cm^{-1}, $\omega' = 912.5$ cm^{-1}, $x'\omega' = 3.7$ cm^{-1}, $\omega'' = 883.7$ cm^{-1} and $x''\omega'' = 5.0$ cm^{-1}. The ω'' value to be expected on the basis of the observed frequencies of $TiCl_4$ and the theory of J. E. Rosenthal, based on the Urey-Bradley potential function, is 450. The discrepancy is probably due to the fact that the assumed potential function is not valid for $TiCl_4$.

139. Some Alpha-Ray and Proton Tracks in Photographic Emulsions. T. R. WILKINS, W. RAYTON AND H. ST. HELENS, *University of Rochester.*—Tracks (both alpha-ray and proton) have been observed showing Rutherford scattering. Pairs of proton tracks with an evident meeting point when produced backward in 3 dimensions seem to indicate ejection by a neutron since no track is observable near the junction. Crossing and single secondary proton tracks diverging from a straight proton track have also been photographed. This latter may be an example of delayed nuclear ejection since if it were an ordinary collision a bend would be observed. Finally, an analysis has been made of the tracks observed when collimated alpha-rays fall on a chromic acid sensitized emulsion. Two groups of tracks at random directions to the incident alpha-rays have been examined—the one group having a range approximately equal to that of the incident rays. The second group is considerably longer and seems to indicate a characteristic proton. The random tracks are approximately equal in number to the collimated tracks. This discovery greatly complicates the analysis of alpha-ray isotopes by the emulsion method unless collimation can be used. In ordinary emulsions, the proton tracks would not be distinguishable from alpha-ray tracks as without special emulsions and sensitization only a short section of the proton track is registered.

140. A High Frequency Parallel Rod Method for the Determination of Alpha-Ray Speeds. T. R. WILKINS, W. RAYTON AND H. ST. HELENS, *University of Rochester.*—If charged particles are sent longitudinally between two rods on which a high frequency is impressed, it is shown that the particles will emerge without a sidewise component to their velocity provided that they are between the rods for a time $t = L/V_p = TV_w/(V_w - V_p)$ where L is the length of the rods, V_w = speed of e.m. waves on rods, V_p = speed of the particles. The experiment can also be used to determine V_w by applying the waves at the far end of the rods. Two equations then result. $V_p = 2L/(T_1 + T_2)$; $V_w = 2L/(T_1 - T_2)$. In our first experiments an interesting phenomenon was observed. The particles were detected by tracks in a photographic emulsion. At a critical frequency the tracks in the emulsion were curved at 90°. We interpret this not as alpha-ray bending for which a field of 10^8 gauss would be required but in terms of a resonance frequency in the emulsion. The frequency was 15,680 kc for the special emulsion used. The method is applicable to charged particles of any kind and gives a direct determination of speeds in terms of a length and a quartz-crystal controlled frequency.

141. Qualitative Experiment on Scattering of Neutrons. ALLAN C. G. MITCHELL AND EDGAR J. MURPHY, *New York University.*—The scattering of neutrons by several elements was investigated by measuring the increase in radioactivity of a silver foil produced by scatters placed on the opposite side of the foil from the neutron source. The source, consisting of radon and beryllium, was encased in paraffin. Neutrons issuing from the source passed through 6 cm of paraffin and struck a silver foil 6×10 cm. Various thicknesses of scattering material, cut to the same size as the silver foil, were placed on the side of the foil

away from the source. Copper and iron were found to be good scatterers, a thickness of about 3.5 cm of either being sufficient to give maximum scattering which was about 54 percent for copper, and 88 percent for iron. In the case of copper a sheet of cadmium 1 mm thick caused a marked decrease in the effect, showing that slow neutrons were being scattered. Evidence was found that some fast neutrons were also scattered back. The scattering by mercury appeared to be quite small.

142. The Diffusion of Radioactive Atoms. J. A. GRAY AND J. F. HINDS, *Queen's University.*—Plates have been placed above a source of radium ($D+E+F$) deposited on glass during the decay of radon. Measurements have been made of the relative rates of deposit on the plates of the three types of atoms and these compared with the equilibrium values. It has been found that these atoms will diffuse through thin metallic foils, the radium E more easily than radium D and radium F.

143. A Simple Circuit for Counting Pulses at High Speed. LOUIS A. TURNER, J. B. H. KUPER AND J. H. RISSER, *Princeton University.*—The discharge of a small condenser (0.002 to 0.1μfd) through a gas triode (RCA 885) as the result of a pulse applied to the grid is found to be a definite, repeatable, uniform process. Every pulse causes a definite quantity of electricity to flow. If such discharges flow through an ordinary microammeter they produce a current directly proportional to the number of pulses per second. This latter quantity, rather than any total number of pulses is the one which is usually of interest. The current has been found to be accurately proportional to the speed up to 420 regularly spaced pulses per second. It has not yet been measured at accurately known higher speeds but less accurate tests show that there is no serious departure from linearity at 1000 regular pulses per second. Adaptation for use as a frequency meter is possible. Using a high resitance (1 megohm) in series with the meter, the two being shunted by a large condenser (10μfd) the meter gave a steady reading for only a few discharges per second. An arrangement in which the discharges are stored until a potential sufficient to discharge another tube has been built up in a condenser operates satisfactorily for ratios of numbers of discharges up to 10.

144. Nuclear States and Moments. D. R. INGLIS, *University of Pittsburgh.*—On comparing the problem of a heavy particle in the nucleus with an outer atomic electron, the binding energies differ by a factor about 10^6, the radii by almost 10^{-6}, and for the spin-orbit magnetic energy the factor $g_s Z_{eff}(\text{magneton})^2/r^3$ gives a ratio around 10^9. The binding-type energies are expected to have no singularity at coincidence of nuclear particles (Majorana) so *may* have relatively smaller nondiagonal elements than have atomic e.s. energies, in the representation of single-particle quantum numbers and diagonal spin-orbit energy. Particles in the same state probably interact most. These are reasons for (jj) coupling of both protons and neutrons at least in heavy nuclei, and for the approximate validity of the single-particle calculations. The order of energies of states is given roughly by nodes of Bessel's functions of half-order (Elsasser). The additional large spin-orbit energies allow the higher doublet level of one state to be above the lower one of the next higher state. The doublet levels correspond to "closed shells." The order of their energies is not quite uniquely given theoretically, but can be chosen to fit observed values of the total angular momentum, limited by the exclusion principle and by a natural tendency of even numbers of like particles to form zero moments. In many cases the angular momentum is then determined uniquely, in other cases three or even more values are possible. Because of the absence of screening, "configurations" are relatively near in energy, and second-order contributions to the magnetic moments are large. First-order calculations of the magnetic moments, using $g_p=5$ and $g_n=-3.5$, thus agree only in sign and in order of magnitude with "experimental" values. Sources of a second-order contribution in the right direction can be found, which is of interest in the cases of the accurately-known ratios.

145. Temperature Variation of Contact Potential. DAVID B. LANGMUIR, *Massachusetts Institute of Technology.*—By a method previously described the contact potential of a thoriated tungsten filament has been measured for different states of activation and temperature. Emission measurements from the same surface and at the same temperatures have also been made. The logarithm of the emission plotted against the contact potential difference is a straight line with exactly the theoretical slope e/kT provided that the zero field emission is used, and that the emission and contact P.D. are measured at the same temperature. If emission under accelerating fields is used the slope does not agree with theory. The contact P.D. between the activated and deactivated states in the experimental temperature range is 1.50 volts. The temperature coefficient of the contact P.D. at constant states of activation has also been measured. For the deactivated state $\partial V/\partial T=0.71\times10^{-4}$ volt per degree, while for the activated state the value is 1.8×10^{-4}. These values would change the value of the constant A in Richardson's equation from 120 to 52 and 15, respectively.

146. X-Ray Diffraction Pattern of Liquid and Solid Glycerine Films. K. LARK-HOROVITZ AND E. P. MILLER, *Purdue University.*—Copper K radiation reflected from a rocksalt crystal was used in producing x-ray diffraction patterns of glycerine at room temperature (liquid) and at -80°C (solid). It has been found that the apparent sharpening of the diffracted lines at lower temperatures as reported previously was due to inhomogeneous radiation. The present experiments show no appreciable sharpening. This is in agreement with the assumption that the molecules in the solid glycerine, which forms a glass, are distributed at random in a way similar to those found in liquids.

AUTHOR INDEX TO ABSTRACTS OF THE WASHINGTON MEETING

Adel, Arthur and V. M. Slipher—No. 10
Allis, W. P.—see Morse
Altar, Wm.—No. 97
Armstrong, A. H.—see Hudson

Ballard, James W. and E. D. Wilson—No. 43
Barker, E. F.—see Migeotte
Barnes, R. Bowling—see Brattain
——, **R. Robert Brattain and R. S. Firestone**—No. 35
Barr, E. S.—see Plyler
Barrett, Charles S.—No. 121
Bartberger, C. L.—No. 93
Bartlett, J. H., Jr., J. J. Gibbons, Jr. and C. G. Dunn—No. 96
Bartlett, William W.—see Harrison
Barton, Henry A.—see Mueller, Donald W.
Bazzoni, Charles B.—see McCorkle
Bearden, J. A.—Nos. 101, 134
Beasley, I. E.—see Glasser
Beck, Guido—No. 125
Bennett, Clarence E.—No. 21
Bennett, Willard H.—No. 26
Bethe, H. A.—No. 49
Bien, R. P.—No. 107
Bleakney, Walker—see Hipple
—— see Smyth
—— **and J. A. Hipple, Jr.**—No. 78
Boyce, J. C.—No. 73
Bradley, Charles A., Jr.—see McKellar
—— **and Andrew McKellar**—No. 38
Bradley, Charles D.—No. 86
Brattain, R. Robert—see Barnes
——, **R. Bowling Barnes and Frederick Seitz**—No. 37
Braun, Milton L.—No. 65
Breazeale, William M.—No. 18
Brickwedde, F. G.—see Scott
—— see Silsbee

Carl, Howard—see Petersen
Carman, Everett F.—see Harkins
Challacombe, C. N. and P. Gerald Kruger—No. 68
Constant, F. Woodbridge—No. 45
Cowie, D. B.—see Swann
Crary, A. P.—see Ewing
——, **Maurice Ewing and E. B. Douglas**—No. 59

Darling, B. T.—see Kruger
Deming, J. H.—see Jauncey
Douglas, E. B.—see Crary
—— see Ewing
Dunn, C. G.—see Bartlett, J. H., Jr.
Dunning, J. R., G. B. Pegram, G. A. Fink and D. P. Mitchell—No. 54

Eaton, William W.—No. 56
Ellis, Cecil and Ralph A. Sawyer—No. 72
Evans, Robley D.—see Livingston
——, **Gladys D. Finney, Arthur F. Kip and Raymond Mugele**—No. 30
Ewing, Maurice—see Crary
——, **A. P. Crary and E. B. Douglas**—No. 60

Failla, G.—No. 106
Fearon, Robert E.—No. 85
Feenberg, Eugene—No. 124
Fink, G. A.—see Dunning
Finney, Gladys D.—see Evans
Firestone, R. S.—see Barnes
Flowers, J. W.—No. 84
Forsythe, W. E.—No. 20
Fox, M.—see Millman
——, **S. Millman and I. I. Rabi**—No. 81
Frost, A. A. and O. Oldenberg—No. 14
Fussler, Karl H.—see Ruark

Gagge, A. P.—No. 3
Gans, David M. and William D. Harkins—No. 53
Gibbons, J. J., Jr.—see Bartlett, J. H., Jr.
Gilbert, W. P.—No. 92
Gingrich, N. S. and Ralph Hultgren—No. 117
Glasser, Otto and I. E. Beasley—No. 16
Granath, L. P.—see Stranathan, R. K.
Gray, J. A. and J. F. Hinds—No. 142
Gunn, Ross—No. 4

Haines, C. L.—No. 29
Hardy, J. D. and Carl Muschenheim—No. 19
Harkins, William D.—see Gans
——, **Everett F. Carman and Herman E. Ries, Jr.**—No. 63
Harnwell, G. P.—see Smyth
Harrison, George R. and William W. Bartlett—No. 69
Henry, D. E.—see Rentschler
Hickman, Roger W. and Frederick V. Hunt—No. 7
Hinds, J. F.—see Gray
Hipple, J. A., Jr.—see Bleakney
—— **and Walker Bleakney**—No. 87
Hirsh, F. R., Jr. and F. K. Richtmyer—No. 102
Hoffmann, B.—No. 98
Hopfield, John J.—No. 15
Houston, William V.—No. 127
Hudson, J. C., H. G. Vogt and A. H. Armstrong—No. 122
Hultgren, Ralph—see Gingrich
—— **and B. E. Warren**—No. 118
Humphreys, C. J.—No. 74
Hunt, Frederick V.—see Hickman

Ide, John—No. 62
Inglis, D. R.—No. 144

Jauncey, G. E. M. and J. H. Deming—No. 99

Kimball, George E.—No. 128
King, Paul B., Jr. and Harry Rowe Mimno—No. 6
King, Ronold—No. 8
Kip, Arthur F.—see Evans

Knipp, Julian K.—No. 94
Koller, L. R.—No. 110
Kruger, P. Gerald—see Challacombe
—— see Weissberg
—— **and B. T. Darling**—No. 25
Krutter, Harry M.—No. 129
Kuper, J. B. H.—see Turner
Kurie, Franz N. D., J. R. Richardson and H. C. Paxton—No. 57

Lamar, E. S.—see Morse
—— **and E. W. Samson**—No. 27
Langmuir, David B.—No. 145
Lark-Horovitz, K. and E. P. Miller—No. 146
Larkin, Chas. R.—No. 42
Lipson, Harry C. and Allan C. G. Mitchell—No. 115
Livingston, M. Stanley and Robley D. Evans—No. 51
Loughridge, Donald H.—No. 31
Lozier, W. W.—see Smyth

Margenau, Henry—see Pollard
McCorkle, Paul and Charles B. Bazzoni—No. 100
McKellar, Andrew—see Bradley
—— **and Charles A. Bradley, Jr.**—No. 9
McMillan, Edwin—No. 83
McNish, A. G. and G. R. Wait—No. 1
Michels, Walter C. and Barbara Raines—No. 41
Migeotte, M. V. and E. F. Barker—No. 137
Miller, E. P.—see Lark-Horovitz
Millman, S.—see Fox
——, **M. Fox and I. I. Rabi**—No. 82
Mimno, Harry Rowe—see King, Paul B., Jr.
—— see Selvidge
Mitchell, Allan C. G.—see Lipson
—— **and Edgar J. Murphy**—No. 141
Mitchell, D. P.—see Dunning
Mohler, Fred L.—see Taylor
Mooney, R. C. L.—No. 116
Morningstar, O.—see Warren
Morse, Philip M., W. P. Allis and E. S. Lamar—No. 111
Mouzon, J. C. and Newell H. Smith—No. 88
Mueller, Donald W. and Henry A. Barton—No. 55
Mueller, George J.—No. 40
Mueller, Hans—No. 22
Mugele, Raymond—see Evans
Murphy, Edgar J.—see Mitchell, Allan C. G.
Muschenheim, Carl—see Hardy

Neilsen, Harald H.—see Steward
Nordheim, Gertrud—No. 95
Nordheim, L. W.—No. 48
Nottingham, W. B.—No. 108

Oldenberg, O.—see Frost

Parker, Alice H.—see Parker, Allan E.
Parker, Allan E. and Alice H. Parker—No. 138
Parratt, Lyman G. and Lloyd P. Smith—No. 104
Paul, Fred W.—No. 70
Paxton, H. C.—see Kurie
Pegram, G. B.—see Dunning
Petersen, Max and Howard Carl—No. 91
Pfund, A. H. and J. A. Sanderson—No. 34
Phillips, C. J.—No. 32
Pickels, E. G.—No. 61
Pike, Eugene W.—Nos. 89, 133
Plyler, E. K. and E. S. Barr—No. 39
Pollard, Ernest and Henry Margenau—No. 50
Pool, M. L.—see Whitmer
Present, R. D. and J. H. Van Vleck—No. 11
Price, W. C.—No. 13

Rabi, I. I.—see Fox
—— see Millman
Raines, Barbara—see Michels
Ramberg, E. and F. K. Richtmyer—No. 103
Rank, D. H.—see Wood
Rayton, W.—see Wilkins
Rentschler, H. C. and D. E. Henry—No. 113
Richardson, J. R.—see Kurie
Richtmyer, F. K.—see Hirsh
—— see Ramberg
Rieke, Foster F.—No. 12
Ries, Herman E., Jr.—see Harkins
Risser, J. H.—see Turner
Robinson, Howard A.—No. 71
Rose, A.—No. 109
Rose, Morris E. and George E. Uhlenbeck—No. 136
Rosin, S.—No. 66
Ruark, Arthur E. and Karl H. Fussler—No. 24

Samson, E. W.—see Lamar
Sanderson, J. A.—see Pfund
Sawyer, Ralph A.—see Ellis
Schiff, L. I. and L. H. Thomas—No. 23
Schneider, Edwin G.—No. 17
Scott, R. B.—see Silsbee
——, **F. B. Silsbee and F. G. Brickwedde**—No. 46
Seitz, Frederick—No. 130
—— see Brattain
Selvidge, H. and Harry Rowe Mimno—No. 5
Silsbee, F. B.—see Scott
——, **F. G. Brickwedde and R. B. Scott**—No. 47
Simard, G. L. and B. E. Warren—No. 119
Skinner, Selby M.—No. 28
Slipher, V. M.—see Adel
Smith, Lloyd P.—see Parratt
Smith, Newbern—No. 90
Smith, Newell H.—see Mouzon
Smyth, H. D., G. P. Harnwell, W. Bleakney and W. W. Lozier—No. 79
St. Helens, H.—see Wilkins
Steward, Wendell B. and Harald H. Nielsen—No. 36
Stranathan, J. D.—No. 44
Stranathan, R. K. and L. P. Granath—No. 80
Street, J. C.—see Woodward
Swann, W. F. G.—No. 77
—— **and D. B. Cowie**—No. 132

Taylor, Lauriston S. and Fred L. Mohler—No. 105
Thomas, L. H.—No. 126
—— see Schiff
Thompson, L.—No. 135
Tonks, Lewi—No. 112
Turner, Louis A.—No. 114
——, **J. B. H. Kuper and J. H. Risser**—No. 143

Uhlenbeck, George E.—see Rose, Morris E.

Vallarta, M. S.—No. 76
Van Vleck, J. H.—see Present
Vogt, H. G.—see Hudson

Wait, G. R.—Nos. 2, 131
—— see McNish
Warfield, Calvin N.—No. 58
Warren, B. E.—see Hultgren
—— see Simard
—— **and O. Morningstar**—No. 120
Weissberg, S. G. and P. Gerald Kruger—No. 67
White, W. P.—No. 64
Whitmer, C. A. and M. L. Pool—No. 52
Wilkins, T. R., W. Rayton and H. St. Helens—Nos. 139, 140
Wilson, E. D.—see Ballard
Wood, R. W. and D. H. Rank—No. 33
Woodward, R. H. and J. C. Street—No. 75

Young, Lloyd A.—No. 123

THE AMERICAN INSTITUTE OF PHYSICS

INCORPORATED

GOVERNING BOARD

For The American Physical Society:

KARL T. COMPTON, *Chairman*
Massachusetts Institute of Technology

GEORGE B. PEGRAM, *Secretary*
Columbia University

JOHN T. TATE
University of Minnesota

For The Optical Society of America:

E. C. CRITTENDEN
Bureau of Standards

PAUL D. FOOTE
The Gulf Companies

F. K. RICHTMYER
Cornell University

For The Acoustical Society of America:

HARVEY FLETCHER
Bell Telephone Laboratories

VERN O. KNUDSEN
University of California at Los Angeles

WALLACE WATERFALL
The Celotex Company

For The Society of Rheology:

E. C. BINGHAM
Lafayette College

A. STUART HUNTER
du Pont Rayon Company

S. E. SHEPPARD
Eastman Kodak Company

For The American Association of Physics Teachers:

HOMER L. DODGE
University of Oklahoma

PAUL E. KLOPSTEG
Central Scientific Company

FREDERIC PALMER
Haverford College

ADMINISTRATIVE STAFF

HERBERT A. BARTON, *Director* JOHN T. TATE, *Adviser on Publications*

MADELINE M. MITCHELL, *Editorial Secretary*

Office: 11 East 38th Street, New York, New York

JOURNALS

THE PHYSICAL REVIEW

REVIEWS OF MODERN PHYSICS

PHYSICS
JOHN T. TATE, *Editor*
J. W. BUCHTA, *Assistant Editor*
E. C. BINGHAM, *Rheology Editor*

THE JOURNAL OF THE OPTICAL SOCIETY OF AMERICA

THE REVIEW OF SCIENTIFIC INSTRUMENTS
WITH PHYSICS NEWS AND VIEWS
F. K. RICHTMYER, *Editor*

JOURNAL OF THE ACOUSTICAL SOCIETY OF AMERICA
F. R. WATSON, *Editor*

THE JOURNAL OF CHEMICAL PHYSICS
HAROLD C. UREY, *Editor*

THE AMERICAN PHYSICS TEACHER
DUANE ROLLER, *Editor*

The American Institute of Physics is a membership corporation of which five societies are the founding members. These five societies are the principal national societies devoted to pure and applied physics in America. Their names, and those of their representatives who form the Governing Board of the Institute, are given above. The principal work of the Institute is the publication of journals sponsored by the societies or by itself. The names and the editors of the journals are also listed above.

The broad purpose of the Institute is to represent, in all matters of wide or common interest, the five thousand or more members and subscribers associated with the Founder Societies and the journals. It aims to advance the sciences and profession of physics, and to promote cooperation between pure research, the applied sciences and the industries. To achieve these aims, it is greatly in need of an endowment and is empowered by law to administer grants and funds of any kind.

CONTENTS

Rev. [illegible] (1956) MAY 15

[illegible] J. L. NICHERSON 707

[illegible] C. J. HUMPHREYS 712

[illegible] J. C. BOYCE 718

[illegible] G. M. ADAMS AND G. D. KRIDER 721

[illegible] KEN'ICHI SHINOHARA 730

[illegible] P. I. WOLD 735

[illegible] SIDNEY MILLMAN 739

[illegible] H. A. BETHE 747

[illegible] J. L. SYNGE 760

[illegible] M. F. CRAWFORD 768

[illegible] A. EINSTEIN, B. PODOLSKY AND N. ROSEN 777

[illegible] HERMAN GOMMERUP AND JOHN W. COLEMAN 781

[illegible] W. E. CRANE, L. A. DUMANOIS, W. A. FOWLER AND C. C. LAURITSEN 782

[illegible] F. A. JENKINS 783

[illegible] GERHART E. DOAN AND WILLIAM C. SCHULTE 785

[illegible]; Abstracts 1–166; [illegible] 785

LANCASTER PRESS, INC., LANCASTER, PA.